Aus der

Klinik und Poliklinik für Psychiatrie und Psychotherapie

Klinikum der Ludwig-Maximilians-Universität München

Contribution of Genetic and Environmental Circadian Disruptions to the Development of Comorbid Behavioral and Metabolic Deficits in Mice

Dissertation

zum Erwerb des Doctor of Philosophy (Ph.D.)

an der Medizinischen Fakultät der

Ludwig-Maximilians-Universität München

vorgelegt von

Muriel Katja Frisch

aus

Woluwe-Saint-Lambert, Belgien

Jahr

2023

Mit Genehmigung der Medizinischen Fakultät der
Ludwig-Maximilians-Universität München

Erstes Gutachten:	Dr. Dominic Landgraf
Zweites Gutachten:	Prof. Maria Robles PhD
Drittes Gutachten:	Prof. Dr. Christoph Scheiermann
Viertes Gutachten:	Prof. Dr. Jan Rémi

Dekan: Prof. Dr. med. Thomas Gudermann

Tag der mündlichen Prüfung: 27.11.2023

Preface

In 2017, the Nobel Prize in Physiology or Medicine was awarded to Jeffrey C. Hall, Michael Rosbash, and Michael W. Young for their discovery of the molecular circadian clock. This groundbreaking research inspired numerous scientists to delve further into the study of circadian rhythms in health and disease. It is an honor for me to have contributed to the advancement of knowledge in this field.

"These rhythms are one of the signatures of life and an understanding of these biological processes tells us much about ourselves and the world in which we live"

— Foster and Kreitzman

Through my research on the role of circadian rhythms in mental health, I hope to increase awareness and understanding of psychiatric disorders, thereby supporting those who are struggling from and fighting against these conditions.

"On croit parfois que c'est la seule manière de les faire taire

Ces pensées qui nous font vivre un enfer"

— Stromae

Table of contents

Abstract

Background: Mood and metabolic disorders frequently occur concomitantly in individuals, causing a tremendous health burden. The disproportionate comorbidity of these disorders has led to the concept of 'metabolic-mood syndrome', suggesting the existence of common underlying biological mechanisms. Since the circadian system regulates virtually all bodily functions, including brain and metabolic functions, it has been proposed that circadian system disruptions, among others, might be at the root of this comorbidity. The circadian system can be disrupted genetically (e.g., clock gene mutation), environmentally (e.g., shift work) or by a combination of both. Research has shown that genetic and environmental circadian disruptions can lead to behavioral and metabolic deficits in animals and humans. However, not all individuals experience adverse health consequences from shift work, indicating differing genetic susceptibilities to environmental circadian disruptions and highlighting a potential circadian gene-environment interaction (G×E) in the generation of disease. These arguments suggest that genetic and environmental circadian disruptions can each be causal for concomitant mental and metabolic deficits, but their interaction further increases an individual's risk for comorbid conditions. According to this hypothesis, the impact of a genetic or environmental circadian disruption, as well as the influence of their interaction on the development of behavioral and metabolic deficits in mice were assessed in this thesis. More precisely, this thesis investigated comorbid (i.e., occurring in the same animal) behavioral and metabolic deficits in three different mouse models.

Methods: In the first model, a genetic circadian disruption was caused by downregulation of molecular rhythms in the suprachiasmatic nucleus (SCN), the master pacemaker of the circadian system. This was achieved by stereotactic injection of short hairpin RNAs (shRNAs), knocking down the essential clock gene *Bmal1,* into the SCN of mice (SCN-*Bmal1*-KD). In the second mouse model, the environmental circadian disruption was induced by exposing mice to alternating light cycles, mimicking shift work conditions. Based on sexually dimorphic health implications in shift workers, male and female mice were both assessed to investigate sex-specific health effects of an environmental circadian disruption. In the third mouse model, the interaction between a genetic and an environmental circadian disruption was examined by subjecting mice lacking a single copy of *Bmal1* (*Bmal1*$^{+/-}$) to the shift work light paradigm. In all three mouse models, comorbidity of behavioral and metabolic deficits in the same animal was examined through various tests that evaluated depression-, mania-, and anxiety-like behaviors, as well as metabolic variables such as eating behavior, weight gain, and sugar metabolism.

Results: Downregulation of molecular SCN rhythms in SCN-*Bmal1*-KD animals leads to dampened locomotor activity rhythms, mania-like behavior, and alterations in the positive valence system that propose changes in reward-related behavior. Importantly, SCN-*Bmal1*-KD animals also exhibit a striking metabolic phenotype with excessive weight gain in the first weeks following SCN rhythm downregulation. Despite overall levels of metabolic parameters remaining unchanged (e.g., food intake), their rhythmicity is significantly dampened in SCN-*Bmal1*-KD mice. Downregulation of SCN rhythms equally affects glucose homeostasis with SCN-*Bmal1*-KD animals displaying changes in glucose tolerance, hypoglycemia, and a potential loss of glucose rhythms under *ad libitum* feeding. The majority of the observed behavioral and metabolic phenotypes are established rapidly following downregulation of SCN rhythms and do not change following a more chronic downregulation. Interestingly, SCN-*Bmal1*-KD animals exhibit alterations in periaqueductal gray (PAG) rhythmicity and the orexin (ORX) system, suggesting that the observed comorbid behavioral and metabolic deficits following SCN rhythm downregulation might originate from disturbances in subordinate clocks involved in the regulation of brain and metabolic functions.

In the second approach, the environmental circadian disruption, we successfully established a shift work light paradigm, which leads to constant re-entrainment in both, male and female mice. However, adaptation to alternating light cycles is sex-specific with male mice appearing to shift more readily than females. The shift work light paradigm leads to behavioral and metabolic deficits. Interestingly, and according to results in human studies, those deficits are sex-specific. While male mice show reduced helplessness during shift work conditions, females exhibit increased helplessness under these conditions. Further, female shift work animals display increased anxiety-like behavior – an effect, which is not observed in males. In line with this, only female shift work animals display a lengthening of the rhythm of the PAG, a brain region involved in anxious responses. In addition, we observe a sex-specific effect of shift work on weight gain with males displaying a significantly increased weight gain following shift work conditions despite unaltered overall food consumption. Thus, we report sex-specific deficits during shift work conditions with females being more susceptible to increased helplessness and anxiety-related features, and males exhibiting reduced helplessness and subtle metabolic changes.

In the third approach, investigating a circadian G×E in generating comorbid diseases, we show an altered adaptation of locomotor activity of *Bmal1*$^{+/-}$ animals to the shift work light paradigm. Independent of shift work conditions, *Bmal1*$^{+/-}$ mice display hyperactivity and mild signs of anxiety but no changes in mood-associated behaviors or metabolic parameters. Against our expectation, shift work conditions do not alter behavior and have only mild metabolic effects

(i.e., increased weight gain) in *Bmal1*$^{+/-}$ and WT animals. Importantly, we do not report any evidence for an interaction between a genetic and environmental circadian disruption in generating comorbid behavioral and metabolic phenotypes in mice.

Outlook: This thesis provides further evidence for the importance of both, genetically-controlled and environmentally-regulated circadian rhythms for mental and metabolic health. However, we cannot provide evidence for a circadian G×E in generating comorbidities. Our research highlights the importance of SCN rhythms in mental and metabolic health, suggesting that stabilization of these rhythms, for instance via light therapy, might be an effective and easy-to-implement tool for preventing or treating comorbidities. Our findings also contribute to the growing body of evidence suggesting sexually dimorphic health effects of shift work. Given the increasing number of individuals engaged in shift work, we recommend taking into consideration sex-specific prevention and/or therapy of shift work-associated health implications.

List of figures

List of tables

List of supplementary figures

List of supplementary tables

List of abbreviations

AAV	Adeno-associated virus
AgRP	Agouti-related peptide
ANOVA	Analysis of variance
ANS	Autonomic nervous system
AOC	Area of the curve
ARC	Arcuate nucleus
AU	Arbitrary unit
AUC	Area under the curve
AVP	Arginine vasopressin
BAT	Brown adipose tissue
bHLH	Basic helix-loop-helix
BMAL1	Brain and muscle aryl hydrocarbon receptor nuclear translocator-like protein 1, also known as ARNTL or MOP3 (clock protein)
BMI	Body mass index
BP	Bipolar disorder
CCG	Clock controlled gene
cDNA	Complementary DNA
CLOCK	Circadian locomotor output cycles kaput (clock protein)
CRY1/2	Cryptochrome 1/2 (clock protein)
DaLi box	Dark-light box
DBP	D-box albumin promoter binding protein
DD	Constant darkness
DEC1/2	Differentiated embryo chondrocyte protein 1/2
DF	Degrees of freedom
DMH	Dorsomedial hypothalamus
DNA	Deoxyribonucleic acid
E4BP4	E4 promoter-binding protein 4, also known as NFIL3
E-box	Enhancer box
EE	Energy expenditure
EGFP	Enhanced green fluorescent protein
EPM	Elevated plus maze
Fisher's LSD test	Fisher's least significant difference test
FR	Fixed ratio
FST	Forced swim test
G×E	Gene-environment interaction
GRP	Gastrin-releasing peptide

GTT	Glucose tolerance test
GWAS	Genome-wide association studies
gWAT	gonadal white adipose tissue
HDL	High-density lipoprotein
HFD	High-fat diet
HPA	Hypothalamus-pituitary-adrenal
i.e.	id est (Latin), 'that is'
IP	Intraperitoneal
ipRGCs	Intrinsically photosensitive retinal ganglion cells
ITT	Insulin tolerance test
iWAT	Inguinal white adipose tissue
KD	Knockdown
KO	Knockout
LD	Light-dark cycle
LH	Learned helplessness
LHA	Lateral hypothalamic area
LL	Constant light
LUC	Luciferase
MDD	Major depressive disorder
mRNA	messenger ribonucleic acid
NAc	Nucleus accumbens
NIH	National Institutes of Health
NPAS2	Neuronal PAS domain protein 2, also known as MOP4 (clock protein). Paralogue of CLOCK in neural tissues.
n.s.	not significant
OFT	Open field test
ORX	Orexin
PAG	Periaqueductal gray
PBS	Phosphate-buffered saline
PER1/2/3	Period 1/2/3 (clock proteins)
Ppox	Prepro-orexin
PVN	Paraventricular nucleus
qPCR	Quantitative polymerase chain reaction
RER	Respiratory exchange rate
REV-ERBα/β	Reverse-erythroblastosis virus alpha/beta, also known as NR1D1/2 (clock protein)
RHT	Retinohypothalamic tract
RNA	Ribonucleic acid
RORα/β/γ	Retinoic acid receptor-related orphan receptor alpha/beta/gamma, also known as NR1F1/2/3 (clock protein)

SCN	Suprachiasmatic Nucleus
SD	Standard deviation
SEM	Standard error of the mean
shRNA	Short hairpin RNA
SNP	Single nucleotide polymorphism
SPRT	Sequential Probability Ratio Testing
TST	Tail suspension test
TTL	Transcriptional-Translational Feedback Loop
VIP	Vasoactive intestinal polypeptide
VMH	Ventromedial hypothalamus
VTA	Ventral tegmental area
WT	Wild type
ZT	Zeitgeber time

1. Introduction

1.1 Metabolic-Mood comorbidity

Affective disorders, also referred to as mood disorders, is an umbrella term used to summarize the group of mood-related psychiatric disorders. These include diseases such as major depressive disorder (MDD) and bipolar disorder (BP). Patients suffering from affective disorders experience very strong positive and/or negative emotional states or a complete lack of emotions [1]. It is widely recognized that affective disorders often co-occur with anxiety disorders, another class of psychiatric illnesses. Anxiety-related disorders are characterized by excessive and persistent anxiety and worry, restlessness, irritability, and sleep disturbances [1]. According to estimations in 2019, approximately 301 million and 280 million individuals globally were living with anxiety disorders and MDD, respectively. Around 40 million people experienced BP [2]. Affective and anxiety disorders are a leading cause of disability worldwide and majorly contribute to the overall global burden of disease. The global costs of MDD and anxiety disorders are estimated to US$ 1 trillion each year [3]. In addition to affective disorders, metabolic disturbances, such as obesity, hypertension, type 2 diabetes and dyslipidemia are a major public health concern [4]. This cluster of symptoms, known as metabolic syndrome, affects around 1/3 of the adult population in the United States and the cost of this epidemic is estimated in trillions of US$ [5].

Importantly, mood and metabolic disorders are frequently associated. MDD patients exhibit a 50 % increased risk of developing obesity, compared to healthy individuals [6-8]. Equally, patients with BD display a prevalence of metabolic syndrome, which is nearly double as high as in the general population [9, 10]. Along the same lines, depressive symptoms during adolescence are a predictor for increased body mass index (BMI) during adulthood [11]. Importantly, metabolic syndrome in psychiatric patients elevates the risk for cardiovascular events and thereby mortality [12-14]. Conversely, individuals suffering from obesity are more likely to report depressive and/or manic symptoms and individuals primarily diagnosed with type 2 diabetes, display an increased prevalence of comorbid depression [7, 15, 16]. Even though antidepressants used to treat mood disorders have metabolic side effects, studies in unmedicated patients evidence that metabolic dysregulation also occurs independently of drug effects [17, 18]. The epidemiological relevance of this comorbidity has become apparent insofar that both disorders and especially their co-occurrence are associated with a tremendous illness-

associated burden [19, 20]. The close relationship between mood and metabolic disorders has led to the concepts of 'metabolic-mood syndrome' or 'metabolic depression', proposing common underlying biological factors for both diseases [15, 21]. The understanding of the nature of these biological mechanisms remains limited. However, the circadian system has been proposed as one factor [22], which is explored in more detail below.

1.2 The circadian system

1.2.1 Origin of the circadian clock

Life on Earth is characterized by daily recurrent changes in the environment, brought about by the 24-hour rotation of the Earth around its axis. These environmental variations include the light-dark (LD) cycle, temperature oscillations, and fluctuations in food availability. One of the greatest challenges of living organisms is to coordinate their behavior and physiology during these variations in environmental conditions. Therefore, organisms evolved an internal timekeeping system, called the circadian system, which enables them to anticipate regular 24-hour changes on Earth, thereby enhancing their chance of survival and reproduction [23-26]. In contrast, disruption of the circadian system impairs fitness [27]. "Circadian" derives from the Latin words "circa" and "diem", which signify "approximately a day" i.e., 24 hours. Circadian rhythms have been extensively studied and described in nearly all living organisms including algae, bacteria, fungi and multicellular organisms like animals, and plants [28]. Importantly, circadian rhythms are defined by three characteristics: (1) they are endogenous, self-sustained rhythms of approximately 24 hours, (2) they are entrainable and (3) they are temperature compensated [29]. These features are further explored in the following paragraphs.

1.2.2 The molecular clock

At the cellular level, the circadian system is based on a molecular clock residing in nearly every cell of the body. This clock is formed by an endogenous, cell-autonomous, and self-sustained transcriptional-translational feedback loop (TTL) [30]. In the TTL, the positive limb consists of the activating transcription factors brain and muscle ARNT-like protein 1 (BMAL1; also called ARNTL or MOP3) and circadian locomotor output cycles kaput (CLOCK) or its paralogue neuronal PAS

domain protein 2 (NPAS2; also called MOP4). These transcription factors form BMAL1:CLOCK heterodimers via their PAS domains and bind to enhancer boxes (E-boxes) in promoter regions via basic-helix-loop-helix (bHLH) domains. The binding of BMAL1:CLOCK heterodimers to E-boxes results in the transcription of the core clock genes *Period1/2/3* (*Per1/2/3*) and *Cryptochromes1/2* (*Cry1/2*), as well as of so-called *clock-controlled genes* (*CCGs*). Upon translation in the cytoplasm, PERs and CRYs form heterodimers, which bind to and inhibit BMAL1:CLOCK activity and thus ultimately their own transcription. Over time, PERs and CRYs are ubiquitinated and degraded resulting in BMAL1:CLOCK complexes binding again to E-boxes and starting a new cycle of transcription (Figure 1 A). This core TTL generates cycles of approximately 24 hours, which in contrast to most biological reactions maintain their kinetics over a broad range of temperatures (i.e., temperature compensation). Although the TTL is the main loop generating endogenous oscillations, it is fine-tuned and stabilized by auxiliary loops. The most studied auxiliary loop consists of REV-ERBα/β (also called NR1D1/2) and RORα/β/γ (also called NR1F1/2/3) [31, 32]. The binding of BMAL1:CLOCK to E-boxes drives the transcription of REV-ERBα/β and RORα/β/γ. REV-ERBα/β and RORα/β/γ in turn fine-tune the expression of BMAL1, by repressing and activating *Bmal1* transcription, respectively. However, other auxiliary loops formed by E4 promoter-binding protein (E4BP4, also called NFIL3) and D-box albumin promoter binding protein (DBP) or DEC1/2 (also called SHARP2/1) have been characterized [33-35]. The rhythms of clock genes are superimposed to a large fraction of the genome since E-boxes and other circadian regulatory elements exist in the promoters of most genes. Indeed, over 80 % of protein-coding genes in primates display daily oscillations in at least one tissue [36].

1.2.3 Hierarchical organization of the circadian system

Circadian clocks are present throughout the body. However, they must be coordinated to allow synchrony with the environment as well as within and between tissues. To this end, the circadian system is organized in a hierarchical manner with the master pacemaker, the suprachiasmatic nucleus (SCN), at the top of the hierarchy [37, 38]. The central role of the SCN as a master pacemaker of the circadian system was initially demonstrated in lesion studies. In rats, bilateral SCN lesion results in arrhythmic locomotor and drinking behavior and blunted rhythms of endocrine signals such as corticosterone [39, 40]. Further, transplantation experiments evidenced that SCN grafts in SCN lesion animals restored behavioral rhythms and that the period of restored locomotor activity rhythms reflects the period of the initial graft rhythms [37]. The SCN consists of two nuclei comprised of densely packed neurons located in the ventral

hypothalamus, directly above the optic chiasm [41]. In mice, each nucleus is comprised of approximately 10,000 neurons, which are predominantly GABAergic. Anatomically, the SCN divides in “core” and “shell” subregions characterized by distinct neuropeptide expression patterns. Whereas the core comprises vasoactive intestinal peptide (VIP) and gastrin-releasing peptide (GRP) neurons, the shell contains mainly arginine vasopressin (AVP)-expressing cells [42]. The core receives direct light input via the retinohypothalamic tract (RHT) from intrinsically photosensitive retinal ganglion cells (ipRGCs) in the eye. The SCN then synchronizes subordinate clocks in the brain and the periphery via neuronal projections of the autonomic nervous system (ANS), hormones (e.g., melatonin and glucocorticoids) or via the regulation of body temperature and behavior, notably locomotor activity and food intake (including reward-related feeding) [43-45]. Importantly, the SCN receives feedback from different brain regions and peripheral tissues, which stabilizes the circadian system (Figure 1 B).

1.2.4 Entrainment of circadian clocks

The endogenous circadian rhythm (i.e., internal time) must be synchronized to the environment (i.e., external time). This process is referred to as entrainment and is essential as most endogenous circadian rhythms are not exactly 24 hours [46]. Thus, their phase must be adjusted via environmental stimuli, called *Zeitgebers* (German: ‘time giver’). Since *Zeitgebers* affect and adjust the circadian system, circadian time points are based on *Zeitgeber* times (ZT) with ZT0 corresponding to the beginning of the light phase (i.e., ‘lights on’). Light is the strongest *Zeitgeber* of the circadian system and mainly signals to the SCN. The SCN in turn can either directly influence peripheral clocks via neuronal and hormonal routes or indirectly by influencing behavior [47, 48]. In this vein, the SCN dictates rest-activity cycles, which then drive the rhythmic exposure of the organism to *Zeitgebers* such as the LD cycle, food, or temperature. This rhythmic exposure to *Zeitgebers* can synchronize peripheral clocks. For instance, liver, pancreas, muscle, adipose tissues and non-SCN brain areas (e.g., amygdala and hippocampus) are entrained via metabolic signals from food [49, 50]. Peripheral clocks in turn can influence the SCN via hormonal and metabolic signals. This feedback to the SCN fine-tunes and stabilizes the circadian network. Thus, the entrainment of circadian clocks is a complex, reciprocal process between *Zeitgebers*, the SCN and peripheral clocks (Figure 1 C). Although this bidirectional crosstalk enables stability of the circadian system, it also signifies that disrupting either the SCN, *Zeitgebers* or both will ultimately affect the entire system and thereby perturb body homeostasis.

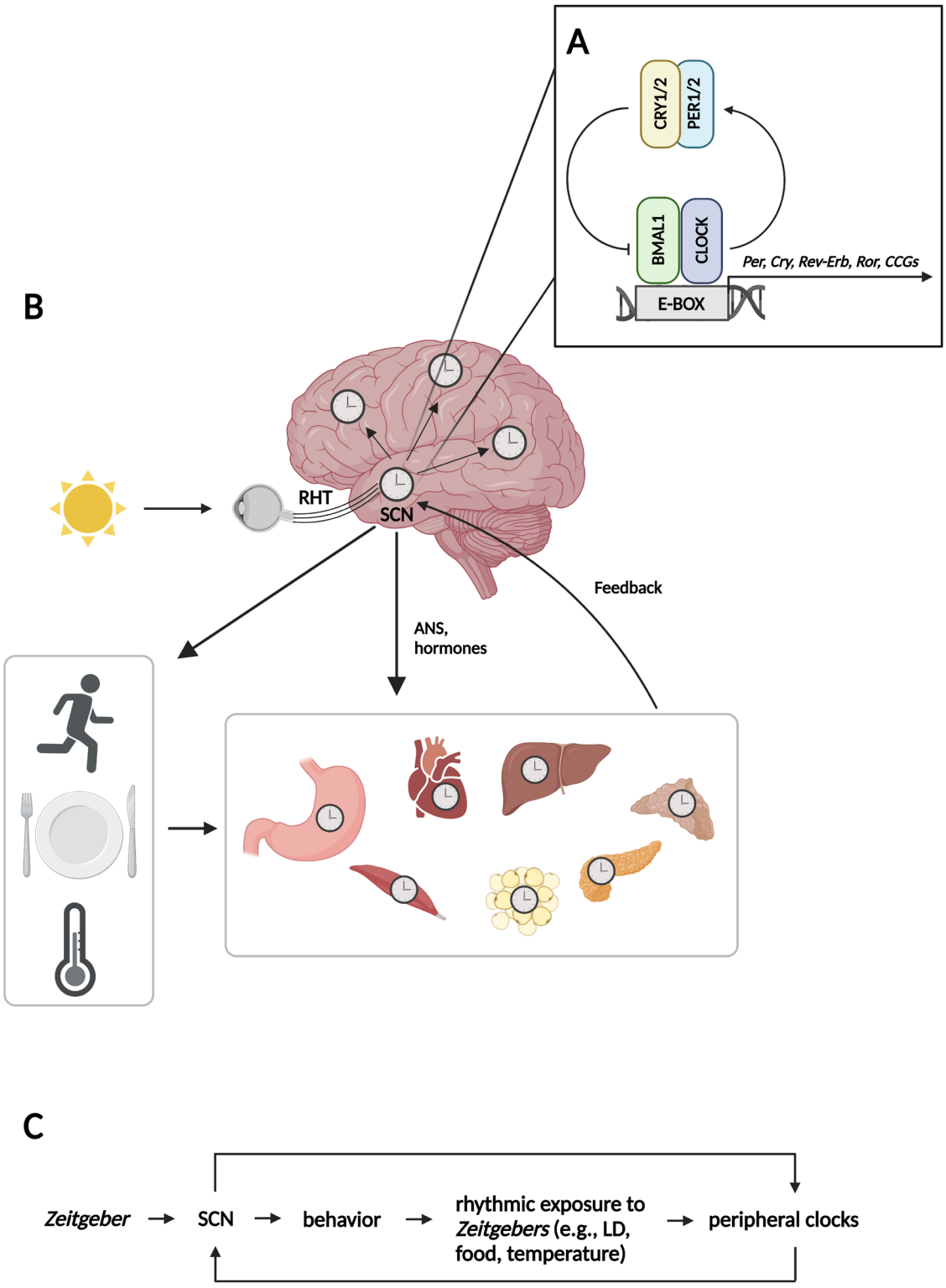

Figure 1. The circadian system in mammals. (A) The molecular clock. In nearly every cell of the body, including in the SCN and peripheral tissues, resides a molecular clock. This molecular clock is formed by a TTL. The positive limb of the TTL consists of the transcription factors BMAL1 and CLOCK, which heterodimerize and bind to E-box elements in promoter regions. This results in the expression of PERs, CRYs and CCGs. PERs and CRYs heterodimerize in the cytoplasm and bind to and inhibit BMAL1:CLOCK activity and hence their own transcription (negative limb). Over time, PERs and CRYs are degraded resulting in BMAL1:CLOCK heterodimers starting a new cycle of transcription. (B) The hierarchical organization of the circadian system. In mammals, light is the strongest *Zeitgeber*. Light information reaches the iPRGCs in the retina and is then transferred to the SCN through the RHT. The SCN is the master pacemaker

and synchronizes subordinate clocks in the brain and periphery via the ANS, hormones or via the regulation body temperature and behavior (notably locomotor activity and food intake). In this manner, subordinate clocks are synchronized with environment and amongst each other. Peripheral circadian oscillators generate outputs that feedback to the brain, further stabilizing the circadian system. (C) Schematic representation of the entrainment of circadian clocks. The bidirectional crosstalk confines stability but also signifies that disrupting one component will ultimately affect the entire circadian system thereby altering body homeostasis. Created with BioRender.

1.3 Circadian regulation of mood and metabolism

The circadian clock is present in virtually all cells of the body and regulates gene expression in a tissue-specific manner. It is therefore not surprising that the circadian system regulates a wide range of physiological, behavioral, and psychological functions, including mood and metabolism. In healthy individuals, a circadian pattern in subjective mood as well as in appetite and hunger has been reported [51-53]. Similarly, neural networks associated with mood and affectivity, including the limbic system and the hypothalamic-pituitary-adrenal (HPA) axis, are all subject to circadian regulation [54, 55]. Moreover, the expression of numerous metabolic enzymes/transporters/receptors is rhythmic and circadian oscillations in food-regulating brain regions including the arcuate nucleus (ARC), the ventromedial hypothalamus (VMH) and the dorsomedial hypothalamus (DMH) have been reported [56].

The link between the circadian clock, mood and metabolism is further strengthened by findings of circadian dysregulation in metabolic and affective disorders. Individuals suffering from MDD display dampened locomotor activity rhythms as well as reduced amplitudes of body temperature and hormone rhythms (e.g., cortisol and melatonin) [57-59]. On the molecular level, a post-mortem human brain study reported dampened circadian gene expression rhythms in mood-regulating brain areas including the nucleus accumbens (NAc) and the amygdala in patients suffering from MDD [55]. In obese individuals, altered hormone secretion and body temperature rhythms and a loss of daily rhythms in glucose and insulin sensitivity have been reported [60, 61].

Interestingly, human data points towards an association between the master pacemaker of the circadian system, the SCN, and both mood and metabolic disorders. Post-mortem studies have found altered neurotransmitter and/or receptor expression in the SCN of individuals who suffered from mood disorders. For instance, increased GABA expression, altered melatonin receptor abundances and increased numbers of AVP-expressing neurons were found in MDD patients [62-64]. Equally, a post-mortem human study found altered numbers of AVP- and VIP-

expressing neurons as well as astroglia in the SCN of type 2 diabetes patients, indicating a potential involvement of the SCN in the disease [65].

The beneficial effects of chronotherapeutic interventions, aiming at stabilizing endogenous circadian rhythms, in affective and metabolic disorders provide another line of evidence for a link between circadian rhythms, mood and metabolism. For instance, chronotherapeutic interventions (e.g., bright light therapy, social rhythm therapy, agomelatine) have been shown to improve symptomatology in patients suffering from affective and/or anxiety disorders [66-69]. Similarly, time-restricted eating and time-restricted feeding, which restrict food intake to the active phase was shown to be successful in alleviating metabolic symptoms in humans and mice, respectively [70-72]. The beneficial effects of chronotherapeutic interventions in affective and metabolic disorders suggest that circadian disruptions might be a common underlying biological mechanism but do not allow to draw definitive conclusions about causality.

Indeed, despite an evident role of the circadian system in mood and metabolism, the question whether blunted physiological rhythms are a predisposing factor for, or a consequence of these disorders remains to be disentangled. To establish a causal role of the circadian clock in metabolic and mood disorders, different models of circadian disruptions have been established and studied.

1.4 Origin and models of circadian disruptions

Circadian rhythms are manifestations of endogenous feedback loops of clock genes, which are entrained to the environment by *Zeitgebers*. Given this, disruptions of the circadian system can be caused genetically and/or environmentally. Circadian disruptions have been linked to pathology and although the mechanisms explaining how genetic and environmental circadian perturbations ultimately lead to pathology remain largely unknown, two expert reviews propose mechanistic concepts including external desynchronization, internal desynchronization at different levels of physiology, reduced rhythm amplitude and changes in sleep architecture [73, 74]. For instance, circadian clocks throughout the body are differentially affected by *Zeitgebers* and disruptive *Zeitgeber* inputs result in the loss of phase coherence within and between tissue clocks (internal desynchronization), altering physiological homeostasis further bringing about various diseases. Some of the described mechanistic concepts will be explored in this thesis in models of genetic and environmental circadian disruptions.

1.4.1 Genetic disruptions of the circadian system

Circadian disruptions can occur due to genetic alterations in clock genes. In humans, genetic polymorphisms mapping to clock genes have been associated with morningness–eveningness preference or circadian rhythm sleep disorder, demonstrating their impact on circadian timing [75]. Importantly, certain human single nucleotide polymorphisms (SNPs) have been associated with disease, including psychiatric and metabolic disorders. For instance, a SNP in the *CLOCK* gene (rs1801260) was significantly associated with increased manic episodes in BP [76, 77], as well as with increased BMI [78]. Moreover, genome-wide association studies (GWAS) have provided compelling evidence of the remarkable overlap between genetic risk loci for major psychiatric disorders and genetic determinants of BMI [79]. As explored below, genetic disruptions of circadian clocks have been more extensively studied in animals, using different strategies.

KO vs. KD

A standard approach for studying the circadian clock involves deleting a clock gene i.e., knockout (KO) and analyzing the phenotypes that ensue. Most of the clock genes are present as paralog pairs (e.g., *Cry1* and *Cry2*), which to some extent can compensate for each other's loss. Thus, single gene KO of most clock genes has shown compensation [80-83]. However, *Bmal1* is a non-redundant clock gene whose single gene KO alone is sufficient to abrogate the functioning of the molecular TTL resulting in arrhythmicity in mice [84]. In contrast to KO, knockdown (KD) of a clock gene is a genetic strategy to study its role without entirely abolishing circadian function and thus might represent a more clinically relevant approach. Landgraf and colleagues, for instance, examined the behavioral and metabolic effects of SCN rhythm disruption by SCN-specific *Bmal1* knockdown (SCN-*Bmal1*-KD) [85]. Given that this thesis employed the genetic approach of Landgraf and colleagues, the advantages of this model and the earlier discoveries are covered in detail below.

Full body vs. local

The investigation of full body clock mutants, i.e., animals lacking a functional molecular clock in every cell of the body, is relevant. However, it often yields a vast range of phenotypes highlighting a significant incentive to investigate the contribution of circadian clocks in a more tissue-specific manner. A primary approach is to lesion a tissue and analyze the resulting

phenotypes. For instance, SCN lesions in rodents do not only result in arrhythmicity but also in reduced behavioral despair and metabolic disturbances including increased fat accumulation, a loss in circadian energy metabolism as well as insulin resistance [39, 40, 86, 87]. However, in addition to perturbing cellular circadian rhythms, brain lesions also eliminate cells and critical neuronal connections, including light input pathways to areas that are involved in regulating other functions than circadian rhythms [88]. Therefore, more targeted approaches have been established to study the role of clock proteins in specific tissues. For instance, tissue-specific KOs of clock genes were achieved using the Cre-lox system. In this system, transgenic mice are created to produce a Cre recombinase transgene under the control of promoters that are specific to the tissue of interest, enabling a tissue- or cell-specific deletion of the targeted clock gene [89]. Another strategy to investigate the role of local cocks is to inject a clock gene-targeting shRNA into a specific brain region. This approach was used, for example, by Landgraf and colleagues, who injected *Bmal1* targeting shRNAs into the SCN of mice to downregulate SCN rhythms [85].

Homozygous vs. heterozygous

An alternative approach to using homozygous clock gene KO mice is the use of heterozygous mice, lacking only one copy of the clock gene. For instance, in contrast to *Bmal1*$^{-/-}$ mice, *Bmal1*$^{+/-}$ mice are healthy under standard conditions e.g., rhythmic behavior, normal weight gain [90, 91]. However, *Bmal1*$^{+/-}$ mice may represent a translational 'circadian susceptibility' model, which upon exposure to an environmental circadian disruption (e.g., shift work) might display adverse health consequences. As explained later, this genetic model was employed in this thesis to examine a potential interaction between a genetic and environmental circadian disruption.

Permanent vs. time point-specific

In contrast to the conventional permanent KO approach, some studies targeted clock genes at a specific time point during development. In these approaches, the clock gene is expressed normally during embryogenesis. For instance, Yang and colleagues investigated the effects of an inducible postnatal global deletion of *Bmal1 (Bmal1*-iKO*)*. Interestingly, many of the adverse health consequences observed in conventional *Bmal1* KO mice (*Bmal1*-cKO) (e.g., reduced lifespan and decreased body weight [84, 92]) were not observed in *Bmal1*-iKO mice [93]. This study helped decipher that some of the phenotypes of *Bmal1*-cKO are a consequence of developmental functions of *Bmal1*, which are not related to its function in the molecular

circadian clock. Moreover, the SCN-*Bmal1*-KD model of Landgraf and colleagues used in this thesis equally eliminates confounds of complete *Bmal1* loss during development since *Bmal1* KD occurs during adulthood [85].

The different genetic manipulations in mice (KO vs. KD; full body vs. local; homozygous vs. heterozygous; permanent vs. time point-specific) have provided valuable models for studying the role of circadian clocks in health and disease. The health consequences of genetic circadian disruptions are further discussed below with particular focus on mental and metabolic health.

1.4.2 Environmental disruptions of the circadian system

In addition to genetic causes of circadian disruptions, environmental alterations can equally perturb the circadian system. In modern society, individuals are frequently exposed to disrupted *Zeitgeber* conditions including shift work, light at night, jet lag, or constant availability of high palatable foods triggering altered feeding behavior (e.g., late night eating). Those conditions promote an uncoupling of external and internal time ultimately favoring the development of many diseases [94]. In particular due to our 24/7 society, there is an increasing proportion of individuals working outside the standard working hours and thus outside their natural active phase. Indeed, approximately 30 % of the working population worldwide is engaged in some form of shift work [95]. Over the last decade, it has become increasingly apparent that shift work is associated with a plethora of adverse health effects. For instance, shift work has been associated with sleep problems [96, 97], mood disorders, such as depression and anxiety [97-99] as well as metabolic disorders including obesity, type 2 diabetes and cardiovascular disease [100-102]. Shift work contributes to pathological outcomes via alteration of *Zeitgebers*. Working schedules of shift workers result for instance in aberrant light exposure, overall reduced as well as shifted and thereby qualitatively compromised sleep, decreased physical activity, or altered food timing – all interfering with normal daily rhythms [73]. Given that research in human subjects is limited in its use for understanding causality and mechanistic underpinnings of the relationship between shift work and adverse health, animal models have been employed to gain further insights. Manipulation of *Zeitgebers* have been used to model shift work in rodents; notably, the use of different light, food, or locomotor activity timings [73]. In line with human findings, murine shift work models reveal an impact of environmental circadian disruptions on metabolism and behavior [73, 103-108]. The mental and metabolic health consequences of environmental circadian disruptions are further explored below.

1.5 Health consequences of genetic circadian disruptions

1.5.1 Mood and anxiety

Several human genetic studies evidence an association between polymorphisms in clock genes and affective or anxiety disorders further indicating an endogenous circadian predisposition for disease. For instance, a polymorphism in the *PER3* gene was shown to affect the age of onset of BP [109]. Moreover, circadian variation in mood in MDD patients was associated with a polymorphism in another circadian gene, *RORA* [110]. Interestingly, a study aiming to generate a predictive model for MDD-to-BD conversion found that eleven SNPs in circadian genes were associated with this conversion [111]. In addition, in the case of anxiety disorders, genetic variants in *PER3* and *ARNTL2* have been linked to the predisposition to these disorders [112, 113]. Lastly, an evening chronotype, a circadian feature strongly influenced by genetic variation, has been associated with adverse mental health in humans [114].

Further causal evidence for a genetic circadian disruption in affective and anxiety disorders stems from animal models of clock gene mutations. For instance, transgenic mice carrying a variant in the human *PER3* gene associated with seasonal affective disorder exhibit a mild depression-like phenotype [115]. *Rev-erbα*$^{-/-}$ mice display both anxiety-like and mania-like phenotypes when exposed to a stressful environment [116]. Further, KD of *Per1* and *Per2* in the NAc of wild type (WT) mice produces anxiety-like behavior suggesting a causal role for the regulation of anxiety by core clock components in the NAc [117]. However, KD of *Rev-erbα* in the same brain area leads to decreased anxiety-like behavior, suggesting that the specific clock gene manipulated may affect the resulting behavioral phenotype [118]. Nevertheless, it is worth noting that the circadian phenotypes of *Per1/2* double KO and *Rev-erbα* double KO mice differ, implying that the behavioral outcomes may be influenced by the overall circadian phenotype resulting from the clock manipulation rather than the specific clock gene targeted [82, 119]. Moreover, these findings highlight the important role that local clocks play in regulating behavior and suggest that clocks in different brain areas may have distinct functions. In line with this, arrhythmicity in the NAc and PAG, two brain regions involved in the reward circuitry, is associated with helpless behavior in mice, proposing that disruption of local clocks in mood-regulation brain regions is associated with depression-like behavior [120]. Not only region-specific but also cell type-specific manipulations of the molecular clock have been investigated with respect to the development of affective and anxiety disorders. For instance, loss of *Per2* in

glial cells of mice reduces anxiety-related behavior and behavioral despair [121]. Moreover, deletion of *Bmal1* exclusively in cortical neurons results in depression-like behavior [122].

As highlighted above, genetic approaches have been increasingly used to assess the role of tissue- or cell type-specific clocks in regulating mood and anxiety. One brain area that has been of particular interest is the master pacemaker, the SCN. Bilateral lesion of the SCN in rats result in reduced immobility in the forced swim test (FST), indicating a protective effect of SCN lesion in the induction of behavioral despair [86, 123]. However, testing during these studies was conducted during the inactive phase when immobility time in the FST may be higher and lesioning the SCN could ameliorate the diurnal variation in this behavior [124]. Regarding the regulation of anxiety-like behavior by the SCN, a study demonstrated that SCN lesions have no effect on anxiety-like behavior in mice that experienced or did not experience social defeat. This study suggested no role of the SCN in regulating anxiety-like behavior [125]. However, drawing definitive conclusions about the role of the SCN in mood regulation based on these SCN lesion studies is limited because behavioral tests were only conducted at a single time point. As a result, there is a lack of information about the behavior of SCN-lesioned animals throughout the day. Additionally, the anatomical connections are disrupted by the lesion, which further complicates the interpretation of results. Nonetheless, more recent studies have investigated the role of the SCN in mood regulation in a neuroanatomically intact system. For instance, disruption of the SCN via optogenetics results in dampened locomotor activity rhythms in mice, which directly correlate with increased anxiety-like behavior [126]. Further, SCN-selective ablation of *Sox2*, a transcription factor regulating *Per2*, results in anxio-depressive-like behavior in mice [127].

1.5.2 Metabolism

Similar to affective and anxiety disorders, multiple genetic studies in humans indicate that there is an association between variations in clock genes and metabolic disorders. For instance, genetic association studies demonstrate that a *CLOCK* polymorphism is a risk factor for diabetes in humans, which depending on the *CLOCK* haplotype is associated with a low or high prevalence of metabolic syndrome [128, 129]. Two *BMAL1* haplotypes have been linked to type 2 diabetes and a missense polymorphism in *PER3* has equally been associated with type 2 diabetes [130, 131]. Further, an evening chronotype, a trait that is strongly influenced by genetic variation, has been linked with metabolic disorders in humans [132].

Genetic studies of clock mutations in rodents have been pivotal in further deciphering the role of circadian disruption in metabolism. Global *Bmal1* KO mice display impaired glucose metabolism, insulin hypersensitivity, decreased fat and muscle mass as well as a decreased lifespan [84, 92, 133]. Moreover, male but not female *Per1/2/3* triple mutant mice display an increased vulnerability to high-fat diet (HFD), indicating sex differences [134]. Systemic KO rodent models do not allow drawing conclusions about the role of specific tissue clocks in energy homeostasis as all tissue clocks including the SCN clock are affected. Peripheral tissues, like liver, pancreas, stomach, muscle, or adipose tissue, orchestrate food intake and metabolic processes. Therefore, clock mutations in peripheral metabolically active organs have been investigated. Liver-specific deletion of *Bmal1* in mice leads to hypoglycemia during fasting and excessive glucose disposal [133]. Moreover, pancreatic deletion of *Bmal1* leads to hypoinsulinemia and impairments in glucose tolerance [135]. Muscle-specific loss of *Bmal1* impairs glucose import and adipose tissue clock ablation leads to hyperphagia and obesity [136, 137]. Surprisingly, intestine-specific *Bmal1* ablation protects against HFD-induced obesity [138], potentially by decreasing intestinal glucose absorption and altering systemic glucose homeostasis [139]. Beyond tissue-specific clock mutants, cell type-specific clock mutants have been characterized. Many appetite- and energy expenditure-regulating neuronal populations reside within the hypothalamus, making those cell populations of particular interest in the investigation of cellular clocks in metabolic health. Disrupting clock function in dopaminergic neurons of ventral tegmental area (VTA) in mice abolishes hedonic appetite rhythms [140]. Further, the clock in Agouti-related peptide (AgRP)-expressing neurons plays a crucial role in hepatic glucose metabolism and *Bmal1* ablation in Sf1 neurons of the VMH alters brown adipose tissue (BAT) function, thermogenesis, and energy expenditure [141, 142]. Cellular populations other than neurons have also been investigated. For instance, *Bmal1* deletion in astrocytes alters glucose homeostasis in mice, which is accompanied by an initial weight increase followed by weight loss due to premature aging [143]. Again, evidence suggests that clock ablation can have protective effects; microglia-specific KO of *Bmal1* is protective against HFD-induced obesity in mice [144].

The role of the master pacemaker of the circadian system in regulating metabolism has been of great interest, similar to its involvement in mood and anxiety. The SCN regulates brain regions involved in food regulation, including the paraventricular nucleus (PVN) and the ARC, but also acts on systemic metabolism through endocrine factors [145]. Rodent models with SCN lesions exhibit a loss of rhythmic food intake, weight gain, and a diabetes-like phenotype [87], but as mentioned earlier, lesion models have many limitations, highlighting the necessity for targeted genetic approaches. For instance, ablating *Bmal1* in the SCN results in weight gain and loss of peripheral clock coordination in mice [146]. In contrast, limiting *Bmal1* expression to the SCN is

sufficient to restore the rhythms of most circulatory metabolites, supporting a role of the master pacemaker in governing metabolic signals [147].

1.5.3 Metabolic-Mood comorbidity

As discussed above, genetic disruptions of the circadian system are associated with both, mood and metabolic disorders. Hence, perturbed circadian clocks have been suggested as modulators of metabolic-mood comorbidities [22]. Evidence in human and animal studies further support such a role of the circadian clock. For example, a SNP in the *CLOCK* gene (rs1801260) was significantly associated with enhanced manic episodes in BP and increased BMI [76-78]. Moreover, GWAS have presented convincing evidence of an extensive overlap between genetic risk loci for major psychiatric disorders and genetic loci for BMI [79]. Further, mice expressing a dominant-negative *Clock* variant (*Clock*Δ19) exhibit mania-like behavior, as well as disrupted feeding patterns, hyperphagia, hyperglycemia and obesity [148-150]. *Cry1/2*$^{-/-}$ mice display increased anxiety-like behavior, manifested by restlessness and compulsive behavior, and exhibit a loss of metabolic rhythms together with insulin resistance [151-153]. Furthermore, SCN lesions result in reduced behavioral despair, a loss of rhythmic food intake as well as weight gain and a diabetes-like phenotype [86, 87, 123]. These studies suggest a role for the SCN in generating metabolic-mood comorbidity. However, metabolic and behavioral assessments of SCN-lesioned mice were conducted in distinct studies and SCN lesions result in a disruption of neuroanatomical connections. To circumvent these issues, Landgraf and colleagues downregulated *Bmal1* expression in the SCN of adult mice (SCN-*Bmal1*-KD) and assessed behavioral and metabolic phenotypes within the same mouse [85]. This approach has numerous advantages as it allows studying the role of SCN rhythms in physiology using an animal model with a functionally developed, anatomically intact brain and light input pathways, where molecular rhythms in all non-SCN brain areas and peripheral organs remain intact. Since KD of *Bmal1* occurs during adulthood, it also eliminates confounds of complete *Bmal1* loss during development. Importantly, SCN-*Bmal1*-KD animals in this study exhibit depression- and anxiety-like behavior together with an increased weight gain [85]. However, a comprehensive metabolic characterization of these mice is still pending to provide a better understanding of the metabolic-mood comorbidity resulting from downregulated SCN rhythms. Moreover, it is yet to be determined which subordinate body clocks mediate these comorbid deficits. Finally, it is worth noting that only the acute effects of downregulated SCN rhythms on behavior and metabolism have been evaluated thus far. Therefore, it is remains to be investigated whether

the comorbid behavioral and metabolic outcomes resulting from chronic downregulation of SCN rhythms differ from those resulting from acute downregulation.

1.6 Health consequences of environmental circadian disruptions

1.6.1 Mood and anxiety

To assess the impact of environmental circadian disruptions on mood and anxiety, numerous human studies in shift workers have been conducted. A plethora of epidemiological studies indicate an association between shift work and poor mental health [154-156]. For instance, shift workers suffer more frequently from depressive and anxiety symptoms than individuals working under regular working schedules [157]. Further, in a Romanian sample, 26 % and 17 % of shift workers were affected by depression and anxiety, respectively [158]. A meta-analysis of 11 studies concluded that compared to daytime workers, night shift workers are 40 % more likely to develop MDD [98]. Similarly, a meta-analysis of 7 longitudinal studies concluded that shift workers, especially women, are more likely to experience mental illness, particularly depressive symptoms [99]. This study suggests that there might be sex differences in the health implications of shift work. Although less studied than shift work, jet lag has also been associated with increased prevalence of affective and anxiety disorders. For instance, a study investigating jet lag in five men found that a 7-hour eastward shift results in significantly disrupted sleep and elevated anxiety and depression scores [159].

Studies in rodents confirm the ability of environmental circadian disruptions to induce altered mood and anxiety phenotypes. Alternations in LD cycles, constant light (LL), light at night, and non-24-hour LD cycles are all used to model shift work using light in mice. These paradigms induce depression-and/or anxiety-like behavior in rodents [103, 105, 160-163]. For instance, exposing mice to a 6-hour phase advance every 3 days leads to enhanced behavioral despair [103]. Equally, 8 weeks of LL increases depression-like behavior in rats and results in a loss of rhythms in locomotor activity, melatonin, and corticosterone [161]. Furthermore, in female Siberian hamsters, 4 weeks of dim light at night (5 Lux) enhances depression-like symptoms [163]. Moreover, exposing rats to cycles of 11 hours light and 11 hours dark induces depression-like behavior [124]. Lastly, McGowan and Coogan observed that mice exposed to alternating LD

cycles mimicking shift work exhibit an increased tendency to stay in the perimeters of the open field, indicating increased anxiety-like behavior [105].

1.6.2 Metabolism

Shift work is linked to mistimed sleeping but naturally also to behavioral rhythm changes (e.g., alterations in eating patterns) all contributing to circadian misalignment and thus ultimately disease. Accordingly, shift work has been repeatedly associated with metabolic disorders [164]. Shift workers evidence higher prevalence of obesity and type 2 diabetes than day workers [165-167]. Shift workers also display higher triglyceride and lower HDL cholesterol [168]. Further, a 5-year follow-up study in female workers found that female employees with persistent rotating shift work exposure have an increased risk of metabolic syndrome [169]. In addition to the long-term consequences of shift work, forced desynchrony protocols have been developed to evidence the immediate effects of circadian environmental disruption. After exposing participants to 10 days of circadian misalignment (28-hour day length cycles), subjects displayed increased glucose and insulin, decreased leptin and a reversed diurnal cortisol rhythm along with elevated blood pressure [170]. Furthermore, studies showed that three days on a night shift schedule are enough to disrupt metabolism in humans. For instance, subjecting individuals to 3 days of stimulated night shift results in altered patterns in the lipidome compared to a day shift schedule [171]. Similarly, following a 3-day stimulated shift work schedule, the majority of metabolites linked to nutrient metabolism dissociate from SCN pacemaker rhythms in humans [172].

Numerous animal models based on altered timing of light, feeding, locomotor activity or sleep have been developed to model shift work and assess its impact on metabolism. For example, under LL, mice display increased food intake, decreased energy expenditure, weight gain and a loss of circadian variation in insulin sensitivity [173]. Another study reported that following dim light at night, mice display an increased weight gain and impaired glucose tolerance, likely resulting from their altered timing of food intake [174]. In a rodent model of simulated night shift (forced activity for 8 hours), glucose rhythms are abolished, and triglyceride rhythms are reversed [108, 175]. Moreover, timed sleep restriction in mice moderately alters locomotion and feeding rhythms and provokes significant disruptions in liver transcriptome rhythms [176]. Equally, housing mice in a 20-hour LD cycle, which is incompatible with their internal timing, results in accelerated weight gain, enhances insulin and leptin levels as well as altered body temperature rhythms [177]. In addition, subjecting female mice to alternating LD cycles (8-hour

phase advance and delay every 3-4 days) results in altered insulin sensitivity during the light phase and shifted glucose tolerance rhythms [178]. Exposing male mice to 8 weeks of rotating light cycles (3 days normal light cycle followed by 4 days of reversed light cycle) promotes weight gain and hepatic lipid accumulation [179]. In addition, chronic LD cycle shifts compromising 6-hour advances twice weekly, induces obesity, glucose intolerance, white adipose fat accumulation and alterations in the expression of metabolic genes in the liver of mice [180]. It should be noted that exposure of female mice to weekly alternating LD cycles (12-hours shifts) has only modest effects on metabolism [181]. This highlights that differences in shift work paradigm, sex and/or rodent strain might have an impact on the metabolic outcomes following shift work conditions. To assess if shift work has a sex-specific effect on metabolic outcomes, a systematic characterization and comparison of the metabolic phenotypes of male and female mice following shift work conditions is required.

1.6.3 Metabolic-Mood comorbidity

As discussed in the previous two chapters, numerous studies evidence that environmental disruptions of the circadian system bring about disturbances in mood and metabolism. This proposes that environmental circadian disruptions might represent a potential mechanism underlying metabolic-mood comorbidities. Crucially, to support this notion, a few humans and rodent studies have assessed metabolic and mood outcomes within the same organism following shift work conditions. For instance, shift work was associated with concurrent adverse metabolic and mental health outcomes in a large population-based study [182]. Further, in a shift work paradigm based on sleep deprivation, male rats show features related to depression and anxiety as well as increased weight gain [102]. Similarly, when kept under short photoperiods mimicking shift work light conditions, diurnal fat sand rats (*Psammomys obesus*) display concomitant mood and metabolic abnormalities [103]. Nonetheless, the so-far conducted studies exploring metabolic-mood comorbidities following shift work conditions are sparse and performed limited behavioral and/or metabolic measurements. Therefore, a detailed metabolic and behavioral characterization in the same animal following shift work conditions remains to be conducted.

Importantly, epidemiological studies have found sex differences in the shift work-associated risk of mental and metabolic disorders [99, 183]. For instance, amongst shift workers, particularly women are at increased risk for adverse mental health and depression [99]. Similarly, for shift work-associated adverse metabolic outcomes, sex differences have been reported although

results have been conflicting. For example, some epidemiological studies showed a stronger and others a weaker association between shift work and metabolic syndrome in women compared men [184-187]. In rodent studies, male mice subjected to shift work-mimicking conditions exhibit metabolic alterations [177, 179, 180]. In contrast, exposure of female mice to alternating light cycles has only modest metabolic effects [181]. Similar to epidemiological studies, these rodent studies may suggest a sexual dimorphism in shift work-associated metabolic dysfunctions. Interestingly, in a population-based study of 277,168 workers in the UK biobank, shift work was associated with poor mental and metabolic outcomes. However, shift work was more strongly associated with adverse metabolic health in women compared to men [182], suggesting sexual dimorphism in the development of comorbid metabolic and mental-related perturbations following shift work.

The sex-dependent vulnerability to adverse health following shift work conditions might be explained by sex differences in the circadian system and its response to shift work light conditions. On the anatomical level, sex-specific differences of the circadian system have been characterized – namely differences in SCN morphology, peptide expression, electrical activity as well as gonadal steroid receptor and target site expression (for an extended review see [188]). Moreover, sex differences in the responses to photic input have been reported. Following a light pulse given during the dark phase, female mice display a larger phase shift than males [189]. Further, in *Octodon degus*, a diurnal rodent, females adjust more rapidly to a 6-hour advance of the LD cycle than males [190]. Despite apparent sex differences in the response of the circadian system to shift work light conditions, less than 7 % of circadian phase shift studies in rodents included females, highlighting the demand for the use of both sexes in future shift work studies [191]. Given the inconsistent findings on sex differences in shift-work associated health implications and the tremendous illness-associated burden of metabolic-mood comorbidities [19, 20], there is an unmet need for a systematic investigation of sex differences in the concomitant behavioral and metabolic outcomes following shift work conditions.

1.7 Health consequences of combined genetic and environmental circadian disruptions

The previous chapters provided evidence that genetic or environmental circadian disruptions can lead to the development of mental and/or metabolic disorders. However, it has become apparent – particularly in the field of psychiatric disorders – that pathological states are often a

product of an interplay between genetic and environmental factors (i.e. gene-environment interaction; G×E) rather than merely their independent primary effects [192, 193]. This means that depending on genetic factors, the impact of environmental conditions on pathology can vary (and vice versa). This concept, the so-called diathesis-stress model, originates from the 1960s, and proposes the interaction of the diathesis, a predisposing vulnerability (e.g., genetic), and stress (i.e., environment) [194-196]. Although G×E have been primarily discussed in the context of psychiatric disorders [197], evidence also points towards a role of G×E in modulating the risk of metabolic disorders [198].

1.7.1 The diathesis-stress model in circadian biology

In the field of circadian biology, the diathesis-stress model can be applied by considering genetic disruptions in clock genes as 'diathesis' and circadian environmental disruptions as 'stress'. However, the research on interactions between circadian genetic and environmental disruptions (circadian G×E) remains limited. Some studies have investigated the impact of chronotype, a circadian feature strongly influenced by genetics, on mood or metabolic parameters in shift workers. For instance, among shift workers, late chronotype was associated with greater depressive symptoms compared to morning chronotype [199]. Equally, in shift workers, evening chronotype was associated with greater BMI compared to morning or intermediate chronotypes [200]. Both studies advocate an interplay between circadian genetic and environmental disruptions in the generation of pathological outcomes. In rodents, the interaction of circadian genetic and environmental disruptions in generating metabolic and/or mood phenotypes remains little explored. Pati and colleagues reported that metabolic aberrations following a chronic circadian disruption light paradigm might depend on the molecular clock [201]. However, total *Bmal1* KO mice used in that study are not a useful model to investigate an interaction between a genetic and environmental circadian disruption in triggering pathology, since they already exhibit many drastic adverse health effects without a circadian environmental disruption. Additionally, total *Bmal1* KO mice are not a translational model, since subtle genetic changes (e.g., polymorphisms) are the most likely scenario in the human population. Given this, a milder circadian genetic manipulation in mice e.g., ablation of a single copy of the *Bmal1* gene (*Bmal1*$^{+/-}$) might be a more appropriate and translational model to investigate a potential interaction between a genetic circadian disruption (i.e., *Bmal1*$^{+/-}$) and

an environmental circadian disruption (e.g., shift work) in triggering behavioral and metabolic pathology. Therefore, this approach was implemented in this thesis.

1.8 Summary – Circadian clocks as modulators of comorbidity

The frequent comorbidity of metabolic and mood disorders has led to the term 'metabolic-mood syndrome' [21]. Since circadian clocks control affective and metabolic processes and both, mood and metabolic disorders are often associated with circadian rhythm dysregulation, disruptions in the circadian system have been proposed to be at the root of this comorbidity [22]. The circadian system can be disrupted genetically, by changes in core clock genes, or environmentally, by exposure to altered *Zeitgebers* (e.g., light).

Human and animal studies evidence a contribution of genetically disrupted circadian clocks to comorbid mood and metabolic disorders. Specifically, molecular circadian rhythms in the master pacemaker of the circadian system, the SCN, have been implicated in metabolic-mood comorbidity. Landgraf and colleagues showed that knocking down *Bmal1* expression in the SCN results in helplessness, behavioral despair, and anxiety-like behavior together with an increased weight gain in the same mouse [85]. Nevertheless, a more detailed characterization of the metabolic phenotype is necessary to better define metabolic-mood comorbidity following genetic SCN rhythm disruption. Additionally, it is important to investigate which subordinate body clocks are responsible for these comorbid deficits, and whether the manifestation of behavioral and metabolic phenotypes observed after acute downregulation of SCN rhythms changes during a more chronic downregulation.

In addition to genetic circadian disruptions, environmental perturbations of the circadian system have also been involved in comorbid metabolic and mood disorders. Nevertheless, investigations of the simultaneous occurrence of metabolic and behavioral alterations following shift work conditions remain scarce. Further, shift work studies have mainly focused on male rodents. Since sexual dimorphism is present in a plethora of physiological functions including brain functions, metabolism, and properties of the circadian system [189, 202, 203], the National Institutes of Health (NIH) supports including both sexes in preclinical and clinical investigations [204]. Crucially, research suggests sexually dimorphic shift work-associated mental and metabolic implications – however, the results remain controversial. Given this, a systematic

characterization of sex differences in circadian, behavioral, and metabolic changes following a shift work paradigm is of utmost importance.

As highlighted above, genetic and environmental circadian disruptions can independently lead to comorbid metabolic and mood disorders. However, according to the diathesis-stress model, pathological states are often a product of the interplay between individual genetic vulnerability and environmental factors (G×E). In the field of circadian biology, the interplay between a genetic circadian disruption and an environmental circadian disruption (i.e., circadian G×E) requires further assessment. In particular, the question if an interaction between a genetic and environmental circadian disruption contributes to comorbid behavioral and metabolic phenotypes remains unexplored.

2. Hypotheses

Because of the influence of circadian clocks on almost all bodily functions, including brain and metabolic functions, and the known links between disturbed circadian clocks and mental and metabolic illness, the overarching hypothesis of this thesis was that disruptions of circadian rhythms, either of genetic or environmental origin or due to a combination of both, can lead to deficits of several bodily functions simultaneously. Accordingly, the same affected individual can develop both, metabolic and mental disorders comorbidly (Figure 2).

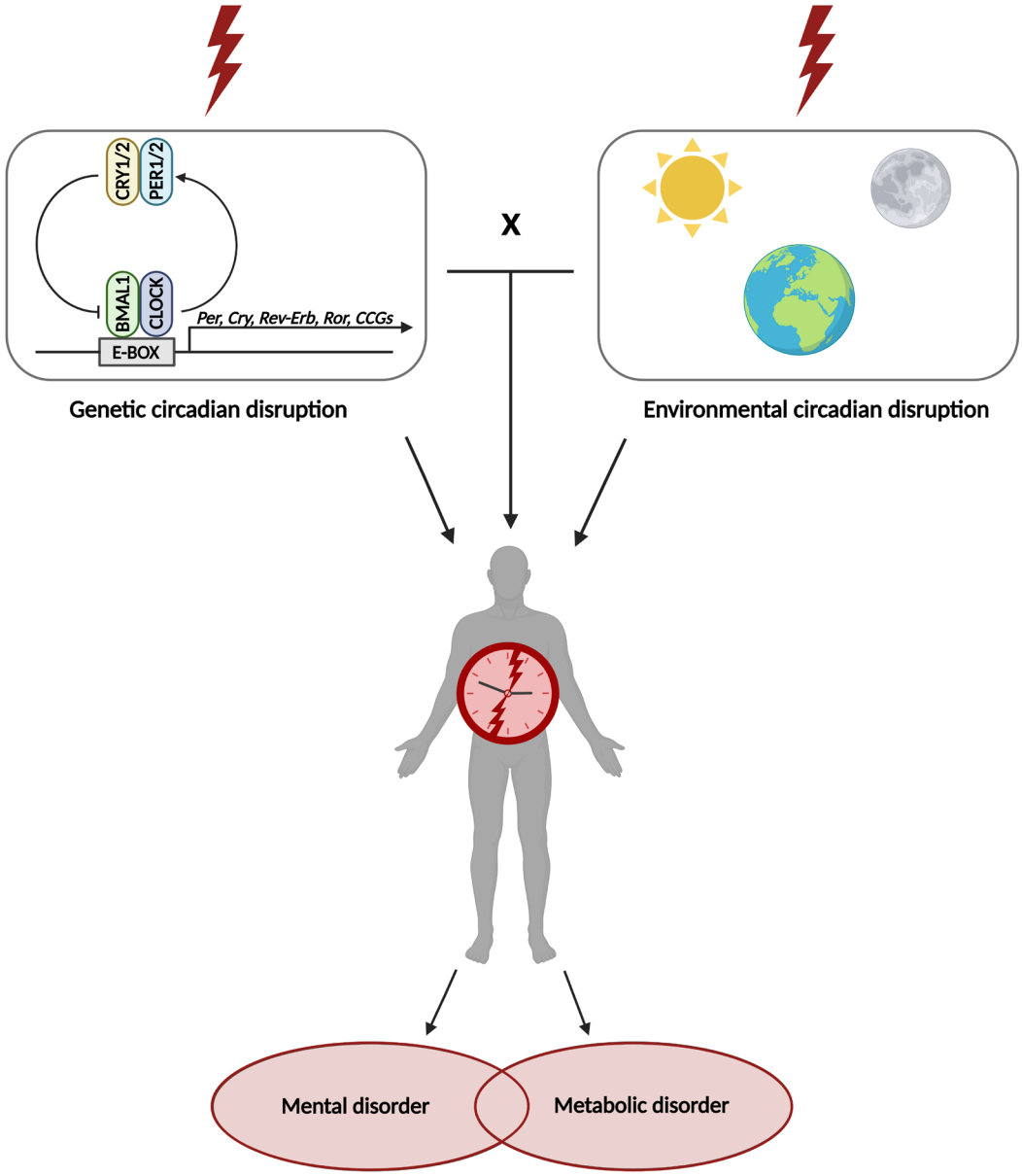

Figure 2. Overarching hypothesis of this thesis. Genetic disruptions of the circadian system (e.g., genetic change in a core clock gene), environmental disruptions of the circadian system (e.g., shift work) or their interaction (x) can perturb circadian clocks throughout the body. Disrupted circadian rhythms bring about the simultaneous development of mental and metabolic disorders. Created with BioRender.com.

To investigate separate aspects of this overarching hypothesis in mice, experiments were conducted in three independent projects.

Project 1 assessed the comorbid behavioral and metabolic outcomes following a genetic disruption of SCN rhythms in male mice.

Project 2 analyzed comorbid behavioral and metabolic outcomes in male and female mice following an environmental circadian disruption, and determined if these outcomes were sex-specific.

Project 3 investigated comorbid behavioral and metabolic outcomes following a combination of both, a genetic and an environmental circadian disruption in female mice.

Each project comprised defined working hypotheses.

Working hypotheses of project 1

(1) In addition to causing behavioral deficits, downregulation of molecular SCN rhythms in male mice also results in several metabolic deficits beyond weight gain in the same animal (Figure 3).

(2) Behavioral and metabolic deficits following downregulation of SCN rhythms in male mice are brought about by changes in subordinate body clocks involved in mood- and anxiety regulation and metabolic functions.

(3) Comorbid behavioral and metabolic outcomes following chronic SCN rhythm downregulation in male mice differ from the outcomes following acute SCN rhythm downregulation.

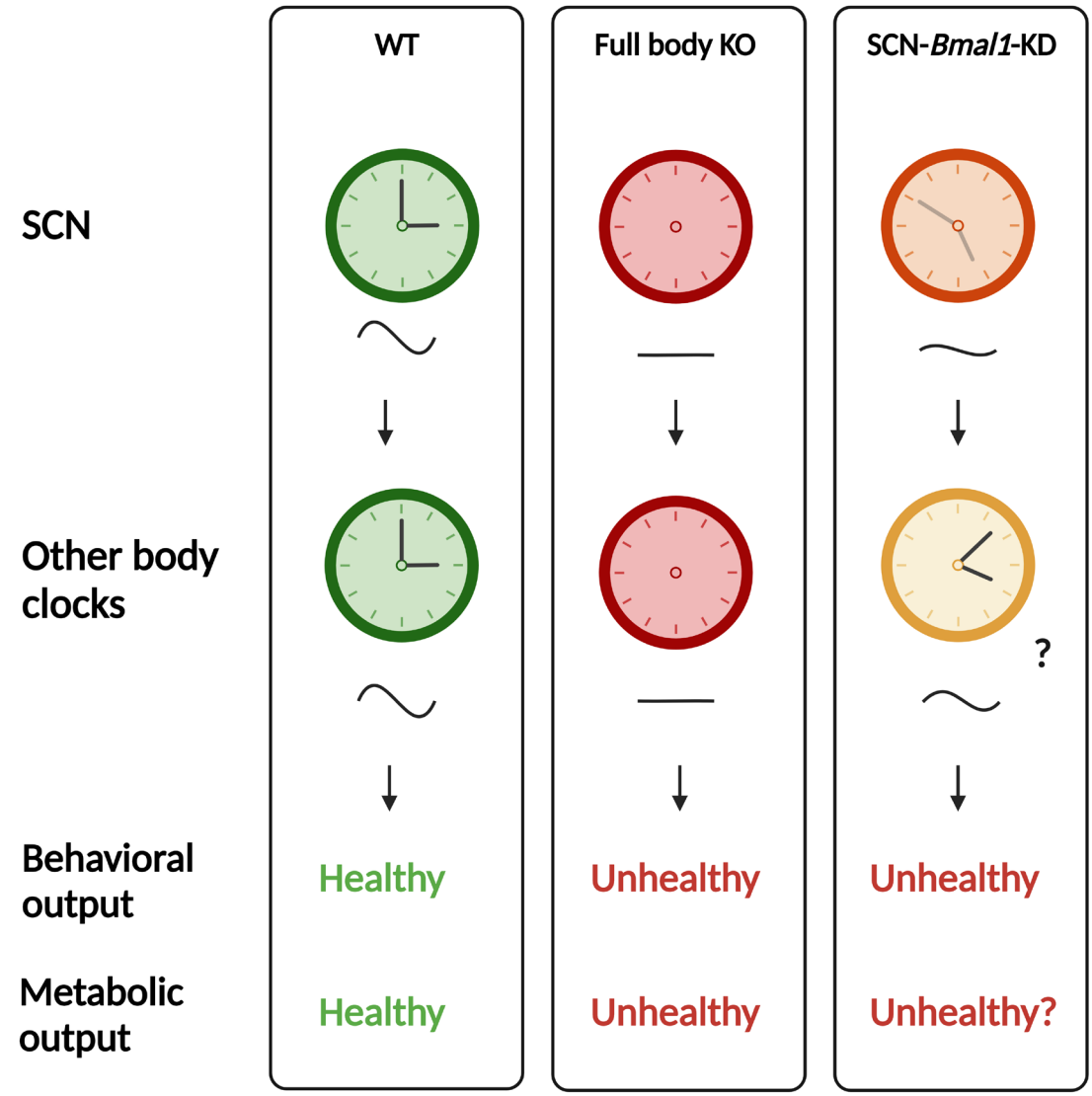

Figure 3. Working hypothesis of project 1. Left column: in WT animals, functional molecular circadian rhythms in the SCN and other body clocks (green clocks) result in a healthy behavioral and metabolic output. Middle column: mice lacking a functional clock in every cell of the body (red clocks), display behavioral and metabolic deficits. Right column: Mice with downregulated SCN rhythms (orange clock) display behavioral deficits and weight gain [85]. Project 1 will further characterize the metabolic phenotype of SCN-*Bmal1*-KD mice to better define the metabolic-mood comorbidity following downregulation of SCN rhythms. It is further hypothesized that downregulated SCN rhythms influence these behavioral and metabolic outcomes by affecting body oscillators involved in mood- and anxiety regulation and metabolic functions (yellow clock). Created with BioRender.com.

Working hypotheses of project 2

(4) Environmental disruptions of the circadian system lead to comorbid behavioral and metabolic deficits in mice (Figure 4).

(5) These deficits are sex-specific.

(6) Environmental disruptions of the circadian system affect molecular TTL rhythms in the SCN, in brain areas crucial for mood- and anxiety regulation, and in peripheral organs governing metabolism.

(7) These changes in molecular TTL rhythms are sex-specific.

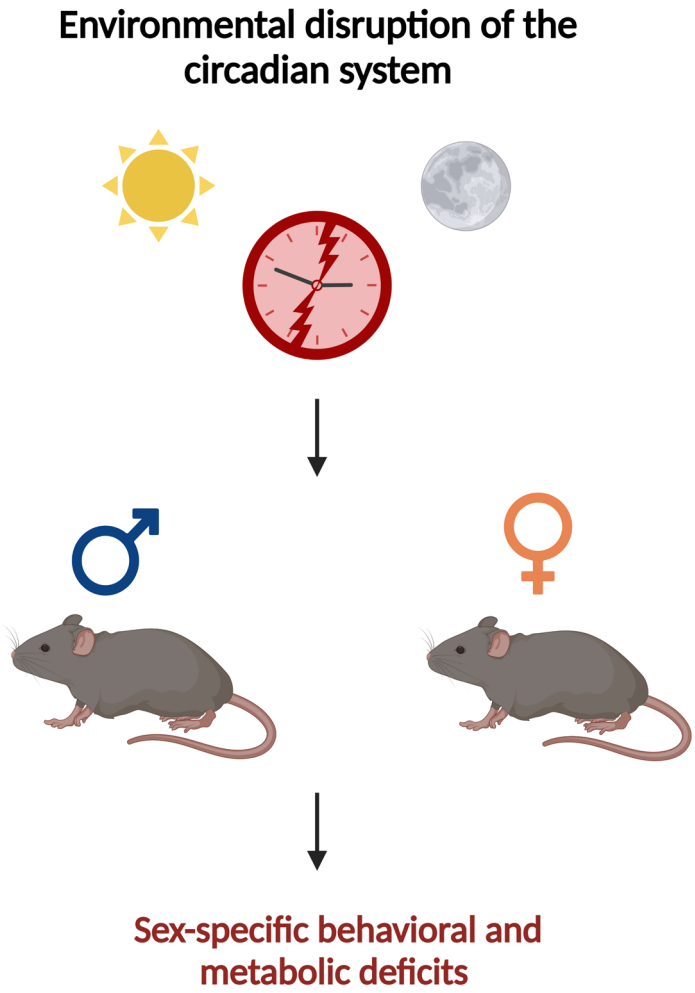

Figure 4. Working hypothesis of project 2. Environmental disruptions of the circadian system bring about comorbid behavioral and metabolic deficits in mice. These deficits are sex-specific. Created with BioRender.com.

Working hypothesis of project 3

(8) Female mice exposed to a combination of both a genetic and environmental circadian disruption, exhibit aggravated comorbid behavioral and metabolic outcomes compared to mice exposed to a single kind of circadian disruption (Figure 5).

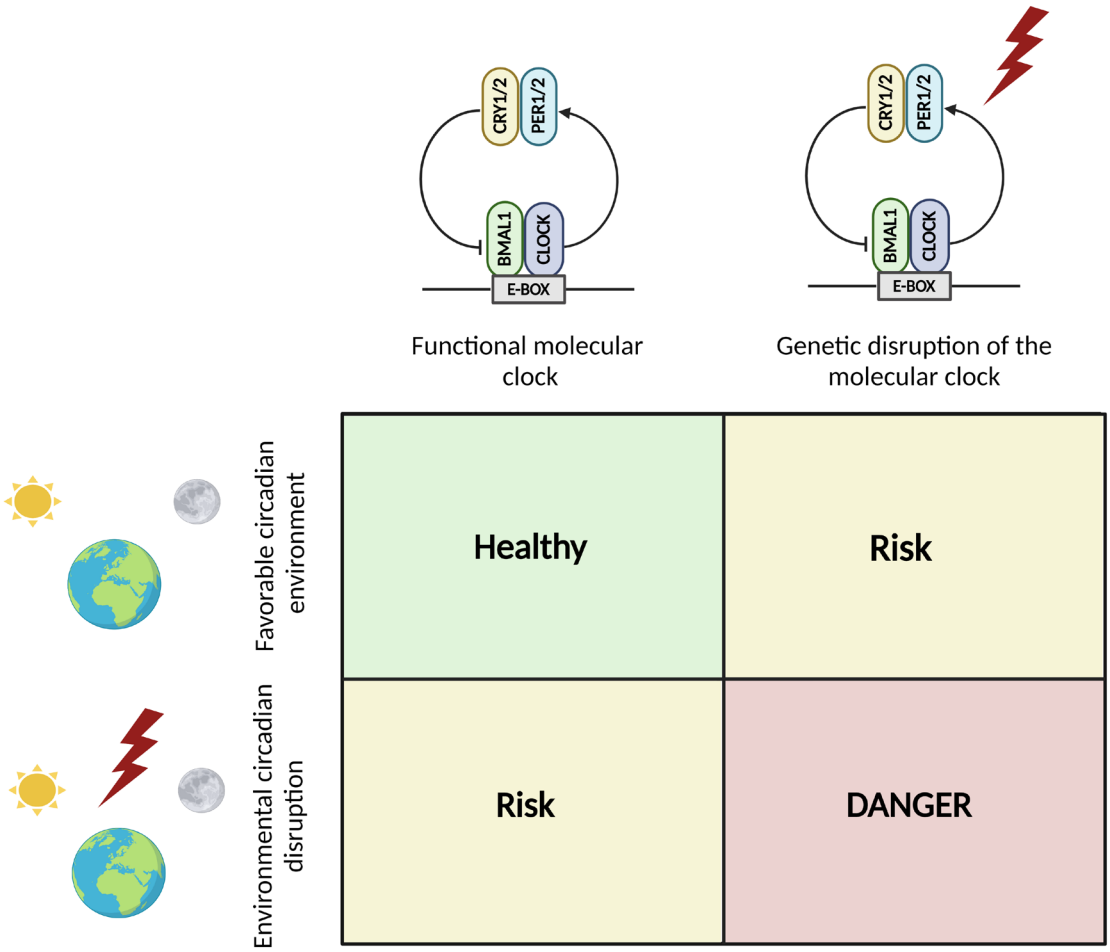

Figure 5. Working hypothesis of project 3. Upper left panel: a functional molecular clock combined with a favorable circadian environment brings about a healthy physiological state (green, 'Healthy'). Upper right panel: Genetic disruption of the molecular circadian clock alone represents a risk factor for comorbid metabolic and behavioral deficits (yellow, 'Risk'). Lower left panel: equally, an environmental circadian disruption as for example during shift work represents a risk factor for comorbid behavioral and metabolic phenotypes (yellow, 'Risk'). Lower right panel: project 3 hypothesizes that genetic and environmental disruptions of the circadian system interact resulting in aggravated comorbid behavioral and metabolic deficits in mice (red, 'DANGER'). Created with BioRender.com.

3. Aims and Objectives

Project 1

To assess if in addition to causing behavioral deficits, downregulation of molecular SCN rhythms in male mice also results in several metabolic deficits beyond weight gain in the same animal (**working hypothesis 1**), the following aims and objectives were defined:

I. Downregulation of molecular SCN rhythms in male mice.

- Stereotactic injection of *Bmal1* shRNAs and control shRNAs into 8-week-old male *Per2*^{Luc} mice generating SCN-*Bmal1*-KD and control mice, respectively.
- Confirmation of injection success by assessment of PER2::LUC bioluminescence rhythms of SCN explants from SCN-*Bmal1*-KD and control animals.

II. Characterization of comorbid behavioral and metabolic dysfunctions in mice following genetic downregulation of molecular SCN rhythms.

- Testing of SCN-*Bmal1*-KD and control animals in several paradigms for mood-, anxiety-, and cognition-related behaviors.
- Monitoring of body weight and food consumption over time of SCN-*Bmal1*-KD and control mice.
- Analysis of circadian rhythmicity and overall levels of locomotor activity and metabolic parameters (i.e., food intake, water intake, respiratory exchange rate (RER), energy expenditure (EE)) of SCN-*Bmal1*-KD and control animals in the metabolic cages.
- Testing glucose and insulin tolerance of SCN-*Bmal1*-KD and control mice.

To assess if behavioral and metabolic deficits following downregulation of SCN rhythms in male mice are brought about by changes in subordinate body clocks involved in mood- and anxiety regulation and metabolic functions (**working hypothesis 2**), the following aims and objectives were defined:

III. Investigation of subordinate circadian oscillators involved in mood- and anxiety regulation and metabolic functions.

- Assessment of PER2::LUC bioluminescence rhythms of PAG and liver explants of SCN-*Bmal1*-KD and control animals.
- Assessment of *Prepro-orexin* (*Ppox*) expression in the lateral hypothalamus of SCN-*Bmal1*-KD and control animals.

To assess if comorbid behavioral and metabolic outcomes following chronic SCN rhythm downregulation in male mice differ from the outcomes following acute SCN rhythm downregulation (**working hypothesis 3**), the following aims and objectives were defined:

IV. Investigation of the consequences of a chronic genetic disruption of molecular SCN rhythms on behavioral and metabolic outcomes.

- Re-assessment of a subset of SCN-*Bmal1*-KD and control animals in the behavioral and metabolic tests at a second time point after stereotactic injection.
- Comparison of the results of the behavioral and metabolic tests conducted at the first and second time point after stereotactic injection.

Project 2

To assess if environmental disruptions of the circadian system lead to comorbid behavioral and metabolic deficits in mice (**working hypothesis 4**) and if those deficits are sex-specific (**working hypothesis 5**), the following aims and objectives were defined.

I. Establishment of a shift work light paradigm and investigation of the adaptation of the circadian system to this paradigm.

- Subjecting one group of mice to alternating light cycles mimicking shift work conditions (shift work). The other group of mice is subjected to standard 12:12 LD conditions (control).
- Using both, male and female mice to investigate sex differences in the behavioral adaptation to the shift work light paradigm by monitoring locomotor activity in the IntelliCage system.

II. Characterization of comorbid behavioral and metabolic outcomes in mice following the shift work light paradigm.

- Assessment of mood- and anxiety-related features in several behavioral paradigms.
- Monitoring of body weight and food intake over time.
- Analysis of circadian rhythmicity and overall levels of metabolic cage readouts (i.e., locomotor activity, food and water consumption, RER, EE).
- Conduction of a glucose and insulin tolerance test.
- Using both, male and female mice to investigate sex differences in the behavioral and metabolic outcomes following the shift work light paradigm.

To address if environmental disruptions of the circadian system affect molecular TTL rhythms in the SCN, in brain areas crucial for mood- and anxiety regulation, and in peripheral organs governing metabolism (**working hypothesis 6**) and if these changes in molecular TTL rhythms are sex-specific (**working hypothesis 7**), the following aims and objectives were defined.

III. Characterization of molecular TTL rhythms of the SCN and subordinate clocks involved in mood- and anxiety regulation and metabolic functions following the shift work light paradigm.

- Assessment of SCN, PAG and liver PER2::LUC bioluminescence rhythms.
- Using both, male and female mice to investigate sex differences in the changes in molecular TTL rhythms following the shift work light paradigm.

Project 3

To address if female mice exposed to a combination of both, a genetic and environmental circadian disruption, exhibit aggravated comorbid behavioral and metabolic outcomes compared to mice exposed to a single kind of circadian disruption (**working hypothesis 8**), the following aims and objectives were defined:

I. Characterization of the circadian system adaptation of female mice with a circadian genetic disruption (*Bmal1*$^{+/-}$) to a shift work light paradigm.

- Subjecting WT and *Bmal1*$^{+/-}$ female mice to alternating light cycles mimicking shift work conditions (WT shift work and *Bmal1*$^{+/-}$ shift work). The other groups of female mice were housed in standard 12:12 LD conditions (WT control and *Bmal1*$^{+/-}$ control).
- Exploring differences in the behavioral adaptation of WT and *Bmal1*$^{+/-}$ shift work mice to alternating light cycles by measuring locomotor activity in the IntelliCage system.

II. Characterization of a circadian G×E in the development of comorbid behavioral and metabolic deficits.

- Assessment of all experimental animals in several behavioral tests for mood- and anxiety-related behaviors.
- Body weight and food consumption monitoring over time.
- Investigation of circadian rhythmicity and overall levels of parameters in the metabolic cages (i.e., locomotor activity, food and water consumption, RER, EE).
- Performance of a glucose and insulin tolerance test.
- Analysis of the interaction effect of a genetic circadian disruption (*Bmal1*$^{+/-}$) and an environmental circadian disruption (shift work) (i.e., circadian G×E) in generating behavioral and metabolic deficits.

4. Materials and Methods

4.1 Animals and Husbandry

4.1.1 Husbandry

Unless otherwise stated, mice were kept in a standard 12:12 LD cycle with lights switched on at 7 a.m. and off at 7 p.m., defined as ZT0 and ZT12, respectively. Food and water were provided *ad libitum*. Mice were group-housed in either type II cages (Tecniplast, 365 x 207 x 140 mm, ground surface: 530 cm^2) or type IV cages (Tecniplast 2000, 612 × 435 × 216 mm, ground surface: 2,065 cm^2). For indirect calorimetry measurements, mice were single-housed. Animal studies were conducted in accordance with the German Animal Protection Law. All efforts were made to reduce animal suffering and minimize animal numbers.

4.1.2 Mouse lines

Per2^{Luc}

In *Per2^{Luc}* mice, the Luciferase gene (*Luc*) has been fused in-frame to the 3' end of the endogenous mouse *Per2* gene. This results in the expression of a PER2::LUC fusion protein allowing the monitoring of circadian oscillations *ex vivo* [205]. *Per2^{Luc}* mice on a C57BL/6J background were kindly provided by Michael Hastings, MRC Laboratory of Molecular Biology, Cambridge, UK and backcrossed as previously described [151]. *Per2^{Luc}* mice were genotyped using the following primers: Forward- CTGTGTTTACTGCGAGAGT (Oligo ID: O2064), Reverse- GGGTCCATGTGATTAGAAAC (Oligo ID: O2065) and Reverse- TAAAACCGGGAGGTAGATGAG (Oligo ID: O2065).

Bmal1$^{+/-}$

In *Bmal1*-fl mice, loxP sequences flank the endogenous *Bmal1* gene, enabling conditional deletion of *Bmal1* in Cre-expressing cells [206]. In EIIa-Cre mice, Cre recombinase is expressed in the early mouse embryo [207]. *Bmal1*-fl mice were kindly provided by Prof. Henrik Oster, University of Lübeck, Lübeck, Germany and EIIa-Cre mice were obtained from The Jackson Laboratory. By crossing *Bmal1*-fl mice with EIIa-Cre mice, *Bmal1$^{+/-}$* mice were generated. These

mice lack one copy on the *Bmal1* gene in the whole body. They were backcrossed for 5 generations from a C57BL/6J background to C57BL/6N by crossing them with Bl/6N mice obtained from Janvier-Labs. *Bmal1*$^{+/-}$ animals and their WT control littermates (*Bmal1*$^{+/+}$) were genotyped using the following primers: Forward- ACTGGAAGTAACTTTATCAAACTG Oligo ID: O3462), Forward – TTTACTGTGCTGCCTGTAG (Oligo ID: O3463), Reverse- CTGACCAACTTGCTAACAATTA (Oligo ID: O3464).

4.2 Experimental timelines

4.2.1 Project 1

All experiments were performed using male *Per2*^{Luc} mice. Only male mice were used as this project was based on and an extension of previous findings obtained in male mice [85]. At the age of 8 weeks, animals were injected either with control shRNAs or with *Bmal1* shRNAs into the SCN. This gave rise to two experimental groups: control and SCN-*Bmal1*-KD mice. To allow for full expression of the virus, all animal experiments started 3 weeks after stereotactic injection. Animals were tested in several behavioral and metabolic tests to assess comorbidity following downregulation of SCN rhythms. To assess whether behavioral and metabolic phenotypes change during a more chronic SCN rhythm downregulation, a subset of animals was re-assessed in several behavioral and metabolic tests at a later time point after stereotactic injection. Animals that underwent the learned helplessness (LH) paradigm were sacrificed and did not undergo further experiments due to the potential long-lasting behavioral and metabolic changes induced by the LH paradigm. Experiments were conducted in two cohorts (Figure 6).

Cohort 1: 12 mice were successfully injected with scrambled shRNAs and 9 animals with *Bmal1* shRNAs (control: n = 12; SCN-*Bmal1*-KD: n = 9). All animals were sacrificed at the end of the experimental timeline, following the LH paradigm.

Cohort 2: 17 mice were successfully injected with scrambled shRNAs and 12 mice with *Bmal1* shRNAs (control: n = 17; SCN-*Bmal1*-KD = 12). 8 control animals and 3 SCN-*Bmal1*-KD were sacrificed in week 8/9, following the LH paradigm. Thereafter, 9 control and 9 SCN-*Bmal1*-KD animals underwent the remaining behavioral and metabolic tests.

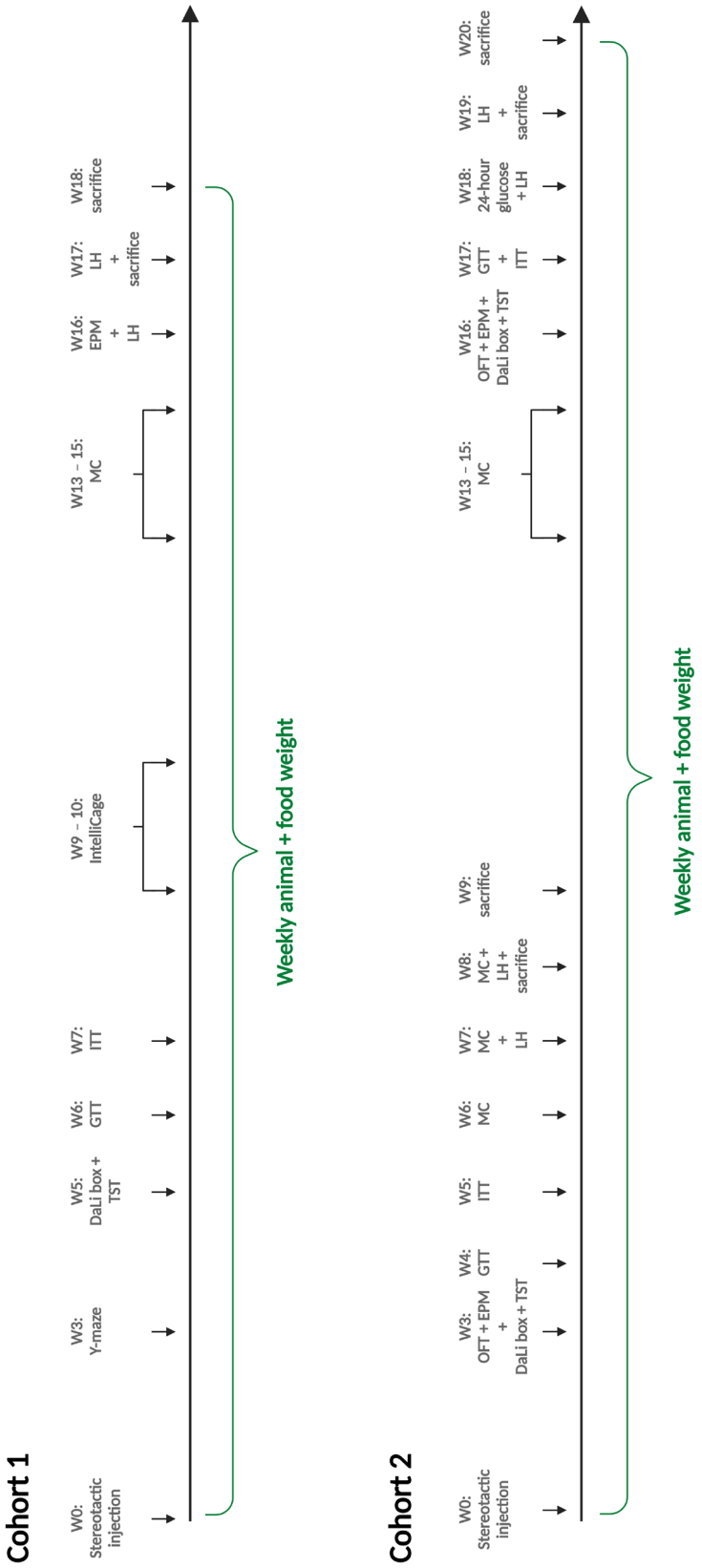

Figure 6. Timelines for the two animal cohorts of project 1. 8-week-old male *Per2*^{Luc} were injected at week 0 (W0). Thereafter, a set of behavioral and metabolic experiments were carried out. Body and food weight were recorded weekly. DaLi box = dark-light box; EPM = elevated plus maze; GTT = glucose tolerance test; ITT = insulin tolerance test; LH = learned helplessness; MC = metabolic cages; OFT = open field test; TST = tail suspension test. Created with BioRender.com.

4.2.2 Project 2

At the age of 8-10 weeks, male and female *Per2*^{Luc} mice were assigned to two different experimental conditions per sex. One group was kept under a standard 12:12 LD cycle (control) whilst the other group of mice was maintained under a shift work light paradigm (shift work). Two different animal cohorts were used for the experiments (Figure 7).

Cohort A: Locomotor activity and sucrose preference in response to control 12:12 LD conditions vs. the light-induced shift work conditions was assessed in a cohort of male and female *Per2*^{Luc} mice (male control: n = 15; male shift work: n = 15; female control: n = 15; female shift work: n = 15). The animal's locomotor activity was tracked during the first 2-3 weeks of the shift work light paradigm using the IntelliCage system (TSESystems GmbH, Bad Homburg, Germany). Following a sucrose preference test in week 3, animals of this cohort were sacrificed without further tissue collection.

Cohort B: Behavioral and metabolic assessments were conducted in male and female *Per2*^{Luc} mice (male control: n = 18; male shift work: n = 18; female control: n = 12; female shift work: n = 12). Animals were exposed to the shift work light paradigm for a total of 7-9 weeks and all metabolic and behavioral experiments started after 3 weeks of alternating light cycles. All experiments were conducted from Monday-Thursday to ensure same *Zeitgeber* conditions in both, control and shift work animals**.**

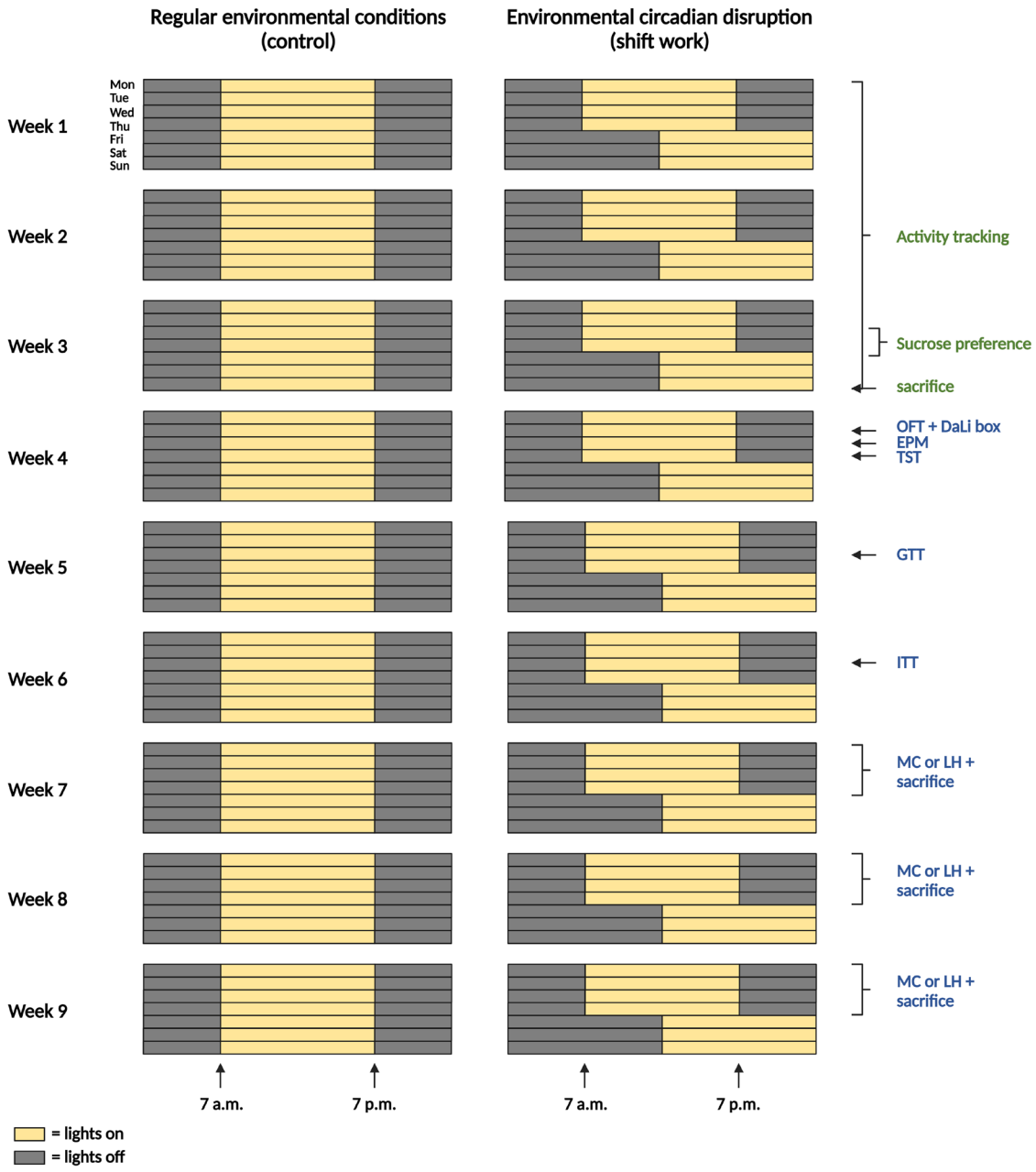

Figure 7. Visualization of the shift work light paradigm and the experimental timeline. Male and female *Per2*^{Luc} animals were subjected to control conditions (left) or a shift work light paradigm (right). All animals underwent the tests indicated on the right, in the respective week indicated on the left. In cohort A (green) locomotor activity and sucrose preference were tracked in the IntelliCage system and animals were sacrificed thereafter. In cohort B (blue) body and food weight were recorded weekly. Further, all other behavioral and metabolic tests were conducted in cohort B. Luminometry data was only collected and analyzed in cohort B upon sacrifice. DaLi box = dark-light box; EPM = elevated plus maze; GTT = glucose tolerance test; ITT = insulin tolerance test; LH= learned helplessness; MC = metabolic cages; OFT = open field test; TST = tail suspension test. Created with BioRender.com.

4.2.3 Project 3

More pronounced shift work-induced behavioral deficits were observed in females compared to males in project 2. Following these results, only female mice were used in project 3. *Bmal1*$^{+/-}$ mice and their *Bmal1*$^{+/+}$ WT littermates were housed according to genotype. At 10 weeks, mice were randomized according to body weight and assigned to either the control or the light-induced shift work conditions. From this, four experimental groups resulted: WT control (n = 11), WT shift work (n = 11), *Bmal1*$^{+/-}$ control (n = 11) and *Bmal1*$^{+/-}$ shift work (n = 12). The experimental timeline as well as the shift work light paradigm were equal to project 2 (Figure 7). The only exception was that in contrast to project 2, in project 3 all experiments were performed in a single cohort.

4.3 Genetic and environmental disruption of circadian clocks

4.3.1 Virus production

Two plasmids containing *Bmal1* shRNAs (pAAV-U6-Bmal1shRNA1-CMV-GFP, pAAV-U6-Bmal1shRNA2-CMV-GFP) and two plasmids containing control scrambled shRNA (pAAV-U6-SCRshRNA1-CMV-GFP, pAAV-U6-SCRshRNA2-CMV-GFP) were kindly provided by Dr. David K. Welsh, University of California San Diego, La Jolla, CA, United States. The shRNA-passenger sequences were as follows: Bmal1shRNA1 = 5'- GTCGATGGTTCAGTTTCAT, Bmal1shRNA2 = 5'-GCATCGATATGATAGATAA, SCRshRNA1 = 5'- GCGCTTAGCTGTAGGATTC, SCRshRNA2= 5'-GCAACAAGATGAAGAGCAC. Details on the generation of the plasmids were described elsewhere and the plasmid maps are visualized (Figure 8) [85]. The plasmids were transfected into HEK293FT cells using the polyethylenimin (Polyscience) transfection method along with pFdelta6 helper plasmid as well as an equimolar mix of the capsid plasmids pH21 (serotype 1) and pRV1 (serotype 2). 72 hours after transfection, HEK293FT cells were collected and lysed using three freeze/thaw cycles to release adeno-associated virus (AAV) particles. Genomic DNA was digested using Benzonase (Sigma) treatment. The lysate was cleared by centrifugation and recombinant AAVs collected from the supernatant. Purification was achieved using an iodixanol gradient. Finally, AAVs were enriched using an Amicon Ultra-15 centrifugal filter 100K device (Millipore) and performing a phosphate-buffered saline (PBS) wash.

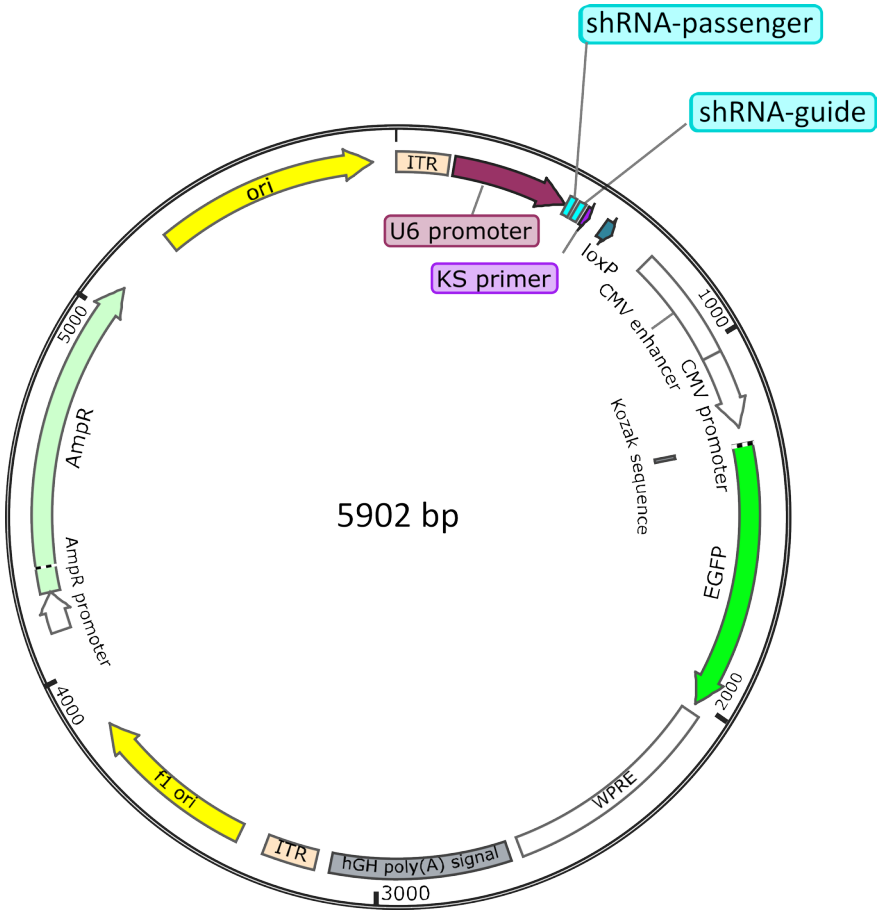

Figure 8. Visualization of a representative vector map. Vector maps of pAAV-U6-Bmal1shRNA1-CMV-GFP and pAAV-U6-Bmal1shRNA2-CMV-GFP as well as pAAV-U6-SCRshRNA1-CMV-GFP and pAAV-U6-SCRshRNA2-CMV-GFP were identical except for the shRNA-passenger and their respective shRNA-guide sequences (blue). In addition to the shRNA located after the U6 promoter (red), another relevant aspect of the vector map is the enhanced green fluorescent protein (EGFP) indicated by the green arrow. Vector map created with SnapGene.

4.3.2 Stereotactic virus injection

Animals were anesthetized by intraperitoneal (IP) injection of an antagonizable anesthetic consisting of midazolam/medetomidine/fentanyl (5.0/0.5/0.05 mg/kg). Prior to surgery, metamizole (400 mg/kg; oral administration) and carprofen (10 mg/kg; subcutaneous) were given as pain prophylaxis. Animals received bilateral virus injection into the SCN. Per injection site, 400 nL were injected at 100 nL per minute. The injection coordinates were the following: AP: - 0.3; ML: +/- 0.3; DV: - 5.5 & - 5.6. Stereotactic injections were performed using a Microinjector (kd Scientific KDS-310-PLUS (78-9311N)) and a 2.5 µL Hamilton Syringe (Hamilton: Microliter Syringe 600 Series 7632-01; Small Hub Removable Needles 7762-06). All mice received a 1:1 mixture of two shRNAs: either both *Bmal1* shRNAs (SCN-*Bmal1*-KD) or both control scrambled shRNAs (control).

Confirmation of stereotactic injection success

Bmal1 knockdown was confirmed by (i) reduced amplitudes in the bioluminescence recordings of organotypic SCN explants (ii) by assessing behavioral activity rhythms in a subset of mice and (iii) by assessing GFP reporter expression in the SCN. For (iii), microscopic images of the 300 µm SCN slices were taken after one week of bioluminescence recordings. Unilateral hits in SCN-*Bmal1*-KD animals were considered as a successful injection when SCN rhythms were significantly downregulated. Animals that did not meet the above-mentioned criteria were categorized as unsuccessful stereotactic injection and were thus excluded from all analyses.

4.3.3 Shift work light paradigm

Mice were group-housed under a 12:12 LD cycle. Lights turned on at 7 a.m., which represented ZT0. At the age of 8-10 weeks, animals were divided over the experimental conditions by randomizing according to the body weight and age. Thereafter, one group of mice was maintained on the standard 12:12 LD cycle (referred to as 'control'). The other group of mice was subsequently housed under alternating light cycles (referred to as 'shift work'). Manipulation of the LD cycle was achieved via an environmental isolation cabinet allowing complete control over the light cycles at ~180 Lux. The alternating light cycles aimed to mimic shift work conditions, and were as follows:

- Monday-Thursday: standard 12:12 LD cycle with lights turned on at 7 a.m. and off at 7 p.m.
- Friday-Sunday: Lights on at 1 p.m. and off at 1 a.m.

This represents a 6-hour phase delay from Thursday to Friday and a 6-hour phase advance from Sunday to Monday every week.

4.4 Behavioral assessment

For all behavioral experiments, mice were allowed to habituate to the testing room for at least 10 minutes before starting the experiment. Between animal testing, the apparatuses were cleaned with 5 % sodium dodecyl sulfate dissolved in water, then water and lastly ethanol to reduce the impact of residual odor on test results.

4.4.1 Open field test

To measure general locomotion and anxiety-related behavior, all animals were tested in the open field test (OFT) similar to previously described [151]. Animals were placed in an open field apparatus (50 cm × 50 cm × 50 cm) facing the wall and video-recorded. Testing started at ZT2 – 3 and illumination was set to 1,600 lux. In project 1, testing time was 10 minutes. In project 2 and 3, the behavior of the mice was tracked for 5 minutes due to high animal numbers. During the testing time, the following parameters were automatically analyzed by the ANY-maze software: total distance traveled (m), center entries and center time (s).

4.4.2 Dark-light box

The dark-light (DaLi) box test is used to assess anxiety-like behavior in mice and was conducted as described before [151]. The DaLi box comprises two compartments joined by an open gate. One compartment contains transparent walls and is illuminated at 1,000 lux. The other compartment has a black lid and black, non-transparent walls that keep the compartment dark (< 10 lux). In project 1, testing started at ZT3 and lasted for 10 minutes. In project 2 and 3, testing started at ZT7 and lasted only 5 min due to high animal numbers. At the beginning of the experiment, animals were placed in the dark compartment facing the wall away from the light compartment. Animals were video-recorded and the relevant parameters automatically analyzed by the ANY-maze software. These parameters included the light compartment entries, time (s), latency to first entry (s) and distance traveled (m).

4.4.3 Elevated plus maze

The elevated plus maze (EPM) is used to assess anxiety-like characteristics in rodents. The EPM is a plus-shaped apparatus, consisting of two opposing open arms (30 cm x 5 cm x 1 cm), two opposing closed arms (30 cm x 5 cm x 16 cm) and a center area (5 cm x 5 cm x 1 cm). The maze was elevated 30 cm above the floor and testing started at ZT2 – 3. Lighting conditions were ~25 lux in the open arms and ~5 lux in the closed arms. At the start of the test, animals were placed in the center, facing an open arm. For project 1, the testing time was 10 minutes. For projects 2 and 3, testing time was shortened to 5 minutes due to high animal numbers. Animals were video-tracked and the relevant parameters recorded by the ANY-maze software. These

parameters included open arm entries, time (s) and distance traveled (m) as well as the overall distance traveled (m). For project 1, heat maps were generated by the ANY-maze software. These represented an occupancy plot of the position of the body center of a representative control and SCN-*Bmal1*-KD animal in the EPM.

4.4.4 Tail suspension test

The tail suspension test (TST) is used to characterize behavioral despair and was performed at ZT3 at a light intensity of 1,600 lux as described previously [208]. Mice were suspended 30 cm above a flat surface for a duration of 6 minutes by using adhesive tape on the tails. To keep the mice from climbing up the tail during the experiment, plastic covers were placed around the tail. Mice were video-recorded and parameters were quantified using the ANY-maze software. Parameters included time immobile (s), latency to first immobile episode (s) and transitions between mobile and immobile episodes.

4.4.5 Learned helplessness

The learned helplessness (LH) paradigm is employed to assess helpless behavior in mice. It was performed as previously described [85, 120, 208]. The paradigm consists of 2 consecutive training days starting at ZT5, followed by one testing day at ZT3. On the training days, mice were placed in restraint tubes and receive 120 shocks to their tails (5 s, every 20-30 s). The shock intensity was gradually increased by 0.05 mA every 15 shocks, starting at 0.25 mA, and going up to 0.60 mA. On the testing day, animals were placed into shuttle boxes (Panlab Harvard Apparatus, Spain) and received 30 electric shocks to their paws through the grid floor (shock intensity: 0.10 mA; shock duration: max. 30 s). During each test shock, the gate between the two compartments of the box remained open and the animals could escape by crossing over to the adjacent compartment. During the trails #1-5 the schedule was fixed ratio (FR) 1, meaning the animals had to cross the gate once to terminate the shock. In the remaining trials #6-30, the schedule was replaced by FR-2 meaning the shock was only terminated once the mice crossed the gate twice. Number of escape failures and escape latency (s) were automatically recorded and only the FR-2 trials were included into data analysis. For project 2, pain sensitivity was later assessed by transferring the mice to shuttle boxes and gradually increasing the shock intensity.

The shock intensity at which animals displayed avoidance behavior (i.e., jumping or climbing the wall) was recorded as pain threshold.

4.4.6 Y-maze

The Y-maze test is used to assess spatial working memory by quantifying spontaneous alternations and has been described before [151]. The Y-maze is a Y-shaped apparatus, consisting of three identical arms (A, B, C). Starting at ZT3, the test was conducted at ~15 lux for 10 minutes. At the start of the test, mice were placed in the center, facing arm A. Spontaneous alternations represent the rate of full sequences of visits (choices) to each arm of the maze without repetition (e.g., A-B-C, B-A-C or B-C-A, but not A-B-A, C-B-C, or B-A-B). Mice were video-tracked and spontaneous alternations were automatically recorded by the ANY-maze software.

4.5 IntelliCage system

The IntelliCage system (TSE Systems, Bad Homburg, Germany) is a fully automated system that can be used for behavioral and cognitive phenotyping. It is composed of a frame that is placed within type IV cages. The frame is made of four corners each containing two doors (one left and one right door). When doors are open, mice can freely access a water bottle located behind them. When doors are closed, mice can open them and access the water bottles by poking the doors. Depending on the experimental paradigm (e.g., reversal learning task), mice can only open a given door. Throughout all IntelliCage experiments, visits to a corner, nosepokes, and licks at water bottles are continuously recorded. To allow corners of the IntelliCage system to identify individual animals, mice are tagged by RFID transponders.

Transponder implantation

To guarantee full recovery from surgery, the transponders were inserted at least 3 days prior to beginning the IntelliCage tests. Following isoflurane anesthesia, mice were shaved in a small section of their dorsocervical region. Dexpanthenol eye ointment was applied to the eyes, 70 % ethanol was used to sterilize the skin and an RFID-transponder was implanted subcutaneously in the neck region. Lastly, one to two sutures were used to close the incision and carprofen (10 mg/kg; subcutaneous) was given as pain prophylaxis. The experimental phases in the IntelliCage

system differed between the projects and will thus be described for each project separately in the following sections.

4.5.1 Project 1

In project 1, the aim was to assess cognitive performance and sucrose preference in SCN-*Bmal1*-KD vs. control animals using the IntelliCage system. To this end, the following order of experiments was performed. Note that 1 day is referring to a timespan of 24 hours and experiments were changed during the light phase:

- **Free adaptation (2 days)**: doors remained open and granted free access to all water bottles.
- **Free adaptation, doors open on visit (1 day)**: doors opened upon entrance of a mouse in a corner (no nosepoke required). Mice had free access to all water bottles.
- **Nosepoke adaptation (2 days)**: doors remained closed until a mouse entered a corner and performed a nosepoke.
- **Nosepoke adaptation at 50 % (1 day)**: similar to 'nosepoke adaptation', however, doors only opened with a 50 % probability following a mouse's nosepoke to prevent a bias for a particular corner by rendering it unreliable.
- **Nosepoke adaptation at 30 % (1 day)**: similar to 'nosepoke adaptation', however, doors only opened with a 30 % probability.
- **Place learning (2 days)**: every mouse was randomly assigned to one of the four corners. Bottles were only accessible following a nosepoke in their assigned corner.
- **Serial reversal learning (3 days)**: similar to 'place learning', however, assignments of the drinking corner for each mouse changed every 24 hours with the new corner being unpredictable for the mouse.
- **Sucrose preference (1 day)**: doors remained open, granting free access to all bottles. However, one of the two bottles in each corner was replaced with a 1 % sucrose solution. The other bottle remained with autoclaved tap water. Preference of mice to drink sucrose solution was recorded for 24 hours and assessed to determine anhedonia in mice.

Place learning and sucrose preference were measured using the preference score $\frac{(A-B)}{(A+B)}$, where A and B represent the number of correct and incorrect trials, respectively. Reversal learning and serial reversal learning phases were calculated using Sequential

Probability Ratio Testing (SPRT). Details on the preference score and the SPRT were described elsewhere [209]. All experiments in the IntelliCage system were only performed in cohort 1. The raw data from each experiment conducted in the IntellliCage system was analyzed using the R based, automated user interface FlowR (XBehavior, Dägerlen, Switzerland).

4.5.2 Project 2 and 3

In project 2 and 3, sucrose preference and behavioral activity in response to control vs. light-induced shift work conditions were assessed. To this end, mice were placed into the IntelliCage system and given 3 days to acclimatize. The animals were exposed to their respective light conditions (i.e., control or shift work). Data recording for analysis started when mice of the shift work group were exposed to their first light cycle shift. Thereafter, data was collected using the following experimental design:

- **Free adaptation (17 days for project 2, 14 days for project 3)**: open doors allowing free access to all bottles. The aim was to measure corner visits as a proxy for behavioral activity of control vs. shift work animals.
- **Sucrose preference (2 days)**: sucrose preference was performed and calculated as described for project 1 with the exception that testing occurred over 2 rather than only 1 day.

Sucrose preference was analyzed using FlowR by calculating the preference score explained above. Behavioral activity in response to the light conditions was analyzed using the R package rethomics [210]. Corner visits were used as a proxy of locomotor activity. Only the start of a mouse corner visit was recorded as one activity event because mice have the tendency to remain in corners for longer periods. Double-plotted actograms were generated, and total locomotor activity was calculated for each mouse. Furthermore, the nocturnality score of locomotor activity was calculated for every mouse by assessing the preference of activity during the dark phase (lights off) over during the light phase (lights on).

4.6 Metabolic assessment

4.6.1 Body and food weight

Body weight and food weight per cage were recorded weekly between ZT3 and ZT5 for project 1, project 2 (cohort B only) and project 3.

4.6.2 Glucose and insulin tolerance test

For the glucose tolerance test (GTT) and the insulin tolerance test (ITT), mice were starved for 6 hours (GTT) or 4 hours (ITT) at ZT0. Glucose (1.5 g/kg body weight) and insulin (1 IU/kg body weight) were injected intraperitoneally for the GTT and ITT, respectively. Blood glucose levels were determined from blood collected by pricking the tail vein and using an Accu-Check Performa glucose meter (Roche, Basel, Switzerland). Measurements were taken prior to injection (0 min) and 15, 30, 60, 90, and 120 min following glucose or insulin injection. Absolute glucose measurements were visualized. By measuring the area under the curve (AUC) and subtracting the area under the baseline, an area of the curve (AOC) was calculated and statistically analyzed for the GTT and ITT.

4.6.3 24-hour blood glucose profile

Mice were transferred to a separate room 48 hours before measurements began. Mice were kept under the standard 12:12 LD cycle with food and water *ad libitum*. Blood was sampled by pricking the tail vein and glucose levels were determined using an Accu-Check Performa glucose meter (Roche, Basel, Switzerland). Blood glucose measurements were taken at ZT1, ZT5, ZT9, ZT13, ZT17 and ZT21. During the time points in the dark phase (i.e., ZT13, ZT17 and ZT21), blood was sampled under dim red light. During sampling, mice were not restrained and were allowed to explore freely. Overall glucose levels during the day vs. during the night were assessed by comparing total glucose levels during the light phase (i.e., ZT1 + ZT5 + ZT9) vs. during the dark phase (i.e., ZT13 + ZT17 + ZT21).

4.6.4 Indirect calorimetry

Locomotor activity, food consumption, water consumption, respiratory exchange rate (RER) and energy expenditure (EE) were assessed using indirect calorimetry in metabolic cages (TSE Systems, Bad Homburg, Germany). The RER represents the ratio of VCO2 produced (ml/h) to VO2 consumed (ml/h). The EE was determined using the formula (3.941 + 1.106 RER) x 0.001 x VO2 and normalized to the body weight [152]. Mice were single-housed and allowed to acclimatize for at least 24 hours. Subsequently data was collected for 48 hours (project 3), 72 hours (project 2) or 96 hours (project 1) in 15-minute intervals. Food and water consumption as well as locomotor activity were summed across the 15 minutes. The RER and EE were determined once every 15 minutes. For all parameters, a mean across two measurements (i.e., 30 minutes) was plotted over time. For locomotor activity, food, and water intake the total sums were calculated for every mouse. For the RER and EE, the mean for each animal across the recorded period was calculated. For analysis of the data, the R package rethomics was used [210]. The function periodogram was used to create Lomb-Scargle periodograms. The function ggetho was used to visualize periodograms and group averages over a period of 24 hours (project 1), 48 hours (project 3) or 72 hours (project 2).

4.7 Animal sacrifice

For project 1, mice were sacrificed 8 or 9 days following the LH testing. For project 2 (cohort B only) and project 3, animals were sacrificed 1 – 2 days after completing LH testing, representing 4 – 5 days after the last light cycle shift. Animals in project 2 and 3 that did not undergo the LH paradigm were sacrificed after 8 weeks of alternating light cycles. All animals were weighed and sacrificed around ZT4 by brief anesthesia with isoflurane followed by decapitation. For all animals, gonadal white adipose tissue (gWAT), inguinal white adipose tissue (iWAT) and interscapular brown adipose tissue (BAT) were dissected and weighed. In project 1, brains were isolated and prepared for bioluminescence recordings and *Ppox* determination as described below. Furthermore, in cohort 1, livers were collected and prepared for recordings. In project 2, for animals that underwent the LH paradigm, livers and brains were collected and prepared for bioluminescence recordings, as described below. In project 3, apart from the fat pad isolation, no further tissues were collected.

4.8 Brain slice cultivation and PER2::LUC luminometry

Brains and livers were collected in half-frozen PBS and further processed for the preparation of organotypic tissue explants (SCN, PAG and liver) as previously described [120, 205, 211]. Livers had to be embedded in in low-melting agarose (Sigma-Aldrich, CAS no. 39346-81-1) before fixation to a Leica vibratome whereas brains were directly fixed to the vibratome. The tissues were kept in cold PBS and 300 µm thin tissue slices were cut. Using a pair of thin scissors, a small piece of liver tissue was cut out. For the brain tissue, the SCN (Bregma: -0.22) and PAG (Bregma: -2.70) were isolated from the appropriate slices. All organotypic tissues were transferred to a tissue culture insert (Millicell Cell Culture Inserts, 30 mm, Millipore, catalog no. PICMORG50) placed in a 35 mm petri dish filled with explant media. The media was adjusted to pH 7.4 and consisted of DMEM powder with 4.5 g/L glucose (Corning, catalog no. 90-013-PB), 4 mM sodium bicarbonate (7.5 % solution, ThermoFisher Scientific, catalog no. 25080094), 10 mM HEPES buffer (PAN-Biotech, catalog no. P05-01100), 52 U/mL penicillin, 52 µg/mL streptomycin, 4mM GlutaMAX™ Supplement (ThermoFisher Scientific, catalog no. 35050061), 4mM B-27 Supplement (ThermoFisher Scientific, catalog no. 17504044) and 1 mM D-luciferin (p.a. free acid, PJK GmbH). The dishes were sealed using silicon grease and a glass cover slip before being placed into a LumiCycle luminometer (Actimetrics, Wilmette, IL) for measurements. PER2::LUC expression patterns were recorded every 10 minutes at 37 °C (without CO_2) and analyzed with the LumiCycle Analysis software (Actimetrics, Wilmette, IL). The raw and baseline subtracted PER2::LUC expression plots were generated. The first day of recordings was excluded from the analysis and the subsequent 3 days of measurements were used to analyze the amplitude, phase, and period of the organotypic slices. To normalize the amplitude to the size of the cultured explant, the sin wave amplitude was divided by the average brightness of the cultured explant. Tissue explants were defined as rhythmic when they displayed at least two PER2::LUC rhythm peaks, a goodness of fit > 1 and clear rhythmicity in the periodogram analysis. When rhythmicity criteria were not met, the normalized amplitude for this issue explant was set to 0 counts/s for analysis. For the analysis of the period and phase, the non-rhythmic tissue explants were excluded.

4.9 *Prepro-orexin* quantificative PCR

From the collected brains, the lateral hypothalamus was dissected between Bregma -1.24 and -1.82 [212]. Tissue was stored overnight in RNAlater™ solution (ThermoFisher Scientific) and subsequently transferred to -80°C. For RNA isolation from frozen tissue, QIAzol Lysis Reagent and RNeasy Mini Kit (Qiagen) were used according to the manufacturer's protocol. The DNAse treatment was included. Complementary DNA (cDNA) was synthesized using the high-capacity RNA-to-cDNA™ kit (Thermo Fisher Scientific). For quantitative PCR (qPCR), primers for β-act (Fw-CCCTGAAGTACCCCATTGAA, Rev-AGGTGTGGTGCCAGATCTTC) and PPO (Fw-TTGGACCACTGCACTGAAGA, Rev-CCCAGGGAACCTTTGTAGAAG) were used [213]. Fold changes were calculated as previously described [214].

4.10 Statistical analysis

The nocturnality score was determined for several parameters as an estimate of the circadian amplitude for the given parameter. The nocturnality score was calculated and normalized to baseline differences using the following formula:

$$\text{Nocturnality of parameter} = \frac{(\text{Parameter during the dark phase} - \text{Parameter during the light phase})}{(\text{Parameter during the dark phase} + \text{Parameter during the light phase})}$$

Statistical analyses and data plotting were conducted using GraphPad Prism 9.3.1 (GraphPad Software, La Jolla, CA, USA) and RStudio (RStudio, Boston, MA, USA). Figures were generated using Adobe Illustrator, InkScape or Biorender. Biological and technical outliers (e.g., animal not detected by camera) were excluded from all analyses.

For all cohorts, results were visualized as mean ± standard error of the mean (SEM) together with the individual data points. Significance threshold was set to $p = 0.05$. Details on the descriptive statistics including n-numbers, the statistical tests that were conducted and their outcomes are indicated in the supplementary tables of this thesis.

4.10.1 Project 1

Animals of cohort 1 and 2 were pooled for analyses to increase statistical power and highlight the reproducibility of the results across two independent cohorts. Pooling occurred for the behavioral and metabolic tests that were performed at the same time point after stereotactic injection (+/- 2 weeks). However, since not all behavioral and metabolic experiments were done with animals of both cohorts, n-numbers differed between the experiments. All analyses aimed to statically test for differences between control and SCN-*Bmal1*-KD mice to assess the metabolic and behavioral impact of dampened SCN rhythms. Following normality testing using D'Agostino and Pearson normality test, a parametric unpaired t-test was used for normally distributed data. The Mann-Whitney U test was used when normality was not met. For correlation analysis, a Pearson correlation coefficient was calculated. For quantification of the distribution of rhythmic vs. arrhythmic PAG slices, a Fisher's exact test was conducted. For repeated measures, a two-way repeated measures analysis of variance (ANOVA) was used. When a data point from an animal was missing, a mixed-effects analysis was employed instead. Thereafter, pairwise comparisons were conducted using the Fisher's least significant difference (LSD) post-hoc test (uncorrected p-value) with Bonferroni correction (corrected p-value). For the day vs. night comparison between the two experimental groups, two-way ANOVAs were conducted and equally followed by pairwise comparisons. The effect of a more chronic SCN rhythm downregulation on behavioral and metabolic parameters was assessed, by statistically comparing the measurements of the subset of re-tested animals using two-way repeated-measures ANOVAs.

4.10.2 Project 2

Male control, male shift work, female control and female shift work mice were statistically compared to detect sex effects (male vs. female), shift work effects (control vs. shift work) and interaction effects (sex x shift work). Statistical outliers in each experimental group were assessed using the two-sided Grubb's test (significance threshold, $p = 0.05$) and excluded from analyses. Two-way ANOVAs were used for comparison of the four experimental groups. For repeated measures, three-way ANOVAs were used. When a data point from an animal was missing, mixed-effects analyses were used instead. Following two- and three-way ANOVA as well as mixed effects analyses, Fisher's LSD post-hoc test with Bonferroni correction was used for the

following pairwise comparisons: male control vs. male shift work and female control vs. female shift work.

4.10.3 Project 3

WT control, WT shift work, *Bmal1*$^{+/-}$ control and *Bmal1*$^{+/-}$ shift work mice were characterized to assess the impact of genotype (WT vs. *Bmal1*$^{+/-}$), shift work (control vs. shift work) or their interaction (genotype x shift work). Outlier detection was performed as outlined for project 2. Two-way ANOVAs were used for comparison of the four experimental groups. For repeated measures, three-way ANOVAs were used. When a data point from an animal was missing, mixed-effects analyses were used instead. When an interaction effect was detected during statistical testing, the following pairwise post-hoc comparisons were performed using a Fisher's LSD post-hoc test with Bonferroni correction:

- WT control vs. WT shift work (to identify the effect of shift work in WT animals)
- WT control vs. *Bmal1*$^{+/-}$ control (to identify baseline genotype differences)
- *Bmal1*$^{+/-}$ control vs. *Bmal1*$^{+/-}$ shift work (to identify the effect of shift work in *Bmal1*$^{+/-}$ animals).

5. Results

5.1 Comorbid behavioral and metabolic deficits in male mice following *Bmal1* downregulation in the suprachiasmatic nucleus

5.1.1 SCN rhythms are dampened in SCN-*Bmal1*-KD animals

The primary aim of project 1 was to downregulate the molecular SCN rhythms in *Per2*^{Luc} animals. As expected, downregulation of *Bmal1* by shRNAs leads to a significant reduction in amplitude of PER2::LUC expression, in some cases to such an extent that significant rhythms are no longer detectable (Figure 9 A – C, S1, Table S1). Moreover, the KD of *Bmal1* in the SCN causes its circadian period to lengthen significantly and a phase delay occurs (Figure 9 D, E). The site of injection was identified using the GFP reporter that was present in all AAV vectors. GFP expression in the organotypic explants confirms for all samples included in the analysis, precise injections of shRNAs into the SCN (Figure 9 F, S2, S3).

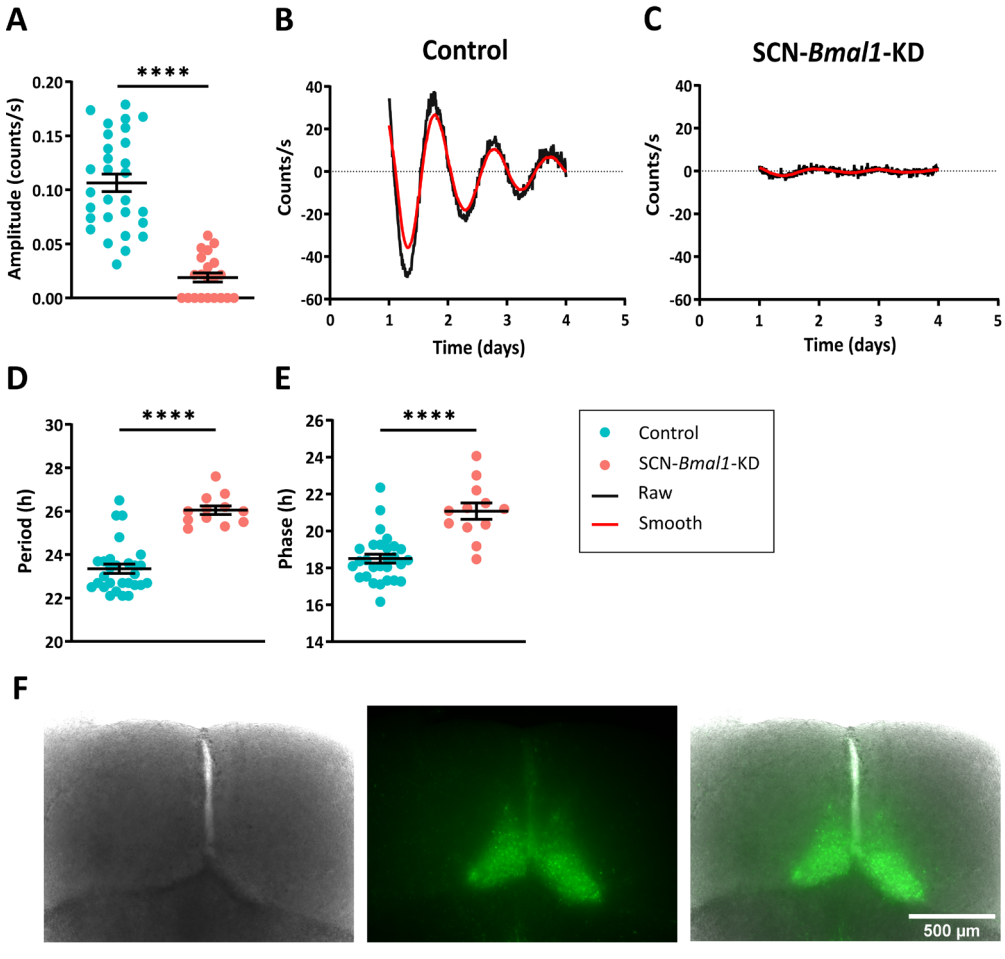

Figure 9. Successful stereotactic injection results in SCN rhythm downregulation in SCN-*Bmal1*-KD animals. SCN slices from SCN-*Bmal1*-KD and control animals were collected upon sacrifice and PER2::LUC rhythmicity and GFP expression of AAV vectors assessed. (A) Normalized amplitude of PER2::LUC rhythm of SCN explants (control: n = 29, SCN-*Bmal1*-KD: n = 21, unpaired t-test). (B) Representative SCN explant PER2::LUC expression plots from a control and (C) an SCN-*Bmal1*-KD animal. Black and red lines represent the baseline subtracted raw data and smoothed curves, respectively. (D) Period and (E) phase of SCN explant PER2::LUC rhythms (control: n = 28, SCN-*Bmal1*-KD: n = 12, Mann-Whitney U test). (F) Representative SCN image from an injected animal (left to right: bright field image, GFP image, and merged image). Scale bar represents 500 µm. **** indicates $p < 0.0001$. Details on the statistical tests and n-values can be found in Table S1. PER2::LUC expression plots and SCN images of all injected animals can be found in Figure S1 – S3. Data points in panels A, D and E represent SCN explants from individual experimental animals. Error bars indicate mean ± SEM.

5.1.2 SCN-*Bmal1*-KD animals display reduced anxiety-like behavior

Downregulation of SCN rhythms was previously shown to lead to anxiety-like behavior in mice [85]. To reconfirm the comorbidity of anxiety-related and metabolic phenotypes following SCN rhythm downregulation within the same mouse, anxiety-related features of SCN-*Bmal1*-KD mice were re-tested in this project using the EPM, DaLi box and OFT. In contrast to the previous findings, SCN-*Bmal1*-KD animals in this project display reduced anxiety-related traits in the EPM. Notably, they evidence increased locomotion in the EPM, as well as increased open arm entries, time and distance traveled (Figure 10 A – F, Table S2). In accordance, SCN-*Bmal1*-KD animals display reduced anxiety-like behavior in the DaLi box test. SCN-*Bmal1*-KD animals exhibit increased light compartment entries and a trend for a decreased latency to the first light compartment entry (Figure 10 G, H). The time in the light compartment is unaltered by KD of *Bmal1* in the SCN (Figure 10 I). Of note, in the OFT, SCN-*Bmal1*-KD animals do not show changes in anxiety-related parameters (Figure 10 J – L).

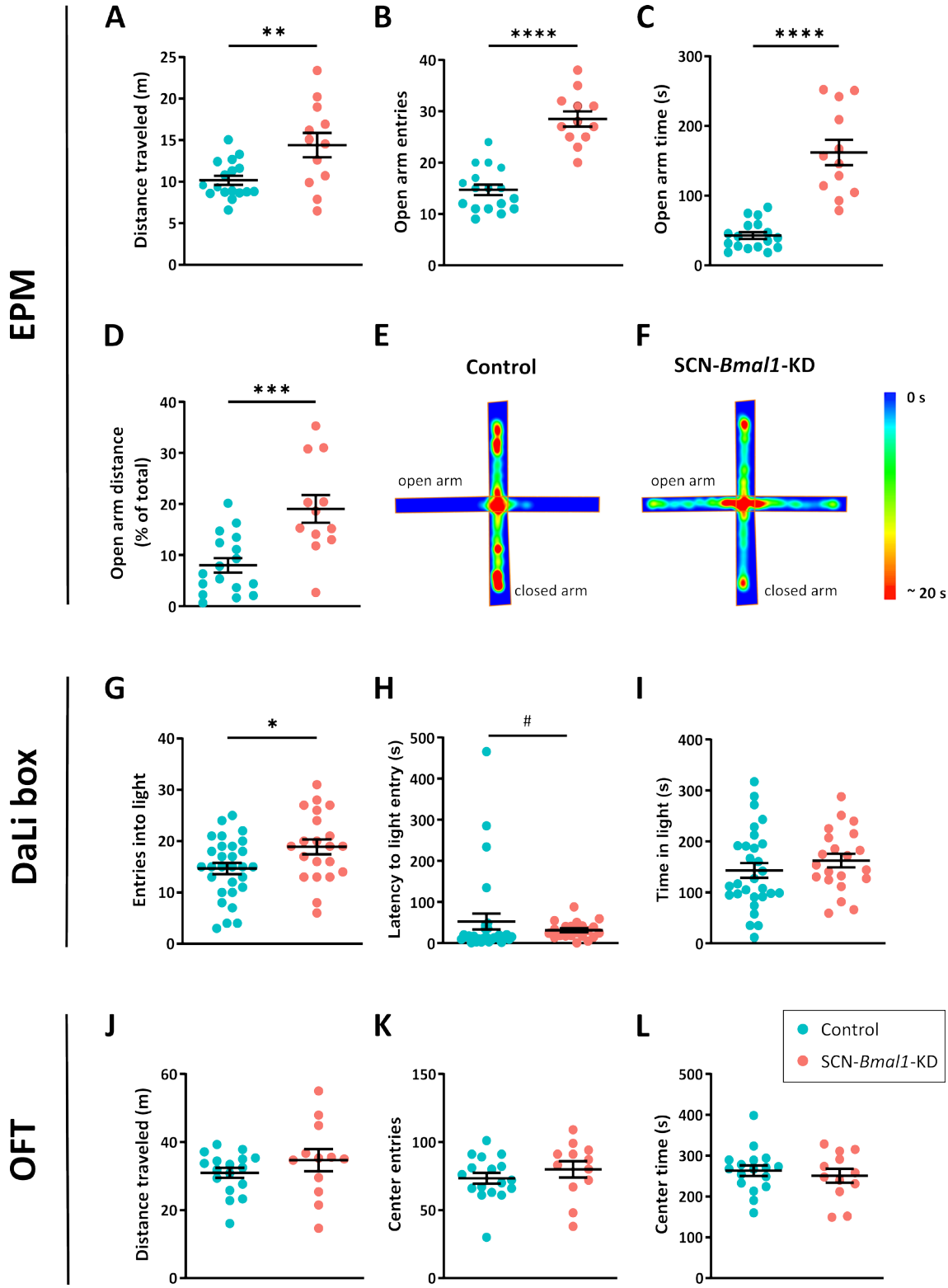

Figure 10. SCN-*Bmal1*-KD animals display reduced anxiety-related behavior. Anxiety-related behavior was assessed in SCN-*Bmal1*-KD and control animals using the EPM, DaLi box and OFT. EPM: (A) total distance traveled, (B) open arm entries, (C) open arm time and (D) open arm distance as a percentage of total distance traveled. (E) Heat map of the animal's center point of a representative control animal and (F) a representative SCN-*Bmal1*-KD animal in the EPM task over the total test duration of 10 min. The scale bar is indicated on the right (0 – 20 s). DaLi box: (G) entries into the light compartment, (I) latency to the first entry into the light compartment and (I) time spent in the light compartment. OFT: (J) total distance traveled, (K) center entries and (L) center time. For the OFT and EPM: n = 17 (control) and n = 12 (SCN-*Bmal1*-KD). For the DaLi box: n = 29 (control) and n = 21 (SCN-*Bmal1*-KD). The control and

SCN-*Bmal1*-KD group were statistically compared using an unpaired t-test or a Mann-Whitney U test when normality was not met. # indicates $p < 0.1$; * indicates $p < 0.05$; *** indicates $p < 0.001$; **** indicates $p < 0.0001$. Details on the statistical tests and n-values can be found in Table S2. DaLi box = dark-light box; EPM = elevated plus maze; OFT = open field test. Data points represent individual experimental animals. Error bars indicate mean ± SEM.

One hypothesis of this project was that comorbid behavioral and metabolic outcomes resulting from a chronic downregulation of SCN rhythms differ from those resulting from acute downregulation. To investigate this hypothesis, a subset of animals was re-tested in the EPM, DaLi box and OFT at a later time point after downregulation of SCN rhythms (i.e., 16 weeks after stereotactic injection). Importantly, the reduced anxiety-related phenotype following KD of *Bmal1* in the SCN persists over time after SCN rhythm downregulation (Figure 11 A – F). Time after stereotactic injection does not significantly affect the anxiety-related parameters that are altered by downregulated SCN rhythms (EPM: distance traveled, open arm entries, open arm time, open arm distance; DaLi: entries into light, latency to light entry) (Table S3). For the anxiety-related parameters that are unaltered by downregulated SCN rhythms (DaLi: time in light; OFT: distance traveled, center entries, center time), an effect of time is observed (Figure 11 G – J, Table S4). However, this effect is independent of the experimental group as indicated by a lack of a significant group x time interaction. Thus, the effect of time likely results from re-testing rather than reflecting a change in the behavioral phenotype after a more chronic *Bmal1* KD in the SCN. Overall, the results indicate that the reduced anxiety-like behavior in SCN-*Bmal1*-KD animals is quickly established after downregulation of SCN rhythms (i.e., 3 weeks after injection) and does not change during a more chronic SCN rhythm downregulation (i.e., 16 weeks after injection).

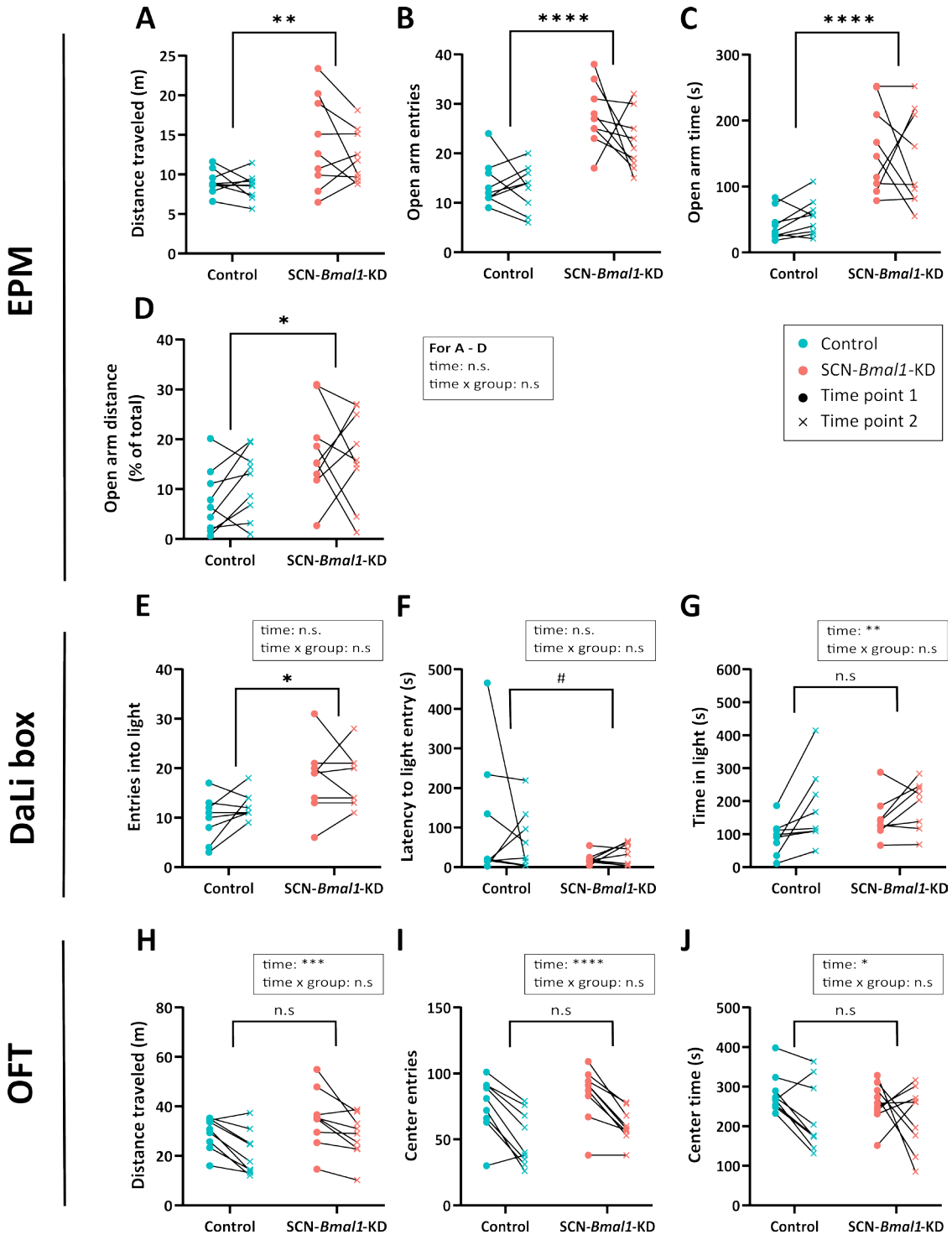

Figure 11. Reduced anxiety-related behavior of SCN-*Bmal1*-KD animals persists over time after downregulation of molecular SCN rhythms. Anxiety-related behaviors were measured at 3 weeks after stereotactic injection and re-assessed at 16 weeks after stereotactic injection in a subset of SCN-*Bmal1*-KD and control animals. EPM: (A) total distance traveled, (B) open arm entries, (C) open arm time and (D) open arm distance as a percentage of total distance traveled. DaLi box: (E) entries into the light compartment, (F) latency to the first entry into the light compartment and (G) time spent in the light compartment. OFT: (H) total distance traveled, (I) center entries and (J) center time. For all tests: n = 8 – 9 per experimental group. Two-way repeated measures ANOVA was performed with the time and interaction effects indicated for each parameter. The group effect (control vs. SCN-*Bmal1*-KD) is indicated above the comparison bar between the experimental groups. Details on the statistical tests and n-values can be found in Table S3 and S4. n.s. = not significant; # indicates $p < 0.1$; * indicates $p < 0.05$; ** indicates $p < 0.01$; *** indicates $p < 0.001$;

**** indicates $p < 0.0001$. DaLi box = dark-light box; EPM = elevated plus maze; OFT = open field test. Data points represent individual experimental animals. Error bars indicate mean ± SEM.

5.1.3 SCN-*Bmal1*-KD animals do not display behavioral despair or helpless behavior

The SCN has been involved in the regulation of mood. SCN rhythm downregulation in SCN-*Bmal1*-KD animals was previously shown to result in behavioral despair and helplessness [85]. To reaffirm the coexistence of mood-related and metabolic phenotypes in the same mouse, affect-related phenotypes were re-assessed in SCN-*Bmal1*-KD animals in this project. SCN-*Bmal1*-KD animals in this project evidence no signs of behavioral despair in the TST. The time immobile, transitions between mobile and immobile episodes as well as the latency to the first immobile episode is not significantly altered by *Bmal1* KD in the SCN (Figure 12 A – C, Table S5). Further, the lack of a behavioral despair phenotype in SCN-*Bmal1*-KD persists during a more chronic downregulation of SCN rhythms in the same animals (Figure 12 D – F, Table S6). In the LH test, SCN rhythm downregulation does not appear to alter escape latencies or failures; however, statistical assessment was not feasible due to low n-numbers (Figure 12 G, H, Table S6). Since animals were sacrificed after LH testing, helpless behavior could not be re-tested following a more prolonged SCN rhythm downregulation in the same animals. Nevertheless, LH testing during a later time point after stereotactic injections using other experimental animals yields comparable results. Indeed, 16 – 19 weeks after stereotactic injection, there is no statistically significant effect of *Bmal1* KD in the SCN on escape latencies or failures (Figure 12 I, J, Table S5). Thus, likewise to the reduced anxiety-related phenotype of SCN-*Bmal1*-KD animals, the absence of behavioral despair and helplessness persists during a more chronic SCN rhythm downregulation.

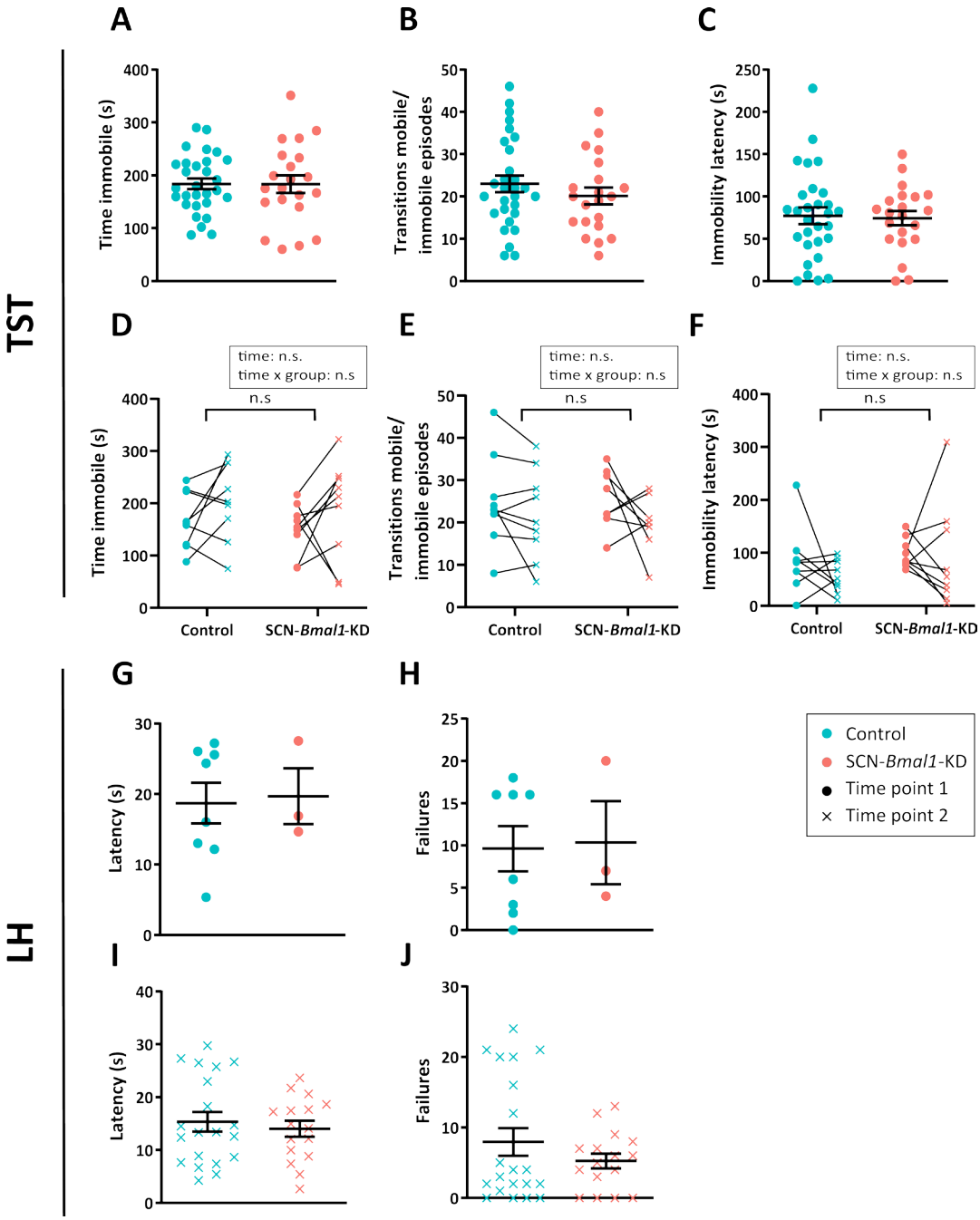

Figure 12. SCN-*Bmal1*-KD animals do not exhibit behavioral despair or helpless behavior. To assess mood-related phenotypes, SCN-*Bmal1*-KD and control animals were tested in the TST and the LH test. Results of the first TST (3 – 5 weeks after stereotactic injection): (A) time immobile, (B) transitions between mobile and immobile episodes and (C) immobility latency (control: n = 29, SCN-*Bmal1*-KD: n = 21). In a subset of animals (n = 9 per experimental group) behavioral despair was re-assessed 16 weeks after stereotactic injection. Comparison of the first and second TST: (D) time immobile, (E) transitions between mobile and immobile episodes and (F) immobility latency. Two-way repeated measures ANOVAs were performed with the time and interaction effect indicated for each parameter. The group effect (control vs. SCN-*Bmal1*-KD) is indicated above the comparison bar between the experimental groups. First LH test (7 – 8 weeks after stereotactic injection): (G) escape latency and (H) escape failure (control: n = 8, SCN-*Bmal1*-KD: n = 3). The n - value for the SCN-*Bmal1*-KD group was too small for statistical analyses. Second LH test (16 – 19 weeks after stereotactic injection): (I) escape latency and (J) escape failure (control: n = 20, SCN-*Bmal1*-KD: n = 16). In panels A, B, C, I and J, the control and SCN-*Bmal1*-KD group were statistically compared using unpaired t-tests. Details on the statistical tests and n-values can be found in Table S5 and S6. LH = learned helplessness; TST = tail suspension test. Data points represent individual experimental animals. Error bars indicate mean ± SEM.

5.1.4 Reward-related behavior is enhanced in SCN-*Bmal1*-KD animals

Affective disorders are linked to changes in the reward system and clock mutants display reward-related phenotypes [148, 215-217]. Thus, we next assessed reward-related behavior following SCN rhythm downregulation by measuring different aspects of positive valence using the IntelliCage system. The positive valence system is involved in the responses to positive events, including the sustained responsiveness to reward and reward learning [209, 218]. These two parameters can be assessed in the IntelliCage system by measuring sucrose preference and place preference, respectively. In the sucrose preference test, SCN-*Bmal1*-KD display increased total licks, with enhanced sucrose but decreased water licks, resulting in an overall higher sucrose preference than control animals (Figure 13 A – D, Table S7). Indeed, when given the choice, SCN-*Bmal1*-KD nearly only consume sucrose solution and close to no water, indicative of a hyperhedonic state. The sustained responsiveness to a reward — in this case sugar — of SCN-*Bmal1*-KD animals reflects an alteration in the positive valence system. Equally, reward learning, assessed by measuring place learning in the IntelliCage system, is increased in SCN-*Bmal1*-KD animals (Figure 13 E). Thus, SCN-*Bmal1*-KD animals evidence changes in the positive valence system as evidenced by their hyperhedonic state and their increased reward learning.

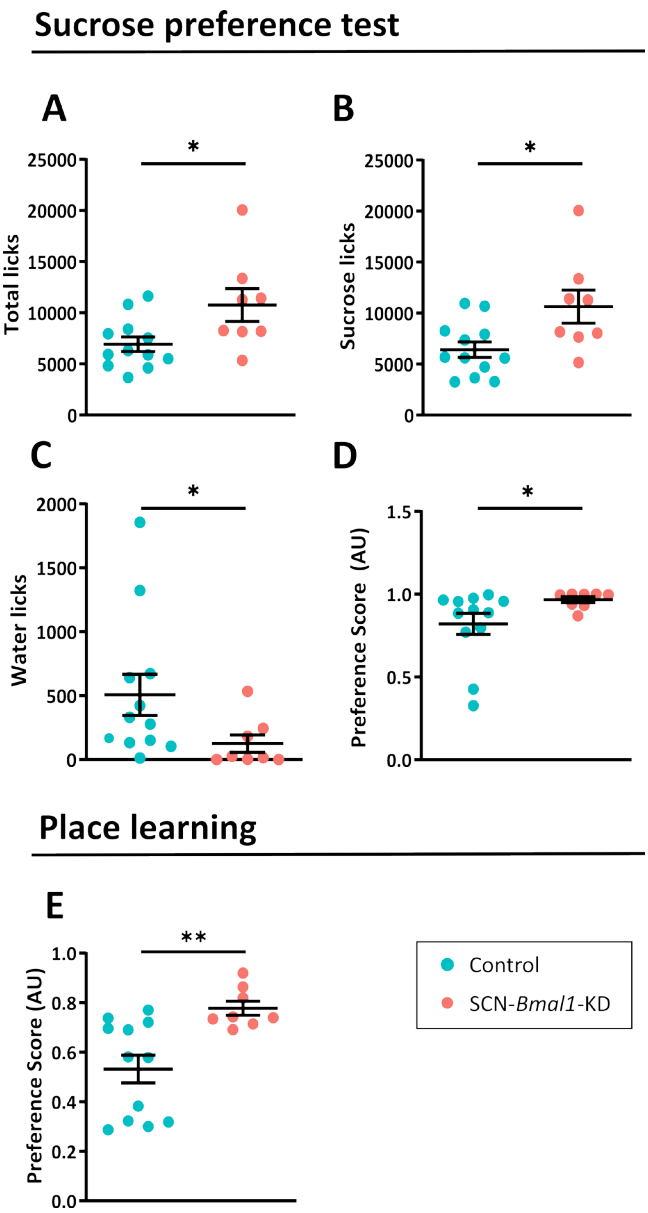

Figure 13. SCN-*Bmal1*-KD animals exhibit enhanced reward-related behavior. SCN-*Bmal1*-KD and control animals were tested in the IntelliCage system to assess parameters of the positive valence system. Sucrose preference test: (A) total licks, (B) sucrose licks, (C) water licks and (D) sucrose preference score. (E) Place learning score. For all tests n = 12 (control) and n = 8 (SCN-*Bmal1*-KD). The control and SCN-*Bmal1*-KD group were statistically compared using an unpaired t-test or a Mann-Whitney U test when normality was not met. * indicates $p < 0.05$; ** indicates $p < 0.01$. Details on the statistical tests and n-values can be found in Table S7. AU = arbitrary unit. Data points represent individual experimental animals. Error bars indicate mean ± SEM.

5.1.5 SCN-*Bmal1*-KD animals do not display cognitive changes

Mental disorders are often associated with cognitive impairments and a role of the SCN in regulating cognitive functions has been discussed [219, 220]. Thus, cognitive performance of SCN-*Bmal1*-KD animals was tested for the first time using the Y-maze and the IntelliCage system. In the Y-maze task, SCN-*Bmal1*-KD and control animals perform similar amounts of spontaneous alternations, a measure for short-term spatial working memory (Figure 14 A, Table S7). Further, SCN-*Bmal1*-KD animals show no changes in reversal learning or serial reversal learning in the IntelliCage system (Figure 14 B, C), arguing for unaltered cognition following SCN rhythm downregulation.

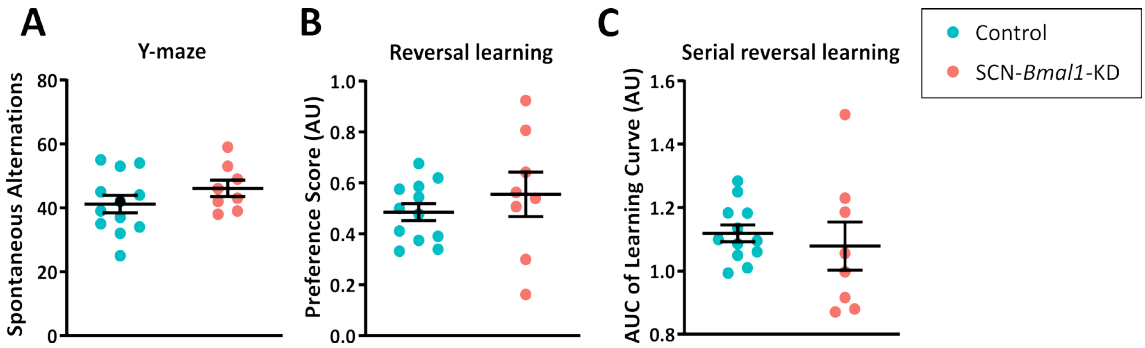

Figure 14. SCN-*Bmal1*-KD animals exhibit unaltered cognition. SCN-*Bmal1*-KD and control animals were tested in the Y-maze and IntelliCage system to assess parameters of cognition. (A) Spontaneous alternations in the Y-maze. (B) Reversal learning and (C) serial reversal learning in the IntelliCage system. For all tests n = 12 (control) and n = 8 (SCN-*Bmal1*-KD). The control and SCN-*Bmal1*-KD group were statistically compared using an unpaired t-test. Details on the statistical tests and n-values can be found in Table S7. AU = arbitrary unit; AUC = area under the curve. Data points represent individual experimental animals. Error bars indicate mean ± SEM.

5.1.6 SCN-*Bmal1*-KD animals display increased weight gain during the first weeks after stereotactic injection

The main hypothesis of project 1 was that downregulation of molecular SCN rhythms negatively affects behavior and metabolism concomitantly. Thus, the same animals that were characterized behaviorally also underwent metabolic characterization. Disruption of SCN rhythms causes animals to gain weight rapidly following *Bmal1* KD in the SCN (Figure 15 A, B, Table S8 – S10). For instance, 3 weeks after stereotactic injection, SCN-*Bmal1*-KD animals display an increased percent body weight gain, with 26.80 ± 16.48 % (mean ± SD) compared to 13.48 ± 9.309 % (mean ± SD) in control animals. However, whilst control animals continue to steadily increase body weight, the weight gain curve of SCN-*Bmal1*-KD animals plateaus. At around 6 weeks after stereotactic injection, the weight of SCN-*Bmal1*-KD and control animals reach a similar level (Figure 15 A, B). Analyzing two time windows separately (i.e., 0 – 6 weeks and 7 –17 weeks after stereotactic injection) confirms this observation statistically. During the first 6 weeks after stereotactic injection, a significant group effect underpins the increased weight gain of SCN-*Bmal1*-KD animals compared to their control littermates (Figure 15 C, Table S10). When analyzing the time frame of 7 – 17 weeks after stereotactic injection, a group effect is lacking, highlighting that SCN-*Bmal1*-KD and control animals reach a similar final weight after 6 weeks (Figure 15 D, Table S10). Importantly, the initial increased weight gain in SCN-*Bmal1*-KD is not related to altered food consumption over time following *Bmal1* KD (Figure 15 E, Table S8 – S10). At the time point of sacrifice, SCN-*Bmal1*-KD animals display similar percent gWAT and

iWAT compared to control animals (Figure 15 F, G, Table S11). However, there is a trend for a decrease in the percent BAT in SCN-*Bmal1*-KD animals (Figure 15 H).

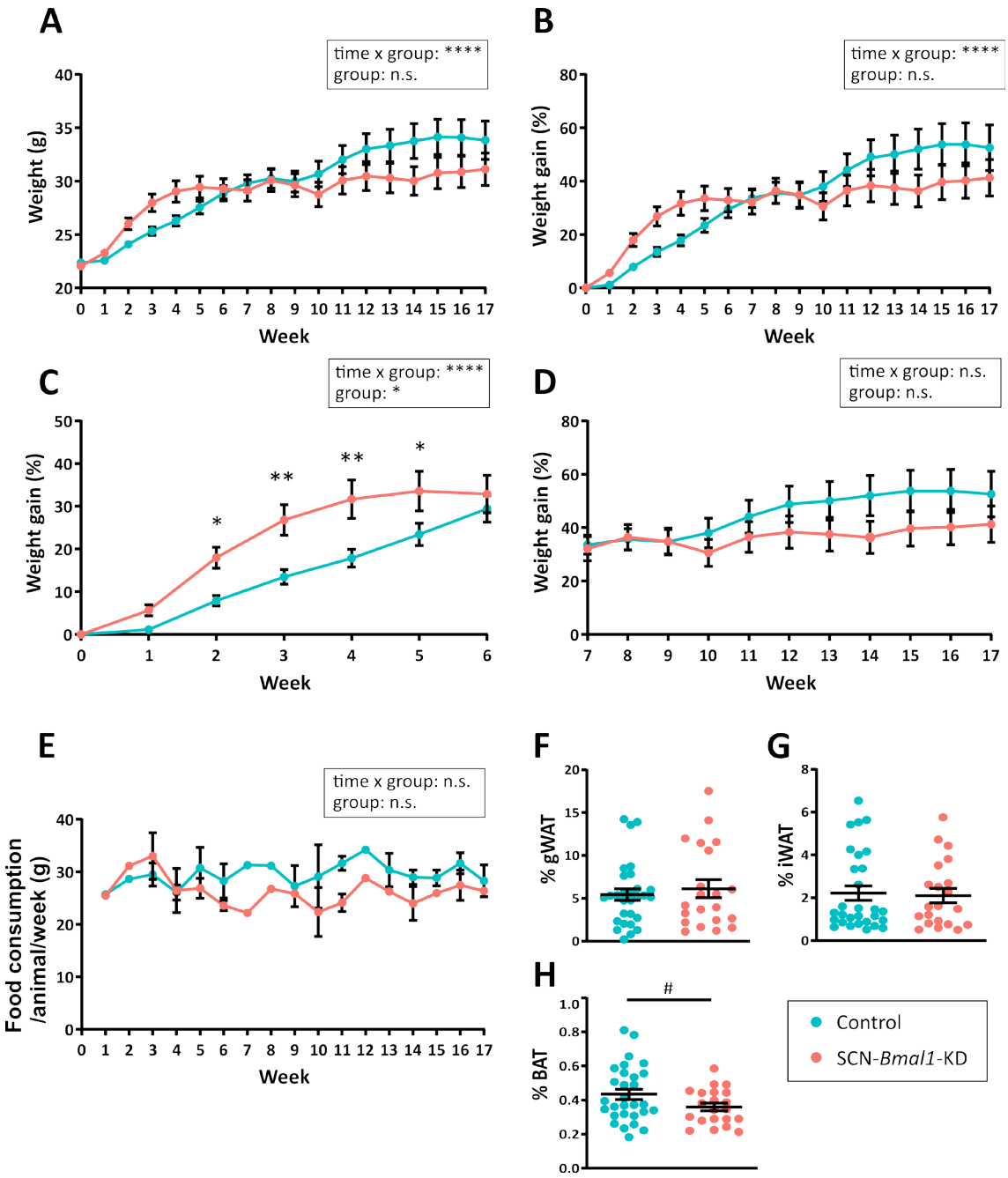

Figure 15. SCN-*Bmal1*-KD display altered weight gain without changes in overall food consumption. Body weight and food consumption of SCN-*Bmal1*-KD and control animals were measured weekly. Upon sacrifice, fat pads were isolated and weighed. (A) Curve of absolute weight over time. (B) Curve of percent weight gain over time. (C) Percent weight gain over the first 6 weeks after stereotactic injection. (D) Percent weight gain from week 7 – 17 after stereotactic injection. (E) Curve of food consumption per animal over time. (F) Percent gWAT, (G) percent iWAT and (H) percent BAT of total body weight at sacrifice. For panels A – D and F – H, n = 21 – 29 (control) and n = 18 – 21 (SCN-*Bmal1*-KD). For panel E, n= 1 – 2 (per time point per group). For panels A – E, the groups were compared using a two-way repeated measures ANOVA or a mixed-effects analysis when single values were missing. A significant effect of the experimental group is indicated by 'group', a significant interaction effect of the experimental group and time is indicated by 'time x group'. Fisher's LSD post-hoc test followed by Bonferroni correction (control vs. SCN-*Bmal1*-KD) was performed for every week in panels A – E but yielded only significant effects for weeks 2, 3, 4 and 5 in panel

C, indicated by (*) or (**). For panels F – H, the control and SCN-*Bmal1*-KD group were statistically compared using an unpaired t-test or a Mann-Whitney U test when normality was not met. Data points represent individual experimental animals. n.s. = not significant; # indicates $p < 0.1$; * indicates $p < 0.05$; **** indicates $p < 0.0001$. Details on the statistical tests and n-values can be found in Table S8 – S11. BAT = brown adipose tissue; gWAT = gonadal white adipose tissue; iWAT = inguinal white adipose tissue. Error bars indicate mean ± SEM.

5.1.7 *Bmal1* KD in the SCN results in strongly dampened locomotor activity and metabolic rhythms in 12:12 LD conditions

SCN-*Bmal1*-KD animals display altered body weight gain over time despite similar food consumption. To further explore metabolic changes in SCN-*Bmal1*-KD animals, mice were placed into metabolic cages during 12:12 LD conditions. In both, control and SCN-*Bmal1*-KD animals, a pattern of circadian locomotor activity rhythm is observed, with a peak of activity at the start of the dark phase. However, these locomotor rhythms are strongly attenuated in SCN-*Bmal1*-KD animals (Figure 16 A, B, Table S12, S13). A roughly 24-hour period can be detected following *Bmal1* KD in the SCN. Nevertheless, the robustness of the locomotor activity period is reduced in SCN-*Bmal1*-KD animals as evidenced by their reduced periodogram peak compared to control (Figure 16 C). Further, SCN-*Bmal1*-KD animals exhibit decreased overall locomotor activity (Figure 16 D, Table S14); most likely resulting from decreased activity during the dark phase (Figure 16 A). Similar results are observed for food and water consumption rhythms, which are strongly dampened following *Bmal1* KD in the SCN. For food consumption, to such an extent that significant rhythms are no longer detectable in SCN-*Bmal1*-KD animals (Figure 16 E – G, I – K). Although a water intake rhythm is still present in SCN-*Bmal1*-KD, the period of the rhythm is less robust compared to the control (Figure 16 K). Importantly, overall food and water intake do not differ between control and SCN-*Bmal1*-KD animals (Figure 16 H, L). Beyond rhythmicity of feeding and drinking behavior, RER and EE rhythms were also measured to assess differences in fuel utilization between SCN-*Bmal1*-KD and control animals. Whilst in control animals circadian RER and EE rhythms are detected, significant rhythms are no longer detectable in SCN-*Bmal1*-KD animals (Figure 16 M – O, Q – S). Interestingly, the 24-hour mean levels of RER and EE are not significantly different between control and SCN-*Bmal1*-KD animals (Figure 16 P, T). Thus, whilst overall levels of metabolic parameters are unchanged in SCN-*Bmal1*-KD animals, locomotor activity and metabolic rhythms are dampened, in some cases to such an extent that significant rhythms are no longer detectable in SCN-*Bmal1*-KD animals.

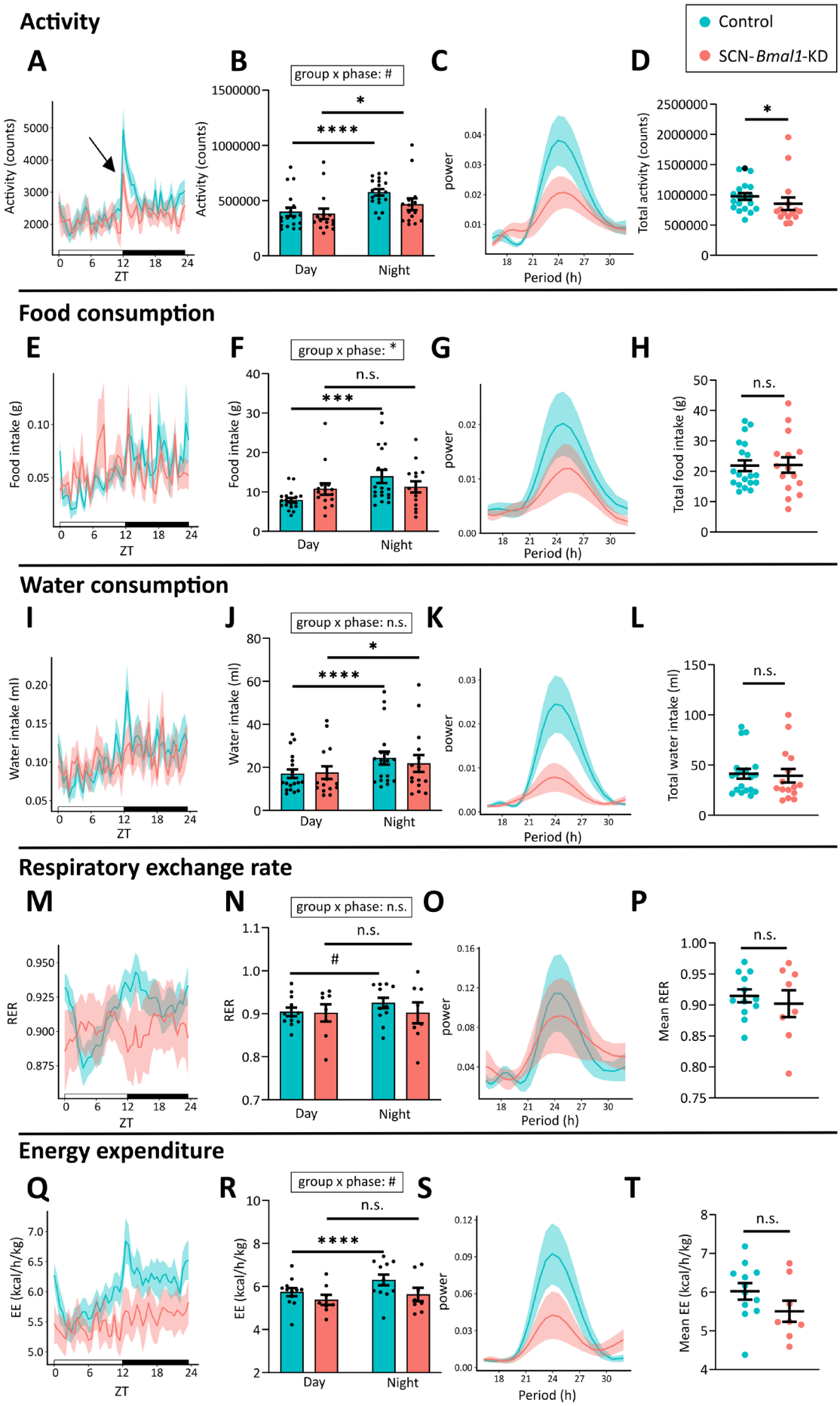
Activity
Control
SCN-Bmal1-KD
A
B
C
D
group x phase: #
Activity (counts)
ZT
Day
Night
power
Period (h)
Total activity (counts)
Food consumption
E
F
G
H
group x phase: *
Food intake (g)
Total food intake (g)
Water consumption
I
J
K
L
group x phase: n.s.
Water intake (ml)
Total water intake (ml)
Respiratory exchange rate
M
N
O
P
RER
Mean RER
Energy expenditure
Q
R
S
T
EE (kcal/h/kg)
Mean EE (kcal/h/kg)
n.s.

Figure 16. SCN-*Bmal1*-KD animals exhibit dampened locomotor activity and metabolic rhythms. SCN-*Bmal1*-KD animals were placed into metabolic cages to measure their locomotor activity, food and water consumption, RER, and EE. After 2 days of acclimatization, all parameters were recorded for 4 days. Animals were kept in 12:12 LD conditions. (A, E, I, M, Q) Recordings from the metabolic cages for locomotor activity (A), food consumption (E), water consumption (I), RER (M) and EE (Q). Averages from 4 days of recording across each experimental group are plotted over a 24-hour day. The shaded area represents ± SEM. The black arrow in (A) points towards the bout of locomotor activity of control and SCN-*Bmal1*-KD animals at the start of the dark phase. (B) Overall locomotor activity during the light phase (day) versus overall locomotor activity during the dark phase (night) is summed across the 4 days of recording and plotted for each experimental group. (F, J) Overall food consumption (F) and overall water consumption (J) during the day versus during the night were added across the recoding time and are plotted for each experimental group. (N, R) For each experimental group, the mean RER (N) and the mean EE (R) during the day versus during the night are plotted. For B, F, J, N, R the results for the interaction effect of experimental group and phase of a two-way repeated measures ANOVA are indicated by 'group x phase'. The results from a Fisher's LSD post-hoc test followed by Bonferroni correction comparing control day vs. control night and SCN-*Bmal1*-KD day vs. SCN-*Bmal1*-KD night are indicated by the comparison bars. (C, G, K, O, S) Periodograms for each experimental group for locomotor activity (C), food consumption (G), water consumption (K), RER (O) and EE (S). (D) Total locomotor activity, (H) total food consumption and (L) total water consumption over the 4 days of recording. (P) Mean RER and (T) mean EE across the 4 days of recording. For panels D, H, L, P and T, the control and SCN-*Bmal1*-KD group were statistically compared using an unpaired t-test or a Mann-Whitney U test when normality was not met. Control: n = 19 or 12, SCN-*Bmal1*-KD: n = 15 or 8. Due to technical issues the n-values for RER and EE are lower. n.s. = not significant; # indicates $p < 0.1$; * indicates $p < 0.05$; *** indicates $p < 0.001$; **** indicates $p < 0.0001$. Details on the n-values can be found in Tables S12 – S14. EE = energy expenditure; RER = respiratory exchange rate. The data points in panels B, D, F, H, J, L, N, P, R, and T represent individual experimental animals. Error bars indicate mean ± SEM.

5.1.8 Glucose homeostasis is altered in SCN-*Bmal1*-KD mice

To assess the impact of SCN rhythm downregulation on glucose homeostasis, SCN-*Bmal1*-KD animals were subjected to a GTT and ITT. During the GTT, SCN-*Bmal1*-KD animals exhibit a reduced response to the glucose injection (Figure 17 A, Table S15). This increased glucose tolerance of SCN-*Bmal1*-KD animals is further supported by their lowered AOC (Figure 17 B, Table S16). Strikingly, during the GTT, SCN-*Bmal1*-KD animals exhibit significantly reduced baseline starvation glucose levels (Figure 17 C). During the ITT, SCN-*Bmal1*-KD mice appear to have an increased glucose response to the insulin injection, suggesting a greater insulin sensitivity (Figure 17 D, Table S15). Nonetheless, similar to the observations during the GTT, SCN-*Bmal1*-KD mice exhibit significantly reduced baseline glucose levels during the ITT (Figure 17 E). This can influence the result of two-way repeated measures ANOVA testing. The AOC corrects for such baseline glucose differences and is thus deemed a more reliable measure for characterizing differing insulin sensitivities [221]. The AOC for the ITT is not significantly changed in SCN-*Bmal1*-KD animals, arguing for an overall unaltered insulin sensitivity following SCN rhythm downregulation (Figure 17 F, Table S16). Similar to the behavioral tests characterizing

anxiety- and mood-related behavior, glucose and insulin tolerance were re-assessed in a subset of animals at a later time point after stereotactic injection to investigate the impact of a chronic SCN rhythm downregulation. There is no effect of time after injection on the results of the GTT and ITT (Figure 17 G – J, Table S17). Thus, the increased glucose tolerance, unaltered insulin sensitivity and hypoglycemia of SCN-*Bmal1*-KD animals during starvation does not change during a more chronic KD of *Bmal1* in the SCN. Thus, the alterations in glucose homeostasis of SCN-*Bmal1*-KD animals are established within 4 – 8 weeks after stereotactic injection and persist over time after SCN rhythm downregulation.

Since SCN-*Bmal1*-KD animals display hypoglycemia following starvation, the question arose whether glucose levels under *ad libitum* feeding and over the course of 24 hours are also altered. Interestingly, as during starvation, SCN-*Bmal1*-KD animals display lower glucose levels over the course of the day during *ad libitum* feeding. This hypoglycemia in SCN-*Bmal1*-KD is even more apparent during the dark phase, since control animals display an increase in glucose levels compared to the light phase – an effect, which is not detected in SCN-*Bmal1*-KD animals (Figure 17 K, Table S18, S19). Indeed, in SCN-*Bmal1*-KD animals there is no significant difference in the glucose levels during the dark vs. light phase suggesting that *Bmal1* KD in the SCN might result in a loss of blood glucose rhythms during *ad libitum* feeding (Figure 17 L).

Overall, SCN-*Bmal1*-KD animals display altered glucose tolerance and consistently exhibit a hypoglycemia phenotype – under fasted and *ad libitum* feeding conditions – together with a potential loss of an endogenous glucose rhythm under non-fasted conditions.

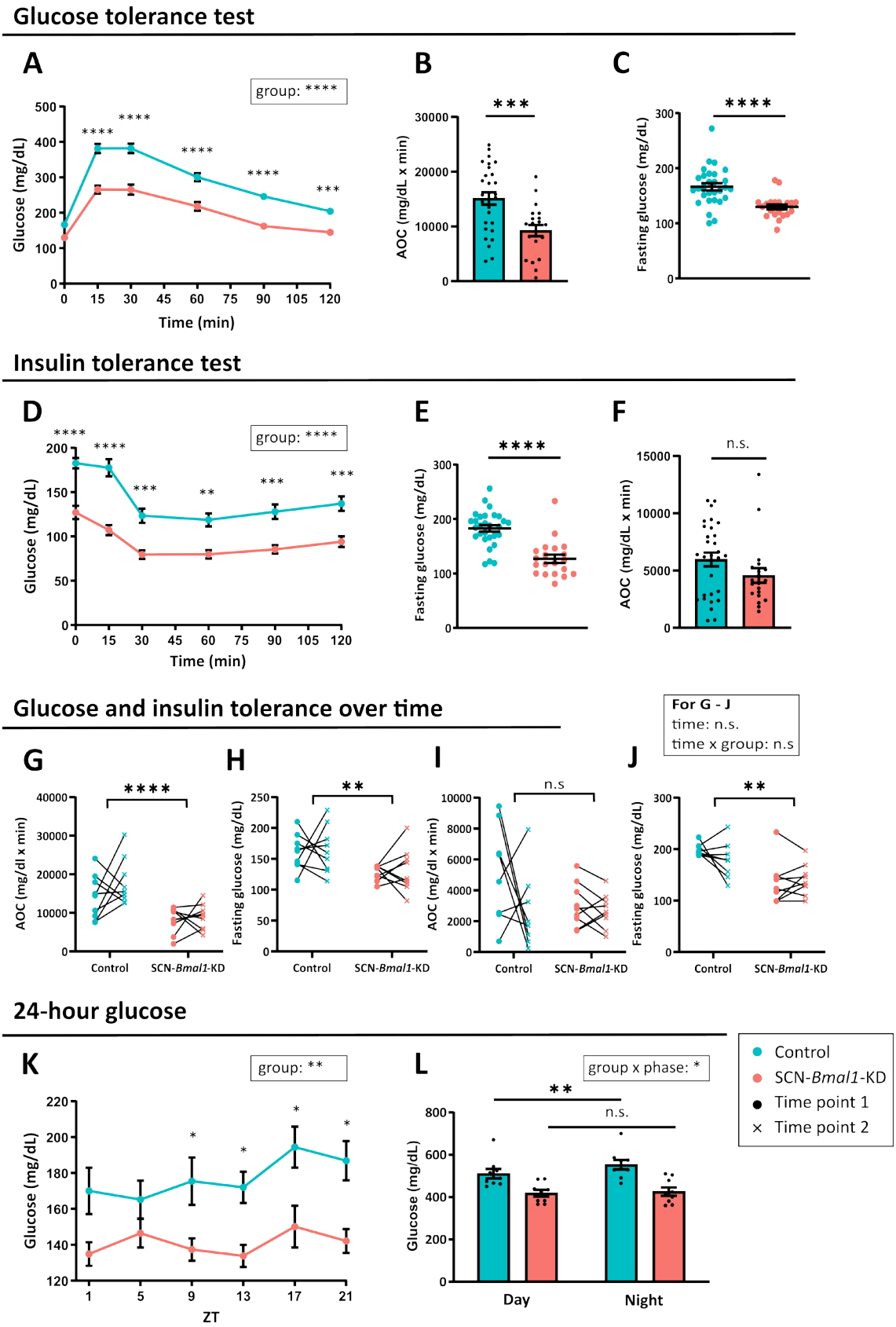

Figure 17. SCN-*Bmal1*-KD animals display altered glucose homeostasis. SCN-*Bmal1*-KD animals were subjected to two GTTs and ITTs. Furthermore, endogenous glucose levels were measured over the 24-hour day during *ad libitum* feeding conditions. First GTT at 4 – 6 weeks after stereotactic injection (control: n = 29; SCN-*Bmal1*-KD: n = 21): (A) glucose curve during the GTT, (B) area of the glucose curve and (C) glucose levels after 6 hours of fasting (i.e., time point '0 min' of GTT). First ITT at 5 – 7 weeks after stereotactic injection (control: n = 29; SCN-*Bmal1*-KD: n = 20): (D)

glucose curve during the ITT, (E) glucose levels after 4 hours of fasting (i.e., time point '0 min' of ITT) and (F) area of the glucose curve. For panels A and D, the groups were compared using a two-way repeated measures ANOVA where a significant effect of the experimental group is indicated by 'group'. The result of Fisher's LSD post-hoc test followed by Bonferroni correction, comparing control vs. SCN-*Bmal1*-KD, is indicated above every time point assessed. For panels B, C, E and F, the control and SCN-*Bmal1*-KD group were statistically compared using an unpaired t-test or a Mann-Whitney U test when normality was not met. In a subset of animals, the GTT and ITT were performed again at 17 weeks after stereotactic injection (n = 8 – 9 per experimental group). Comparison of first and second GTT and ITT: (G) AOC of the glucose curve during the GTT, (H) fasting glucose during the GTT, (I) AOC of the glucose curve during the ITT and (J) fasting glucose during the ITT. Two-way repeated measures ANOVAs were performed with the time and interaction effect indicated. The group effect (control vs. SCN-*Bmal1*-KD) is indicated above the comparison bar between the experimental groups. (K) Glucose levels under *ad libitum* feeding over the 24-hour cycle and (L) Cumulative day glucose vs. cumulative night glucose levels (n = 9 per experimental group). For panel K, statistical analyses were performed like in A and D. For panel L, a two-way repeated measures ANOVA was conducted, and the significant interaction effect of the experimental group and phase is indicated by 'group x phase'. Comparison bars indicate the results of the Fisher's LSD post-hoc test followed by Bonferroni correction for control animals and SCN-*Bmal1*-KD animals. Data points represent individual experimental animals. n.s. = not significant; ** indicates $p < 0.01$; *** indicates $p < 0.001$; **** indicates $p < 0.0001$. Details on the statistical tests and n-values can be found in Table S15 – S19. AOC = area of the curve. Error bars indicate mean ± SEM.

5.1.9 Downregulation of SCN rhythms affects downstream circadian oscillators involved in mood- and anxiety regulation and metabolic functions

The SCN, as the master pacemaker of the circadian system, largely affects physiology through its impact on subordinate clocks. Thus, the observed comorbid deficits in behavioral and metabolic processes in SCN-*Bmal1*-KD animals were likely mediated through alterations in downstream oscillators governing these processes. Given this, the impact of SCN rhythm downregulation on circadian oscillators involved in mood- and anxiety regulation (PAG and lateral hypothalamus) and metabolism (liver and lateral hypothalamus) was determined.

The PAG has been linked to anxiety-related responses and reward-seeking behavior, receives direct projections from the SCN and expresses stable circadian rhythms *in vitro* [120, 222, 223]. Thus, we wondered how downregulated SCN rhythms may affect PAG explant rhythms. The amplitude of PER2::LUC rhythms of PAG slices is significantly reduced following *Bmal1* KD in the SCN (Figure 18 A, Table S1). Further, SCN-*Bmal1*-KD animals display a significantly increased proportion of non-rhythmic PAG slices compared to control (Figure 18 B). To ensure the absence of ectopic *Bmal1* shRNA expression in the PAG, GFP expression was examined. No GFP expression was observed in PAG slices, indicating the absence of shRNA expression in the PAG (data not shown). Due to the low number of rhythmic PAG slices of SCN-*Bmal1*-KD animals

(n = 1), the period and phase of PER2::LUC rhythms could not be statistically assessed (Figure 18 C, D).

The lateral hypothalamus is a brain region that contains the orexin (ORX) neuronal system, which is involved in mood and metabolic regulation [22]. Expression of *Ppox*, which encodes the common precursor peptide of ORX-A and -B [224], is under circadian control [225]. Moreover, ORX rhythms are abolished in SCN-lesioned animals and evidence suggests a direct projection from the SCN to ORX neurons [226-228]. Thus, we next examined the impact of downregulated SCN rhythms on *Ppox* expression in the lateral hypothalamus. *Bmal1* KD in the SCN does not alter overall levels of *Ppox* at ZT3 – 4 (Figure 18 E). Interestingly, control animals evidence a significant positive correlation between the SCN amplitude and *Ppox* levels (Figure 18 F). This correlation is not detectable in SCN-*Bmal1*-KD animals (Figure 18 G).

Lastly, the rhythmicity of the liver, a metabolically active organ, was assessed. Visual examination of liver PER2::LUC rhythms does not suggest any marked differences in rhythmicity (i.e., amplitude, period and phase) between liver slices of SCN-*Bmal1*-KD and control animals (Figure 18 H – J). However, it should be noted that low n-numbers following exclusion of animals with unsuccessful stereotactic injection, did not allow statistical assessment.

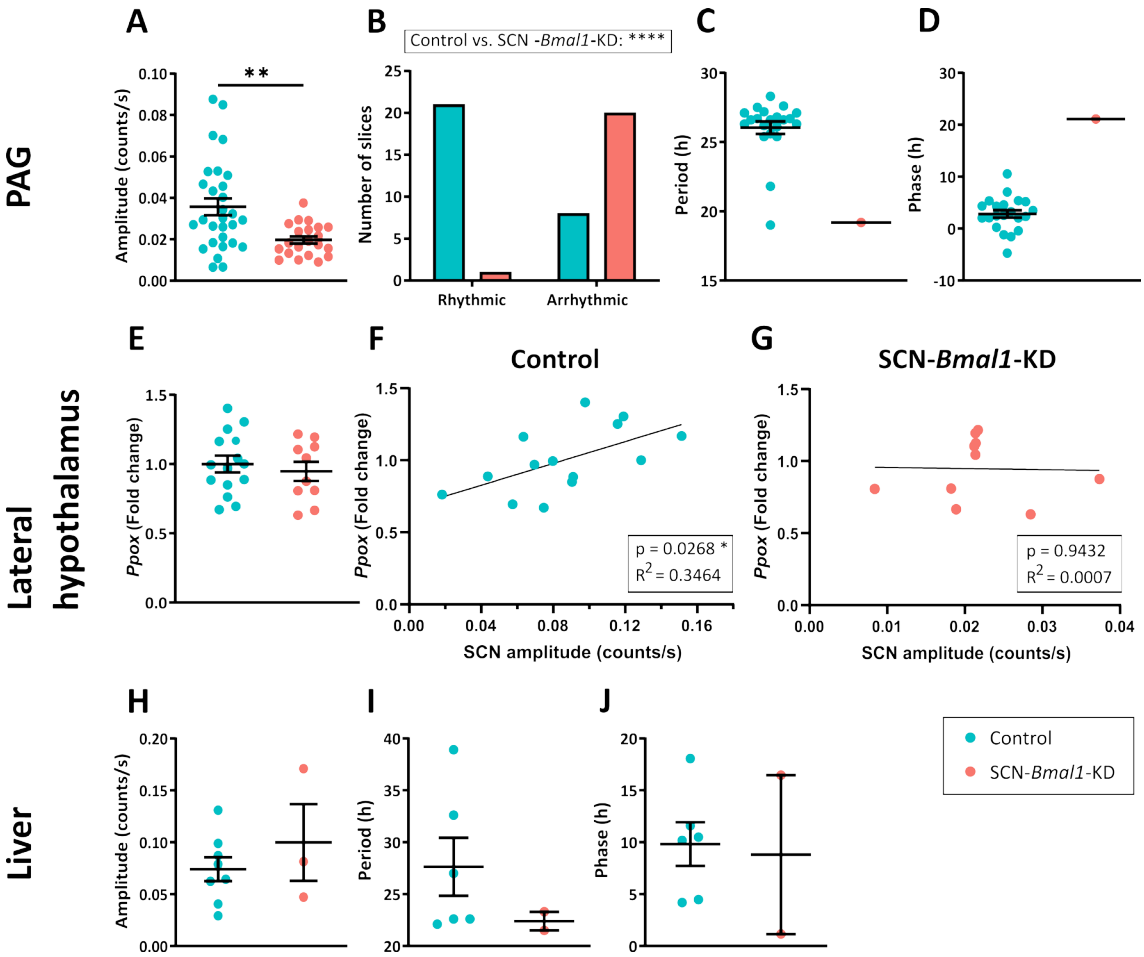

Figure 18. Downregulation of SCN rhythms affects downstream circadian oscillators. Upon sacrifice at ZT3 – 4, PAG and liver slices from experimental animals were collected and their rhythmicity assessed. Lateral hypothalamus slices were also collected and *Ppox* expression determined. Comparison of PER2::LUC rhythms of PAG slices of SCN-*Bmal1*-KD and control animals: (A) normalized amplitude of PER2::LUC rhythms (unpaired t-test, control: n = 29 and SCN-*Bmal1*-KD: n = 21), (B) number of rhythmic and arrhythmic PAG slices (Fisher's exact test, control: 21 rhythmic slices and 8 non-rhythmic slices, SCN-*Bmal1*-KD: 1 rhythmic slice and 20 non-rhythmic slices), (C) period and (D) phase of PAG PER2::LUC rhythms. Comparison of *Ppox* expression in the lateral hypothalamus of SCN-*Bmal1*-KD and control animals: (E) *Ppox* expression (unpaired t-test, control: n = 14 and SCN-*Bmal1*-KD: n = 10). (F) Correlation of normalized SCN amplitude and *Ppox* expression in control animals (n = 14) and (G) SCN-*Bmal1*-KD animals (n = 10) (Pearson correlation coefficient). *Ppox* quantification was kindly performed by Dr. Charlotte Kling. Comparison of PER2::LUC rhythms of liver slices of SCN-*Bmal1*-KD and control animals: (H) normalized amplitude, (I) period and (J) phase of liver PER2::LUC rhythms. For panels C, D, H, I, and J, n-values were too small for statistical comparisons. Data points represent explants from individual experimental animals. * indicates $p < 0.05$; ** indicates $p < 0.01$; **** indicates $p < 0.0001$. Details on the statistical tests and n-values can be found in Table S1. PAG = periaqueductal gray. Error bars indicate mean ± SEM.

5.2 Sex-specific behavioral and metabolic phenotypes following light-induced shift work conditions in mice

5.2.1 The shift work light paradigm leads to constant re-entrainment with sex-specific adaptation of locomotor activity to alternating light cycles

The primary aim of project 2 was to implement a shift work light paradigm to evaluate the behavioral and metabolic consequences of an environmental circadian disruption. To ensure that the chosen shift work light paradigm achieves the desired circadian disruption, locomotor adaptation to alternating light cycles in the shift work light paradigm was assessed in a first cohort. As expected, control animals of both sexes entrain to the rhythmic 12:12 LD cycle (Figure 19 A, B, S4, S5). Upon exposure to the shift work-mimicking alternating light cycles, both, male and female mice constantly try to re-entrain to the given light cycle (Figure 19 C, D, S6, S7). Two-way ANOVA testing reveals an effect of sex on the overall locomotor activity with female mice displaying increased activity compared to males. Moreover, shift work conditions reduce the overall locomotor activity with male and female shift work animals displaying decreased activity compared to their respective sex-matched controls (Figure 19 E, Table S20). Interestingly, there is a significant interaction effect of shift work and sex on the locomotor activity nocturnality score. Female shift work animals display a significantly decreased activity nocturnality score compared to their sex-matched controls – an effect, which is also present but not as pronounced in male animals (Figure 19 F, Table S20).

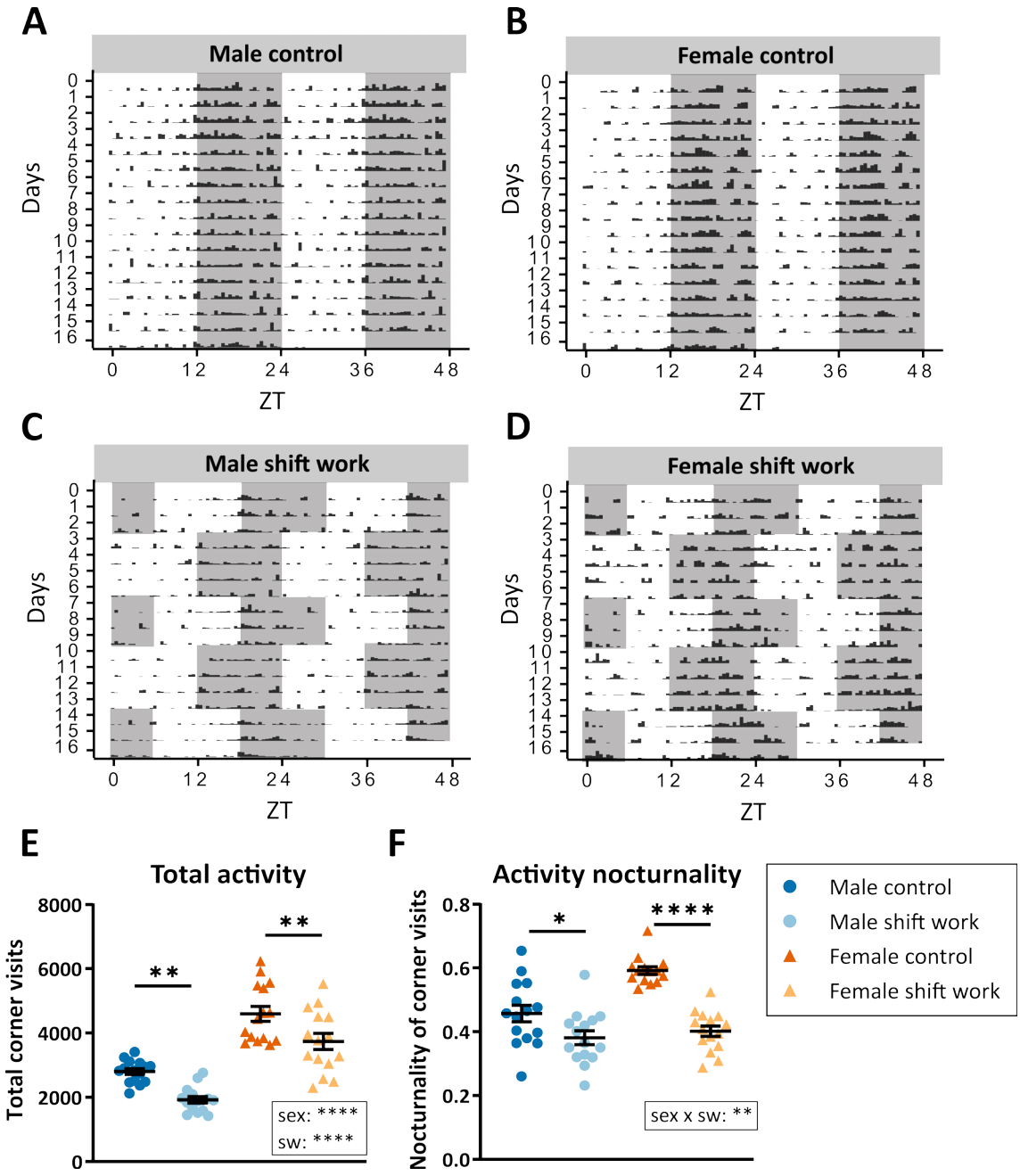

Figure 19. Sex-specific re-entrainment of locomotor activity to alternating light cycles. Male and female animals were placed into the IntelliCage system and subjected to either a standard 12:12 LD cycle (control) or to alternating light cycles (shift work). Corner visits were tracked as a proxy for the animal's locomotor activity. (A – D) Representative double-plotted actograms for (A) male control, (B) female control, (C) male shift work and (D) female shift work. The shading of the double-plotted actograms represents the LD cycle that the animal was subjected to. The black bars of the actograms indicate the locomotor activity of the respective animal. Double-plotted actograms of all experimental animals can be found in Figure S4 – S7. (E) Overall corner visits. (F) Locomotor activity nocturnality score. In panels E and F, two-way ANOVAs were conducted where a significant sex effect is indicated by 'sex', a significant shift work effect is indicated by 'sw' and a significant interaction effect between sex and shift work is indicated by 'sex x sw'. A Fisher's LSD post-hoc test with Bonferroni correction was used to compare the following groups: male control vs. male shift work and female control vs. female shift work. The results of these post-hoc comparisons are indicated by the black comparison bars. Data points in panels E and F represent individual experimental animals (male control: n = 15; male shift work: n = 15; female control: n = 14 – 15; female shift work: n = 15). * indicates $p < 0.05$; ** indicates $p < 0.01$; **** indicates $p < 0.0001$. Details on statistical tests and n-values can be found in Table S20. Error bars indicate mean ± SEM.

5.2.2 Light-induced shift work conditions lead to an anxiety-like phenotype in female but not male mice

A separate cohort of male and female animals was used for the characterization of comorbid behavioral and metabolic phenotypes following light-induced shift work conditions. To investigate anxiety-related behavior, all experimental animals were subjected to several behavioral tests. In the OFT, shift work conditions have no impact on the distance traveled, center entries or center time in neither of both sexes (Figure 20 A – C, Table S21, S22). There is a trend for an effect of sex on center time, with male mice spending more time in the center of the open field (Figure 20 C, Table S21, S22). In the EPM, a statistically significant interaction between the effects of shift work and sex is observed for open arm entries and time. Males exhibit a trend towards increased open arm entries during shift work conditions. On the contrary, in females, shift work conditions decrease open arm entries (Figure 20 D, Table S23, S24). Similarly, shift work conditions significantly decrease open arm time in female mice – an effect that is not observed in male mice (Figure 20 E, Table S23, S24). Further, a trend for an interaction between shift work and sex on the open arm distance is observed. Nonetheless, post-hoc testing does not reveal a significant difference between male or female shift work animals and their respective sex-matched controls (Figure 20 F, Table S23, S24). During the DaLi box test, female shift work animals exhibit a trend towards decreased entries into the light compartment – an effect, which is not detected in male animals (Figure 20 G, Table S23, S24). Although not robust to Bonferroni correction, female shift work animals display a trend for a reduced time in the light compartment compared to their sex-matched controls. In male animals, no difference between shift work and control animals is observed (Figure 20 H, Table S23, S24). Further supporting the sex-specific anxiety phenotype of female shift work animals in the EPM, shift work conditions cause females to travel less distance in the light compartment – an effect, which is not detected in males (Figure 20 I, S23, S24). To further characterize effects of shift work conditions on anxiety-like behavior, the transitions between mobile and immobile episodes were quantified in the OFT and TST. This parameter was assessed as a proxy for restlessness, which is often characterized as anxiety-like behavior. In the OFT and the TST, a significant interaction and a trend for an interaction between sex and shift work on restless behavior is observed, respectively (Figure 20 J, K, Table S21, S22). Female shift work animals exhibit increased restlessness compared to their sex-matched controls, although not reaching statistical significance in the OFT after Bonferroni correction. This effect of shift work conditions on restless behavior is not detected in male mice. Overall, behavioral testing reveals that light-induced shift work conditions lead to an anxiety-like phenotype in female but not male mice.

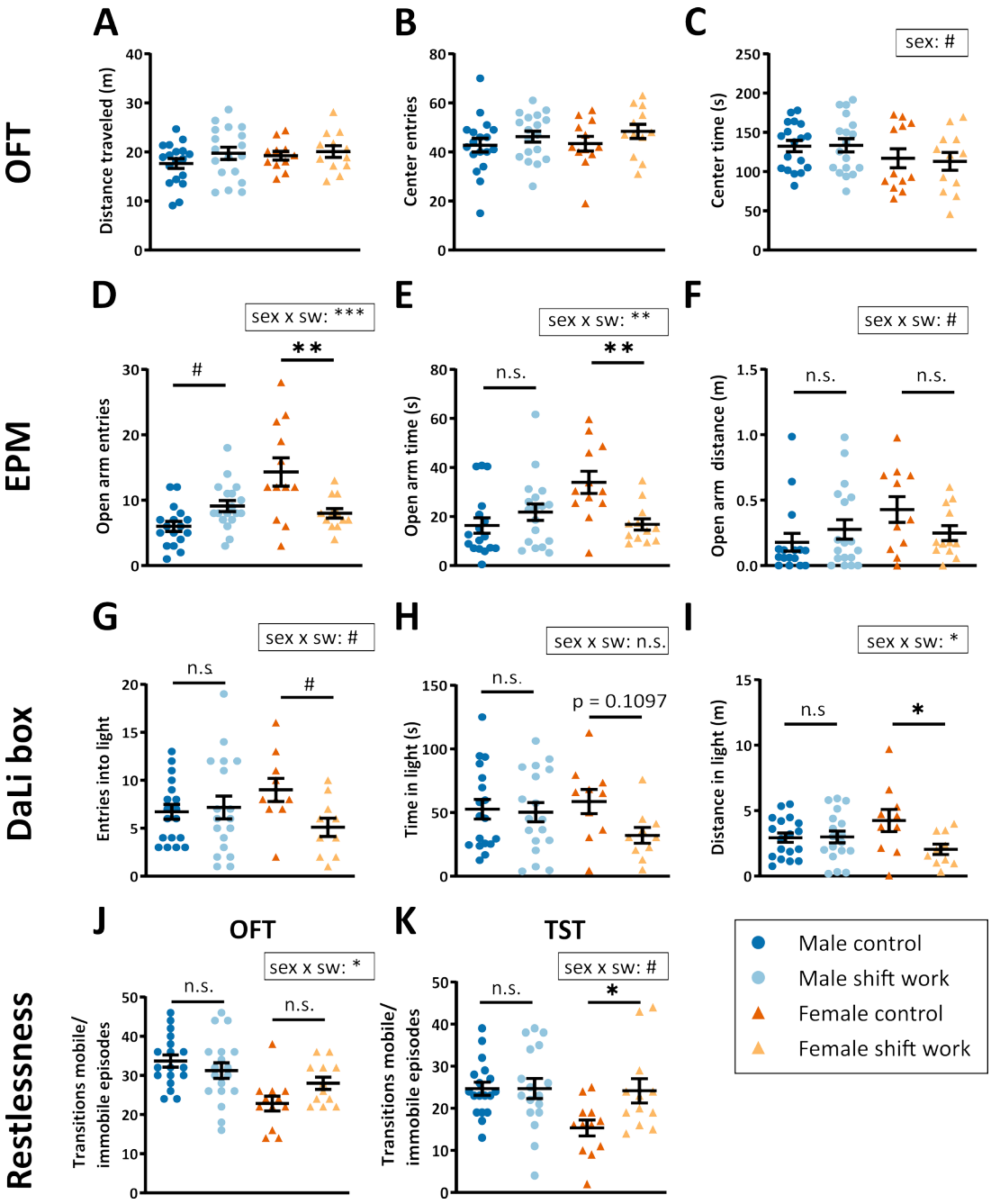

Figure 20. Light-induced shift work conditions result in anxiety-like behavior in female but not male mice. Animals were tested in the OFT, EPM, DaLi box test and TST to assess anxiety-like behavior. OFT: (A) distance traveled, (B) center entries and (C) center time. EPM: (D) open arm entries, (E) open arm time and (F) open arm distance. DaLi: (G) entries into the light compartment, (H) time in the light compartment and (I) distance traveled in the light. (J, K) Transitions between mobile and immobile episodes in the OFT (J) and the TST (K). For all parameters, two-way ANOVAs were conducted where a significant sex effect is indicated by 'sex' and a significant interaction effect between sex and shift work is indicated by 'sex x sw'. A Fisher's LSD post-hoc test with Bonferroni correction was used to compare the following groups: male control vs. male shift work and female control vs. female shift work. The results of these post-hoc comparisons are indicated by the black comparison bars. Data points represent individual experimental animals (male control: n = 17 – 18; male shift work: n = 17 – 18; female control: n = 10 – 12; female shift work: n = 10 – 12). n.s. = not significant; # indicates $p < 0.1$; * indicates $p < 0.05$; ** indicates $p < 0.01$; *** indicates $p < 0.001$. Details on statistical tests and n-values can be found in Table S21 – S24. DaLi box = dark-light box; EPM = elevated plus maze; OFT = open field test; TST = tail suspension test. Error bars indicate mean ± SEM.

5.2.3 Sex-specific effects of light-induced shift work conditions on helpless behavior but not on features of behavioral despair or anhedonia

Next, the effect of the shift work light paradigm on the development of depression-like behavior was investigated using the TST, sucrose preference test and LH paradigm. Neither in male nor female mice, shift work conditions affect behavioral despair quantified by the time immobile and immobility latency in the TST (Figure 21 A, B, Table S25, S26). Equally, the shift work light paradigm has no effect on anhedonia-like behavior assessed with the sucrose preference score (Figure 21 C). Of note, sex alone has an impact on the immobility time in the TST and sucrose preference with females displaying decreased immobility time and sucrose preference. In the LH paradigm the motivation to avoid an escapable electric shock is quantified. During LH testing, a statistically significant interaction between sex and shift work is observed for the escape latencies and failures (Figure 21 D, E, Table S25, S26). Male shift work animals exhibit significantly reduced escape latencies and failures compared to male controls (i.e., more motivation to escape the electric shock and thus less helpless behavior). In contrast, females display increased escape latencies and failures following shift work conditions, although this effect does not reach statistical significance during post-hoc testing. Thus, shift work conditions have a sex-specific effect on helpless behavior with male and female shift work animals displaying decreased and increased helplessness compared to their sex-matched controls, respectively. To test if the differences of LH results between the two sexes were the result of varying pain sensitivities, the animals' pain thresholds were determined. Females exhibit an increased pain threshold compared to males (Figure 21 F, Table S25, S26).

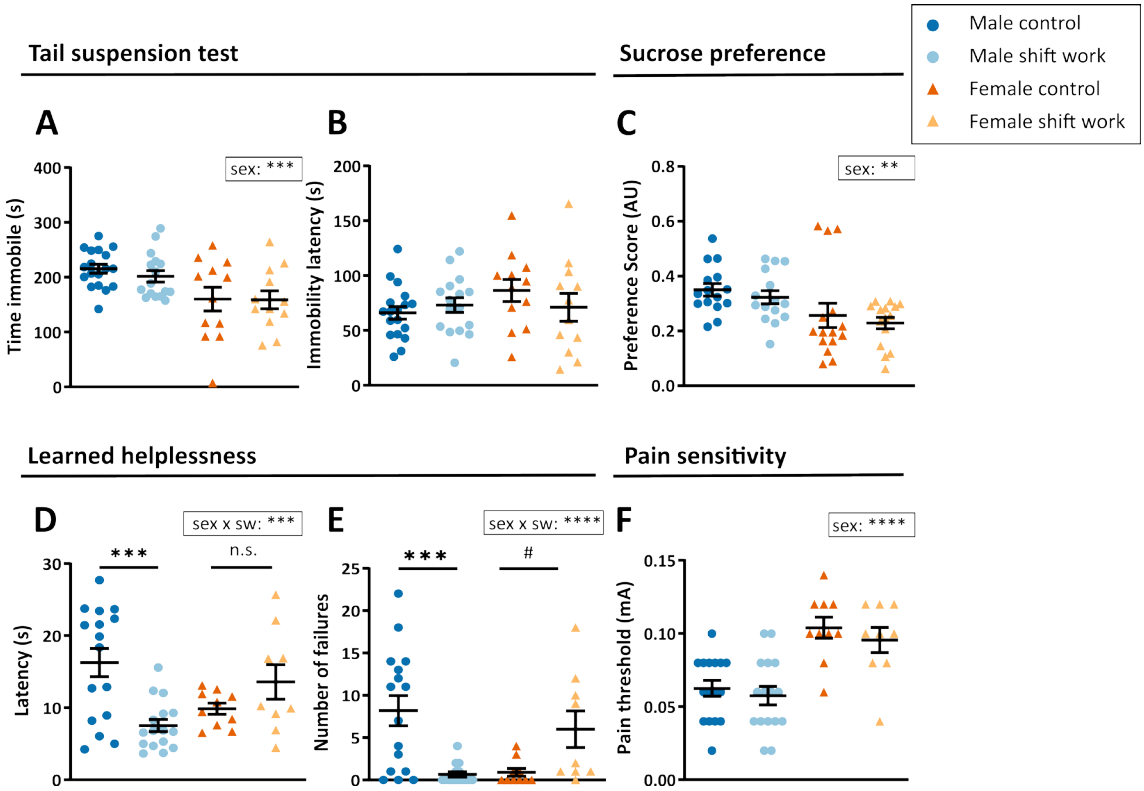

Figure 21. Sex-specific effects of light-induced shift work conditions on helpless behavior but not on behavioral despair or anhedonia. Animals were subjected to the TST, sucrose preference test, and LH paradigm to investigate effects on behavioral despair, anhedonia-like behavior, and helplessness. TST: (A) time immobile and (B) immobility latency. (C) Sucrose preference score. LH test: (D) Latency to escape the electrical shock and (E) failures to escape the electrical shock. (F) Electric shock intensity of pain threshold. For all parameters, two-way ANOVAs were conducted where a significant sex effect is indicated by 'sex' and a significant interaction effect between sex and shift work is indicated by 'sex x sw'. A Fisher's LSD post-hoc test with Bonferroni correction was used to compare the following groups: male control vs. male shift work and female control vs. female shift work. The results of these post-hoc comparisons are indicated by the black comparison bars. Data points represent individual experimental animals (male control: n = 15 – 18; male shift work; n = 15 – 16; female control: n = 10 – 15; female shift work: n = 9 – 15). n.s. = not significant; # indicates $p < 0.1$; ** indicates $p < 0.01$; *** indicates $p < 0.001$; **** indicates $p < 0.0001$. Details on statistical tests and n-values can be found in Table S25 and S26. Error bars indicate mean ± SEM.

5.2.4 Light-induced shift work conditions cause mild sex-specific metabolic alterations in mice

Shift work does not only affect mood and anxiety but has also been associated with metabolic disturbances [229]. Accordingly, the hypothesis of project 2 was that light-induced shift work conditions lead to comorbid behavioral and metabolic phenotypes in the same mouse. Therefore, the animals that were characterized behaviorally also underwent metabolic assessment. As expected, males displayed an increased body weight compared to females at the start of the shift work light paradigm. Importantly, there were no baseline weight differences

between male control and male shift work animals or between female control and female shift work animals (Figure 22 A, Table S27, S28). Upon exposure to the shift work light paradigm, shift work animals display overall a similar absolute weight gain compared to their sex-matched controls (Figure 22 B, Table S29, S30). Nonetheless, male shift work animals appear to have a steeper absolute weight gain compared to male controls. This effect is further highlighted by an interaction between the effects of sex and shift work on the percent weight gain over the weeks. Male shift work animals display an increased percent body weight gain compared to male controls – a shift work-induced effect, which is not detected in female mice (Figure 22 C, Table S30). Accordingly, only in males, shift work conditions result in a significantly increased percent body weight gain at sacrifice (Figure 22 D, Table S28). Interestingly, food consumption over the weeks is unchanged in shift work animals (Figure 22 E), suggesting that the increased weight gain in males following shift work conditions does not result from altered food consumption. As expected, there is an effect of sex on food consumption, with males ingesting more food, in line with their heavier body weights (Figure 22 E, Table S30). To assess if the shift work-induced weight gain in males results from increased fat depositions, the percentages of gWAT, iWAT and BAT at sacrifice were quantified. Surprisingly, the percentages of gWAT, iWAT and BAT are unchanged in shift work animals (Figure 22 F – H, Table S28). Of note, female mice display an increased percent iWAT compared to male mice (Figure 22 G).

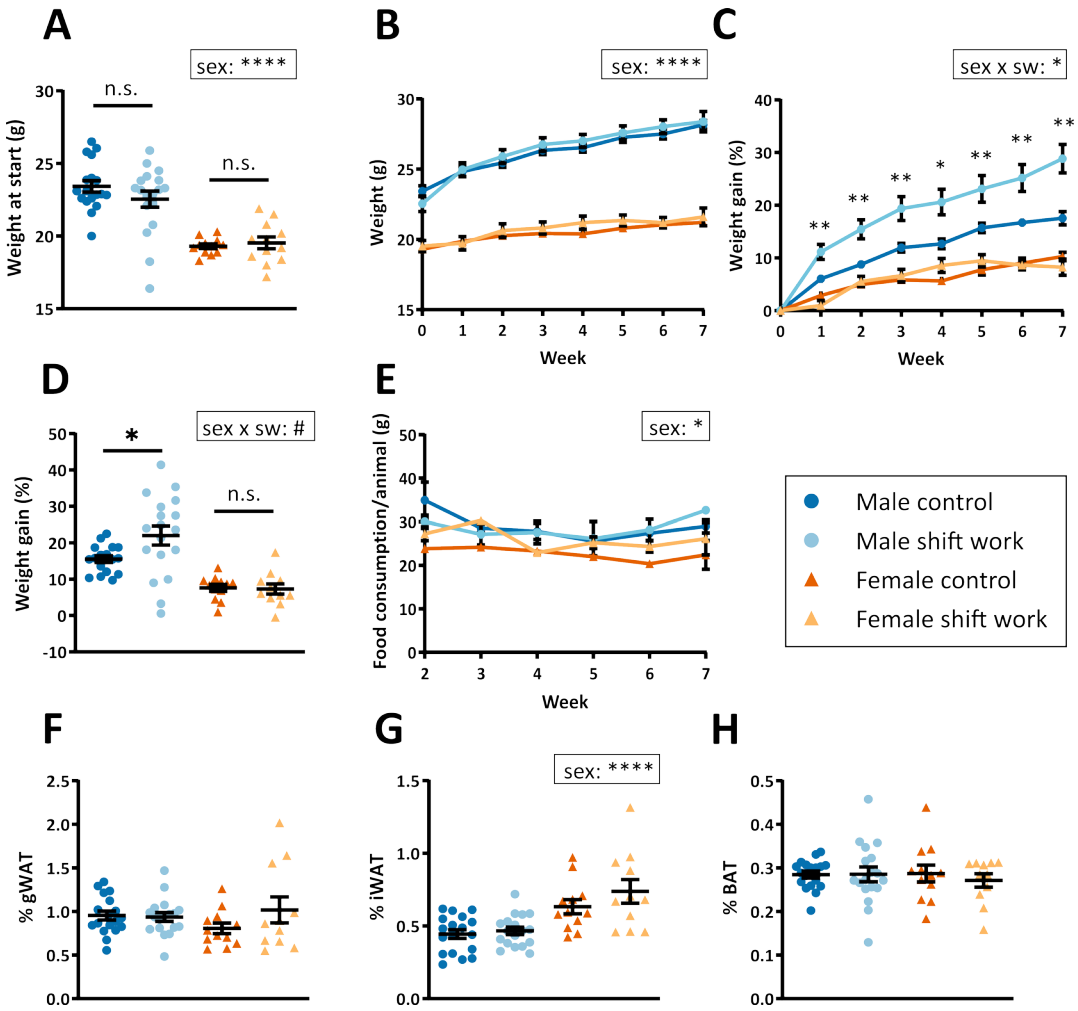

Figure 22. Mild sex-specific metabolic alterations following light-induced shift work conditions in mice. The body weight of all experimental animals and their food intake were recorded weekly. During sacrifice, fat pads were isolated and weighed. (A) Absolute body weight of the experimental animals before initiation of the shift work light paradigm i.e., baseline body weight. (B) Curve of absolute body weight over time. (C) Curve of percent weight gain over time. (D) Percent weight gain at sacrifice. (E) Curve of food consumption per animal over time. Percent gWAT (F), iWAT (G) and BAT (H) of total body weight at sacrifice. For the parameters in panels A, D, F, G and H, two-way ANOVAs were conducted where a significant sex effect is indicated by 'sex' and an interaction effect between sex and shift work is indicated by 'sex x sw'. A Fisher's LSD post-hoc test with Bonferroni correction was used to compare the following groups: male control vs. male shift work and female control vs. female shift work. The relevant results of these post-hoc comparisons are indicated by the black comparison bars. In panels B, C and E, groups were compared using mixed-effects analysis where 'sex' indicates a significant effect of sex and 'sex x sw' indicates a significant interaction effect of sex and shift work. In panel C, the results of Fisher's LSD post-hoc tests followed by Bonferroni correction, comparing male control vs. male shift work is indicated above every time point assessed. For all panels except panel E: n = 17 – 18 (male control); n = 18 (male shift work); n = 12 (female control); n = 12 (female shift work). For panel E: n= 1 – 3 (per time point per group). Data points in panels A, D, F, G and H represent individual experimental animals. n.s. = not significant; # indicates $p < 0.1$; * indicates $p < 0.05$; ** indicates $p < 0.01$; **** indicates $p < 0.0001$. Details on statistical tests and n-values can be found in Table S27 – S30. BAT = brown adipose tissue; gWAT = gonadal white adipose tissue; iWAT = inguinal white adipose tissue. Error bars indicate mean ± SEM.

Male shift work animals display an increased percent body weight gain compared to their sex-matched controls despite similar overall food consumption. To further explore the effects of light-induced shift work conditions on metabolism, mice from all experimental groups were placed into metabolic cages. Experiments started on a Monday to ensure the same *Zeitgeber* conditions (lights on: 7 a.m.; lights off: 7 p.m.) for all mice. Thus, the shift work animals underwent a light cycle shift before the start of the experiment. Whereas male control and male shift work animals display similar locomotor activity profiles, female shift work animals exhibit a delayed locomotor activity onset on day 1 compared to their sex-matched controls (Figure 23 A, B). This delayed locomotor activity of female shift work animals is no longer present on day 2, indicating a gradual adaptation of female shift work animals to the given light cycle (Figure 23 B). Locomotor activity periodograms reveal a roughly 24-hour rhythm for all experimental animals (Figure 23 C, D). Overall locomotor activity in the metabolic cages is unaltered in shift work animals (Figure 23 E). Interestingly, two-way ANOVA testing reveals a significant interaction between sex and shift work on locomotor activity nocturnality. Female shift work animals have a significantly decreased locomotor activity nocturnality compared to female controls – a shift work-induced effect, which is not present in males (Figure 23 F, Table S31, S32). Thus, in accordance with the IntelliCage locomotor activity data (Figure 19 F), there is a sex-specific behavioral adaptation to the given light cycle with female animals exhibiting a greater loss of locomotor activity nocturnality following shift work conditions. Regarding food consumption, no major differences between control and shift work animals in neither sex are observed over the days (Figure 23 G, H). However, periodogram analyses of food consumption evidence a decreased power peak for shift work animals compared to their sex-matched controls (Figure 23 I, J). This suggests a more variable period in shift work animals, likely resulting from the gradual shifting of food consumption rhythms to the given light cycle. In accordance with the previously discussed data, shift work conditions do not affect overall food consumption (Figure 23 K). Further, food intake nocturnality is unchanged by the shift work light paradigm (Figure 23 L). Similar to food consumption, no major differences between control and shift work animals are observed when plotting the water intake over the days (Figure 23 M, N). However, periodogram analyses evidence a less robust period of the water intake rhythms in shift work animals, likely originating from the gradual adaptation of the water intake rhythm to the given light cycle (Figure 23 O, P). Further, a sex-specific effect of shift work conditions on overall water intake is observed with female shift work animals ingesting more water than their sex-matched controls (Figure 23 Q). Regarding the water intake nocturnality, a trend for an effect of shift work was observed with shift work animals displaying decreased nocturnality, indicating an attenuated water intake rhythm (Figure 23 R).

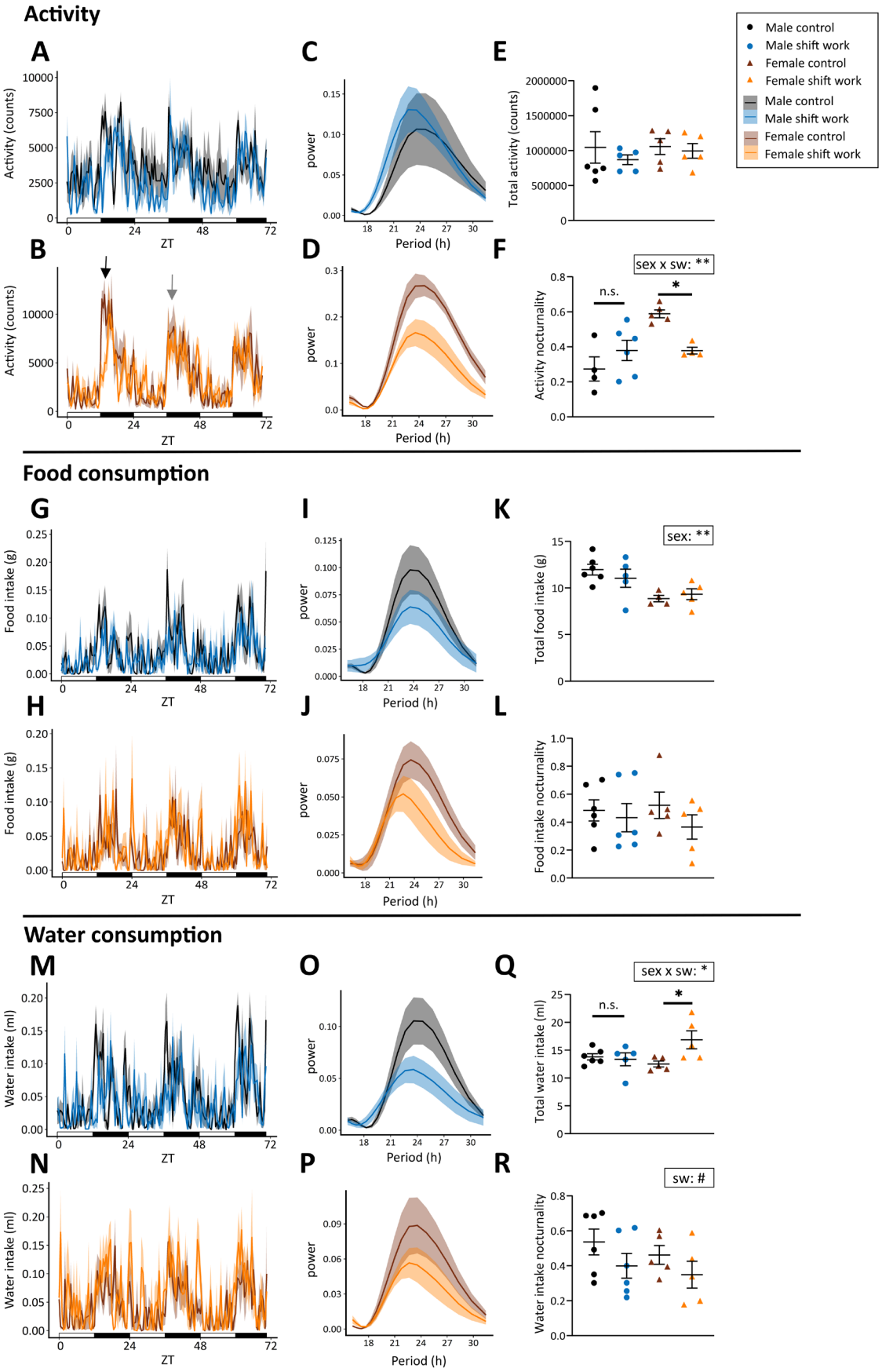

Figure 23. Effects of sex, shift work and their interaction on locomotor activity, food, and water intake. Experimental animals were placed into metabolic cages to measure their locomotion, food intake and water consumption. After 1 day of acclimatization, parameters were recorded for 3 days. During the experiment, animals

were housed in 12:12 LD conditions (lights on: 7 a.m.; lights off: 7 p.m.). (A, B, G, H, M, N) Plots from recordings of the metabolic cages for locomotor activity (A, B), food consumption (G, H) and water consumption (M, N). Averages across each experimental group are plotted over time with the shaded area indicating ± SEM. In panel B, the black and gray arrows indicate the parameter onset on day 1 and day 2 of the recording, respectively. (C, D, I, J, O, P) Corresponding periodograms for each experimental group for locomotor activity (C, D), food consumption (I, J) and water consumption (O, P). (E, K, Q) Total locomotor activity (E), food consumption (K) and water consumption (Q) summed across the 3 days of recording. (F, L, R) Nocturnality score for the locomotor activity (F), food consumption (L) and water consumption (R). For panels E, F, K, L, Q and R, two-way ANOVAs were conducted where a significant sex effect is indicated by 'sex', an effect of shift work is indicated by 'sw' and a significant interaction effect between sex and shift work is indicated by 'sex x sw'. A Fisher's LSD post-hoc test with Bonferroni correction was used to compare the following groups: male control vs. male shift work and female control vs. female shift work. The relevant results of these post-hoc comparisons are indicated by the black comparison bars. Data points represent individual experimental animals. Male control: n = 4 – 6; male shift work: n = 5 – 6; female control: n = 4 – 5; female shift work: n = 4 – 5. n.s = not significant; # indicates $p < 0.1$; * indicates $p < 0.05$; ** indicates $p < 0.01$. Details on statistical tests and n-values can be found in Table S31 and S32. Error bars indicate mean ± SEM.

Beyond feeding and drinking behavior, RER and EE were also recorded to assess the effect of the shift work light paradigm on fuel utilization. Visual examination of RER and EE rhythmicity over the days reveals no major differences between shift work animals and their sex-matched controls (Figure 24 A – D). Nevertheless, the power of the periodogram peaks is decreased in shift work animals, suggesting a more variable RER and EE rhythm period in shift work animals likely resulting from the gradual shifting (Figure 24 E – H). Light-induced shift work conditions do not affect mean RER. However, there is an effect of sex with female mice displaying an increased RER compared to males (Figure 24 I, Table S33, S34). Further, RER nocturnality is not significantly affected by shift work conditions. Of note, there is a trend for a reduced RER nocturnality in females compared to males (Figure 24 J). Further, a significant interaction between sex and shift work on the mean EE is observed. Female shift work animals display an increased overall EE compared to female controls – a shift work-induced effect that is not detected in males (Figure 24 K). Regarding the EE nocturnality, an effect of sex and shift work alone is observed. Females display a higher EE nocturnality than males and shift work animals exhibit a lower EE nocturnality than controls. Post-hoc testing reveals that female shift work animals evidence a significantly reduced EE nocturnality compared to female controls – a shift work-induced effect that does not reach statistical significance in males (Figure 24 L).

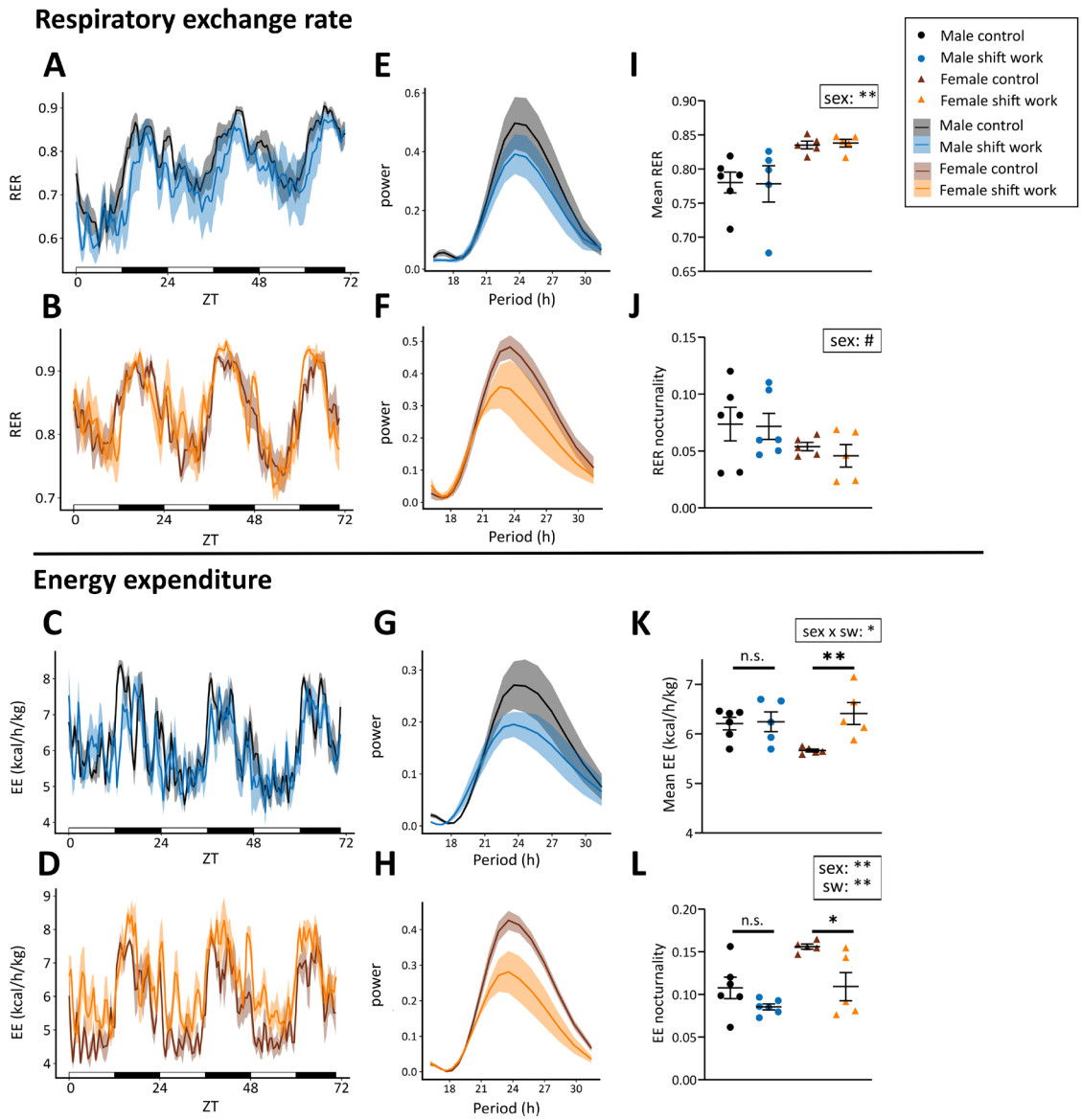

Figure 24. Effects of sex, shift work and their interaction on respiratory exchange rate and energy expenditure. Experimental animals were placed into metabolic cages to measure their RER and EE. Parameters were recorded for 3 days following 1 day of acclimatization. Mice were maintained in 12:12 LD conditions (lights on: 7 a.m.; lights off: 7 p.m.). (A, B, C, D) Recordings from 3 days of metabolic cage experiments for RER (A, B) and EE (C, D). The mean ± SEM for each experimental group is plotted over time. (E, F, G, H) Corresponding periodograms for each experimental group for RER (E, F) and EE (G, H). (I, K) Mean RER (I) and mean EE (K) across the 3 days of recording. (J, L) Nocturnality score for RER (J) and EE (L). For panels I, J, K and L, two-way ANOVAs were conducted where a sex effect is indicated by 'sex', an effect of shift work is indicated by 'sw' and an interaction effect between sex and shift work is indicated by 'sex x sw'. A Fisher's LSD post-hoc test with Bonferroni correction was used to compare the following groups: male control vs. male shift work and female control vs. female shift work. The relevant results of these post-hoc comparisons are indicated by the black comparison bars. Data points represent individual experimental animals. Male control: n = 6; male shift work: n = 5 – 6; female control: n = 5; female shift work: n = 5. n.s. = not significant; # indicates $p < 0.1$; * indicates $p < 0.05$; ** indicates $p < 0.01$. Details on statistical tests and n-values can be found in Table S33 and S34. EE = energy expenditure; RER = respiratory exchange rate. Error bars indicate mean ± SEM.

To assess the impact of light-induced shift work conditions on glucose homeostasis, all experimental animals were subjected to a GTT and ITT. Shift work conditions do not significantly alter glucose tolerance in male or female mice (Figure 25 A, B, Table S35, S36). Of note, sex alone has a significant effect with male mice displaying higher plasma glucose levels following the glucose injection (Figure 25 A, B). During the ITT, shift work animals of both sexes appear to display a greater glucose drop following the insulin injection. In females, this shift work-induced effect appears to be stronger than in males (Figure 25 C, Table S37). However, this shift work-induced effect on insulin sensitivity is not detected when correcting for differing baseline glucose values by generating the AOC (Figure 25 D). Of note, sex alone affects the AOC with male mice exhibiting an increased AOC i.e., enhanced glucose response to the insulin injection.

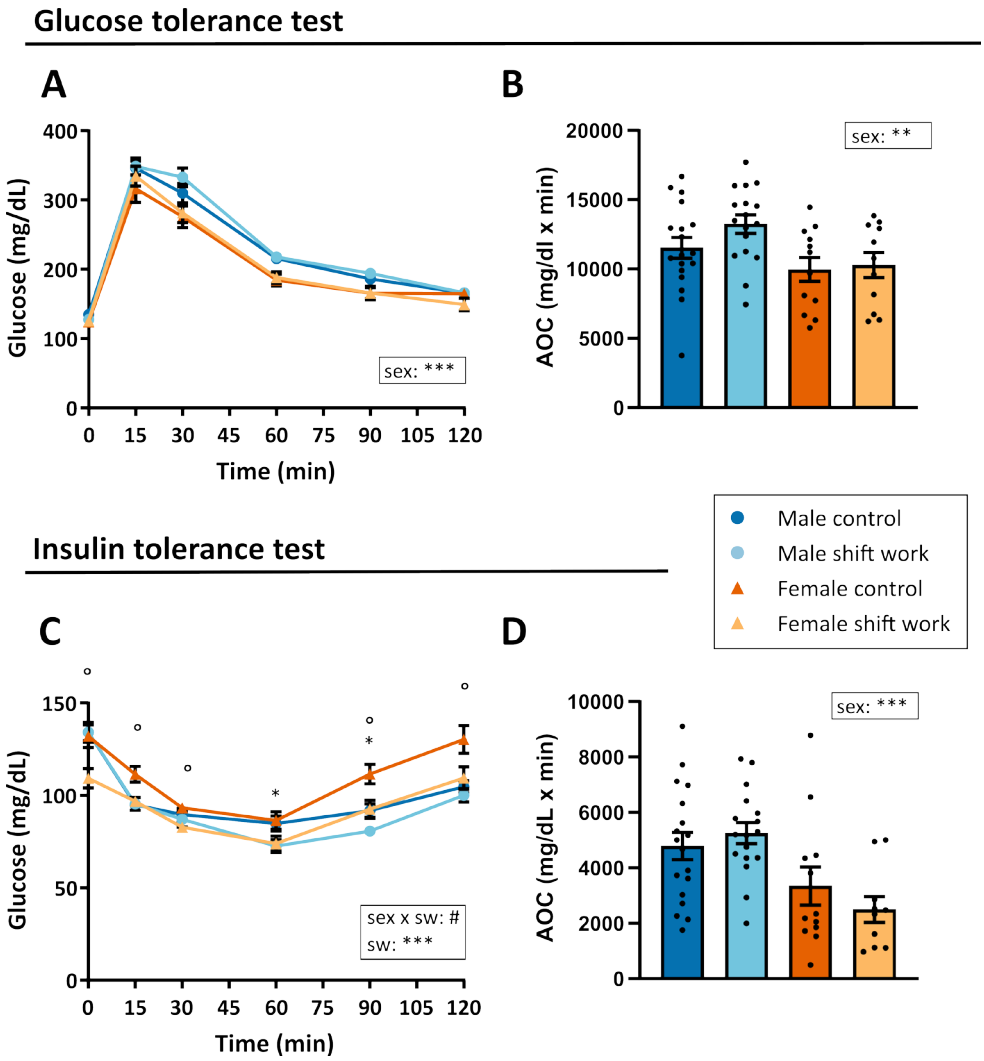

Figure 25. Light-induced shift work conditions do not alter glucose and insulin tolerance in a sex-specific manner. All animals were subjected to a GTT and ITT. (A) Glucose curve during the GTT. (B) Area of the glucose curve from the GTT. (C) Glucose curve during the ITT. (D) Area of the glucose curve from the ITT. For panels A and C, three-way ANOVAs were conducted where a sex effect is indicated by 'sex', an effect of shift work is indicated by 'sw' and an interaction effect between sex and shift work is indicated by 'sex x sw'. Significant results of Fisher's LSD post-hoc

tests followed by Bonferroni correction are indicated above the time point assessed (Meaning of the symbols: * = male control vs. male shift work; ° = female control vs. female shift work. Number of symbols: $^{x}p < 0.05$). For the panels B and D, two-way ANOVAs were conducted where a sex effect is indicated by 'sex'. Data points represent individual experimental animals. Male control: n = 18; male shift work: n = 17 – 18; female control: n = 12; female shift work: n = 10 – 11. # indicates $p < 0.1$; ** indicates $p < 0.01$, *** indicates $p < 0.001$. Details on the statistical tests and n-values can be found in Table S35 – S37. AOC = area of the curve. Error bars indicate mean ± SEM.

5.2.5 Light-induced shift work conditions lead to slight changes in molecular rhythms, some of which are sex-specific

Next, the effect of the shift work light paradigm on molecular rhythms in tissue explants was examined. Since molecular SCN rhythms are directly impacted by light and the shift work paradigm was based on alternating light cycles, SCN rhythms were assessed. As expected, the phase of the SCN explant PER2::LUC rhythm is altered by shift work conditions (Figure 26 A, Table S38, S39). A delayed phase is observed in shift work animals because of their maintenance in a delayed light cycle 4-5 days prior to sacrifice. Additionally, sex affects the phase of the SCN rhythm with females displaying a delayed phase compared to males (Figure 26 A). Regarding the amplitude and period of the SCN rhythm, no effect of the shift work light paradigm is detected (Figure 26 B, C). To investigate the impact of shift work conditions on the rhythmicity of a brain region involved in anxious responses, the rhythmicity of PAG explants was assessed based on PER2::LUC expression. The phase and amplitude of the PAG rhythm is unchanged by shift work conditions (Figure 26 D, E). However, there is a significant effect of sex, with females displaying a delayed phase and increased amplitude of the PAG rhythm compared to males. Interestingly, a statistically significant interaction between sex and shift work is observed for the period of the PAG PER2::LUC rhythm (Figure 26 F, Table S38, S39). Although not robust to Bonferroni correction, females display a trend for a prolonged period of the PAG rhythm following shift work conditions. In contrast, no difference between the period of the PAG rhythm is observed between male control and male shift work animals (Figure 26 F). This highlights a sex-specific effect of shift work conditions on the period of the PAG rhythm. Additionally, the effect of shift work conditions of the rhythmicity of a metabolically active organ, namely the liver, was investigated. Shift work conditions do not alter the phase, amplitude or period of the liver explant PER2::LUC rhythm in either sex (Figure 26 G – I, Table S40, S41). Next, to measure internal desynchrony, the phase relationship between the SCN (master pacemaker) and subordinate clocks was quantified. Shift work conditions decrease the phase difference between the SCN and PAG tissue explant rhythms but do not affect the phase difference between the SCN and liver explant rhythms (Figure 26 J, K, Table S40, S41).

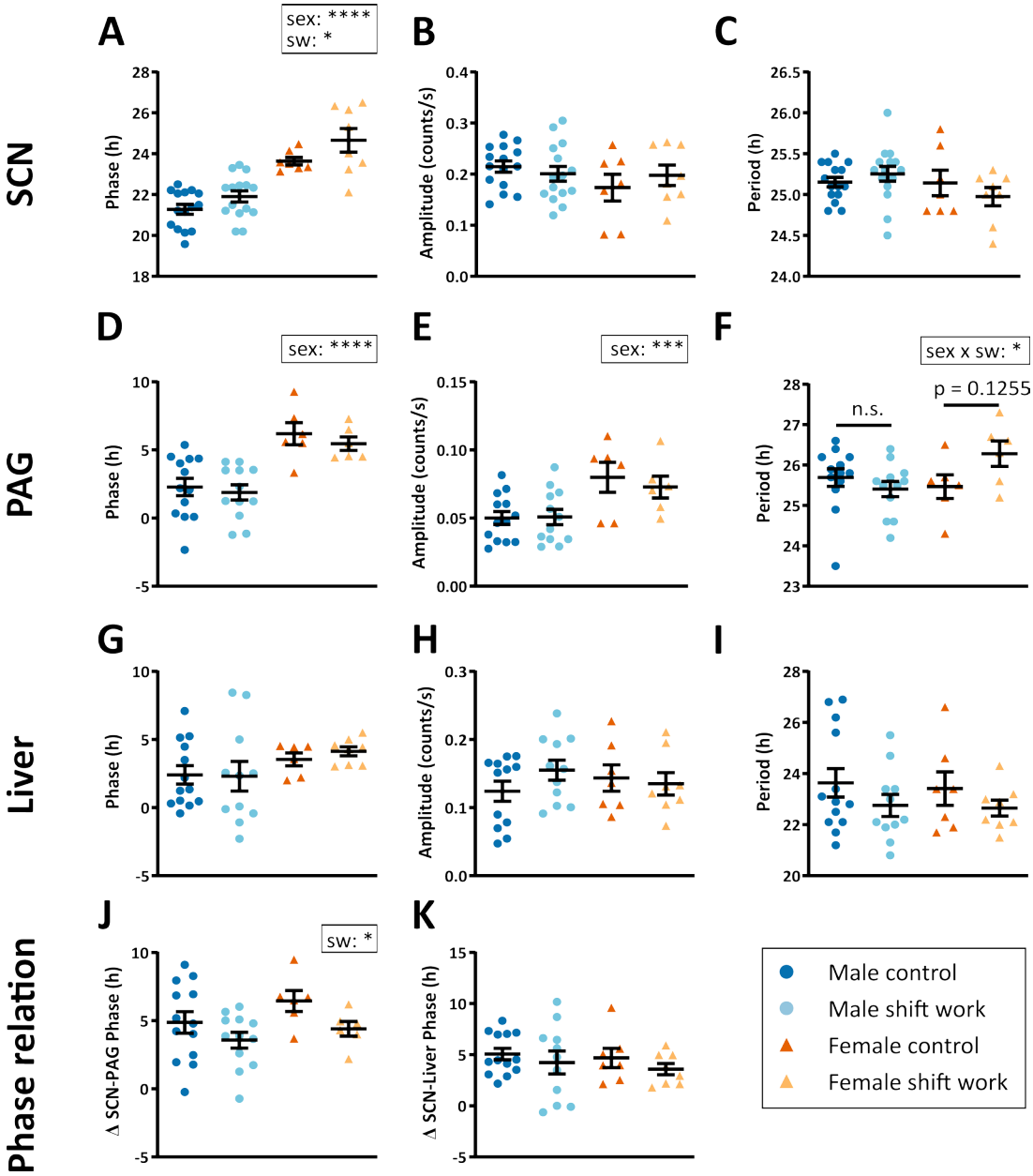

Figure 26. Subtle changes in molecular rhythms following light-induced shift work conditions. Experimental animals were sacrificed 7-9 weeks after initiation of the shift work light paradigm and 4-5 days after the last light cycle shift. SCN, PAG and liver tissue explants were collected and their rhythmicity was determined based on PER2::LUC oscillations. SCN slices: (A) phase, (B) amplitude and (C) period. PAG slices: (D) phase, (E) amplitude and (F) period. Liver slices: (G) phase, (H) amplitude, (I) period. (J) Phase relationship between SCN and PAG rhythms. (K) Phase relationship between SCN and liver rhythms. For all parameters, two-way ANOVAs were conducted where a sex effect is indicated by 'sex', an effect of shift work is indicated by 'sw' and an interaction effect between sex and shift work is indicated by 'sex x sw'. Data points represent tissue explants from individual experimental animals (male control: n = 12 – 15; male shift work; n = 11 – 15; female control: n = 6 – 7; female shift work: n = 6 – 8). n.s. = not significant; * indicates $p < 0.05$; *** indicates $p < 0.001$; **** indicates $p < 0.0001$. Details on the statistical tests and n-values can be found in Table S38 – S41. PAG = periaqueductal gray; SCN = suprachiasmatic nucleus. Error bars indicate mean ± SEM.

5.3 Absence of an interaction between a genetic and environmental circadian disruption in comorbid behavioral and metabolic phenotypes in female mice

In project 3, the interaction between a genetic circadian disruption (*Bmal1*$^{+/-}$) and an environmental circadian disruption (shift work) was investigated to assess whether a circadian G×E affects behavioral and metabolic outcomes in female mice concomitantly.

5.3.1 *Bmal1*$^{+/-}$ mice display altered adaptation of locomotor activity to alternating light cycles

In a first step, differences in the behavioral adaptation of WT and *Bmal1*$^{+/-}$ mice to alternating light cycles mimicking shift work were assessed. To this end, locomotor activity of WT and *Bmal1*$^{+/-}$ mice housed in 12:12 LD conditions (control) or light-induced shift work conditions (shift work) was tracked in the IntelliCage system. Both WT and *Bmal1*$^{+/-}$ animals entrain to 12:12 LD control conditions and display rhythmic behavior (Figure 27 A, B, S8, S9). When subjected to light-induced shift work conditions, WT and *Bmal1*$^{+/-}$ animals constantly re-entrain to the given light cycle (Figure 27 C, D, S10, S11). The shift work conditions do not alter overall locomotor activity. However, *Bmal1*$^{+/-}$ animals exhibit an increased overall locomotor activity compared to WT animals (Figure 27 E, Table S42). Next, activity nocturnality was determined to quantify the preference of locomotor activity during the dark vs. light phase and to assess differences in the behavioral adaptation to alternating light cycles. There is a significant interaction between genotype and shift work for locomotor activity nocturnality (Figure 27 F, Table S42). *Bmal1*$^{+/-}$ control animals display a higher locomotor activity nocturnality compared to WT control animals, suggesting that under standard 12:12 LD conditions, lacking one copy of the essential clock gene *Bmal1* results in an increased amplitude of the locomotor activity rhythm. Furthermore, *Bmal1*$^{+/-}$ animals react differently to light-induced shift work conditions compared to WT animals. In *Bmal1*$^{+/-}$ animals, light-induced shift work conditions significantly reduce locomotor activity nocturnality – a shift work-induced effect, which is not detected in WT animals (Figure 27 F).

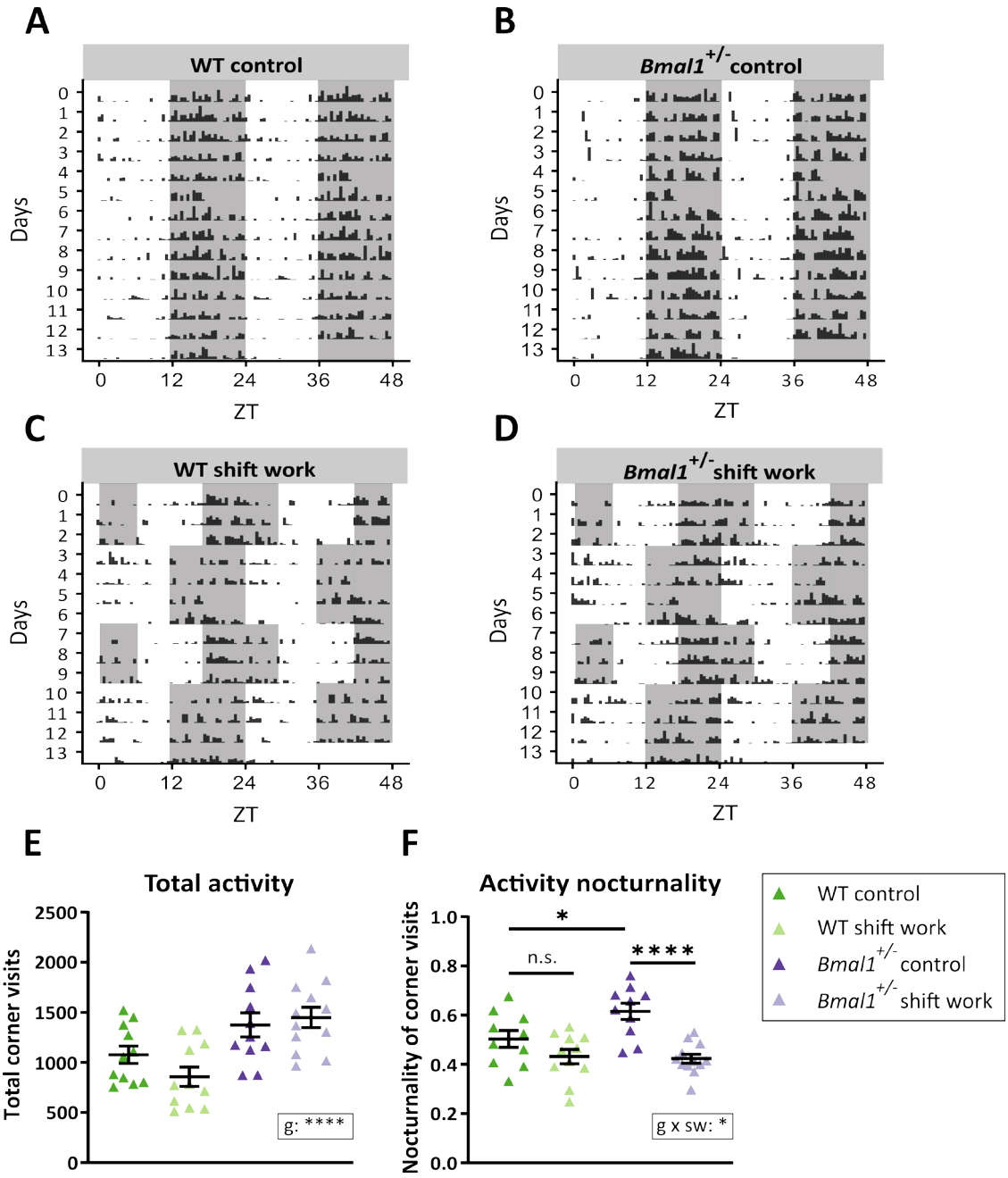

Figure 27. *Bmal1*$^{+/-}$ display altered re-entrainment to alternating light cycles. WT and *Bmal1*$^{+/-}$ animals were placed into the IntelliCage system and subjected to standard 12:12 LD conditions (control) or to alternating light cycles (shift work). Corner visits were tracked as a measure for the animal's locomotor activity. (A – D) Representative double-plotted actogram for (A) WT control, (B) *Bmal1*$^{+/-}$ control, (C) WT shift work and (D) *Bmal1*$^{+/-}$ shift work. Corner visits are indicated by the black bars on the actograms. Due to technical reasons, some data measurements on day 5 were missing, resulting in a recording gap. The shading of the double-plotted actograms represents the LD cycle that the animal was subjected to. Double-plotted actograms of all experimental animals can be found in Figure S8 – S11. (E) Overall corner visits for each experimental group. (F) Nocturnality score for locomotor activity. In panels E and F, all groups were compared using a two-way ANOVA where a significant genotype effect is indicated by 'g' and a significant interaction effect between genotype and shift work is indicated by 'g x sw'. When an interaction effect was observed, the following comparisons were tested using a Fisher's LSD post-hoc test with Bonferroni correction: WT control vs. *Bmal1*$^{+/-}$ control, WT control vs. WT shift work and *Bmal1*$^{+/-}$ control vs. *Bmal1*$^{+/-}$ shift work. Data points in panels E and F represent individual experimental animals (WT control: n = 10 – 11; WT shift work: n = 11; *Bmal1*$^{+/-}$ control: n = 10 – 11; *Bmal1*$^{+/-}$ shift work: n = 12). n.s. = not significant; * indicates $p < 0.05$; **** indicates $p < 0.0001$. Details on the statistical tests and n-values can be found in Table S42. Error bars indicate mean ± SEM.

5.3.2 No evidence for a circadian G×E in the generation of anxiety- or depression-related behaviors

To determine if there is an interaction between a genetic and environmental circadian disruption in the generation of anxiety-related behaviors, all experimental animals were tested in the OFT, EPM and DaLi box test. For the OFT, no statistically significant interaction between genotype and shift work on the distance traveled, center entries or center time is detected (Figure 28 A – C, Table S43). Independent of genotype, animals subjected to shift work conditions display increased overall distance traveled and center entries in the OFT (Figure 28 A, B). However, shift work animals do not display increased center time, arguing that shift conditions increase locomotion in the OFT rather than reducing anxiety-related behavior (Figure 28 C). Further, *Bmal1*$^{+/-}$ animals travel a larger distance and enter the center more often than WT animals independent of shift work conditions (Figure 28 A, B). Nevertheless, despite increased entries into the center of the open field, *Bmal1*$^{+/-}$ animals spent significantly less time in it, arguing for an increased anxiety-like behavior in *Bmal1*$^{+/-}$ compared to WT animals independent of shift work conditions (Figure 28 C). In accordance with the result in the OFT, genotype and shift work conditions increase the distance traveled in the EPM (Figure 28 D). Interestingly, a significant interaction between genotype and shift work is detected for the entries into the open arm (Figure 28 E, Table S44). There is no baseline difference in open arm entries between WT and *Bmal1*$^{+/-}$ control animals. However, shift work conditions significantly increase open arm entries in WT animals – a shift work-induced effect that is not observed in *Bmal1*$^{+/-}$ animals (Figure 28 E). Regarding the open arm time, merely a trend for an effect of shift work conditions is detected, with shift work animals displaying slightly increased open arm time (Figure 28 F). In the DaLi box test, two-way ANOVA testing reveals no statistically significant interaction between genotype and shift work for any of the assessed parameters (i.e., entries into light, time in light, distance in light, latency to first entry into the light) (Figure 28 G – J, Table S45). In line with the increased locomotion of shift work animals in the OFT and EPM, shift work conditions increase and decrease light entries and latency to first light entry, respectively (Figure 28 G, J).

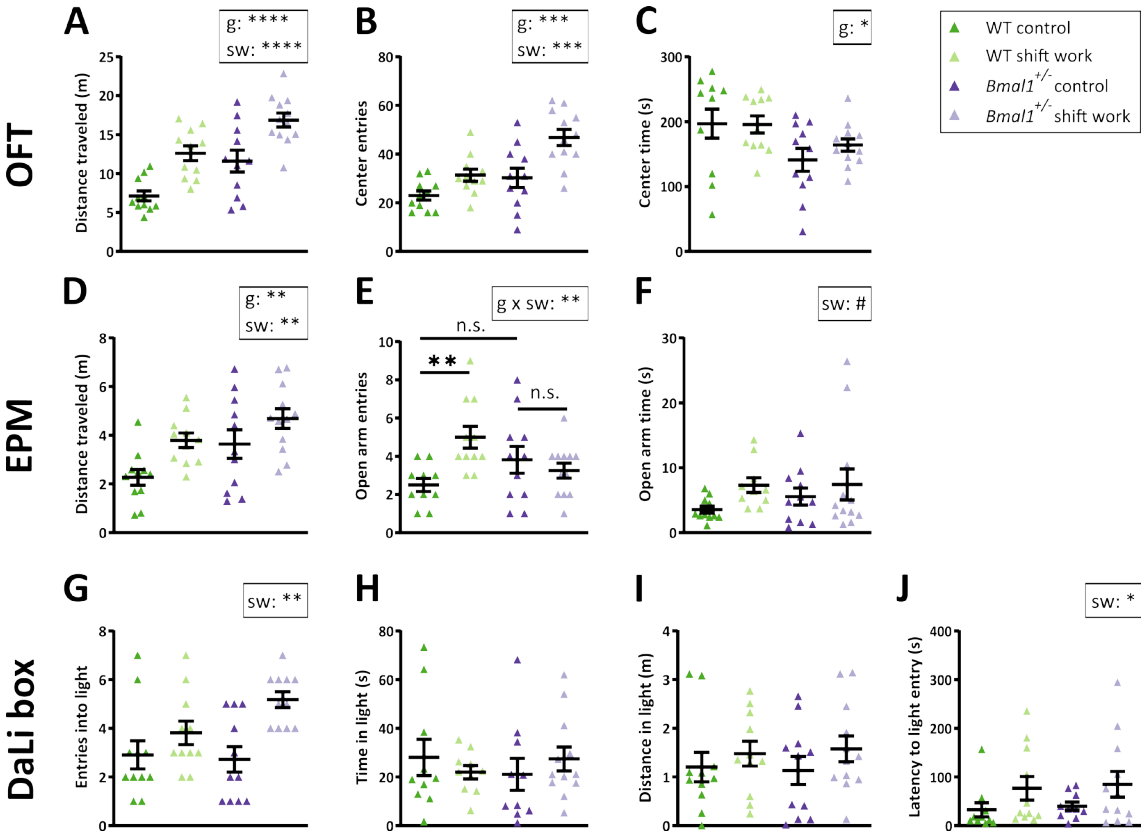

Figure 28. No evidence for a circadian G×E in the generation of anxiety-like behavior. Following 3 weeks of experimental light paradigm, anxiety-like behavior was tested in the OFT, EPM and DaLi box test. OFT: (A) distance traveled, (B) center entries and (C) center time. EPM: (D) distance traveled, (E) open arm entries and (F) time spent in the open arm. DaLi: (G) entries into the light compartment, (H) time spent in the light compartment, (I) distance traveled in the light compartment and (J) latency to the first entry into the light compartment. For all parameters, all groups were compared using a two-way ANOVA where a genotype effect is indicated by 'g', a shift work effect is indicated by 'sw' and an interaction effect between genotype and shift work is indicated by 'g x sw'. When an interaction effect was observed, the following comparisons were tested using a Fisher's LSD post-hoc test with Bonferroni correction: WT control vs. *Bmal1*$^{+/-}$ control, WT control vs. WT shift work and *Bmal1*$^{+/-}$ control vs. *Bmal1*$^{+/-}$ shift work. Data points represent individual experimental animals (WT control: n = 10 – 11; WT shift work: n = 10 – 11; *Bmal1*$^{+/-}$ control: n = 10 – 11; *Bmal1*$^{+/-}$ shift work: n = 11 – 12). # indicates $p < 0.1$; * indicates $p < 0.05$; ** indicates $p < 0.01$; *** indicates $p < 0.001$: **** indicates $p < 0.0001$. Details on statistical tests and n-values can be found in Table S43 – S45. DaLi box = dark-light box; EPM = elevated plus maze; OFT = open field test. Error bars indicate mean ± SEM.

Next, the effect of a genetic circadian disruption (*Bmal1*$^{+/-}$), an environmental circadian disruption (shift work) and their interaction on depression-like behavior was assessed. To this end, all animals were subjected to the TST, sucrose preference test and LH paradigm. Genotype, shift work or their interaction do not significantly affect behavior in the TST, sucrose preference test or LH test (Figure 29, Table S46). Thus, there is no evidence for a circadian G×E in the generation of anxiety- or depression-like phenotypes.

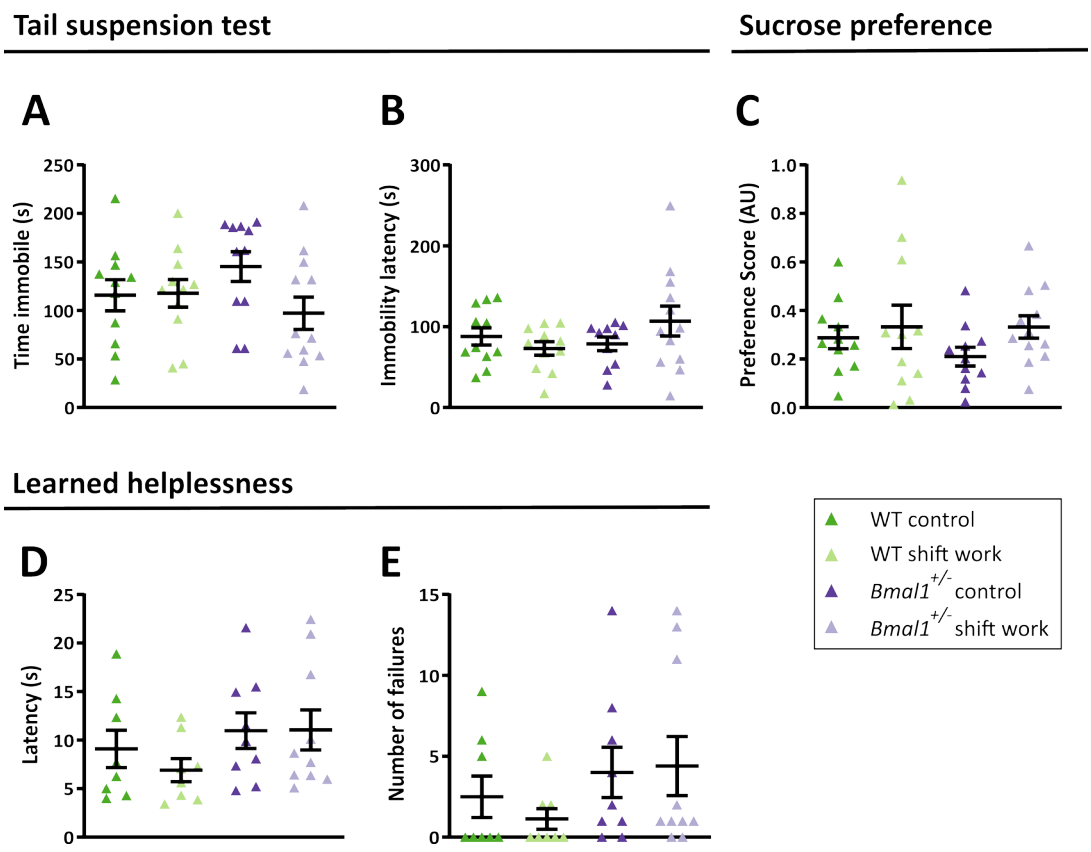

Figure 29. No evidence for a circadian G×E in the generation of depression-like behavior. All experimental animals were tested in the TST, sucrose preference test, and LH test to assess the effects of genotype, shift work and their interaction on depression-like phenotypes. TST: (A) time immobile and (B) immobility latency. (C) Sucrose preference score. LH test: (D) latency to escape the electrical shock and (E) failures to escape the electrical shock. For every parameter, all groups were compared using two-way ANOVAs, which yielded no effect of genotype, shift work or their interaction. Data points represent individual experimental animals (WT control: n = 8 or 11; WT shift work: n = 8 or 11; *Bmal1*$^{+/-}$ control: n = 9 – 11; *Bmal1*$^{+/-}$ shift work: n = 10 or 12). Details on statistical tests and n-values can be found in Table S46. Error bars indicate mean ± SEM.

5.3.3 No evidence for a circadian G×E in the generation of metabolic phenotypes

The hypothesis of project 3 was that genetic and environmental circadian disruptions interact and result in adverse comorbid behavioral and metabolic outcomes the same mouse. To explore this, all experimental animals that were profiled behaviorally were also assessed for metabolic comorbidities. The initial body weight of the mice, prior to initiation of the shift work light paradigm, was similar in all experimental groups (Figure 30 A, Table S47). Mixed-effects analyses reveal no significant interaction between genotype and shift work for the absolute or percent weight gain over time (Figure 30 B, C, Table S48, S49). However, shift work conditions increase the percent weight gain (Figure 30 C). Further, despite this shift work-induced effect on weight, food consumption does not appear profoundly different between the experimental groups

(Figure 30 D). To investigate if the increased percent weight gain in shift work animals was accompanied by enhanced fat deposition, gWAT, iWAT and BAT were isolated and weighed at sacrifice. The percentages of gWAT, iWAT and BAT are similar in all experimental groups (Figure 30 E – G, Table S47).

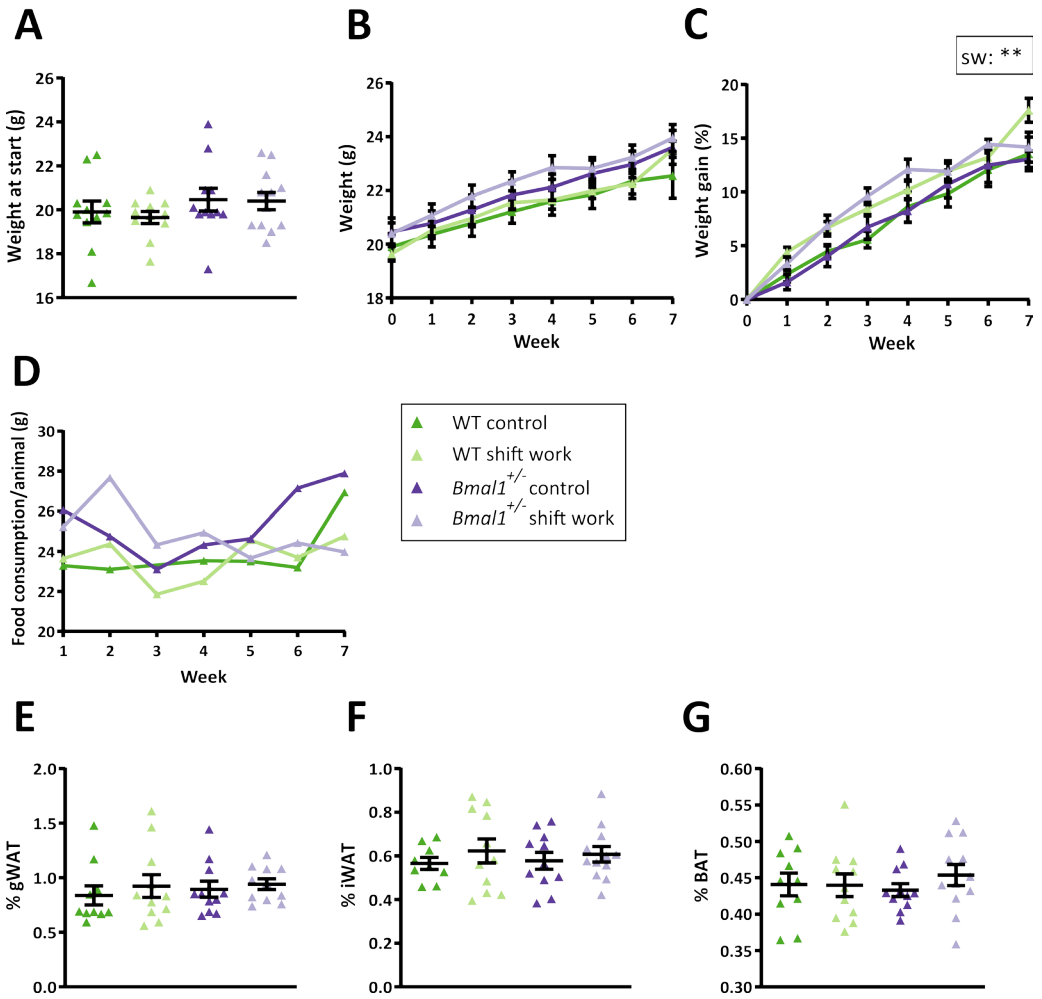

Figure 30. No evidence for a circadian G×E on body weight or food consumption. Body weights and cage food were measured weekly. Upon sacrifice, fat pads were isolated and weighed. (A) Absolute body weight of the experimental animals before the start of the shift work light paradigm i.e., baseline body weight. (B) Curve of absolute body weight over time. (C) Curve of the percent weight gain over time. (D) Curve of food consumption per animal over time. (E-G) Percent gWAT (E), iWAT (F), BAT (G) of total body weight at sacrifice. For the parameters in A, E, F and G, all groups were compared using a two-way ANOVA that yielded no effect of genotype, shift work or their interaction. Data points represent individual experimental animals. In panels B and C, the groups were compared using mixed-effects analysis where 'sw' indicates a shift work effect. For all panels except panel D: n = 9 – 11 (WT control); n = 11 (WT shift work); n = 11 (*Bmal1*$^{+/-}$ control); n = 11 – 12 (*Bmal1*$^{+/-}$ shift work). For panel D: n = 1 (per time point per group). ** indicates $p < 0.01$. Details on statistical tests and n-values can be found in Table S47 – S49. BAT = brown adipose tissue; gWAT = gonadal white adipose tissue; iWAT = inguinal white adipose tissue. Error bars indicate mean ± SEM.

To further explore the interaction of a genetic and environmental circadian disruption in generating metabolic phenotypes, animals from all four experimental groups were placed into

metabolic cages. To ensure the same *Zeitgeber* conditions (lights on: 7 a.m.; lights off: 7 p.m.) for all mice, experiments started on a Monday. Thus, shift work animals were subjected to a light cycle shift 1 day prior to recordings. On the first day of recording, the locomotor activity onset of shift work animals is delayed compared to their genotype-matched controls (Figure 31 A, B, black arrows). This effect is no longer present on the second day of recording due to behavioral adaptation of the shift work animals to the given light cycle (Figure 31 A, B, gray arrows). The gradual forward activity shifting of shift work animals is also highlighted by their shortened locomotor activity period (Figure 31 C, D). Of note, in both genotypes shift work animals display an increased locomotor activity bout on the first day of recording compared to control (Figure 31 A, B). Overall locomotor activity and activity nocturnality are not significantly different between the experimental groups (Figure 31 E, F, Table S50). Similar to the locomotor activity rhythm, shift work animals display a slightly delayed feeding onset on the first but no longer on the second day of recording (Figure 31 G, H, black and gray arrows). This gradual forward shifting of the feeding rhythm in shift work animals is also supported by their less robust feeding rhythm period (Figure 31 I, J). Overall food intake and feeding nocturnality is similar between the experimental groups (Figure 31 K, L). In terms of water intake, a gradual shifting of the drinking rhythm is observed in shift work animals (Figure 31 M, N, black and gray arrows). This is also supported by the more variable period of the water intake rhythm in shift work animals (Figure 30 O, P). For the overall water intake and drinking nocturnality, no interaction between a genetic and environmental circadian disruption is observed (Figure 31 Q, R, Table S50). However, there is an effect of genotype with *Bmal1*$^{+/-}$ animals displaying a higher overall water consumption than WT animals (Figure 31 Q). Further, shift work conditions significantly decrease drinking nocturnality (Figure 31 R).

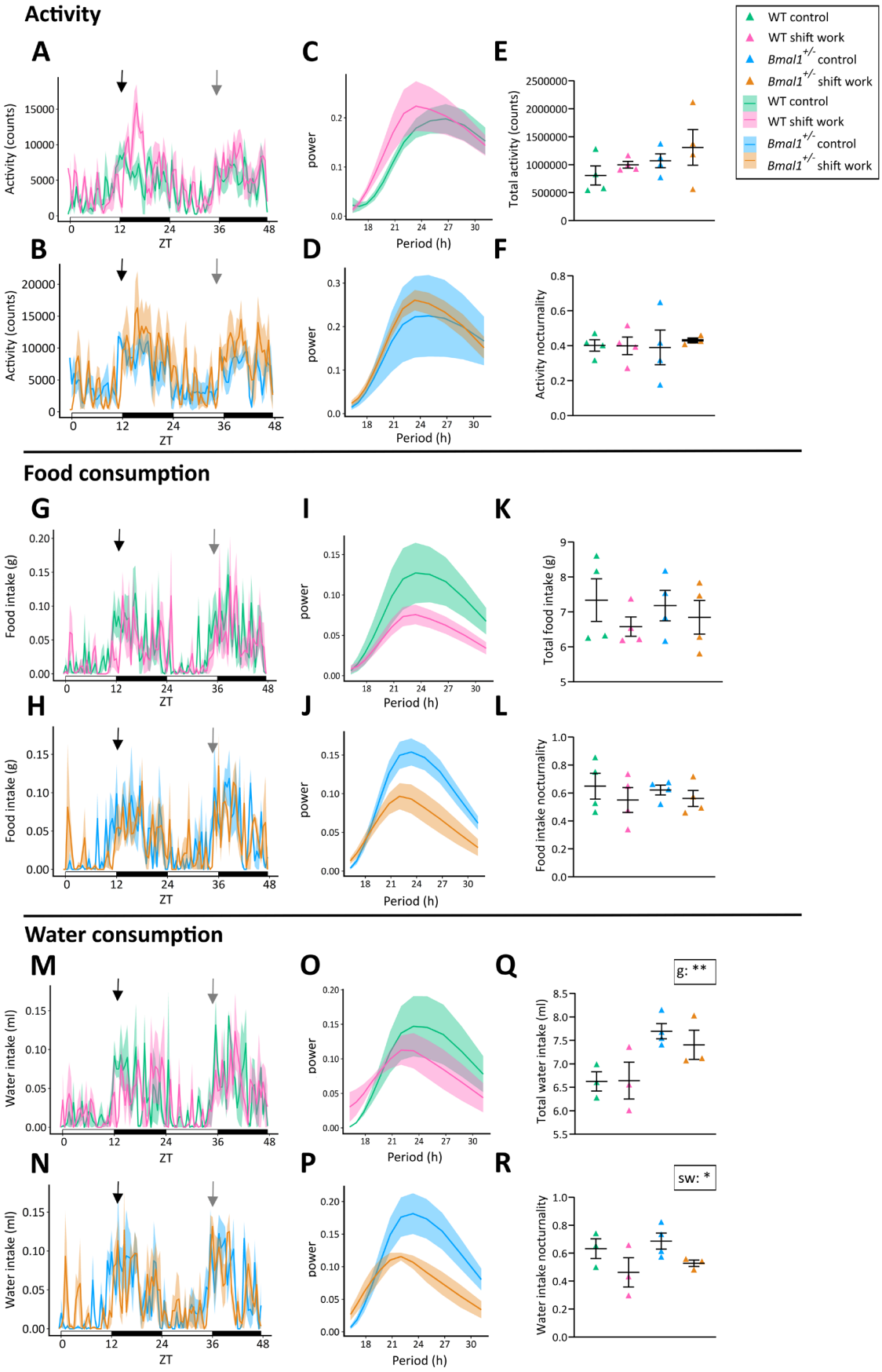

Figure 31. No evidence for a circadian G×E on locomotor activity, food, and water consumption. Locomotion, food, and water intake were recorded in the metabolic cages. After 1 day of acclimatization, parameters were recorded for 2 days. Animals were maintained in 12:12 LD conditions (lights on: 7 a.m.; lights off: 7 p.m.). (A, B) Average locomotor

activity plots across each experimental group over the recording time. The shaded area represents ± SEM. (C, D) Corresponding locomotor activity periodograms. (E) Sum of locomotor activity over the 2 days of recording. (F) Nocturnality score for the locomotor activity. (G, H) Average food consumption plots across each experimental group over the recording time. Shaded areas represent ± SEM. (I, J) Corresponding food consumption periodograms. (K) Overall food consumption across the 2 days of recording. (L) Nocturnality score for food consumption. (M, N) Water intake over the recording time. Averages ± SEM are plotted for each experimental group. (O, P) Corresponding water consumption periodograms. (Q) Total water intake over the 2 days of recording. (R) Nocturnality score for the water consumption. For panels E, F, K, L, Q and R, all groups were compared using a two-way ANOVA where 'g' represents a significant genotype effect and 'sw' represents a significant shift work effect. In panels A, B, G, H, M and N, the black and gray arrows indicate the parameter onset on day 1 and day 2 of the recording, respectively. In panels E, F, K, L, Q and R, data points represent individual experimental animals. WT control: n = 3 – 4; WT shift work: n = 3 – 4; *Bmal1*$^{+/-}$ control: n = 4; *Bmal1*$^{+/-}$ shift work: n = 3 – 4. * indicates $p < 0.05$; ** indicates $p < 0.01$. Details on statistical tests and n-values can be found in Table S50. Error bars indicate mean ± SEM.

Besides feeding and drinking behavior, RER and EE were measured to examine energy utilization. As for the food and water intake rhythms, shift work animals exhibit a gradual shifting for both the RER and EE rhythms (Figure 32 A – D, black and gray arrows). The RER and EE periodograms suggest a less stable period of the RER and EE rhythm in shift work animals, further highlighting the shifting of those rhythms (Figure 32 E – H). The mean RER, RER nocturnality and mean EE is similar in all experimental groups (Figure 32 I – L). For the EE nocturnality, no interaction between the effect of genotype and shift work is observed. However, shift work animals exhibit a decreased EE nocturnality score and a trend for *Bmal1*$^{+/-}$ animals displaying an increased EE nocturnality score is observed (Figure 32 L, Table S51). Overall, metabolic cage experiments evidence no significant interaction between a genetic and environmental circadian disruption for the metabolic parameters assessed.

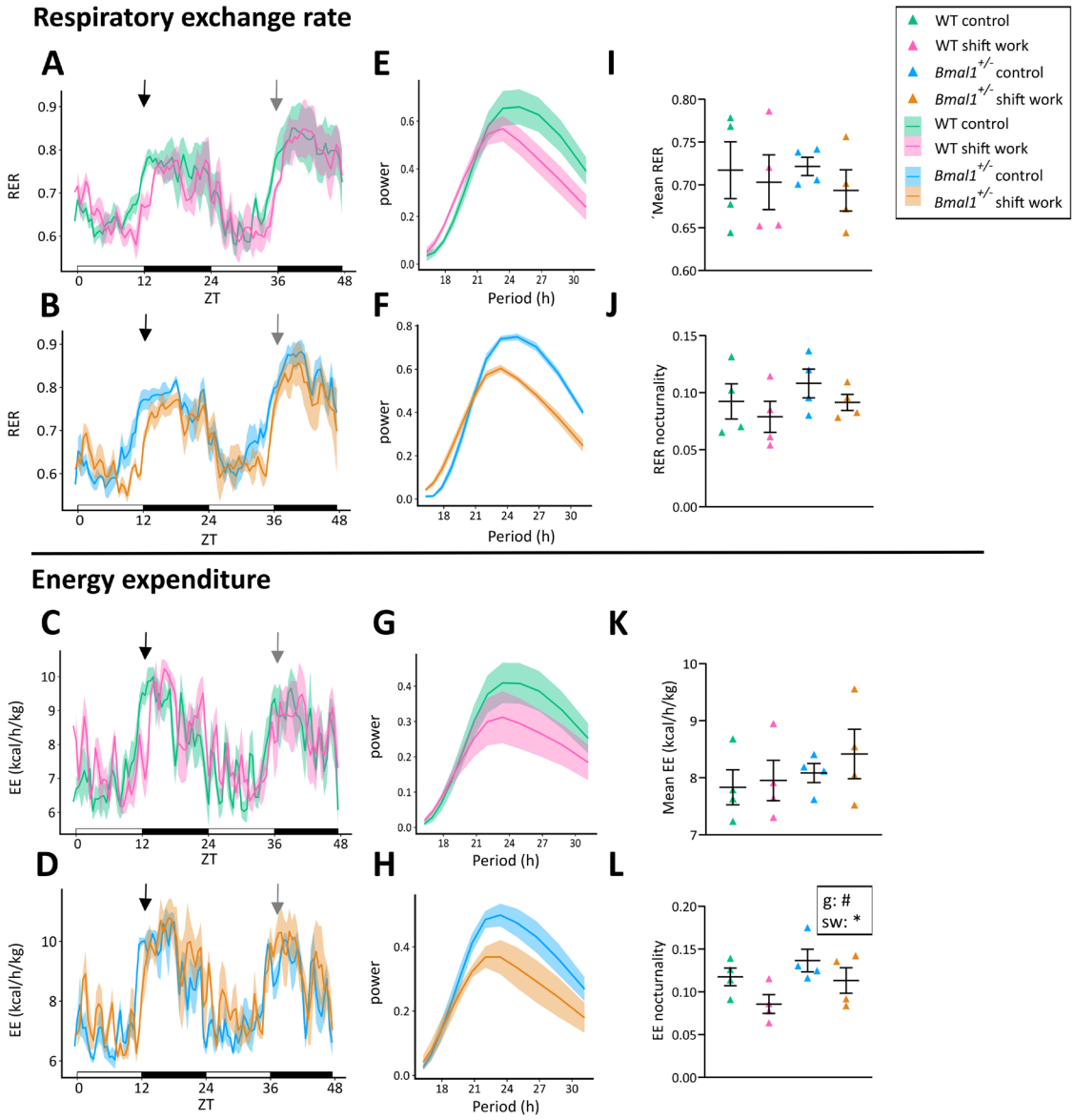

Figure 32. No evidence for a circadian G×E on respiratory exchange rate and energy expenditure. Following 1 day of acclimatization, the RER and EE were measured for 2 days in the metabolic cages. Animals were housed in 12:12 LD conditions (lights on: 7 a.m.; lights off: 7 p.m.). (A, B) Average RER plots across each experimental group over the recording time. The shaded area represents ± SEM. The black arrows indicate the delay of RER rhythm of shift work animals on day 1 of recording. The gray arrows indicate that shift work animals aligned their RER rhythm by day 2 of recording. (C, D) EE over the recording time. Averages ± SEM are plotted for each experimental group. The black arrows indicate the delay of EE rhythm of shift work animals on day 1 of recording. On day 2 of recording, this delay is absent (gray arrows). (E, F) RER periodograms. (G, H) EE periodograms. (I) Mean RER across the 2 days of recording. (J) Nocturnality score for the RER. (K) Mean EE across the 2 days of recording. (L) Nocturnality score for the EE. For panels I, J, K and L, all groups were compared using a two-way ANOVA where 'g' represents a genotype effect and 'sw' represents a significant shift work effect. Data points in panels I, J, K and L represent individual experimental animals. WT control: n = 4; WT shift work: n = 4; *Bmal1*$^{+/-}$ control: n = 4; *Bmal1*$^{+/-}$ shift work: n = 4. # indicates $p < 0.1$; * indicates $p < 0.05$. Details on statistical tests and n-values can be found in Table S51. EE = energy expenditure; RER = respiratory exchange rate. Error bars indicate mean ± SEM.

Next, glucose homeostasis was examined by subjecting all experimental animals to a GTT and ITT. For the glucose and insulin tolerance, no interaction between a genetic circadian disruption (*Bmal1*$^{+/-}$) and an environmental circadian disruption (shift work) is detected (Figure 33). Shift work conditions appear to enhance glucose tolerance and insulin sensitivity compared to control light conditions (Figure 33 A, B, Table S52, S53). However, this apparent shift work-induced effect on glucose and insulin tolerance is not detected when correcting for baseline glucose values by generating the AOCs (Figure 32 C, D, Table S54). Therefore, genotype, shift work or their interaction have no significant impact on the response to a glucose or insulin injection in this project.

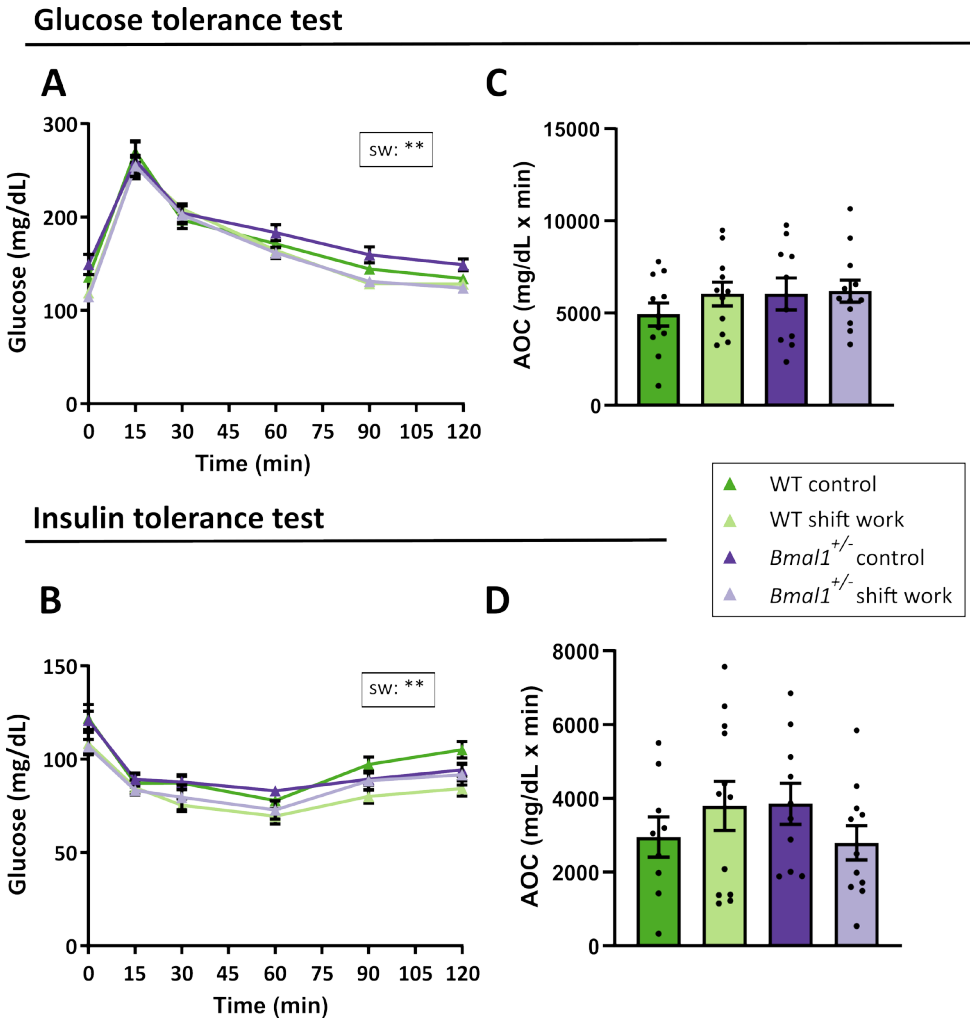

Figure 33. No evidence for a circadian G×E on glucose homeostasis. All animals underwent a GTT and ITT. (A, B) Plasma glucose curve during the GTT (A) and ITT (B). (C, D) Area of the glucose curve during the GTT (C) and ITT (D). For panels A and B, all groups were compared using three-way ANOVA testing where 'sw' indicates a shift work effect. For the panels C and D, all groups were compared using two-way ANOVAs, which yielded no effects for genotype, shift work or their interaction. Data points represent individual experimental animals. WT control: n = 9 – 11; WT shift work: n = 11; *Bmal1*$^{+/-}$ control: n = 10 – 11; *Bmal1*$^{+/-}$ shift work: n = 11 – 12. ** indicates $p < 0.01$. Details on the statistical tests and n-values can be found in Table S52 – S54. AOC = area of the curve. Error bars indicate mean ± SEM.

6. Discussion

6.1 Comorbid behavioral and metabolic deficits in male mice following *Bmal1* downregulation in the suprachiasmatic nucleus

Psychiatric and metabolic diseases often coexist in the same individuals [6, 7, 230], putting a tremendous burden on patients while also challenging therapists to treat numerous illnesses concurrently. The frequent co-occurrence of psychiatric and metabolic disorders has led to the concept of 'metabolic-mood syndrome', proposing the existence of common biological mechanisms at the root of this comorbidity [15, 21]. The knowledge about these biological components remains however, scarce. Because circadian clocks influence brain and metabolic functions and both, mental and metabolic disorders are frequently associated with circadian rhythm disturbance, circadian system disruptions may play a role in the etiology of such comorbidities. Numerous prior genetic rodent studies have verified the influence of circadian clock disruption in the generation of behavioral and metabolic phenotypes. For instance, *Clock*Δ19 mice exhibit mania-like traits and were shown to develop obesity, hyperlipidemia, and hyperglycemia [148, 149]. *Cry1/2*$^{-/-}$ mice suffer from anxiety-related traits and metabolic deficits when subjected to HFD [151, 152, 231]. Further, Landgraf and colleagues demonstrated that SCN rhythm disruption by *Bmal1* knockdown in the SCN (SCN-*Bmal1*-KD) results in anxiety-related behavior, helplessness, and behavioral despair together with an increased weight gain [85]. However, a detailed metabolic profiling of SCN-*Bmal1*-KD animals is yet to be performed. Further, it is also unclear which subordinate body clocks might mediate the behavioral and metabolic deficits and whether comorbid outcomes following a chronic SCN rhythm downregulation differ from the outcomes following acute downregulation. The SCN-*Bmal1*-KD model has several advantages as it enables studying the importance of SCN rhythms in a mouse model with an anatomically intact brain, where molecular TTL rhythms in all non-SCN brain areas and peripheral tissues remain functional. Since *Bmal1* KD occurs during adulthood, this model also excludes confounds of complete *Bmal1* KO during development.

In project 1 of this thesis, the animal model of Landgraf and colleagues was used, and the metabolic phenotype of SCN-*Bmal1*-KD mice was further characterized. In order to examine comorbidity, several mood-, anxiety- and cognitive- related parameters were determined in the same animals that underwent metabolic profiling. Changes in subordinate body clocks were assessed by examining rhythmicity of the PAG and liver and *Ppox* expression in the lateral hypothalamus in SCN-*Bmal1*-KD animals. Additionally, most parameters were assessed at two

discrete time points after stereotactic injection, to investigate whether the comorbid behavioral and metabolic outcomes following a more chronic SCN rhythm downregulation differ from the outcomes following acute downregulation.

6.1.1 SCN rhythms are dampened in SCN-*Bmal1*-KD animals

The amplitude of PER2::LUC rhythms of SCN explants generated after all phenotyping tests was used to estimate the knockdown efficiency for each experimental animal. SCN explant rhythms of SCN-*Bmal1*-KD animals display a significantly downregulated PER2::LUC amplitude, together with a prolonged period and a delayed phase. In line with the prominent dampening of SCN rhythms, SCN-*Bmal1*-KD animals display a downregulated locomotor activity rhythm during LD conditions. This is in contrast with findings from Landgraf and colleagues where *Bmal1* downregulation in the SCN did not affect locomotor activity rhythms in LD [85]. It equally contrasts findings from Kolbe and colleagues where KO of *Bmal1* in the SCN did not affect behavioral rhythms under LD conditions and only resulted in a loss of locomotor activity rhythms during constant darkness (DD) [146]. Downregulated LD locomotor activity rhythms of SCN-*Bmal1*-KD animals in this project suggest that *Bmal1* KD in the SCN might have affected light masking (i.e. the direct effect of light on locomotor activity independent of the circadian clock), similarly to the reported abnormal light masking in mice lacking *Bmal1* in the forebrain/SCN [232]. Deficits in light masking were also observed in SCN-lesioned animals, where LD locomotor activity rhythms are completely lost and masking no longer works [233]. Importantly, in microscopic images of SCN explants from SCN-*Bmal1*-KD animals, no visible lesions were observed, arguing for an anatomically intact SCN. Further supporting this, PER2::LUC expression was detected in all SCN explants of SCN-*Bmal1*-KD animals, arguing for a viable SCN. Therefore, stereotactic injections were successful and resulted in a strong downregulation of SCN and locomotor activity rhythms in SCN-*Bmal1*-KD animals, highlighting once more the non-redundant role of *Bmal1* [84].

6.1.2 Downregulation of SCN rhythms leads to comorbid behavioral and metabolic deficits

6.1.2.1 Behavioral features of SCN-*Bmal1*-KD animals are reminiscent of the manic state in bipolar disorder

Downregulation of SCN rhythms in SCN-*Bmal1*-KD animals results in slightly lower overall locomotor activity in the metabolic cages due to decreased locomotion during the dark phase. Nonetheless, SCN-*Bmal1*-KD mice display enhanced locomotion in the EPM. These results demonstrate that SCN-*Bmal1*-KD animals exhibit hyperactivity in response to novelty but not over the entire LD cycle. Importantly, hyperactivity is one of the defining symptoms of a manic episode of patients suffering from BP [1]. Further, SCN-*Bmal1*-KD animals display decreased anxiety-related behavior in the EPM and DaLi box test. This contrasts the findings from Landgraf and colleagues where downregulated SCN rhythms resulted in enhanced anxiety-like behavior [85]. However, the here presented project differs from the study from Landgraf and colleagues in terms of methodological approaches (e.g., different stereotactic injection methods), *Bmal1* knockdown efficiency as well as genetic background and housing conditions of the mice. Further, potentially reconciling these contrasting results, Otsuka and colleagues recently evidenced that *Rev-erbα*$^{-/-}$ mice exhibit both, anxiety-related and mania-like features when exposed to stressful environments [116], suggesting that genetic disruption of a clock gene can principally result in both phenotypes concomitantly. In line with the observed mania-like behavior of SCN-*Bmal1*-KD animals, some other clock mutants, for instance *Clock*Δ19 and *Per2*$^{Brdm1-/-}$ mice, also display mania-like features [148, 217]. Similarly, SCN-lesioned animals evidence reduced immobility time in the forced swim test, a response associated with mania-like characteristics [86]. Another clinical aspect of mania is the enhanced response to rewarding stimuli [215]. To explore the sustained responsiveness to reward and reward learning, sucrose preference and place learning were determined, respectively. SCN-*Bmal1*-KD animals display enhanced sucrose preference (hyperhedonia) and place learning, suggesting changes in the positive valence system [218]. This indicates aberrations in reward behaviors, reminiscent of mania symptoms. In line with altered responses to rewarding stimuli of clock mutants, *Clock*Δ19 animals show enhanced behavioral responses to a psychostimulant (cocaine) and a natural reward (sucrose) [148, 216]. Similarly, mutations in *Per1* and *Per2* affect cocaine reward in mice [217]. Of note, given the previously observed mood-associated changes in SCN-*Bmal1*-KD animals [85], and the here presented findings for mania-related behavior in SCN-*Bmal1*-KD animals, it is surprising that we observe no effects in the TST and LH testing.

Since the SCN does not only play a role in mood and anxiety but has also been implicated in cognitive processes and mental-related disorders are often linked with cognitive deficits [219, 220], SCN-*Bmal1*-KD animals underwent cognitive assessments. SCN-*Bmal1*-KD animals do not display any marked alterations in the Y-maze task or in reversal and serial reversal learning. This is in line with findings in *Cry1/2*$^{-/-}$ mice, which display only mild cognitive abnormalities [151]. Interestingly, in Siberian hamster, a one-time photic treatment inducing SCN arrhythmicity leads to recognition and spatial memory deficits, which can be reversed by SCN lesion [234]. This argues that for perturbed SCN signals to cause cognitive deficits, the SCN circuitry must be genetically and anatomically intact. In line with this, in SCN-*Bmal1*-KD animals where SCN circuitries are genetically perturbed, cognition is unaltered. Nevertheless, in future studies the impact of genetic SCN rhythm downregulation on other cognitive domains such as trace memory learning should be assessed.

Overall, behavioral phenotyping of SCN-*Bmal1*-KD animals reveals disturbed circadian rhythms, hyperactivity in certain novel environments (EPM), reduced anxiety-like behavior, hyperhedonia and an enhanced propensity towards reward. Thus, behavioral features of SCN-*Bmal1*-KD mice strikingly resemble the manic state of a patient suffering from BP disorder [1].

6.1.2.2 SCN-*Bmal1*-KD animals display metabolic abnormalities despite unchanged overall food consumption

The comorbidity of behavioral and metabolic changes following downregulation of SCN rhythms was the primary focus of this project. For this reason, the same animals that underwent behavioral assessment were also characterized metabolically. Importantly, in addition to the observed behavioral deficits, the downregulation of SCN rhythms also caused several comorbid metabolic deficits. In the first weeks following stereotactic injection, SCN-*Bmal1*-KD animals display a significantly increased weight gain, despite similar overall food intake. This phenotype replicates the previous findings from Landgraf and colleagues, who observed a significantly increased weight gain of SCN-*Bmal1*-KD animals 5 weeks after AAV injection, despite unaltered overall food consumption [85]. This increased body weight was also observed in several clock mutants, including *Clock*Δ19 animals, as well as SCN-lesioned mice [87, 149]. Similar to our findings, a study reported that complete KO of *Bmal1* in the SCN of mice equally results in increased weight gain despite unchanged overall food intake [146]. However, it is worth noting that excessive weight gain of SCN-*Bmal1*-KO mice was only observed in DD and not under LD conditions — directly contrasting our findings obtained in LD conditions [146]. Interestingly, a

recently published study further characterized the above-mentioned SCN-*Bmal1*-KO mice and observed changes in the microbiome, proposing that microbial changes might represent an early step in the progression of metabolic phenotypes following a complete loss of *Bmal1* in the SCN [235]. The steep weight gain of SCN-*Bmal1*-KD animals in the first weeks following SCN rhythm downregulation plateaus approximately 6 weeks after AAV injection. This weight curve of SCN-*Bmal1*-KD animals is consistent with previous findings in constitutive *Bmal1*$^{-/-}$ animals and in mice with astrocytic *Bmal1* deletion [92, 133, 143]. In these clock mutants, the increased weight gain was followed by a steady weight decline, a phenotype that was interpreted as a sign of premature aging [92]. Further, we were wondering whether body composition (fat vs. lean mass) was altered following SCN rhythm downregulation. Although the percent gWAT and iWAT are not altered by *Bmal1* KD in the SCN, SCN-*Bmal1*-KD animals exhibit a decreased percent BAT, a tissue involved in body heat production [236]. This finding is surprising, since constitutive *Bmal1*$^{-/-}$ and adipocyte-specific *Bmal1* deletion in mice results in increased BAT formation [237]. However, in our model *Bmal1* was exclusively downregulated in the SCN, potentially explaining the contrasting result. Regardless of the direction of change of the percent BAT, the balance of white and brown adipose tissue is impaired in SCN-*Bmal1*-KD animals; a phenomenon that is known to contribute to the development of obesity [238]. Overall, we show an increased body weight gain in the first weeks following SCN rhythm downregulation, which does not result from altered overall food consumption.

6.1.2.3 SCN-*Bmal1*-KD animals display a dampening of metabolic rhythms

SCN-*Bmal1*-KD animals display altered weight gain curves despite unchanged overall food consumption. However, SCN-*Bmal1*-KD animals lose their feeding rhythms, giving a potential explanation for the aberrant weight gain. Indeed, food timing is known to play a crucial role for metabolic homeostasis. *Clock*Δ19, *Cry1/2*$^{-/-}$, and SCN-lesioned mice, all exhibit arrhythmic feeding and increased weight gain [87, 149, 152]. Further supporting our findings, SCN-specific KO of *Bmal1* (SCN-*Bmal1*-KO) causes a loss of feeding rhythms and excessive weight gain despite unchanged overall food intake in mice [146]. Interestingly, by reintroducing rhythmic food intake behavior through time-restricted feeding, metabolic regulation in SCN-*Bmal1*-KO mice was restored. The importance of rhythmic feeding for metabolic health was shown by several rodent and human studies. For instance, restricting the food access to the active phase in mice rescues the metabolic deficits caused by HFD [70], even in the absence of a functional circadian clock [71]. In humans, restricting the eating window to 10 – 11 hour daily to the active phase reduces body weight in overweight individuals [72]. In addition to unaltered total food

consumption, overall levels of other metabolic parameters (i.e., RER, EE, and water intake) are also unchanged in SCN-*Bmal1*-KD animals. However, like feeding rhythms, rhythms of RER, EE and water intake are dampened or lost in SCN-*Bmal1*-KD animals in this project. In line with these findings, *Bmal1* KO in the SCN also causes blunted RER and oxygen consumption rhythms during LD conditions [146]. Further supporting a role of the central pacemaker in controlling rhythmic metabolic signals, limiting *Bmal1* expression to the SCN is sufficient to drive the rhythms of the majority of circulating metabolites [147]. Overall, we show that SCN rhythms are important for the rhythmic expression of metabolic parameters but do not affect their overall levels. Our findings further support the notion that rhythmicity rather than overall levels of metabolic parameters is essential for metabolic homeostasis.

6.1.2.4 SCN-*Bmal1*-KD animals display altered glucose homeostasis

Given that several clock mutants display altered glucose homeostasis, we wondered whether downregulated SCN rhythms affect sugar metabolism. During the GTT, SCN-*Bmal1*-KD animals display a decreased response to the glucose injection, commonly interpreted as an increased glucose tolerance. This is in contrast with findings in SCN-*Bmal1*-KO mice, which display unaltered glucose tolerance in LD and decreased glucose tolerance in DD [146]. It equally contrasts findings from several clock mutants, including *Clock*Δ19 and *Cry1/2*$^{-/-}$, which display reduced glucose tolerance [135, 152]. However, the here observed increased glucose tolerance in SCN-*Bmal1*-KD animals likely represents an artefact from their significantly decreased fasting glucose levels. Glucose transport occurs primarily through diffusion along its concentration gradient. This phenomenon, referred to as 'glucose efficacy' occurs even in the absence of insulin action [221]. During a hypoglycemic state, this passive glucose transport results in a large uptake of glucose by the muscle and thus immediate clearance from the blood. Therefore, in SCN-*Bmal1*-KD mice, the large glucose uptake during the GTT is a direct consequence of their hypoglycemia phenotype. An alternative explanation for the enhanced glucose tolerance of SCN-*Bmal1*-KD animals is given by a study of SCN-lesioned rats [239]. SCN lesions resulted in an enhancement of glucose tolerance (i.e., high glucose uptake) during the rat's inactive (light) phase — an effect that was not observed when the GTT was performed during the active (dark) phase. Therefore, the authors concluded that SCN lesions result in a loss of the daily rhythm in glucose tolerance and increased glucose uptake during the inactive phase [239]. Given this, SCN-*Bmal1*-KD animals should be subjected to a GTT during their active phase, since the strong downregulation of SCN rhythms likely affected glucose tolerance/uptake rhythm similarly to

what has been observed in SCN-lesioned rats. Additionally, SCN-*Bmal1*-KD animals in this project do not display any changes in insulin sensitivity during the light phase. This is in line with the unaltered insulin sensitivity in SCN-lesioned rats during the light phase [239]. Similarly, insulin sensitivity is unaltered in SCN-*Bmal1*-KO mice in both, LD and DD conditions [146]. We observe that SCN-*Bmal1*-KD animals display a hypoglycemic state after 6 hours of fasting (i.e., GTT) and after 4 hours of fasting (i.e., ITT). To further investigate this hypoglycemia phenotype, we measured glucose levels over the 24-hour circadian cycle under *ad libitum* feeding conditions. Strikingly, also during *ad libitum* food access, SCN-*Bmal1*-KD animals display hypoglycemia throughout the 24-hour cycle, despite unchanged overall food intake. In line with those findings, hypoglycemia has been observed in mice with *Bmal1* deletion in the liver or in astrocytes [133, 240]. Furthermore, in SCN-lesioned rats, the plasma glucose concentration throughout the 24-hour cycle remains at the sham-operated rats' lowest level, resulting in a hypoglycemic state during the dark phase [241]. In addition to the observed hypoglycemia in SCN-*Bmal1*-KD animals, we also provide evidence that blood glucose rhythms may be lost in LD conditions under *ad libitum* feeding. Glucose rhythms are dictated by the SCN rather than local peripheral clocks and hence SCN-lesioned animals display a blunted glucose rhythm [242]. Thus, it is not surprising that downregulation of SCN rhythms as in SCN-*Bmal1*-KD animals, impacted glucose rhythms. Overall, SCN-*Bmal1*-KD animals display altered glucose tolerance and a hypoglycemia phenotype – under fasted and *ad libitum* feeding conditions – together with a potential loss of an endogenous glucose rhythm under non-fasted conditions.

6.1.3 Downregulation of SCN rhythms affects downstream circadian oscillators involved in mood- and anxiety regulation and metabolic functions

Metabolic and mood disorders are frequently linked to disrupted circadian rhythms. Due to its tight oscillator network, the SCN is extremely resistant to perturbations, whilst other tissues display less stable circadian rhythms, making them more prone to disturbances [243]. Thus, downstream circadian oscillators involved in mood- and anxiety regulation and metabolic functions have been proposed as a potential root cause for the simultaneous development of psychiatric and metabolic diseases [22]. For this reason, we assessed whether downregulated SCN rhythms affect downstream circadian oscillators involved in mood- and anxiety regulation (PAG), metabolism (liver) or both (lateral hypothalamus), further potentially contributing the observed comorbid behavioral and metabolic deficits in SCN-*Bmal1*-KD animals.

The PAG has been implicated in anxious responses and reward-seeking behavior and receives direct projections from the SCN [222, 223]. It was also reported that the PAG exhibits stable circadian rhythms *in vitro* [120]. Thus, alterations in PAG rhythmicity in SCN-*Bmal1*-KD animals could have been at the root of the observed mania-like and reward-related phenotype. Indeed, SCN-*Bmal1*-KD animals display a decreased amplitude in *ex vivo* PAG explant rhythms. Further, we show a lower percentage of rhythmic PAG slices in SCN-*Bmal1*-KD animals compared to controls, contrasting previous findings using the same animal model [85]. Results of this project suggest that the downstream PAG clock is affected by SCN rhythm downregulation. Crucially, no GFP expression was observed in PAG slices of SCN-*Bmal1*-KD animals (data not shown), suggesting that changes in PAG rhythmicity were not the result of ectopic *Bmal1* shRNA expression in the PAG but rather an indirect effect of downregulated SCN rhythms. It is worth noting that the loss of PAG tissue rhythmicity in SCN-*Bmal1*-KD animals could be resulting from two different scenarios. Firstly, the individual PAG cells could be arrhythmic resulting in tissue arrythmicity. Since the molecular TTL is likely intact in PAG cells of SCN-*Bmal1*-KD animals, this scenario is unexpected. It is rather likely that the individual PAG cells are no longer synchronized among each other (i.e., out of phase), resulting in an overall arrhythmic output of the PAG tissue.

The lateral hypothalamus contains the ORX neuronal system, which regulates a variety of body functions, including sleep/wake states, feeding behavior, energy homeostasis, reward, anxiety, and mood [244]. Accordingly, altered ORX signaling has been associated with various conditions including obesity, diabetes, depression, and BP [245-248]. To explore changes in the ORX system, we quantified the expression levels of *Ppox*, which encodes the common precursor peptide of ORX-A and -B [224], in the lateral hypothalamus at ZT3 – 4. We find that overall levels of *Ppox* are similar in SCN-*Bmal1*-KD and control animals. Interestingly, in control animals we observe a positive correlation between the amplitude of PER2::LUC oscillations in the SCN and *Ppox* expression at ZT3 – 4. In line with this, a regulation of ORX neurons by the SCN is supported by studies in diurnal and nocturnal organisms evidencing a direct projection of the SCN to ORX neurons [227, 228]. In SCN-*Bmal1*-KD animals, the correlation between the SCN PER2::LUC rhythm amplitude and *Ppox* expression is not detected. This argues for a dysregulation of the relationship between SCN amplitude and *Ppox* levels, suggesting a disturbed communication between the SCN and lateral hypothalamus. In SCN-lesioned animals and in *Clock*Δ19, ORX oscillations are lost [149, 226], advocating an involvement of the SCN in the generation of these rhythms. Thus, the strong downregulation of SCN rhythms in SCN-*Bmal1*-KD animals could have affected ORX rhythms. Importantly, similar to SCN-*Bmal1*-KD animals, SCN-lesioned rodents and *Clock*Δ19 mice display metabolic and mania-like phenotypes. However, a time-course

experiment needs to be conducted to draw a definitive conclusion about the ORX rhythm in SCN-*Bmal1*-KD animals.

The SCN regulates metabolism and mood, by directly projecting to brain regions involved in metabolic and mood regulation, including as discussed, the PAG and lateral hypothalamus. However, the SCN can also influence peripheral circadian oscillators involved in metabolism via endocrine factors [145]. We thus investigated the effect of downregulated SCN rhythms on PER2::LUC oscillations of the liver, a peripheral organ that governs metabolism. SCN-*Bmal1*-KD animals do not exhibit apparent changes in *ex vivo* liver explant rhythms. This is in line with findings from Izumo and colleagues, who found that in mice with *Bmal1* deletion in the forebrain/SCN, rhythmic clock gene expression is unchanged in peripheral tissues, including the liver [232]. However, the loss of feeding rhythms in SCN-*Bmal1*-KD animals could have affected rhythmic liver gene expression without affecting hepatic core clock gene expression. Indeed, under arrhythmic feeding, 70 % of the rhythmic mouse liver transcriptome loses rhythmicity without the rhythmic expression of core clock genes being affected [249].

Overall, our findings propose that downregulated SCN rhythms directly affect oscillators in brain areas (lateral hypothalamus and PAG) but not in peripheral tissues (liver). Changes in these oscillators can potentially mediate the observed comorbid behavioral and metabolic deficits in SCN-*Bmal1*-KD animals.

6.1.4 Strengths and weaknesses of this project

A strength of this project is that it provides a detailed behavioral and metabolic profiling of the same animals meaning that comorbidity is precisely characterized. Further, most behavioral and metabolic tests were performed at two differing time points after stereotactic injection. This approach enabled to show that comorbid behavioral and metabolic outcomes resulting from chronic downregulation of SCN rhythms do not differ from the outcomes following acute downregulation. Hence, all observed phenotypes are quickly established after SCN rhythm downregulation (~ 3 weeks) and persist over time. This indicates that SCN rhythm disruption perturbs body homeostasis — an effect, which is not compensated over time. A limitation of this project is that testing was performed only at a single time point during the inactive phase. Diurnal variations in behavior and metabolism (e.g., glucose and insulin tolerance) could have been lost in SCN-*Bmal1*-KD animals due to their heavily suppressed rhythmicity. Therefore, it would be essential to assess the phenotypes over circadian time scales to exclude the potential

confound of rhythmicity dampening on behavioral and metabolic parameters. Lastly, all experiments were only conducted in male mice, leaving any sex-specific effects unexplored.

6.1.5 Conclusion

In this project, we assessed the impact of a genetic disruption of the circadian system on comorbid behavioral and metabolic outcomes in mice. Genetic downregulation of molecular SCN rhythms results in a mania-like phenotype, without affecting features of behavioral despair or helplessness. Equally, cognitive parameters are unaltered following SCN rhythm dampening. However, SCN-*Bmal1*-KD animals display alterations in the positive valence system, suggesting changes in reward-related behavior following downregulation of SCN rhythms. Importantly, SCN-*Bmal1*-KD animals do not only exhibit behavioral changes, but also evidence concomitant metabolic deficits. SCN-*Bmal1*-KD mice show aberrant weight gain, with enhanced weight accumulation in the first weeks following SCN rhythm dampening, which thereafter plateaus. Interestingly, overall levels of metabolic parameters, including food consumption, are unchanged. However, SCN-*Bmal1*-KD animals display dampened metabolic rhythms in LD conditions, which might be at the root of the weight phenotype. Further, SCN-*Bmal1*-KD animals exhibit altered glucose tolerance and hypoglycemia – under fasted and non-fasted conditions – as well as a potential loss of the endogenous glucose rhythm under *ad libitum* feeding. This suggests alterations in glucose homeostasis following SCN rhythm dampening. Strikingly, the behavioral phenotypes of SCN-*Bmal1*-KD animals resemble clinical symptoms of the manic state of a patient suffering from BP disorder. Similarly, the metabolic deficits of SCN-*Bmal1*-KD animals resemble metabolic alterations observed in BP patients (Table 1).

Table 1. A comparison of clinical symptoms of the manic state in BP/metabolic alterations in BP and the phenotypes of SCN-*Bmal1*-KD animals.

	Clinical symptoms of the manic state in BP / Metabolic alterations in BP	**SCN-*Bmal1*-KD mice**
Behavior	Disturbed circadian rhythms [148]	Disturbed circadian rhythms
	Hyperactivity [148]	Hyperlocomotion in certain novel environments (EPM)
	Enhanced risk-taking [148]	Decreased anxiety-like behavior
	Extreme euphoria [148]	Hyperhedonia
	Propensity towards reward [148]	Enhanced sucrose preference and reward learning
Metabolism	Weight gain following the first manic episode [250]	Excessive initial weight gain
	Impaired glucose metabolism [251]	Altered glucose tolerance, hypoglycemia, and potential loss of glucose rhythms

Interestingly, SCN-*Bmal1*-KD animals display changes in PAG rhythmicity and the ORX system. Thus, the observed comorbid behavioral and metabolic deficits following SCN rhythm downregulation might result from disturbances in subordinate oscillators influencing anxiety-, reward- and metabolic-related functions.

This project was one of the first to directly address the role of the master pacemaker in the comorbidity of behavioral and metabolic outcomes by downregulating molecular rhythms in the SCN (Figure 34). Interestingly, in another study, we used the reverse approach and restored SCN rhythms in an arrhythmic *Cry1/2*$^{-/-}$ double KO animal [153]. We found that restoration of molecular SCN rhythms rescued several of the comorbid anxiety-related and metabolic phenotypes. Combined, both studies highlight an important role of SCN rhythms for behavioral and metabolic health.

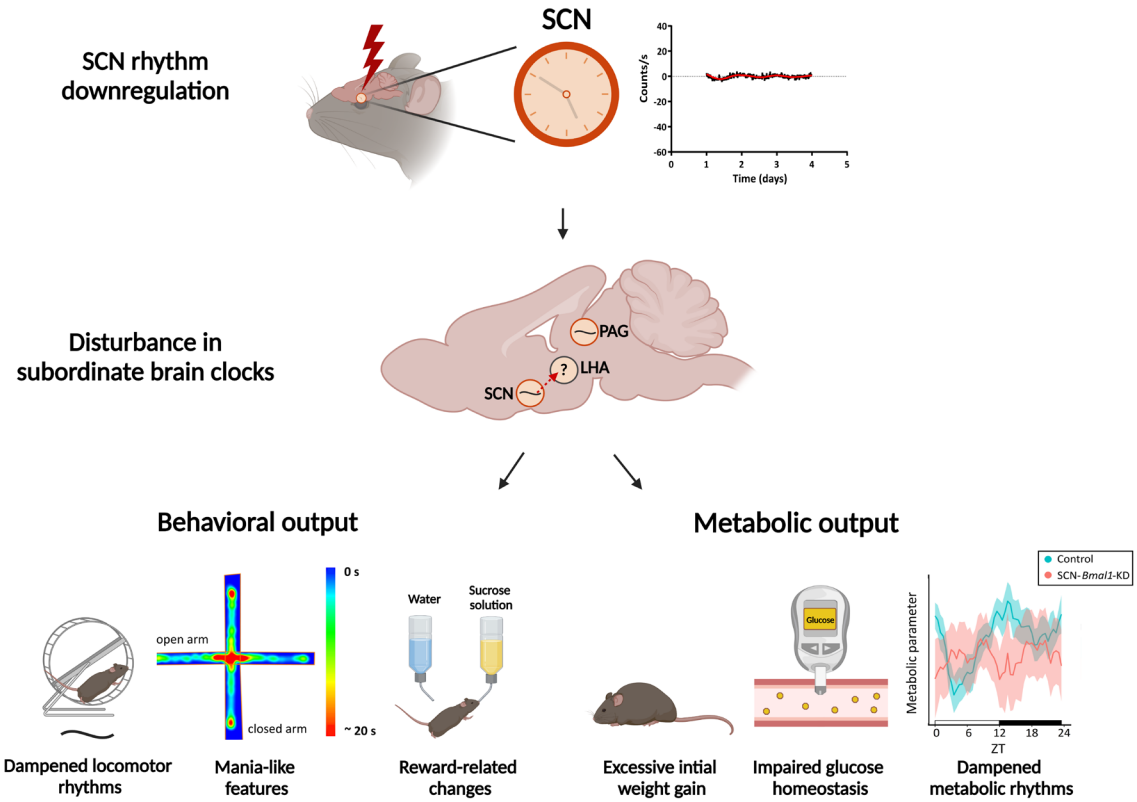

Figure 34. Summary figure for project 1. Downregulation of SCN rhythms (orange clock) leads to comorbid behavioral and metabolic deficits in mice. Following SCN rhythm downregulation, PAG rhythmicity is reduced (orange circle with dampened amplitude rhythm) and the communication between the SCN and the lateral hypothalamic area (LHA) is disturbed (dotted red arrow). Whether the rhythmicity of the LHA is altered remains to be assessed (indicated by "?"). Thus, comorbid deficits may result from the observed disturbances in subordinate circadian oscillators involved in behavioral and metabolic functions (i.e., PAG and LHA). Created with BioRender.com.

6.2 Sex-specific behavioral and metabolic phenotypes following light-induced shift work conditions in mice

In project 1, we investigated the impact of a genetic disruption of the circadian system – namely the genetic downregulation of molecular SCN rhythms – on the development of metabolic-mood comorbidity in mice. Nonetheless, the circadian system cannot only be perturbed genetically but also environmentally. A well-known environmental disruption of the circadian system is shift work. Because of our 24/7 society, an increasing proportion of individuals work outside the standard working hours with around 30 % of the working population involved in shift work [95]. Working schedules of shift workers promote a loss of synchronization between the environment (external time) and the endogenous circadian rhythms (internal time) ultimately favoring the development of many health issues, including mental and metabolic disorders [157, 229, 252]. Thus, an environmental disruption of the circadian system might represent a potential mechanism underlying mental and metabolic comorbidities.

Supporting this notion, in a large population-based study of 277,168 workers in the UK biobank, shift work was associated with concomitant adverse metabolic and mental health outcomes [182]. Despite few investigations, not many studies have explored metabolic-mood comorbidities within the same organism. Importantly, epidemiological studies have found sex differences in the shift work-associated risk of mental and metabolic disorders [99, 183]. However, the results on sex-dependent vulnerability to adverse health are often conflicting. For instance, some studies display a stronger and others a weaker association of shift work and adverse metabolic health in females compared to males [184-187]. Further, sex differences in the anatomy of the circadian system and its response to light have been reported [188, 189], potentially explaining sexual dimorphisms in shift work-associated adverse health outcomes. Despite these apparent sex differences, most studies still solely examine the impact of shift work on a single sex, leaving any potential sex-specific effects unexplored.

In project 2, we subjected mice to alternating light cycles mimicking shift work, as light is the dominant *Zeitgeber*. We assessed the direct effects of this environmental circadian disruption on comorbid behavioral and metabolic outcomes in the same animal and systematically characterized sex differences in those outcomes.

6.2.1 The shift work light paradigm leads to constant re-entrainment with sex-specific adaptation of locomotor activity to alternating light cycles

Understanding how the circadian system adapts to alternating light cycles is critical to understanding the health repercussions of shift work. Thus, we explored the behavioral response of mice to alternating light cycles, resembling schedules experienced by shift workers. We wondered whether mice entrain to alternating light cycles or start to free-run – a phenomenon that occurs when light cycle switches are performed too frequently. During free-running conditions an organism no longer responds to external *Zeitgebers* (e.g., light) and merely follows its internal rhythm. We find that following the shift work light paradigm both, male and female mice, constantly re-entrain to the given light cycle rather than entering free-running conditions. This has health implications since physiologically, free-running conditions might allow the maintenance of body homeostasis whilst constant re-entrainment is often associated with a state of internal desynchrony, further resulting in health issues [74, 170]. Accordingly, it was hypothesized that fast rotating schedules may be more tolerable for shift workers than slow rotating schedules, as lack of entrainment to faster rotating schedules might prevent the adverse health consequences of rhythms having to continuously re-entrain [253, 254]. Endorsing the notion of health benefits under missing entrainment, in rats subjected to LD rotation patterns those that free-run rather than re-entrain have favorable outcomes after being injected with a lung tumor-inducing substance [255]. Further supporting a constant re-entrainment of shift work animals, we observe a decreased locomotor activity nocturnality score in shift work animals in the IntelliCage system and the metabolic cages. The nocturnality score for the locomotor activity of shift work animals is an indirect measure for the adaptation phase to the new light cycle (i.e., behavioral shifting to the new light cycle). A high nocturnality score indicates that the animal's locomotor activity rapidly aligns with the new light cycle. In contrast, a low nocturnality score evidences a slower adaptation of the animal's locomotor activity to the given light cycle. Interestingly, female shift work animals display a greater loss of locomotor activity nocturnality compared to female controls than male shift work animals to male controls. Thus, the behavioral adaptation to light cycle alternations is sex-specific with alternating light cycles affecting female mice more than male mice. This finding is in line with observed sex differences in the phase shift responses to photic inputs [256]. Additionally, we observe a greater locomotor activity nocturnality of female compared to male mice, in line with the previously observed stronger daily wheel running rhythm in female mice [257]. Interestingly, low amplitude oscillators have been reported to be more easily shifted (i.e., greater resetting

sensitivity) [258]. Thus, the lower locomotor activity nocturnality in male mice in this project could explain why male mice are more readily shifted during the shift work light paradigm.
At the tissue level, we also report phase shifting following the shift work light paradigm. As expected, the phase of the *ex vivo* SCN explant rhythm is delayed in shift work animals. The SCN receives direct light input from the retina and hence a delayed phase of the SCN rhythm in shift work animal is a direct consequence of the light cycle shifts [259]. Of note, the amplitude and period of the SCN rhythm is unaffected by shift work conditions, suggesting that our shift work light paradigm does not affect the functioning of the molecular TTL within the SCN. As discussed above, the shift work light paradigm results in re-entrainment rather than free-running in both sexes. This leads to a temporary loss of synchronicity between the organism and the environment, further resulting in internal desynchronization. The first layer of internal desynchronization is defined by alterations in the phase relationship between the master pacemaker and other tissue clocks [74]. Interestingly, we show that the phase relationship between the SCN and the PAG rhythm is altered by shift work conditions, arguing for desynchronization between these two tissues. Contrarily, we do not detect such a desynchronization between the SCN and the liver. Nonetheless, future studies should focus on better quantifying the state of internal desynchrony and its potential sexual dimorphism following shift work conditions by for instance using EEG or time course experiments.

6.2.2 Light-induced shift work conditions lead to sex-specific behavioral and metabolic deficits

6.2.2.1 Light-induced shift work conditions lead to an anxiety-like phenotype in female but not male mice

Since sex-specific differences in the adaptation of locomotor activity to alternating light cycles were observed, we next addressed the question whether shift work conditions affect anxiety-related outcomes differently in male and female mice. Interestingly, shift work conditions result in enhanced anxiety-related behavior in the EPM and DaLi box test in female but not male mice. Furthermore, we find a sex-specific effect of shift work on restless behavior, with female shift work animals displaying increased transitions between mobile and immobile episodes in the OFT and TST compared to their sex-matched controls. Since restlessness and anxiety disorders are closely associated, the DSM-V includes restlessness as a defining symptom of generalized anxiety disorders [260]. Thus, the increased restlessness in female shift work animals further

supports the notion that shift work conditions lead to an anxiety-related phenotype in female mice. We do not find increased anxiety-related features in male mice following shift work. This finding contrasts the study of McGowan and Coogan, who reported signs of elevated anxiety-like behavior in males following light-induced shift work conditions [105]. However, whilst McGowan and Coogan assessed anxiety-related behaviors only in the OFT, we used several tests and consistently found unaltered anxiety-like behavior in male shift work animals. These contrasting results might stem from differences in the light paradigms used, the different housing conditions (single housing vs. group housing) or the different strains employed (CD-1 vs. C57BL/6J). Further, whilst we focused on the acute effects of light-induced shift work conditions, McGowan and Coogan investigated long-term effects of their shift work light paradigm [105]. The increased anxiety-related behavior in female but not male shift work animals in our project is in line with the increased prevalence of anxiety disorders in women compared to men [261]. Interestingly, we also observe a sex-specific effect of shift work on the period of the *ex vivo* PAG rhythm. Female shift work animals display a longer PAG rhythm period compared to their sex-matched controls – an effect, which is not found in male mice. Given that the PAG has been involved in anxious responses [223], a prolonged PAG circadian period might represent a potential mechanism for the observed sex-specific anxiety-related traits of female shift work animals.

6.2.2.2 Light-induced shift work conditions have sex-specific effects on helpless behavior but not on features of behavioral despair or anhedonia

Beyond anxiety-related features, helpless behavior and aspects related to behavioral despair and anhedonia were examined. We report no effects of shift work or its interaction with sex on parameters of the TST or the sucrose preference test. Thus, light-induced shift work conditions do not seem to affect despair- or anhedonia-related behavioral features in male or female mice. Studies using different light exposure manipulation paradigms found contrasting results to the ones obtained in this project. For instance, subjecting female Siberian hamsters to 4 weeks of dim light at night, results in decreased sucrose preference (i.e., increased anhedonia features) and enhanced floating behavior in the forced swim test (i.e., increased behavioral despair) [163]. Equally, LeGates and colleagues found reduced sucrose preference (i.e., enhanced anhedonia features) and increased floating time in the forced swim test (i.e., increased behavioral despair) in male mice exposed to an aberrant light cycle (i.e., cycles of 3.5 hours of light followed by 3.5 hours of dark) [160]. Despite the absence of despair- or anhedonia-related phenotypes following

our paradigm, we observe a sex-specific effect of shift work on helpless behavior. Male mice show decreased latencies and failures to escape electrical shocks during the LH test under shift work conditions, while the opposite effect is observed in female mice. This implies that shift work conditions reduce helpless behavior in males but enhance it in females. The results suggest that exposure to a primary stressor, such as shift work light conditions, may build resistance to a secondary stressor, the LH paradigm, in males, but enhance susceptibility in females. The sex-specific increase of helpless behavior in female shift work animals is in line with the observed increased prevalence of depression among female shift workers compared to male shift workers [99]. Of note, the sex-specific differences in helpless behavior following shift work conditions could also reflect sex differences in coping strategies following the electrical stressor (i.e., active coping by escaping the stressor vs. passive coping by enduring the stressor). Further, in our project, female mice display higher pain sensitivity to an electrical stimulus compared to male mice, potentially also affecting the results of the LH paradigm.

6.2.2.3 Light-induced shift work conditions cause mild sex-specific metabolic alterations in mice

Shift work has not only been linked to depression and anxiety, but also to metabolic abnormalities [229]. Therefore, we assessed behavioral and metabolic comorbidities by performing a concomitant metabolic characterization of the same animals that we also profiled behaviorally. We find that when subjected to light-induced shift work conditions, male animals display an increased percent body weight gain compared to their sex-matched controls – an effect that is not observed in female animals. Importantly, the body weight at the start of the shift work light paradigm was not different between the shift work animals and their sex-matched controls. Thus, the increased percent weight gain in male shift work animals compared to male controls did not result from differing initial body weights. In line with our findings of sex-specific body weight gain in males following shift work, previous studies reported a higher susceptibility of men to shift work-associated metabolic deficits [186, 262]. Increased body weight gain can primarily result from increased food consumption and/or decreased locomotor activity – resulting in an imbalance between energy intake and energy expenditure [263]. We observe no differences in the total locomotor activity of shift work animals compared to controls in the metabolic cage recordings. In contrast, we find that shift work conditions decrease overall locomotor activity in the IntelliCages in both sexes – a finding which was previously reported [257]. However, this effect is not sex-specific and thus cannot explain the observed sexual dimorphism in body weight increase following shift work conditions. Further, the observed

increased percent body weight gain in male shift work animals also does not result from increased overall food consumption. Indeed, shift work conditions do not increase food consumption in either sex. Accordingly, previous studies consistently found little or no difference in the overall food intake in shift workers compared to non-shift workers [264, 265]. Overall, we report a sex-specific enhanced weight gain in male shift work animals, despite unchanged overall food consumption.

6.2.2.4 Light-induced shift work conditions cause gradual shifting of metabolic parameters independent of sex

Although we do not observe a difference in overall food intake during shift work, the period of the feeding rhythm appears less robust in both, male and female shift work animals likely due to their gradual shifting to the given light cycle. In accordance, previous studies suggested that meal frequency and timing is severely disturbed amongst shift workers [264], with the likelihood of shift workers developing metabolic syndrome being linked to meal timing rather than total energy consumption [265]. Further, numerous human and rodent studies demonstrate the importance of rhythmic feeding for metabolic health [70-72]. In addition to the more variable period of the food consumption rhythm, we equally observe a less robust period of the rhythms of other metabolic parameters (i.e., water intake, EE, RER). This is in line with human and rodent shift work studies evidencing a disruption of metabolic rhythms including a loss of metabolic gene rhythmicity in the liver during shift work conditions [266]. Furthermore, we do not evidence a clear sexual dimorphism in the effect of shift work on metabolic parameter rhythmicity. Thus, whilst metabolic rhythms are similarly (un)affected by shift work conditions in male and female mice, only male mice display a significantly increased percent body weight gain following light-induced shift work conditions. This suggests the presence of other sexually dimorphic metabolic responses following shift work, which remain to be explored.

6.2.2.5 Light-induced shift work conditions do not alter glucose or insulin tolerance

Numerous human and rodent studies evidence an association between shift work and type 2 diabetes [178, 267-269]. Thus, in contrast to our expectations, we do not show an effect of shift work or its interaction with sex on glucose tolerance or insulin sensitivity. It should be noted that we observe a greater glucose response of males compared to females to both, a glucose

and insulin injection during the GTT and ITT, respectively. These results, however, likely represent an experimental artefact rather than a meaningful biological finding. Glucose and insulin injection volumes were based on body weight and since males were heavier than females, they received larger injection volumes likely explaining the observed sex effect.

6.2.2.6 Lack of metabolic deficits following shift work paradigms

Overall, we observe only minor effects of our shift work light paradigm on metabolic parameters. Total food consumption, body weight as well as glucose and insulin tolerance are only mildly — if at all – affected by our shift work light paradigm. Equally liver rhythms and the SCN-liver rhythm phase relationship are unaffected by light-induced shift work conditions. Given that shift work has repeatedly been associated with major adverse metabolic outcomes [270], our results seem surprising at first. Nonetheless, others equally observe only minor metabolic alterations following shift work conditions. For instance, exposure of female FVB mice to alternating light cycles affected metabolic parameters only moderately [181]. We propose that multiple factors might affect the results of rodent shift work studies. These include the paradigm used to mimic shift work, the duration of the paradigm, the housing conditions as well as the sex and the genetic background of the mice. Moreover, an additional metabolic trigger e.g., HFD might be needed to trigger a strong metabolic phenotype during our shift work light paradigm. In fact, HFD triggers hedonic feeding, and a preliminary study proposes that hedonic pathways contribute to weight gain in shift workers [271].

6.2.3 Strengths and weaknesses of this project

This project is the first to systematically assess sex differences in the behavioral and metabolic outcomes following a shift work light paradigm in mice. It assesses the impact of merely modulating the LD cycle on behavioral and metabolic outcomes. This allows uncoupling the effect of disturbed circadian rhythms from other lifestyle factors associated with shift work (e.g., poor diet, smoking), which also represent a major risk for disease and are frequently confounding factors in human shift work studies. However, a weakness of this project is that our shift work light paradigm does not mimic natural shift work conditions. Our protocol to investigate shift work in mice involves alternating light cycles with a distinct light and dark phase, which are unlikely to occur during a shift worker’s life. Shift work represent a particular challenge

for humans, as the external light cycle is not aligned to their work schedule – an aspect that is not fully reproduced in our shift work light paradigm. Additionally social aspects of shift work are not mimicked in our paradigm. The fact that shift workers are out of sync with family, friends, and society has a major impact on their well-being [272]. Lastly, we only assessed acute consequences of our shift work light paradigm. Long-lasting effects should be investigated, especially given that persistent behavioral changes following an environmental circadian disruption have been reported [105].

6.2.4 Conclusion

In this project, we assessed the impact of an environmental disruption of the circadian system on behavioral and metabolic outcomes in the same animal. Given the conflicting data on sexual dimorphism in shift work-associated health implications, we also assessed whether health deficits following the shift work light paradigm were sex-specific. We report the successful establishment of a shift work paradigm based on alternating light cycles. During this paradigm, mice constantly re-entrain to the given light cycle and do not enter free-running conditions. In line with constant re-entrainment, we provide preliminary evidence for internal desynchronization, namely a change in the SCN-PAG rhythm phase relationship, following shift work conditions. Importantly, we show sex-specific behavioral adaptation to alternating light cycles with male mice appearing to be more readily shifted than females. In addition, we observe sex-specific effects of the shift work light paradigm on mood- and anxiety-related behaviors. Male mice display reduced helplessness during shift work conditions, while females exhibit increased helplessness under such conditions. Moreover, female but not male mice show enhanced anxiety-like behavior following shift work conditions. In accordance, the period of the PAG rhythm, a brain region involved in anxious responses, was lengthened in female shift work animals in a sex-dependent manner. In addition to the behavioral deficits, we also observe mild shift work-induced metabolic deficits. Importantly, these metabolic changes are also sex-specific with male shift work animals displaying an enhanced percent weight gain despite unaltered total food intake. Overall, the findings from our project reveal a sex-dependent effect of shift work conditions on behavioral and metabolic outcomes in mice. Specifically, while females show increased susceptibility to anxiety-related behavior and helplessness during shift work conditions, male mice exhibit reduced helplessness and subtle comorbid metabolic deficits under the same conditions (Figure 35).

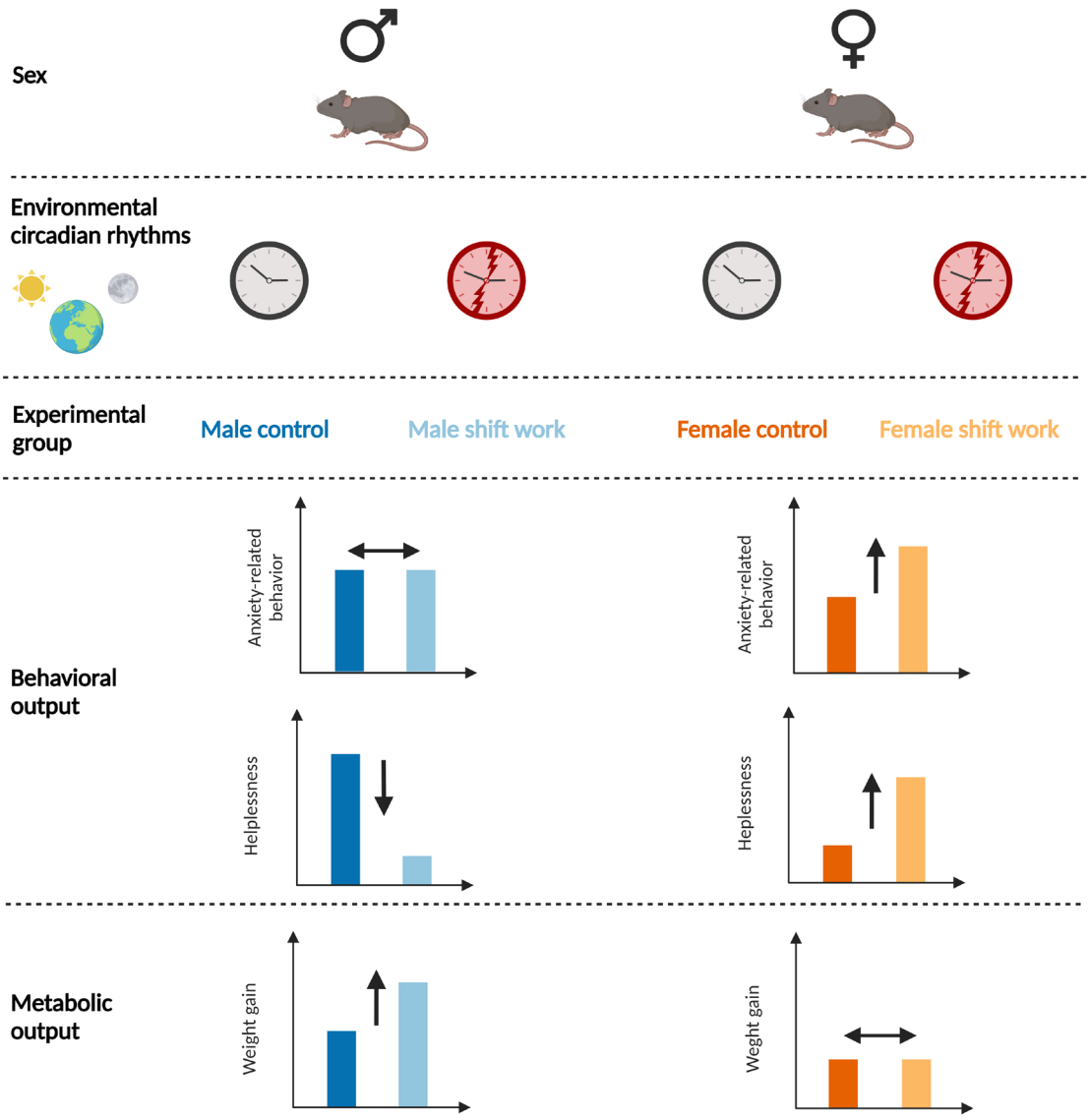

Figure 35. Summary figure for project 2. Male and female mice were exposed to control 12:12 LD conditions (intact clock) or to shift work-mimicking light conditions (broken red clock). Following shift work conditions, animals develop sex-specific behavioral and metabolic phenotypes. Whereas male mice display unaltered anxiety-related behavior and reduced helplessness during shift work conditions, females display increased anxiety-related features and helplessness under the same conditions. Additionally, male shift work animals simultaneously exhibit enhanced weight gain compared to their sex-matched controls – a phenomenon that is not observed in females. Created with BioRender.com.

6.3 Absence of an interaction between a genetic and environmental circadian disruption in comorbid behavioral and metabolic phenotypes in female mice

Shift work is associated with adverse mental and metabolic health [182]. Nonetheless, not all shift workers develop psychiatric and metabolic disturbances. This suggests the presence of predisposing genetic susceptibility factors in some shift workers, favoring the development of poor mental and metabolic outcomes following the environmental circadian disruption that their work schedule represents. Indeed, it has been acknowledged that pathology is frequently the result of a combination of both, genetic and environmental factors [193]. G×E have been predominantly discussed in relation to psychiatric disorders [197], however, there is growing evidence to suggest that G×E equally influence the risk for metabolic disorders [198]. Nevertheless, in the field of circadian biology, studies investigating the interplay between a predisposing genetic circadian disruption and an environmental circadian disruption (i.e., circadian G×E) in mediating pathology are scarce. A recent study aimed to look for such an interaction by subjecting complete *Bmal1*$^{-/-}$ KO mice to a chronic circadian disruption paradigm. The authors report that metabolic aberrations following light cycle disruption might be dependent on the molecular clock [201]. However, complete *Bmal1*$^{-/-}$ KO mice at the age of 5-7 months used in that study display drastic health consequences and are therefore an inadequate model to investigate potential additional impacts of an environmental circadian disruption [92]. Further, complete *Bmal1*$^{-/-}$ KO mice are not a translational model, because modest genetic alterations (e.g., polymorphisms) are more likely to occur in the human population. Therefore, we used *Bmal1*$^{+/-}$ mice, lacking a single copy of the *Bmal1* gene, as a circadian genetic susceptibility model.

In project 1 and 2 of this thesis the impact of a genetic and environmental circadian disruption on comorbid behavioral and metabolic outcomes in mice was investigated. Given the concept of G×E in triggering pathology, the aim of project 3 was to investigate the interaction of a genetic and an environmental circadian rhythm disruption in triggering comorbid behavioral and metabolic deficits. To this end, *Bmal1*$^{+/-}$ mice (i.e., genetic circadian disruption) were subjected to alternating light cycles (i.e., environmental circadian disruption) and profiled behaviorally and metabolically.

6.3.1 *Bmal1*$^{+/-}$ mice display altered adaptation of locomotor activity to alternating light cycles

We show that WT and *Bmal1*$^{+/-}$ mice both entrain to control 12:12 LD conditions. Indeed, in contrast to complete *Bmal1*$^{-/-}$ KO mice, which are arrhythmic even in LD conditions, it has been previously reported that *Bmal1*$^{+/-}$ mice are rhythmic in LD and DD conditions [273]. Interestingly, in the IntelliCage experiment we observe an increased locomotor activity amplitude in *Bmal1*$^{+/-}$ control animals compared to WT control animals. BMAL1 transactivation is negatively regulated by SHARP1 and SHARP2 directly or indirectly binding to DNA [33, 274]. Thus, our observation of an enhanced locomotor activity amplitude in *Bmal1*$^{+/-}$ animals is in line with the finding of a reduced locomotor activity nocturnality of mice lacking SHARP1 and SHARP2 [275]. Before investigating the health-associated implications of our shift work light paradigm, it is crucial to understand the adaptation of WT and *Bmal1*$^{+/-}$ animals to the shift work light paradigm. When exposed to alternating light cycles, WT and *Bmal1*$^{+/-}$ mice constantly re-entrain to the given light cycle rather than entering free-running conditions. Nonetheless, *Bmal1*$^{+/-}$ animals display a significantly reduced locomotor activity nocturnality following shift work conditions – an effect which is not detected in WT animals. This could indicate a more gradual adaptation of *Bmal1*$^{+/-}$ animals to alternating light cycles compared to WT animals. Contrarily, in mice lacking *Npas2*, a heterodimer partner of *Bmal1*, an accelerated adaptation to rapidly shifting LD cycles was reported [276]. Equally contrasting our result, inducible *Bmal1* deletion in mice facilitates adaptation to disrupted LD conditions [277]. Nonetheless, since *Bmal1*$^{+/-}$ animals in our project display an increased locomotor activity amplitude, the interpretation of a more gradual adaptation of *Bmal1*$^{+/-}$ animals to alternating light cycles is in line with the theory that high amplitude oscillators are less readily shifted [258].

6.3.2 No evidence for a circadian G×E in the generation of comorbid behavioral and metabolic deficits

6.3.2.1 No evidence for a circadian G×E in the generation of anxiety-like behavior

In the behavioral tests measuring anxiety-related features, we observe a genotype effect on locomotor activity, with *Bmal1*$^{+/-}$ animals displaying increased activity. This finding is in line with a previous study that reported increased distance traveled in the open field by *Bmal1*$^{+/-}$ animals

[278, 279]. We equally observe an effect of shift work on locomotion, with shift work animals displaying increased activity independent of genotype. However, we do not find an effect of shift work on the total activity throughout the 24-hour cycle. Thus, the increased locomotion of shift work animals in the behavioral tests is likely related to the gradual locomotor activity adaptation during the light cycle shifts rather than a general hyperactivity phenotype. Interestingly, *Bmal1*$^{+/-}$ animals spent less time in the center of the open field. This finding has been previously reported [279], and is equally in line with findings of anxiety-related behavior in BMAL1-deficient monkeys [280]. Nonetheless, we do not observe this increased anxiety-like phenotype of *Bmal1*$^{+/-}$ mice in any other parameter measuring anxiety-related behavior. Given that *Bmal1*$^{+/-}$ animals adapt differently to alternating light cycles and that transient re-entrainment is associated with internal desynchronization [74, 170], we expected different health repercussion in *Bmal1*$^{+/-}$ animals compared to WT when subjected to shift work conditions. We observe an interaction effect of genotype (*Bmal1*$^{+/-}$) and shift work on EPM open arm entries. Shift work conditions significantly increase open arm entries in WT animals – an effect, which is absent in *Bmal1*$^{+/-}$ animals. However, this apparent genotype-specific decrease in anxiety-related behavior could not be replicated in any other anxiety-measuring parameter. Indeed, it might represent an artefact from the observed hyperlocomotion discussed above. Thus, we conclude that in our project there is no clear interaction between a genetic circadian disruption (*Bmal1*$^{+/-}$) and an environmental circadian disruption (shift work) in the generation of anxiety-related behavior in female mice.

6.3.2.2 No evidence for a circadian G×E in the generation of depression-like phenotypes

Depression-like phenotypes were characterized by assessing behavioral despair in the TST, anhedonia-like features using the sucrose preference test and helplessness in the LH paradigm. For all three behavioral tests, we do not observe an effect of the *Bmal1*$^{+/-}$ genotype. This demonstrates that a single copy of the *Bmal1* gene is enough to prevent a depression-like phenotype and directly contrasts results in animals where both *Bmal1* copies were targeted. For instance, BMAL1-deficient monkeys display depression-like behavior and *Bmal1* deficiency in mice results in depression-like features in the TST [280] [281]. Furthermore, ablating *Bmal1* in the cerebral cortex results in a depression-like behavioral state [85, 122]. For all three behavioral tests examining depression-like features, we do not observe an effect of shift work. This contrasts numerous human and rodent studies evidencing increased depressive symptoms

following shift work conditions [157, 160, 163]. Notably, it differs from our result in project 2, which indicates enhanced helplessness in females following shift work conditions. Potential reasons for these contrasting results are explored below. Most importantly, we do not observe a circadian G×E in the TST, sucrose preference test or LH paradigm. Therefore, we cannot provide evidence for a circadian G×E in the generation of behavioral despair, anhedonia-related behavior, or helplessness traits in female mice.

6.3.2.3 No evidence for a circadian G×E in the generation of metabolic phenotypes

Metabolic profiling was performed in the same animals that were characterized behaviorally. We find no interaction effect of a genetic circadian disruption (*Bmal1*$^{+/-}$) and an environmental circadian disruption (shift work) on the major metabolic parameters assessed. Notably, for the percent weight gain, fat deposition and food consumption, no circadian G×E is detected. We equally do not observe an effect of the *Bmal1*$^{+/-}$ genotype on major metabolic outcomes. For instance, the initial weight or the fat deposition is not different in *Bmal1*$^{+/-}$ animals compared to WT animals. These findings highlight that a single copy of the *Bmal1* gene is enough to maintain metabolic homeostasis. In contrast, mice lacking both copies of *Bmal1* display lower body weights and altered fat deposition together with an early-aging phenotype [92, 282]. Regarding the overall food consumption, we find no pronounced difference between *Bmal1*$^{+/-}$ and WT animals. This is in line with previous reports of unaltered daily food intake in *Bmal1*$^{-/-}$ mice [283]. Additionally, in this project we observe that shift work conditions increase the percent body weight gain in female mice independent of genotype. This is in line with the increased prevalence of obesity among shift workers and with animal studies reporting increased weight gain in animals subjected to shift work-mimicking paradigms [165-167, 177, 179, 180, 235]. However, our results of project 2 indicate no differences in weight gain following shift work conditions in female mice. Potential explanations for the contrasting results are given below.

Since there are no circadian G×E for the major metabolic outcomes, we wondered whether the rhythmicity of parameters was affected. In the metabolic cages, we observe a genotype-independent minor delay of locomotor activity and metabolic rhythms in shift work animals on the first day of recording. This finding once more shows the gradual adaptation of shift work animals to the given light cycle. Importantly, there are no circadian G×E for the nocturnality score of the metabolic cage parameters. We merely find a genotype-independent effect of shift work on EE nocturnality with shift work animals displaying a significantly decreased EE nocturnality. Since rhythmicity rather than overall levels of physiological parameters might be

important for metabolic health, the decreased EE nocturnality may explain the observed increased percent body weight gain in shift work animals. Importantly, we overall conclude that there is no evidence for a circadian G×E in triggering metabolic deficits in female mice.

6.3.2.4 No evidence for a circadian G×E in glucose or insulin tolerance

Genetic and environmental disruptions of the circadian system have been shown to alter glucose tolerance and insulin sensitivity [152, 167, 174, 283]. However, whether genetic and environmental circadian disruptions interact and thereby potentially result in worse glucose tolerance and insulin sensitivity remained unassessed. Therefore, we performed a GTT and ITT. In our project, *Bmal1*$^{+/-}$ mice do not display changes in glucose or insulin tolerance. Against our expectations, the shift work light paradigm equally has no effect on the response to a glucose or insulin injection when correcting for baseline glucose. Most crucially, we find no interaction effect of a genetic circadian disruption (*Bmal1*$^{+/-}$) and an environmental circadian disruption (shift work) on the outcomes of the GTT and ITT. Thus, we cannot provide evidence for a circadian G×E in glucose homeostasis in female mice.

6.3.3 Strengths and weaknesses of this project

One of the strengths of this project was the use of *Bmal1*$^{+/-}$ mice, which we believed to be a more appropriate and translational model for investigating a circadian G×E compared to complete *Bmal1* KO mice. To model environmental circadian disruption, we utilized the shift work light paradigm, which we had previously established, and which has both strengths and weaknesses, as outlined in project 2. Another strength of this project, as for all the projects in this thesis, was that we examined a wide variety of behavioral and metabolic parameters in the same animals, allowing for a precise characterization of comorbidity. However, a weakness of this project was that we only used female mice, which means that any potential sex-specific effects remain unexplored. Additionally, as in project 2, we merely explored acute effects of the shift work light paradigm and thus, potential long-term implications remain unexplored. Furthermore, the sample size utilized in this project may have been insufficient to identify G×E, which are known to necessitate larger samples for the necessary statistical power.

6.3.4 Conclusion

To our knowledge, this project was the first to systematically investigate if there is an interaction between a genetic and environmental circadian disruption in the generation of comorbid behavioral and metabolic deficits. Against our expectations, the shift work-induced behavioral and metabolic effects were very mild if present at all. This is in contrast with many human and rodent studies, demonstrating a significant impact of shift work on mental and metabolic health [73, 105, 154, 270]. Indeed, in project 2, we equally observe more pronounced health effects following our shift work light paradigm. The differences in the animals' health outcomes might be explained by differences in genetic backgrounds. For instance, C57/Bl6J mice (used in project 2) display significantly lower baseline anxiety-related features compared to C57/Bl6N mice (used in project 3)[284]. This highlights that preclinical studies should take differences between genetic backgrounds into account. Further, we demonstrate that *Bmal1*$^{+/-}$ mice exhibit hyperlocomotion and mild signs of anxiety but no alterations in depression-like behavior or metabolism. Thus, a single copy of the *Bmal1* gene is enough to prevent most of the drastic health consequences observed in complete *Bmal1*$^{-/-}$ KO mice [92]. Importantly, we show that although *Bmal1*$^{+/-}$ mice display altered adaptation of locomotor activity to the shift work light paradigm, they do not evidence any clear shift work-induced behavioral or metabolic phenotypes. Therefore, we provide no evidence for a circadian G×E in the generation of comorbid behavioral and metabolic pathology in female mice (Figure 36). Given that the development of shift work-associated pathology likely results from predisposing genetic susceptibility, we recommend continuing following this line of research, despite the provided lack of evidence, using alternative approaches. For instance, mice carrying human variants of clock genes could be used as a circadian genetic susceptibility model (e.g., mice carrying a human *PER3* variant [115]). Further, an alternative shift work-mimicking paradigm could be employed (e.g., different light paradigm, forced activity, sleep deprivation, restricted feeding) [73]. Equally, factors such as the duration of the shift work-mimicking paradigm or the genetic background, sex and housing conditions of the mice should be taken into consideration. Furthermore, increasing the sample size of the animal cohorts studied might enhance the chances to uncover such G×E, well known to require larger samples to provide the required statistical power.

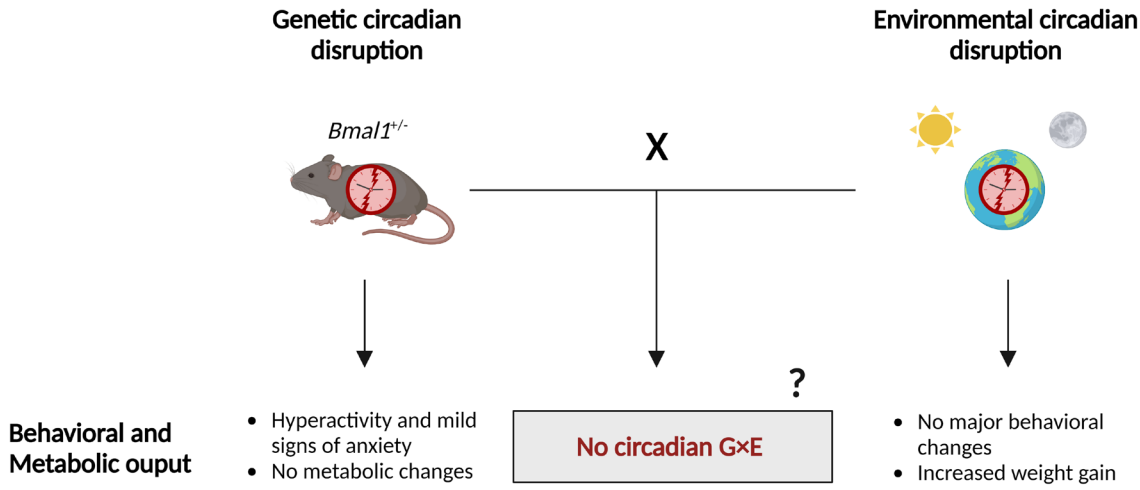

Figure 36. Summary figure for project 3. Following a genetic environmental disruption (i.e., *Bmal1*$^{+/-}$), female mice evidence mild behavioral but no metabolic changes. Following an environmental circadian disruption (i.e., light-induced shift work conditions), female mice unexpectedly display no major behavioral phenotypes and only minor metabolic deficits. Importantly, we find no evidence for an interaction between a genetic and environmental circadian disruption in the generation of comorbid behavioral and metabolic outcomes in female mice ("No circadian G×E"). However, a potential circadian G×E in the generation of comorbidities cannot be excluded as further investigations using larger sample sizes are warranted (indicated by "?"). Created with BioRender.com.

7. Overall conclusion and perspective

This thesis emphasizes the role of circadian clocks in modulating metabolic-mood comorbidities and highlights the importance of genetic and environmental circadian rhythms for mental and metabolic health.

We underscore the significance of genetic circadian rhythms by demonstrating that disrupting molecular SCN rhythms leads to behavioral and metabolic deficits in the same mouse. Nonetheless, future investigations should assess phenotypes across the circadian cycle to eliminate the possibility of rhythmicity dampening confounding behavioral and metabolic outcomes. Additionally, it remains to be examined whether superimposed environmental rhythms, for instance time-restricted feeding, can prevent comorbid phenotypes following SCN rhythm downregulation. Since dampening of SCN rhythms in this project affects subordinate clocks, future studies should differentiate the physiological processes that rely more on local canonical clocks versus those that depend directly on SCN rhythms. Despite these uncertainties, our findings suggest that stabilizing SCN rhythms, for instance by light therapy, could be a promising and easy-to-implement approach for treating or preventing comorbid metabolic and mood disorders.

This thesis also presents compelling evidence for the significance of environmental circadian rhythms in maintaining mental and metabolic health. We demonstrate that environmental circadian disruptions, such as those experienced during shift work, can have sex-specific effects on behavior and metabolism in mice. Whereas females display enhanced anxiety-related behavior and helplessness during shift work conditions, male mice exhibit reduced helplessness and subtle metabolic deficits under the same conditions. These findings underscore the need for a sex-specific approach to the prevention and treatment of shift work-associated health implications. Nonetheless, it would be pertinent to evaluate if the hereby reported sexually dimorphic health implications following shift work can be reproduced using alternative shift work-mimicking paradigms. Further, our project raises the question whether different light cycle shifts (i.e., different shift work schedules) may be more tolerable and would thus not induce the observed health deficits. Indeed, in a broader sense our findings suggest that continuous re-entrainment is associated with poor health outcomes and thereby support the notion that faster rotating work schedules may be more tolerable for shift workers due to the lack of entrainment. In future, long-term effects of our shift work-mimicking paradigm should be explored to distinguish acute effects from chronic implications, which may represent an even greater health and economic burden.

In the third project of this thesis, we were the first to systematically evaluate a potential circadian G×E in the generation of metabolic-mood comorbidities. While we did not find evidence for such an interaction in our model, we believe that further research in this area is warranted, given that shift work-associated health implications are likely influenced by genetic susceptibility. In view of the increasing numbers of individuals engaged in shift work and the significant burden of shift work-associated diseases, it would be beneficial to understand the genetic predisposition to these diseases. This knowledge could be used to identify at-risk individuals via screening, thereby preventing the development of comorbid mental and metabolic disorders. It would equally ease the development of targeted therapies for individuals suffering from health consequences of a circadian G×E by enhancing the mechanistic understanding of the affected pathways.

Overall, this thesis offers valuable insights into the impact of genetic and environmental circadian rhythms on mental and metabolic health (Figure 37). The shift work light paradigm presented in this thesis can be utilized in future studies to enhance the understanding of shift work-associated diseases and their underlying pathological mechanisms. The ultimate aim is to apply the knowledge gained from our and future research into clinical practice, thereby advancing patient care and enhancing their quality of life.

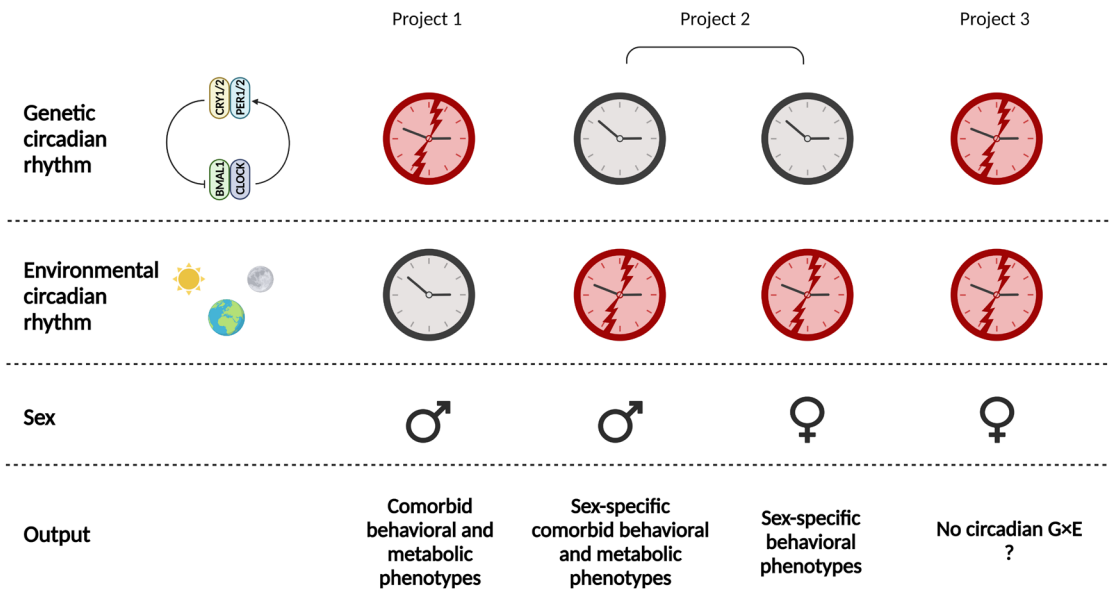

Figure 37. Summary figure for this thesis. The overarching hypothesis of this thesis was that disruptions of circadian rhythms, either of genetic or environmental origin or due to a combination of both, can lead to comorbid behavioral and metabolic deficits in mice. The distinct aspects of this overarching hypothesis were investigated in three independent projects. In project 1, a genetic circadian disruption in the SCN of male mice leads to comorbid behavioral and metabolic phenotypes. In project 2, an environmental circadian disruption has sex-specific effects on behavior and metabolism. In project 3, we find no evidence for an interaction between a genetic and environmental circadian disruption in generating comorbidities ("No circadian G×E"). However, further investigations are needed (indicated by "?"). Created with BioRender.com.

References

1. American Psychiatric Association. Diagnostic and Statistical Manual of Mental Disorders. 5th ed. Washington, DC2013.

2. Institute of Health Metrics and Evaluation. Global Health Data Exchange (GHDx) 2019 [Available from: https://vizhub.healthdata.org/gbd-results/.

3. World Health Organisation. Mental health 2022 [Available from: https://www.who.int/health-topics/mental-health#tab=tab_2.

4. Huang PL. A comprehensive definition for metabolic syndrome. Disease models & mechanisms. 2009;2(5-6):231-7.

5. Saklayen MG. The Global Epidemic of the Metabolic Syndrome. Current hypertension reports. 2018;20(2):12.

6. Blaine B. Does depression cause obesity?: A meta-analysis of longitudinal studies of depression and weight control. Journal of health psychology. 2008;13(8):1190-7.

7. Luppino FS, de Wit LM, Bouvy PF, Stijnen T, Cuijpers P, Penninx BW, et al. Overweight, obesity, and depression: a systematic review and meta-analysis of longitudinal studies. Archives of general psychiatry. 2010;67(3):220-9.

8. Toups MS, Myers AK, Wisniewski SR, Kurian B, Morris DW, Rush AJ, et al. Relationship between obesity and depression: characteristics and treatment outcomes with antidepressant medication. Psychosomatic medicine. 2013;75(9):863-72.

9. Silarova B, Giltay EJ, Van Reedt Dortland A, Van Rossum EF, Hoencamp E, Penninx BW, et al. Metabolic syndrome in patients with bipolar disorder: comparison with major depressive disorder and non-psychiatric controls. Journal of psychosomatic research. 2015;78(4):391-8.

10. Moreira FP, Jansen K, Cardoso TA, Mondin TC, Magalhães P, Kapczinski F, et al. Metabolic syndrome in subjects with bipolar disorder and major depressive disorder in a current depressive episode: Population-based study: Metabolic syndrome in current depressive episode. Journal of psychiatric research. 2017;92:119-23.

11. Pine DS, Cohen P, Brook J, Coplan JD. Psychiatric symptoms in adolescence as predictors of obesity in early adulthood: a longitudinal study. American journal of public health. 1997;87(8):1303-10.

12. Ringen PA, Engh JA, Birkenaes AB, Dieset I, Andreassen OA. Increased mortality in schizophrenia due to cardiovascular disease - a non-systematic review of epidemiology, possible causes, and interventions. Frontiers in psychiatry. 2014;5:137.

13. Vancampfort D, Vansteelandt K, Correll CU, Mitchell AJ, De Herdt A, Sienaert P, et al. Metabolic syndrome and metabolic abnormalities in bipolar disorder: a meta-analysis of prevalence rates and moderators. The American journal of psychiatry. 2013;170(3):265-74.

14. Ohaeri JU, Akanji AO. Metabolic syndrome in severe mental disorders. Metabolic syndrome and related disorders. 2011;9(2):91-8.

15. Vogelzangs N, Beekman AT, Boelhouwer IG, Bandinelli S, Milaneschi Y, Ferrucci L, et al. Metabolic depression: a chronic depressive subtype? Findings from the InCHIANTI study of older persons. The Journal of clinical psychiatry. 2011;72(5):598-604.

16. Semenkovich K, Brown ME, Svrakic DM, Lustman PJ. Depression in type 2 diabetes mellitus: prevalence, impact, and treatment. Drugs. 2015;75(6):577-87.

17. Guha P, Bhowmick K, Mazumder P, Ghosal M, Chakraborty I, Burman P. Assessment of insulin resistance and metabolic syndrome in drug naive patients of bipolar disorder. Indian journal of clinical biochemistry : IJCB. 2014;29(1):51-6.

18. van Reedt Dortland AK, Giltay EJ, van Veen T, Zitman FG, Penninx BW. Metabolic syndrome abnormalities are associated with severity of anxiety and depression and with tricyclic antidepressant use. Acta psychiatrica Scandinavica. 2010;122(1):30-9.

19. Everson SA, Maty SC, Lynch JW, Kaplan GA. Epidemiologic evidence for the relation between socioeconomic status and depression, obesity, and diabetes. Journal of psychosomatic research. 2002;53(4):891-5.

20. Kemp DE, Sylvia LG, Calabrese JR, Nierenberg AA, Thase ME, Reilly-Harrington NA, et al. General medical burden in bipolar disorder: findings from the LiTMUS comparative effectiveness trial. Acta psychiatrica Scandinavica. 2014;129(1):24-34.

21. Mansur RB, Brietzke E, McIntyre RS. Is there a "metabolic-mood syndrome"? A review of the relationship between obesity and mood disorders. Neuroscience and biobehavioral reviews. 2015;52:89-104.

22. Barandas R, Landgraf D, McCarthy MJ, Welsh DK. Circadian Clocks as Modulators of Metabolic Comorbidity in Psychiatric Disorders. Current psychiatry reports. 2015;17(12):98.

23. Ouyang Y, Andersson CR, Kondo T, Golden SS, Johnson CH. Resonating circadian clocks enhance fitness in cyanobacteria. Proceedings of the National Academy of Sciences of the United States of America. 1998;95(15):8660-4.

24. Bhadra U, Thakkar N, Das P, Pal Bhadra M. Evolution of circadian rhythms: from bacteria to human. Sleep medicine. 2017;35:49-61.

25. Hurd MW, Ralph MR. The significance of circadian organization for longevity in the golden hamster. Journal of biological rhythms. 1998;13(5):430-6.

26. Vaze KM, Sharma VK. On the adaptive significance of circadian clocks for their owners. Chronobiology international. 2013;30(4):413-33.

27. Fisk AS, Tam SKE, Brown LA, Vyazovskiy VV, Bannerman DM, Peirson SN. Light and Cognition: Roles for Circadian Rhythms, Sleep, and Arousal. Frontiers in neurology. 2018;9:56.

28. Bell-Pedersen D, Cassone VM, Earnest DJ, Golden SS, Hardin PE, Thomas TL, et al. Circadian rhythms from multiple oscillators: lessons from diverse organisms. Nature reviews Genetics. 2005;6(7):544-56.

29. Honma S. The mammalian circadian system: a hierarchical multi-oscillator structure for generating circadian rhythm. The journal of physiological sciences : JPS. 2018;68(3):207-19.

30. Reppert SM, Weaver DR. Molecular analysis of mammalian circadian rhythms. Annual review of physiology. 2001;63:647-76.

31. André E, Conquet F, Steinmayr M, Stratton SC, Porciatti V, Becker-André M. Disruption of retinoid-related orphan receptor beta changes circadian behavior, causes retinal degeneration and leads to vacillans phenotype in mice. The EMBO journal. 1998;17(14):3867-77.

32. Triqueneaux G, Thenot S, Kakizawa T, Antoch MP, Safi R, Takahashi JS, et al. The orphan receptor Rev-erbalpha gene is a target of the circadian clock pacemaker. Journal of molecular endocrinology. 2004;33(3):585-608.

33. Honma S, Kawamoto T, Takagi Y, Fujimoto K, Sato F, Noshiro M, et al. Dec1 and Dec2 are regulators of the mammalian molecular clock. Nature. 2002;419(6909):841-4.

34. Rossner MJ, Oster H, Wichert SP, Reinecke L, Wehr MC, Reinecke J, et al. Disturbed clockwork resetting in Sharp-1 and Sharp-2 single and double mutant mice. PloS one. 2008;3(7):e2762.

35. Mitsui S, Yamaguchi S, Matsuo T, Ishida Y, Okamura H. Antagonistic role of E4BP4 and PAR proteins in the circadian oscillatory mechanism. Genes & development. 2001;15(8):995-1006.

36. Mure LS, Le HD, Benegiamo G, Chang MW, Rios L, Jillani N, et al. Diurnal transcriptome atlas of a primate across major neural and peripheral tissues. Science (New York, NY). 2018;359(6381).

37. Ralph MR, Foster RG, Davis FC, Menaker M. Transplanted suprachiasmatic nucleus determines circadian period. Science (New York, NY). 1990;247(4945):975-8.

38. Silver R, LeSauter J, Tresco PA, Lehman MN. A diffusible coupling signal from the transplanted suprachiasmatic nucleus controlling circadian locomotor rhythms. Nature. 1996;382(6594):810-3.

39. Stephan FK, Zucker I. Circadian rhythms in drinking behavior and locomotor activity of rats are eliminated by hypothalamic lesions. Proceedings of the National Academy of Sciences of the United States of America. 1972;69(6):1583-6.

40. Moore RY, Eichler VB. Loss of a circadian adrenal corticosterone rhythm following suprachiasmatic lesions in the rat. Brain research. 1972;42(1):201-6.

41. Ma MA, Morrison EH. Neuroanatomy, Nucleus Suprachiasmatic. StatPearls. Treasure Island (FL): StatPearls Publishing

Copyright © 2022, StatPearls Publishing LLC.; 2022.

42. Hastings MH, Maywood ES, Brancaccio M. Generation of circadian rhythms in the suprachiasmatic nucleus. Nature reviews Neuroscience. 2018;19(8):453-69.

43. Buijs RM, la Fleur SE, Wortel J, Van Heyningen C, Zuiddam L, Mettenleiter TC, et al. The suprachiasmatic nucleus balances sympathetic and parasympathetic output to peripheral organs through separate preautonomic neurons. The Journal of comparative neurology. 2003;464(1):36-48.

44. Kalsbeek A, Palm IF, La Fleur SE, Scheer FA, Perreau-Lenz S, Ruiter M, et al. SCN outputs and the hypothalamic balance of life. Journal of biological rhythms. 2006;21(6):458-69.

45. Balsalobre A, Brown SA, Marcacci L, Tronche F, Kellendonk C, Reichardt HM, et al. Resetting of circadian time in peripheral tissues by glucocorticoid signaling. Science (New York, NY). 2000;289(5488):2344-7.

46. Daan S, Aschoff J. The Entrainment of Circadian Systems. In: Takahashi JS, Turek FW, Moore RY, editors. Circadian Clocks. Boston, MA: Springer US; 2001. p. 7-43.

47. Schibler U, Gotic I, Saini C, Gos P, Curie T, Emmenegger Y, et al. Clock-Talk: Interactions between Central and Peripheral Circadian Oscillators in Mammals. Cold Spring Harbor symposia on quantitative biology. 2015;80:223-32.

48. Dibner C, Schibler U, Albrecht U. The mammalian circadian timing system: organization and coordination of central and peripheral clocks. Annual review of physiology. 2010;72:517-49.

49. Stenvers DJ, Jonkers CF, Fliers E, Bisschop P, Kalsbeek A. Nutrition and the circadian timing system. Progress in brain research. 2012;199:359-76.

50. Begemann K, Neumann AM, Oster H. Regulation and function of extra-SCN circadian oscillators in the brain. Acta physiologica (Oxford, England). 2020;229(1):e13446.

51. Emens JS, Berman AM, Thosar SS, Butler MP, Roberts SA, Clemons NA, et al. Circadian rhythm in negative affect: Implications for mood disorders. Psychiatry research. 2020;293:113337.

52. Boivin DB, Czeisler CA, Dijk DJ, Duffy JF, Folkard S, Minors DS, et al. Complex interaction of the sleep-wake cycle and circadian phase modulates mood in healthy subjects. Archives of general psychiatry. 1997;54(2):145-52.

53. Scheer FA, Morris CJ, Shea SA. The internal circadian clock increases hunger and appetite in the evening independent of food intake and other behaviors. Obesity (Silver Spring, Md). 2013;21(3):421-3.

54. Oster H, Damerow S, Kiessling S, Jakubcakova V, Abraham D, Tian J, et al. The circadian rhythm of glucocorticoids is regulated by a gating mechanism residing in the adrenal cortical clock. Cell metabolism. 2006;4(2):163-73.

55. Li JZ, Bunney BG, Meng F, Hagenauer MH, Walsh DM, Vawter MP, et al. Circadian patterns of gene expression in the human brain and disruption in major depressive disorder. Proceedings of the National Academy of Sciences of the United States of America. 2013;110(24):9950-5.

56. Stütz AM, Staszkiewicz J, Ptitsyn A, Argyropoulos G. Circadian expression of genes regulating food intake. Obesity (Silver Spring, Md). 2007;15(3):607-15.

57. Pinho M, Sehmbi M, Cudney LE, Kauer-Sant'anna M, Magalhães PV, Reinares M, et al. The association between biological rhythms, depression, and functioning in bipolar disorder: a large multi-center study. Acta psychiatrica Scandinavica. 2016;133(2):102-8.

58. Difrancesco S, Lamers F, Riese H, Merikangas KR, Beekman ATF, van Hemert AM, et al. Sleep, circadian rhythm, and physical activity patterns in depressive and anxiety disorders: A 2-week ambulatory assessment study. Depression and anxiety. 2019;36(10):975-86.

59. Germain A, Kupfer DJ. Circadian rhythm disturbances in depression. Human psychopharmacology. 2008;23(7):571-85.

60. Ferrari E, Fraschini F, Brambilla F. Hormonal circadian rhythms in eating disorders. Biological psychiatry. 1990;27(9):1007-20.

61. Lee A, Ader M, Bray GA, Bergman RN. Diurnal variation in glucose tolerance. Cyclic suppression of insulin action and insulin secretion in normal-weight, but not obese, subjects. Diabetes. 1992;41(6):750-9.

62. Wu YH, Ursinus J, Zhou JN, Scheer FA, Ai-Min B, Jockers R, et al. Alterations of melatonin receptors MT1 and MT2 in the hypothalamic suprachiasmatic nucleus during depression. Journal of affective disorders. 2013;148(2-3):357-67.

63. Wu X, Balesar R, Lu J, Farajnia S, Zhu Q, Huang M, et al. Increased glutamic acid decarboxylase expression in the hypothalamic suprachiasmatic nucleus in depression. Brain structure & function. 2017;222(9):4079-88.

64. Zhou JN, Riemersma RF, Unmehopa UA, Hoogendijk WJ, van Heerikhuize JJ, Hofman MA, et al. Alterations in arginine vasopressin neurons in the suprachiasmatic nucleus in depression. Archives of general psychiatry. 2001;58(7):655-62.

65. Hogenboom R, Kalsbeek MJ, Korpel NL, de Goede P, Koenen M, Buijs RM, et al. Loss of arginine vasopressin- and vasoactive intestinal polypeptide-containing neurons and glial cells in the suprachiasmatic nucleus of individuals with type 2 diabetes. Diabetologia. 2019;62(11):2088-93.

66. Golden RN, Gaynes BN, Ekstrom RD, Hamer RM, Jacobsen FM, Suppes T, et al. The efficacy of light therapy in the treatment of mood disorders: a review and meta-analysis of the evidence. The American journal of psychiatry. 2005;162(4):656-62.

67. Frank E, Kupfer DJ, Thase ME, Mallinger AG, Swartz HA, Fagiolini AM, et al. Two-year outcomes for interpersonal and social rhythm therapy in individuals with bipolar I disorder. Archives of general psychiatry. 2005;62(9):996-1004.

68. Frank E, Swartz HA, Boland E. Interpersonal and social rhythm therapy: an intervention addressing rhythm dysregulation in bipolar disorder. Dialogues in clinical neuroscience. 2007;9(3):325-32.

69. Robillard R, Carpenter JS, Feilds KL, Hermens DF, White D, Naismith SL, et al. Parallel Changes in Mood and Melatonin Rhythm Following an Adjunctive Multimodal Chronobiological Intervention With Agomelatine in People With Depression: A Proof of Concept Open Label Study. Frontiers in psychiatry. 2018;9:624.

70. Hatori M, Vollmers C, Zarrinpar A, DiTacchio L, Bushong EA, Gill S, et al. Time-restricted feeding without reducing caloric intake prevents metabolic diseases in mice fed a high-fat diet. Cell metabolism. 2012;15(6):848-60.

71. Chaix A, Lin T, Le HD, Chang MW, Panda S. Time-Restricted Feeding Prevents Obesity and Metabolic Syndrome in Mice Lacking a Circadian Clock. Cell metabolism. 2019;29(2):303-19.e4.

72. Gill S, Panda S. A Smartphone App Reveals Erratic Diurnal Eating Patterns in Humans that Can Be Modulated for Health Benefits. Cell metabolism. 2015;22(5):789-98.

73. Opperhuizen AL, van Kerkhof LW, Proper KI, Rodenburg W, Kalsbeek A. Rodent models to study the metabolic effects of shiftwork in humans. Frontiers in pharmacology. 2015;6:50.

74. Hühne A, Welsh DK, Landgraf D. Prospects for circadian treatment of mood disorders. Annals of medicine. 2018;50(8):637-54.

75. Hida A, Kitamura S, Katayose Y, Kato M, Ono H, Kadotani H, et al. Screening of clock gene polymorphisms demonstrates association of a PER3 polymorphism with morningness-eveningness preference and circadian rhythm sleep disorder. Scientific reports. 2014;4:6309.

76. Lee KY, Song JY, Kim SH, Kim SC, Joo EJ, Ahn YM, et al. Association between CLOCK 3111T/C and preferred circadian phase in Korean patients with bipolar disorder. Progress in neuro-psychopharmacology & biological psychiatry. 2010;34(7):1196-201.

77. Benedetti F, Serretti A, Colombo C, Barbini B, Lorenzi C, Campori E, et al. Influence of CLOCK gene polymorphism on circadian mood fluctuation and illness recurrence in bipolar depression. American journal of medical genetics Part B, Neuropsychiatric genetics : the official publication of the International Society of Psychiatric Genetics. 2003;123b(1):23-6.

78. Garaulet M, Corbalán MD, Madrid JA, Morales E, Baraza JC, Lee YC, et al. CLOCK gene is implicated in weight reduction in obese patients participating in a dietary programme based on the Mediterranean diet. International journal of obesity (2005). 2010;34(3):516-23.

79. Bahrami S, Steen NE, Shadrin A, O'Connell K, Frei O, Bettella F, et al. Shared Genetic Loci Between Body Mass Index and Major Psychiatric Disorders: A Genome-wide Association Study. JAMA psychiatry. 2020;77(5):503-12.

80. Takahashi JS. Transcriptional architecture of the mammalian circadian clock. Nature reviews Genetics. 2017;18(3):164-79.

81. Vitaterna MH, Selby CP, Todo T, Niwa H, Thompson C, Fruechte EM, et al. Differential regulation of mammalian period genes and circadian rhythmicity by cryptochromes 1 and 2. Proceedings of the National Academy of Sciences of the United States of America. 1999;96(21):12114-9.

82. Zheng B, Albrecht U, Kaasik K, Sage M, Lu W, Vaishnav S, et al. Nonredundant roles of the mPer1 and mPer2 genes in the mammalian circadian clock. Cell. 2001;105(5):683-94.

83. DeBruyne JP, Weaver DR, Reppert SM. CLOCK and NPAS2 have overlapping roles in the suprachiasmatic circadian clock. Nature neuroscience. 2007;10(5):543-5.

84. Bunger MK, Wilsbacher LD, Moran SM, Clendenin C, Radcliffe LA, Hogenesch JB, et al. Mop3 is an essential component of the master circadian pacemaker in mammals. Cell. 2000;103(7):1009-17.

85. Landgraf D, Long JE, Proulx CD, Barandas R, Malinow R, Welsh DK. Genetic Disruption of Circadian Rhythms in the Suprachiasmatic Nucleus Causes Helplessness, Behavioral Despair, and Anxiety-like Behavior in Mice. Biological psychiatry. 2016;80(11):827-35.

86. Tataroğlu O, Aksoy A, Yilmaz A, Canbeyli R. Effect of lesioning the suprachiasmatic nuclei on behavioral despair in rats. Brain research. 2004;1001(1-2):118-24.

87. Coomans CP, van den Berg SA, Lucassen EA, Houben T, Pronk AC, van der Spek RD, et al. The suprachiasmatic nucleus controls circadian energy metabolism and hepatic insulin sensitivity. Diabetes. 2013;62(4):1102-8.

88. Cryan JF, Mombereau C. In search of a depressed mouse: utility of models for studying depression-related behavior in genetically modified mice. Molecular psychiatry. 2004;9(4):326-57.

89. Meinke G, Bohm A, Hauber J, Pisabarro MT, Buchholz F. Cre Recombinase and Other Tyrosine Recombinases. Chemical reviews. 2016;116(20):12785-820.

90. Rakai BD, Chrusch MJ, Spanswick SC, Dyck RH, Antle MC. Survival of adult generated hippocampal neurons is altered in circadian arrhythmic mice. PloS one. 2014;9(6):e99527.

91. Boden MJ, Varcoe TJ, Voultsios A, Kennaway DJ. Reproductive biology of female Bmal1 null mice. Reproduction (Cambridge, England). 2010;139(6):1077-90.

92. Kondratov RV, Kondratova AA, Gorbacheva VY, Vykhovanets OV, Antoch MP. Early aging and age-related pathologies in mice deficient in BMAL1, the core componentof the circadian clock. Genes & development. 2006;20(14):1868-73.

93. Yang G, Chen L, Grant GR, Paschos G, Song WL, Musiek ES, et al. Timing of expression of the core clock gene Bmal1 influences its effects on aging and survival. Science translational medicine. 2016;8(324):324ra16.

94. Vetter C. Circadian disruption: What do we actually mean? The European journal of neuroscience. 2020;51(1):531-50.

95. Alterman T, Luckhaupt SE, Dahlhamer JM, Ward BW, Calvert GM. Prevalence rates of work organization characteristics among workers in the U.S.: data from the 2010 National Health Interview Survey. American journal of industrial medicine. 2013;56(6):647-59.

96. Vallières A, Azaiez A, Moreau V, LeBlanc M, Morin CM. Insomnia in shift work. Sleep medicine. 2014;15(12):1440-8.

97. Øyane NM, Pallesen S, Moen BE, Akerstedt T, Bjorvatn B. Associations between night work and anxiety, depression, insomnia, sleepiness and fatigue in a sample of Norwegian nurses. PloS one. 2013;8(8):e70228.

98. Lee A, Myung SK, Cho JJ, Jung YJ, Yoon JL, Kim MY. Night Shift Work and Risk of Depression: Meta-analysis of Observational Studies. Journal of Korean medical science. 2017;32(7):1091-6.

99. Torquati L, Mielke GI, Brown WJ, Burton NW, Kolbe-Alexander TL. Shift Work and Poor Mental Health: A Meta-Analysis of Longitudinal Studies. American journal of public health. 2019;109(11):e13-e20.

100. Knutsson A, Kempe A. Shift work and diabetes--a systematic review. Chronobiology international. 2014;31(10):1146-51.

101. Sun M, Feng W, Wang F, Li P, Li Z, Li M, et al. Meta-analysis on shift work and risks of specific obesity types. Obesity reviews : an official journal of the International Association for the Study of Obesity. 2018;19(1):28-40.

102. Torquati L, Mielke GI, Brown WJ, Kolbe-Alexander T. Shift work and the risk of cardiovascular disease. A systematic review and meta-analysis including dose-response relationship. Scandinavian journal of work, environment & health. 2018;44(3):229-38.

103. Chen R, Weitzner AS, McKennon LA, Fonken LK. Chronic circadian phase advance in male mice induces depressive-like responses and suppresses neuroimmune activation. Brain, behavior, & immunity - health. 2021;17:100337.

104. Arble DM, Ramsey KM, Bass J, Turek FW. Circadian disruption and metabolic disease: findings from animal models. Best practice & research Clinical endocrinology & metabolism. 2010;24(5):785-800.

105. McGowan NM, Coogan AN. Circadian and behavioural responses to shift work-like schedules of light/dark in the mouse. Journal of molecular psychiatry. 2013;1(1):7.

106. Bilu C, Einat H, Zimmet P, Vishnevskia-Dai V, Schwartz WJ, Kronfeld-Schor N. Beneficial effects of voluntary wheel running on activity rhythms, metabolic state, and affect in a diurnal model of circadian disruption. Scientific reports. 2022;12(1):2434.

107. Guerrero-Vargas NN, Zárate-Mozo C, Guzmán-Ruiz MA, Cárdenas-Rivera A, Escobar C. Time-restricted feeding prevents depressive-like and anxiety-like behaviors in male rats exposed to an experimental model of shift-work. Journal of neuroscience research. 2021;99(2):604-20.

108. Salgado-Delgado R, Angeles-Castellanos M, Buijs MR, Escobar C. Internal desynchronization in a model of night-work by forced activity in rats. Neuroscience. 2008;154(3):922-31.

109. Benedetti F, Dallaspezia S, Colombo C, Pirovano A, Marino E, Smeraldi E. A length polymorphism in the circadian clock gene Per3 influences age at onset of bipolar disorder. Neuroscience letters. 2008;445(2):184-7.

110. Chen Z, Tao S, Zhu R, Tian S, Sun Y, Wang H, et al. Aberrant functional connectivity between the suprachiasmatic nucleus and the superior temporal gyrus: Bridging RORA gene polymorphism with diurnal mood variation in major depressive disorder. Journal of psychiatric research. 2021;132:123-30.

111. Xu Z, Chen L, Hu Y, Shen T, Chen Z, Tan T, et al. A Predictive Model of Risk Factors for Conversion From Major Depressive Disorder to Bipolar Disorder Based on Clinical Characteristics and Circadian Rhythm Gene Polymorphisms. Frontiers in psychiatry. 2022;13:843400.

112. Sipilä T, Kananen L, Greco D, Donner J, Silander K, Terwilliger JD, et al. An association analysis of circadian genes in anxiety disorders. Biological psychiatry. 2010;67(12):1163-70.

113. Liberman AR, Kwon SB, Vu HT, Filipowicz A, Ay A, Ingram KK. Circadian Clock Model Supports Molecular Link Between PER3 and Human Anxiety. Scientific reports. 2017;7(1):9893.

114. Fares S, Hermens DF, Naismith SL, White D, Hickie IB, Robillard R. Clinical correlates of chronotypes in young persons with mental disorders. Chronobiology international. 2015;32(9):1183-91.

115. Zhang L, Hirano A, Hsu PK, Jones CR, Sakai N, Okuro M, et al. A PERIOD3 variant causes a circadian phenotype and is associated with a seasonal mood trait. Proceedings of the National Academy of Sciences of the United States of America. 2016;113(11):E1536-44.

116. Otsuka T, Le HT, Thein ZL, Ihara H, Sato F, Nakao T, et al. Deficiency of the circadian clock gene Rev-erbα induces mood disorder-like behaviours and dysregulation of the serotonergic system in mice. Physiology & behavior. 2022;256:113960.

117. Spencer S, Falcon E, Kumar J, Krishnan V, Mukherjee S, Birnbaum SG, et al. Circadian genes Period 1 and Period 2 in the nucleus accumbens regulate anxiety-related behavior. The European journal of neuroscience. 2013;37(2):242-50.

118. Zhao C, Gammie SC. The circadian gene Nr1d1 in the mouse nucleus accumbens modulates sociability and anxiety-related behaviour. The European journal of neuroscience. 2018;48(3):1924-43.

119. Cho H, Zhao X, Hatori M, Yu RT, Barish GD, Lam MT, et al. Regulation of circadian behaviour and metabolism by REV-ERB-α and REV-ERB-β. Nature. 2012;485(7396):123-7.

120. Landgraf D, Long JE, Welsh DK. Depression-like behaviour in mice is associated with disrupted circadian rhythms in nucleus accumbens and periaqueductal grey. The European journal of neuroscience. 2016;43(10):1309-20.

121. Martini T, Ripperger JA, Stalin J, Kores A, Stumpe M, Albrecht U. Deletion of the clock gene Period2 (Per2) in glial cells alters mood-related behavior in mice. Scientific reports. 2021;11(1):12242.

122. Bering T, Carstensen MB, Wörtwein G, Weikop P, Rath MF. The Circadian Oscillator of the Cerebral Cortex: Molecular, Biochemical and Behavioral Effects of Deleting the Arntl Clock Gene in Cortical Neurons. Cerebral cortex (New York, NY : 1991). 2018;28(2):644-57.

123. Arushanyan EB, Popov AV. Influence of damage to the suprachiasmatic nuclei of the hypothalamus of rats on the dynamics of short-period fluctuations of normal and abnormal behavior. Neuroscience and behavioral physiology. 1995;25(4):290-5.

124. Ben-Hamo M, Larson TA, Duge LS, Sikkema C, Wilkinson CW, de la Iglesia HO, et al. Circadian Forced Desynchrony of the Master Clock Leads to Phenotypic Manifestation of Depression in Rats. eNeuro. 2016;3(6).

125. Tuma J, Strubbe JH, Mocaër E, Koolhaas JM. Anxiolytic-like action of the antidepressant agomelatine (S 20098) after a social defeat requires the integrity of the SCN. European neuropsychopharmacology : the journal of the European College of Neuropsychopharmacology. 2005;15(5):545-55.

126. Vadnie CA, Petersen KA, Eberhardt LA, Hildebrand MA, Cerwensky AJ, Zhang H, et al. The Suprachiasmatic Nucleus Regulates Anxiety-Like Behavior in Mice. Frontiers in neuroscience. 2021;15:765850.

127. Boehler NA, Fung SW, Hegazi S, Cheng AH, Cheng HM. Sox2 Ablation in the Suprachiasmatic Nucleus Perturbs Anxiety- and Depressive-like Behaviors. Neurology international. 2021;13(4):541-54.

128. Scott EM, Carter AM, Grant PJ. Association between polymorphisms in the Clock gene, obesity and the metabolic syndrome in man. International journal of obesity (2005). 2008;32(4):658-62.

129. Valladares M, Obregón AM, Chaput JP. Association between genetic variants of the clock gene and obesity and sleep duration. Journal of physiology and biochemistry. 2015;71(4):855-60.

130. Woon PY, Kaisaki PJ, Bragança J, Bihoreau MT, Levy JC, Farrall M, et al. Aryl hydrocarbon receptor nuclear translocator-like (BMAL1) is associated with susceptibility to hypertension and type 2 diabetes. Proceedings of the National Academy of Sciences of the United States of America. 2007;104(36):14412-7.

131. Below JE, Gamazon ER, Morrison JV, Konkashbaev A, Pluzhnikov A, McKeigue PM, et al. Genome-wide association and meta-analysis in populations from Starr County, Texas, and

Mexico City identify type 2 diabetes susceptibility loci and enrichment for expression quantitative trait loci in top signals. Diabetologia. 2011;54(8):2047-55.

132. Yu JH, Yun CH, Ahn JH, Suh S, Cho HJ, Lee SK, et al. Evening chronotype is associated with metabolic disorders and body composition in middle-aged adults. The Journal of clinical endocrinology and metabolism. 2015;100(4):1494-502.

133. Lamia KA, Storch KF, Weitz CJ. Physiological significance of a peripheral tissue circadian clock. Proceedings of the National Academy of Sciences of the United States of America. 2008;105(39):15172-7.

134. Dallmann R, Weaver DR. Altered body mass regulation in male mPeriod mutant mice on high-fat diet. Chronobiology international. 2010;27(6):1317-28.

135. Marcheva B, Ramsey KM, Buhr ED, Kobayashi Y, Su H, Ko CH, et al. Disruption of the clock components CLOCK and BMAL1 leads to hypoinsulinaemia and diabetes. Nature. 2010;466(7306):627-31.

136. Dyar KA, Ciciliot S, Wright LE, Biensø RS, Tagliazucchi GM, Patel VR, et al. Muscle insulin sensitivity and glucose metabolism are controlled by the intrinsic muscle clock. Molecular metabolism. 2014;3(1):29-41.

137. Paschos GK, Ibrahim S, Song WL, Kunieda T, Grant G, Reyes TM, et al. Obesity in mice with adipocyte-specific deletion of clock component Arntl. Nature medicine. 2012;18(12):1768-77.

138. Yu F, Wang Z, Zhang T, Chen X, Xu H, Wang F, et al. Deficiency of intestinal Bmal1 prevents obesity induced by high-fat feeding. Nature communications. 2021;12(1):5323.

139. Onuma S, Kinoshita S, Shimba S, Ozono K, Michigami T, Kawai M. The lack of Bmal1, a core clock gene, in the intestine decreases glucose absorption in mice. Endocrinology. 2022.

140. Koch CE, Begemann K, Kiehn JT, Griewahn L, Mauer J, Hess ME, et al. Circadian regulation of hedonic appetite in mice by clocks in dopaminergic neurons of the VTA. Nature communications. 2020;11(1):3071.

141. Cedernaes J, Huang W, Ramsey KM, Waldeck N, Cheng L, Marcheva B, et al. Transcriptional Basis for Rhythmic Control of Hunger and Metabolism within the AgRP Neuron. Cell metabolism. 2019;29(5):1078-91.e5.

142. Orozco-Solis R, Aguilar-Arnal L, Murakami M, Peruquetti R, Ramadori G, Coppari R, et al. The Circadian Clock in the Ventromedial Hypothalamus Controls Cyclic Energy Expenditure. Cell metabolism. 2016;23(3):467-78.

143. Barca-Mayo O, Boender AJ, Armirotti A, De Pietri Tonelli D. Deletion of astrocytic BMAL1 results in metabolic imbalance and shorter lifespan in mice. Glia. 2020;68(6):1131-47.

144. Wang XL, Kooijman S, Gao Y, Tzeplaeff L, Cosquer B, Milanova I, et al. Microglia-specific knock-down of Bmal1 improves memory and protects mice from high fat diet-induced obesity. Molecular psychiatry. 2021;26(11):6336-49.

145. Ding G, Gong Y, Eckel-Mahan KL, Sun Z. Central Circadian Clock Regulates Energy Metabolism. Advances in experimental medicine and biology. 2018;1090:79-103.

146. Kolbe I, Leinweber B, Brandenburger M, Oster H. Circadian clock network desynchrony promotes weight gain and alters glucose homeostasis in mice. Molecular metabolism. 2019;30:140-51.

147. Petrus P, Smith JG, Koronowski KB, Chen S, Sato T, Greco CM, et al. The central clock suffices to drive the majority of circulatory metabolic rhythms. Science advances. 2022;8(26):eabo2896.

148. Roybal K, Theobold D, Graham A, DiNieri JA, Russo SJ, Krishnan V, et al. Mania-like behavior induced by disruption of CLOCK. Proceedings of the National Academy of Sciences of the United States of America. 2007;104(15):6406-11.

149. Turek FW, Joshu C, Kohsaka A, Lin E, Ivanova G, McDearmon E, et al. Obesity and metabolic syndrome in circadian Clock mutant mice. Science (New York, NY). 2005;308(5724):1043-5.

150. Shostak A, Meyer-Kovac J, Oster H. Circadian regulation of lipid mobilization in white adipose tissues. Diabetes. 2013;62(7):2195-203.

151. Hühne A, Volkmann P, Stephan M, Rossner M, Landgraf D. An in-depth neurobehavioral characterization shows anxiety-like traits, impaired habituation behavior, and restlessness in male Cryptochrome-deficient mice. Genes, brain, and behavior. 2020;19(8):e12661.

152. Barclay JL, Shostak A, Leliavski A, Tsang AH, Jöhren O, Müller-Fielitz H, et al. High-fat diet-induced hyperinsulinemia and tissue-specific insulin resistance in Cry-deficient mice. American journal of physiology Endocrinology and metabolism. 2013;304(10):E1053-63.

153. Hühne-Landgraf A, Frisch MK, Laurent K, Wehr MC, Rossner MJ, Landgraf D. Rescue of Comorbid Behavioral and Metabolic Phenotypes of Arrhythmic Mice by Restoring Circadian Cryptochrome1/2 Expression in the Suprachiasmatic Nucleus. [Manuscript submitted for publication]. 2023;Department of Molecular Neurobiology, Clinic of Psychiatry and Psychotherapy, University Hospital, Ludwig Maximilian University.

154. Brown JP, Martin D, Nagaria Z, Verceles AC, Jobe SL, Wickwire EM. Mental Health Consequences of Shift Work: An Updated Review. Current psychiatry reports. 2020;22(2):7.

155. Bara AC, Arber S. Working shifts and mental health--findings from the British Household Panel Survey (1995-2005). Scandinavian journal of work, environment & health. 2009;35(5):361-7.

156. Kalmbach DA, Fang Y, Arnedt JT, Cochran AL, Deldin PJ, Kaplin AI, et al. Effects of Sleep, Physical Activity, and Shift Work on Daily Mood: a Prospective Mobile Monitoring Study of Medical Interns. Journal of general internal medicine. 2018;33(6):914-20.

157. Pereira H, Fehér G, Tibold A, Monteiro S, Costa V, Esgalhado G. The Impact of Shift Work on Occupational Health Indicators among Professionally Active Adults: A Comparative Study. International journal of environmental research and public health. 2021;18(21).

158. Voinescu BI. Common Sleep, Psychiatric, and Somatic Problems According to Work Schedule: an Internet Survey in an Eastern European Country. International journal of behavioral medicine. 2018;25(4):456-64.

159. Fève-Montange M, Van Cauter E, Refetoff S, Désir D, Tourniaire J, Copinschi G. Effects of "jet lag" on hormonal patterns. II. Adaptation of melatonin circadian periodicity. The Journal of clinical endocrinology and metabolism. 1981;52(4):642-9.

160. LeGates TA, Altimus CM, Wang H, Lee HK, Yang S, Zhao H, et al. Aberrant light directly impairs mood and learning through melanopsin-expressing neurons. Nature. 2012;491(7425):594-8.

161. Tapia-Osorio A, Salgado-Delgado R, Angeles-Castellanos M, Escobar C. Disruption of circadian rhythms due to chronic constant light leads to depressive and anxiety-like behaviors in the rat. Behavioural brain research. 2013;252:1-9.

162. Horsey EA, Maletta T, Turner H, Cole C, Lehmann H, Fournier NM. Chronic Jet Lag Simulation Decreases Hippocampal Neurogenesis and Enhances Depressive Behaviors and Cognitive Deficits in Adult Male Rats. Frontiers in behavioral neuroscience. 2019;13:272.

163. Bedrosian TA, Weil ZM, Nelson RJ. Chronic dim light at night provokes reversible depression-like phenotype: possible role for TNF. Molecular psychiatry. 2013;18(8):930-6.

164. Brum MC, Filho FF, Schnorr CC, Bottega GB, Rodrigues TC. Shift work and its association with metabolic disorders. Diabetology & metabolic syndrome. 2015;7:45.

165. De Bacquer D, Van Risseghem M, Clays E, Kittel F, De Backer G, Braeckman L. Rotating shift work and the metabolic syndrome: a prospective study. International journal of epidemiology. 2009;38(3):848-54.

166. Biggi N, Consonni D, Galluzzo V, Sogliani M, Costa G. Metabolic syndrome in permanent night workers. Chronobiology international. 2008;25(2):443-54.

167. Szosland D. Shift work and metabolic syndrome, diabetes mellitus and ischaemic heart disease. International journal of occupational medicine and environmental health. 2010;23(3):287-91.

168. Karlsson BH, Knutsson AK, Lindahl BO, Alfredsson LS. Metabolic disturbances in male workers with rotating three-shift work. Results of the WOLF study. International archives of occupational and environmental health. 2003;76(6):424-30.

169. Lin YC, Hsiao TJ, Chen PC. Persistent rotating shift-work exposure accelerates development of metabolic syndrome among middle-aged female employees: a five-year follow-up. Chronobiology international. 2009;26(4):740-55.

170. Scheer FA, Hilton MF, Mantzoros CS, Shea SA. Adverse metabolic and cardiovascular consequences of circadian misalignment. Proceedings of the National Academy of Sciences of the United States of America. 2009;106(11):4453-8.

171. Kyle JE, Bramer LM, Claborne D, Stratton KG, Bloodsworth KJ, Teeguarden JG, et al. Simulated Night-Shift Schedule Disrupts the Plasma Lipidome and Reveals Early Markers of Cardiovascular Disease Risk. Nature and science of sleep. 2022;14:981-94.

172. Skene DJ, Skornyakov E, Chowdhury NR, Gajula RP, Middleton B, Satterfield BC, et al. Separation of circadian- and behavior-driven metabolite rhythms in humans provides a window on peripheral oscillators and metabolism. Proceedings of the National Academy of Sciences of the United States of America. 2018;115(30):7825-30.

173. Coomans CP, van den Berg SA, Houben T, van Klinken JB, van den Berg R, Pronk AC, et al. Detrimental effects of constant light exposure and high-fat diet on circadian energy metabolism and insulin sensitivity. FASEB journal : official publication of the Federation of American Societies for Experimental Biology. 2013;27(4):1721-32.

174. Fonken LK, Workman JL, Walton JC, Weil ZM, Morris JS, Haim A, et al. Light at night increases body mass by shifting the time of food intake. Proceedings of the National Academy of Sciences of the United States of America. 2010;107(43):18664-9.

175. Salgado-Delgado R, Angeles-Castellanos M, Saderi N, Buijs RM, Escobar C. Food intake during the normal activity phase prevents obesity and circadian desynchrony in a rat model of night work. Endocrinology. 2010;151(3):1019-29.

176. Barclay JL, Husse J, Bode B, Naujokat N, Meyer-Kovac J, Schmid SM, et al. Circadian desynchrony promotes metabolic disruption in a mouse model of shiftwork. PloS one. 2012;7(5):e37150.

177. Karatsoreos IN, Bhagat S, Bloss EB, Morrison JH, McEwen BS. Disruption of circadian clocks has ramifications for metabolism, brain, and behavior. Proceedings of the National Academy of Sciences of the United States of America. 2011;108(4):1657-62.

178. Zhong LX, Li XN, Yang GY, Zhang X, Li WX, Zhang QQ, et al. Circadian misalignment alters insulin sensitivity during the light phase and shifts glucose tolerance rhythms in female mice. PloS one. 2019;14(12):e0225813.

179. Christie S, Vincent AD, Li H, Frisby CL, Kentish SJ, O'Rielly R, et al. A rotating light cycle promotes weight gain and hepatic lipid storage in mice. American journal of physiology Gastrointestinal and liver physiology. 2018;315(6):G932-g42.

180. Oike H, Sakurai M, Ippoushi K, Kobori M. Time-fixed feeding prevents obesity induced by chronic advances of light/dark cycles in mouse models of jet-lag/shift work. Biochemical and biophysical research communications. 2015;465(3):556-61.

181. Schilperoort M, van den Berg R, Dollé MET, van Oostrom CTM, Wagner K, Tambyrajah LL, et al. Time-restricted feeding improves adaptation to chronically alternating light-dark cycles. Scientific reports. 2019;9(1):7874.

182. Wyse CA, Celis Morales CA, Graham N, Fan Y, Ward J, Curtis AM, et al. Adverse metabolic and mental health outcomes associated with shiftwork in a population-based study of 277,168 workers in UK biobank<sup/>. Annals of medicine. 2017;49(5):411-20.

183. Qian J, Morris CJ, Caputo R, Wang W, Garaulet M, Scheer F. Sex differences in the circadian misalignment effects on energy regulation. Proceedings of the National Academy of Sciences of the United States of America. 2019;116(47):23806-12.

184. Silva-Costa A, Rotenberg L, Nobre AA, Schmidt MI, Chor D, Griep RH. Gender-specific association between night-work exposure and type-2 diabetes: results from longitudinal study of adult health, ELSA-Brasil. Scandinavian journal of work, environment & health. 2015;41(6):569-78.

185. Guo Y, Rong Y, Huang X, Lai H, Luo X, Zhang Z, et al. Shift work and the relationship with metabolic syndrome in Chinese aged workers. PloS one. 2015;10(3):e0120632.

186. Gan Y, Yang C, Tong X, Sun H, Cong Y, Yin X, et al. Shift work and diabetes mellitus: a meta-analysis of observational studies. Occupational and environmental medicine. 2015;72(1):72-8.

187. Son M, Ye BJ, Kim JI, Kang S, Jung KY. Association between shift work and obesity according to body fat percentage in Korean wage workers: data from the fourth and the fifth Korea National Health and Nutrition Examination Survey (KNHANES 2008-2011). Annals of occupational and environmental medicine. 2015;27:32.

188. Bailey M, Silver R. Sex differences in circadian timing systems: implications for disease. Frontiers in neuroendocrinology. 2014;35(1):111-39.

189. Kuljis DA, Loh DH, Truong D, Vosko AM, Ong ML, McClusky R, et al. Gonadal- and sex-chromosome-dependent sex differences in the circadian system. Endocrinology. 2013;154(4):1501-12.

190. Goel N, Lee TM. Sex differences and effects of social cues on daily rhythms following phase advances in Octodon degus. Physiology & behavior. 1995;58(2):205-13.

191. Lee R, Tapia A, Kaladchibachi S, Grandner MA, Fernandez FX. Meta-analysis of light and circadian timekeeping in rodents. Neuroscience and biobehavioral reviews. 2021;123:215-29.

192. Kendler KS, Eaves LJ. Models for the joint effect of genotype and environment on liability to psychiatric illness. The American journal of psychiatry. 1986;143(3):279-89.

193. Plomin R, Owen MJ, McGuffin P. The genetic basis of complex human behaviors. Science (New York, NY). 1994;264(5166):1733-9.

194. Meehl PE. Schizotaxia, schizotypy, schizophrenia. American Psychologist. 1962;17:827-38.

195. Bleuler M. Conception of Schizophrenia Within the Last Fifty Years and Today [Abridged]. Proceedings of the Royal Society of Medicine. 1963;56(10):945-52.

196. Rosenthal D. A suggested conceptual framework. The Genain quadruplets: A case study and theoretical analysis of heredity and environment in schizophrenia. New York, NY, US: Basic Books; 1963. p. 505-11.

197. Assary E, Vincent JP, Keers R, Pluess M. Gene-environment interaction and psychiatric disorders: Review and future directions. Seminars in cell & developmental biology. 2018;77:133-43.

198. Ordovas JM, Shen J. Gene-environment interactions and susceptibility to metabolic syndrome and other chronic diseases. Journal of periodontology. 2008;79(8 Suppl):1508-13.

199. Togo F, Yoshizaki T, Komatsu T. Association between depressive symptoms and morningness-eveningness, sleep duration and rotating shift work in Japanese nurses. Chronobiology international. 2017;34(3):349-59.

200. Hulsegge G, Picavet HSJ, van der Beek AJ, Verschuren WMM, Twisk JW, Proper KI. Shift work, chronotype and the risk of cardiometabolic risk factors. European journal of public health. 2019;29(1):128-34.

201. Pati P, Colson J, Dunaway L, Pollock DM, Pollock JS. Environmental Circadian Disruption Alters Body Composition and Impairs Energy Expenditure Rhythm Dependent on the Clock Gene, Bmal1. The FASEB Journal 2022;36(S1).

202. Mauvais-Jarvis F. Sex differences in metabolic homeostasis, diabetes, and obesity. Biology of sex differences. 2015;6:14.

203. Seney ML, Sibille E. Sex differences in mood disorders: perspectives from humans and rodent models. Biology of sex differences. 2014;5(1):17.

204. Sandberg K, Umans JG. Recommendations concerning the new U.S. National Institutes of Health initiative to balance the sex of cells and animals in preclinical research. FASEB journal : official publication of the Federation of American Societies for Experimental Biology. 2015;29(5):1646-52.

205. Yoo SH, Yamazaki S, Lowrey PL, Shimomura K, Ko CH, Buhr ED, et al. PERIOD2::LUCIFERASE real-time reporting of circadian dynamics reveals persistent circadian oscillations in mouse peripheral tissues. Proceedings of the National Academy of Sciences of the United States of America. 2004;101(15):5339-46.

206. Storch KF, Paz C, Signorovitch J, Raviola E, Pawlyk B, Li T, et al. Intrinsic circadian clock of the mammalian retina: importance for retinal processing of visual information. Cell. 2007;130(4):730-41.

207. Lakso M, Pichel JG, Gorman JR, Sauer B, Okamoto Y, Lee E, et al. Efficient in vivo manipulation of mouse genomic sequences at the zygote stage. Proceedings of the National Academy of Sciences of the United States of America. 1996;93(12):5860-5.

208. Landgraf D, Long J, Der-Avakian A, Streets M, Welsh DK. Dissociation of learned helplessness and fear conditioning in mice: a mouse model of depression. PloS one. 2015;10(4):e0125892.

209. Volkmann P, Stephan M, Krackow S, Jensen N, Rossner MJ. PsyCoP - A Platform for Systematic Semi-Automated Behavioral and Cognitive Profiling Reveals Gene and Environment Dependent Impairments of Tcf4 Transgenic Mice Subjected to Social Defeat. Frontiers in behavioral neuroscience. 2020;14:618180.

210. Geissmann Q, Garcia Rodriguez L, Beckwith EJ, Gilestro GF. Rethomics: An R framework to analyse high-throughput behavioural data. PloS one. 2019;14(1):e0209331.

211. Landgraf D, Tsang AH, Leliavski A, Koch CE, Barclay JL, Drucker DJ, et al. Oxyntomodulin regulates resetting of the liver circadian clock by food. eLife. 2015;4:e06253.

212. Mickelsen LE, Kolling FWt, Chimileski BR, Fujita A, Norris C, Chen K, et al. Neurochemical Heterogeneity Among Lateral Hypothalamic Hypocretin/Orexin and Melanin-Concentrating Hormone Neurons Identified Through Single-Cell Gene Expression Analysis. eNeuro. 2017;4(5).

213. Kim TK, Kim JE, Park JY, Lee JE, Choi J, Kim H, et al. Antidepressant effects of exercise are produced via suppression of hypocretin/orexin and melanin-concentrating hormone in the basolateral amygdala. Neurobiology of disease. 2015;79:59-69.

214. Pfaffl MW. A new mathematical model for relative quantification in real-time RT-PCR. Nucleic acids research. 2001;29(9):e45.

215. Whitton AE, Treadway MT, Pizzagalli DA. Reward processing dysfunction in major depression, bipolar disorder and schizophrenia. Current opinion in psychiatry. 2015;28(1):7-12.

216. McClung CA, Sidiropoulou K, Vitaterna M, Takahashi JS, White FJ, Cooper DC, et al. Regulation of dopaminergic transmission and cocaine reward by the Clock gene. Proceedings of the National Academy of Sciences of the United States of America. 2005;102(26):9377-81.

217. Abarca C, Albrecht U, Spanagel R. Cocaine sensitization and reward are under the influence of circadian genes and rhythm. Proceedings of the National Academy of Sciences of the United States of America. 2002;99(13):9026-30.

218. Morris SE, Cuthbert BN. Research Domain Criteria: cognitive systems, neural circuits, and dimensions of behavior. Dialogues in clinical neuroscience. 2012;14(1):29-37.

219. Robinson OJ, Vytal K, Cornwell BR, Grillon C. The impact of anxiety upon cognition: perspectives from human threat of shock studies. Frontiers in human neuroscience. 2013;7:203.

220. Perini G, Cotta Ramusino M, Sinforiani E, Bernini S, Petrachi R, Costa A. Cognitive impairment in depression: recent advances and novel treatments. Neuropsychiatric disease and treatment. 2019;15:1249-58.

221. Virtue S, Vidal-Puig A. GTTs and ITTs in mice: simple tests, complex answers. Nature metabolism. 2021;3(7):883-6.

222. Kriegsfeld LJ, Leak RK, Yackulic CB, LeSauter J, Silver R. Organization of suprachiasmatic nucleus projections in Syrian hamsters (Mesocricetus auratus): an anterograde and retrograde analysis. The Journal of comparative neurology. 2004;468(3):361-79.

223. Motta SC, Carobrez AP, Canteras NS. The periaqueductal gray and primal emotional processing critical to influence complex defensive responses, fear learning and reward seeking. Neuroscience and biobehavioral reviews. 2017;76(Pt A):39-47.

224. Sakurai T, Amemiya A, Ishii M, Matsuzaki I, Chemelli RM, Tanaka H, et al. Orexins and orexin receptors: a family of hypothalamic neuropeptides and G protein-coupled receptors that regulate feeding behavior. Cell. 1998;92(4):573-85.

225. Hühne A, Echtler L, Kling C, Stephan M, Schmidt MV, Rossner MJ, et al. Circadian gene × environment perturbations influence alcohol drinking in Cryptochrome-deficient mice. Addiction biology. 2022;27(1):e13105.

226. Zhang S, Zeitzer JM, Yoshida Y, Wisor JP, Nishino S, Edgar DM, et al. Lesions of the suprachiasmatic nucleus eliminate the daily rhythm of hypocretin-1 release. Sleep. 2004;27(4):619-27.

227. Abrahamson EE, Leak RK, Moore RY. The suprachiasmatic nucleus projects to posterior hypothalamic arousal systems. Neuroreport. 2001;12(2):435-40.

228. Schwartz MD, Urbanski HF, Nunez AA, Smale L. Projections of the suprachiasmatic nucleus and ventral subparaventricular zone in the Nile grass rat (Arvicanthis niloticus). Brain research. 2011;1367:146-61.

229. Antunes LC, Levandovski R, Dantas G, Caumo W, Hidalgo MP. Obesity and shift work: chronobiological aspects. Nutrition research reviews. 2010;23(1):155-68.

230. McElroy SL, Kotwal R, Malhotra S, Nelson EB, Keck PE, Nemeroff CB. Are mood disorders and obesity related? A review for the mental health professional. The Journal of clinical psychiatry. 2004;65(5):634-51, quiz 730.

231. De Bundel D, Gangarossa G, Biever A, Bonnefont X, Valjent E. Cognitive dysfunction, elevated anxiety, and reduced cocaine response in circadian clock-deficient cryptochrome knockout mice. Frontiers in behavioral neuroscience. 2013;7:152.

232. Izumo M, Pejchal M, Schook AC, Lange RP, Walisser JA, Sato TR, et al. Differential effects of light and feeding on circadian organization of peripheral clocks in a forebrain Bmal1 mutant. eLife. 2014;3.

233. Easton A, Meerlo P, Bergmann B, Turek FW. The suprachiasmatic nucleus regulates sleep timing and amount in mice. Sleep. 2004;27(7):1307-18.

234. Fernandez F, Lu D, Ha P, Costacurta P, Chavez R, Heller HC, et al. Circadian rhythm. Dysrhythmia in the suprachiasmatic nucleus inhibits memory processing. Science (New York, NY). 2014;346(6211):854-7.

235. Altaha B, Heddes M, Pilorz V, Niu Y, Gorbunova E, Gigl M, et al. Genetic and environmental circadian disruption induce weight gain through changes in the gut microbiome. Molecular metabolism. 2022:101628.

236. Cannon B, Nedergaard J. Brown adipose tissue: function and physiological significance. Physiological reviews. 2004;84(1):277-359.

237. Nam D, Guo B, Chatterjee S, Chen MH, Nelson D, Yechoor VK, et al. The adipocyte clock controls brown adipogenesis through the TGF-β and BMP signaling pathways. Journal of cell science. 2015;128(9):1835-47.

238. Froy O, Garaulet M. The Circadian Clock in White and Brown Adipose Tissue: Mechanistic, Endocrine, and Clinical Aspects. Endocrine reviews. 2018;39(3):261-73.

239. la Fleur SE, Kalsbeek A, Wortel J, Fekkes ML, Buijs RM. A daily rhythm in glucose tolerance: a role for the suprachiasmatic nucleus. Diabetes. 2001;50(6):1237-43.

240. Barca-Mayo O, Pons-Espinal M, Follert P, Armirotti A, Berdondini L, De Pietri Tonelli D. Astrocyte deletion of Bmal1 alters daily locomotor activity and cognitive functions via GABA signalling. Nature communications. 2017;8:14336.

241. Yamamoto H, Nagai K, Nakagawa H. Role of SCN in daily rhythms of plasma glucose, FFA, insulin and glucagon. Chronobiology international. 1987;4(4):483-91.

242. La Fleur SE, Kalsbeek A, Wortel J, Buijs RM. A suprachiasmatic nucleus generated rhythm in basal glucose concentrations. Journal of neuroendocrinology. 1999;11(8):643-52.

243. Liu AC, Welsh DK, Ko CH, Tran HG, Zhang EE, Priest AA, et al. Intercellular coupling confers robustness against mutations in the SCN circadian clock network. Cell. 2007;129(3):605-16.

244. Chieffi S, Carotenuto M, Monda V, Valenzano A, Villano I, Precenzano F, et al. Orexin System: The Key for a Healthy Life. Frontiers in physiology. 2017;8:357.

245. Girault EM, Yi CX, Fliers E, Kalsbeek A. Orexins, feeding, and energy balance. Progress in brain research. 2012;198:47-64.

246. Adeghate E. Orexins: tissue localization, functions, and its relation to insulin secretion and diabetes mellitus. Vitamins and hormones. 2012;89:111-33.

247. Nollet M, Leman S. Role of orexin in the pathophysiology of depression: potential for pharmacological intervention. CNS drugs. 2013;27(6):411-22.

248. Tsuchimine S, Hattori K, Ota M, Hidese S, Teraishi T, Sasayama D, et al. Reduced plasma orexin-A levels in patients with bipolar disorder. Neuropsychiatric disease and treatment. 2019;15:2221-30.

249. Greenwell BJ, Trott AJ, Beytebiere JR, Pao S, Bosley A, Beach E, et al. Rhythmic Food Intake Drives Rhythmic Gene Expression More Potently than the Hepatic Circadian Clock in Mice. Cell reports. 2019;27(3):649-57.e5.

250. Bond DJ, Kauer-Sant'Anna M, Lam RW, Yatham LN. Weight gain, obesity, and metabolic indices following a first manic episode: prospective 12-month data from the Systematic Treatment Optimization Program for Early Mania (STOP-EM). Journal of affective disorders. 2010;124(1-2):108-17.

251. Mansur RB, Rizzo LB, Santos CM, Asevedo E, Cunha GR, Noto MN, et al. Impaired glucose metabolism moderates the course of illness in bipolar disorder. Journal of affective disorders. 2016;195:57-62.

252. Rosenberg R, Doghramji PP. Is shift work making your patient sick? Emerging theories and therapies for treating shift work disorder. Postgraduate medicine. 2011;123(5):106-15.

253. Härmä M, Kandolin I. Shiftwork, age and well-being: recent developments and future perspectives. Journal of human ergology. 2001;30(1-2):287-93.

254. Smith MR, Fogg LF, Eastman CI. A compromise circadian phase position for permanent night work improves mood, fatigue, and performance. Sleep. 2009;32(11):1481-9.

255. Logan RW, Zhang C, Murugan S, O'Connell S, Levitt D, Rosenwasser AM, et al. Chronic shift-lag alters the circadian clock of NK cells and promotes lung cancer growth in rats. Journal of immunology (Baltimore, Md : 1950). 2012;188(6):2583-91.

256. Dib R, Gervais NJ, Mongrain V. A review of the current state of knowledge on sex differences in sleep and circadian phenotypes in rodents. Neurobiology of sleep and circadian rhythms. 2021;11:100068.

257. Banks G, Nolan PM, Bourbia N. Shift work-like patterns effect on female and male mouse behavior. Neurobiology of sleep and circadian rhythms. 2022;13:100082.

258. Abraham U, Granada AE, Westermark PO, Heine M, Kramer A, Herzel H. Coupling governs entrainment range of circadian clocks. Molecular systems biology. 2010;6:438.

259. Warren EJ, Allen CN, Brown RL, Robinson DW. Intrinsic light responses of retinal ganglion cells projecting to the circadian system. The European journal of neuroscience. 2003;17(9):1727-35.

260. Tyrer P, Baldwin D. Generalised anxiety disorder. Lancet (London, England). 2006;368(9553):2156-66.

261. McLean CP, Asnaani A, Litz BT, Hofmann SG. Gender differences in anxiety disorders: prevalence, course of illness, comorbidity and burden of illness. Journal of psychiatric research. 2011;45(8):1027-35.

262. Puttonen S, Viitasalo K, Härmä M. The relationship between current and former shift work and the metabolic syndrome. Scandinavian journal of work, environment & health. 2012;38(4):343-8.

263. Hill JO, Wyatt HR, Peters JC. Energy balance and obesity. Circulation. 2012;126(1):126-32.

264. de Assis MA, Kupek E, Nahas MV, Bellisle F. Food intake and circadian rhythms in shift workers with a high workload. Appetite. 2003;40(2):175-83.

265. Esquirol Y, Bongard V, Mabile L, Jonnier B, Soulat JM, Perret B. Shift work and metabolic syndrome: respective impacts of job strain, physical activity, and dietary rhythms. Chronobiology international. 2009;26(3):544-59.

266. Salgado-Delgado RC, Saderi N, Basualdo Mdel C, Guerrero-Vargas NN, Escobar C, Buijs RM. Shift work or food intake during the rest phase promotes metabolic disruption and desynchrony of liver genes in male rats. PloS one. 2013;8(4):e60052.

267. Figueiro MG, Radetsky L, Plitnick B, Rea MS. Glucose tolerance in mice exposed to light-dark stimulus patterns mirroring dayshift and rotating shift schedules. Scientific reports. 2017;7:40661.

268. Ika K, Suzuki E, Mitsuhashi T, Takao S, Doi H. Shift work and diabetes mellitus among male workers in Japan: does the intensity of shift work matter? Acta medica Okayama. 2013;67(1):25-33.

269. Pan A, Schernhammer ES, Sun Q, Hu FB. Rotating night shift work and risk of type 2 diabetes: two prospective cohort studies in women. PLoS medicine. 2011;8(12):e1001141.

270. Zimberg IZ, Fernandes Junior SA, Crispim CA, Tufik S, de Mello MT. Metabolic impact of shift work. Work (Reading, Mass). 2012;41 Suppl 1:4376-83.

271. Vidafar P, Cain SW, Shechter A. Relationship between Sleep and Hedonic Appetite in Shift Workers. Nutrients. 2020;12(9).

272. Costa G. Shift work and occupational medicine: an overview. Occupational medicine (Oxford, England). 2003;53(2):83-8.

273. Park N, Kim HD, Cheon S, Row H, Lee J, Han DH, et al. A Novel Bmal1 Mutant Mouse Reveals Essential Roles of the C-Terminal Domain on Circadian Rhythms. PloS one. 2015;10(9):e0138661.

274. Kato Y, Kawamoto T, Fujimoto K, Noshiro M. DEC1/STRA13/SHARP2 and DEC2/SHARP1 coordinate physiological processes, including circadian rhythms in response to environmental stimuli. Current topics in developmental biology. 2014;110:339-72.

275. Baier PC, Brzózka MM, Shahmoradi A, Reinecke L, Kroos C, Wichert SP, et al. Mice lacking the circadian modulators SHARP1 and SHARP2 display altered sleep and mixed state endophenotypes of psychiatric disorders. PloS one. 2014;9(10):e110310.

276. Dudley CA, Erbel-Sieler C, Estill SJ, Reick M, Franken P, Pitts S, et al. Altered patterns of sleep and behavioral adaptability in NPAS2-deficient mice. Science (New York, NY). 2003;301(5631):379-83.

277. Yang G, Chen L, Zhang J, Ren B, FitzGerald GA. Bmal1 deletion in mice facilitates adaptation to disrupted light/dark conditions. JCI insight. 2019;5(10).

278. Kondratova AA, Dubrovsky YV, Antoch MP, Kondratov RV. Circadian clock proteins control adaptation to novel environment and memory formation. Aging. 2010;2(5):285-97.

279. Singla R, Mishra A, Lin H, Lorsung E, Le N, Tin S, et al. Haploinsufficiency of a Circadian Clock Gene Bmal1 (Arntl or Mop3) Causes Brain-Wide mTOR Hyperactivation and Autism-like Behavioral Phenotypes in Mice. International journal of molecular sciences. 2022;23(11).

280. Qiu P, Jiang J, Liu Z, Cai Y, Huang T, Wang Y, et al. BMAL1 knockout macaque monkeys display reduced sleep and psychiatric disorders. National science review. 2019;6(1):87-100.

281. Akladious A, Azzam S, Hu Y, Feng P. Bmal1 knockdown suppresses wake and increases immobility without altering orexin A, corticotrophin-releasing hormone, or glutamate decarboxylase. CNS neuroscience & therapeutics. 2018;24(6):549-63.

282. Kennaway DJ, Varcoe TJ, Voultsios A, Boden MJ. Global loss of bmal1 expression alters adipose tissue hormones, gene expression and glucose metabolism. PloS one. 2013;8(6):e65255.

283. Shimba S, Ogawa T, Hitosugi S, Ichihashi Y, Nakadaira Y, Kobayashi M, et al. Deficient of a clock gene, brain and muscle Arnt-like protein-1 (BMAL1), induces dyslipidemia and ectopic fat formation. PloS one. 2011;6(9):e25231.

284. Matsuo N, Takao K, Nakanishi K, Yamasaki N, Tanda K, Miyakawa T. Behavioral profiles of three C57BL/6 substrains. Frontiers in behavioral neuroscience. 2010;4:29.

Appendix A: Supplementary figures

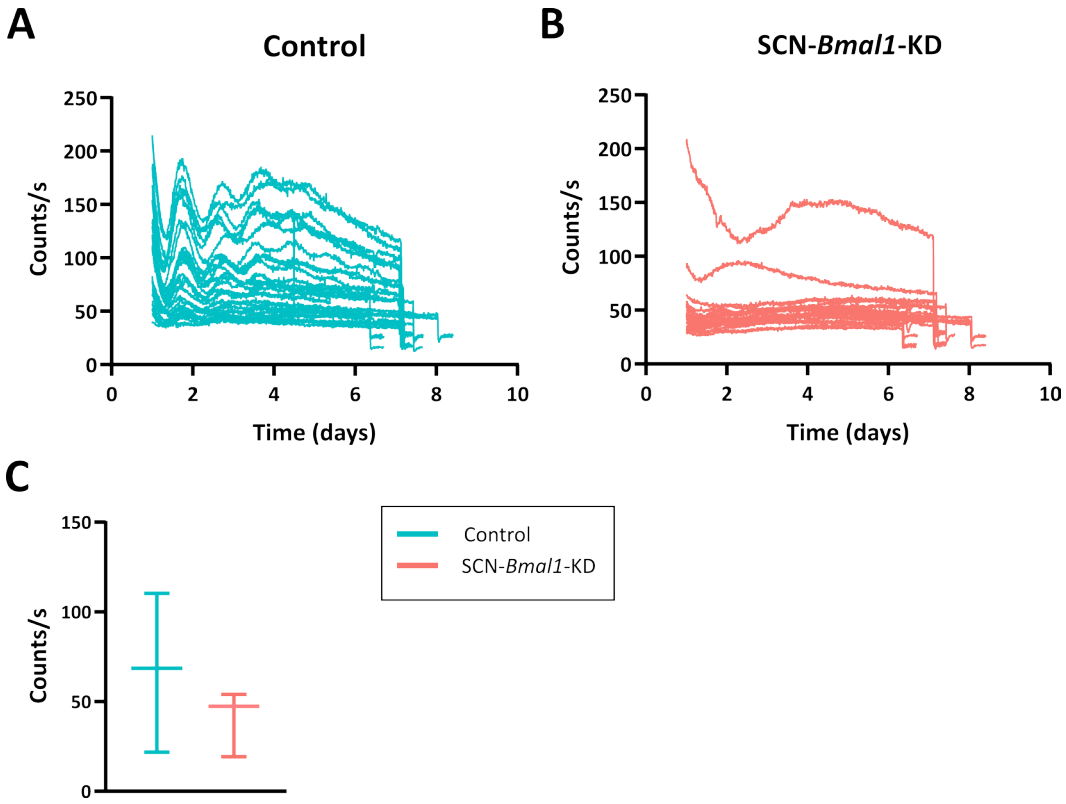

Figure S1. Raw bioluminescence plots of SCN explants from control and SCN-*Bmal1*-KD animals. Upon sacrifice, brains of control and SCN-*Bmal1*-KD animals were collected. A 300 µm thick SCN slice was isolated from every experimental animal and placed into the LumiCycle for recordings of SCN PER2::LUC rhythms. (A) Individual raw bioluminescence plots for all experimental control animals (n = 29). (B) Individual raw bioluminescence plots for all experimental SCN-*Bmal1*-KD animals (n = 21). The dips at the end of the recording plots in A and B represent the measurements after the samples were taken out of the LumiCycle (i.e., empty recording well). Since the counts dropped once the tissues were taken out of the LumiCycle (i.e., dips), the dips are an indication that the tissues were still viable in the LumiCycle. (C) Mean and range for the bioluminescence recordings in A (control: n = 29) and B (SCN-*Bmal1*-KD: n = 21). Control: mean = 68.60 counts/s, min = 21.77 counts/s, max = 110.3 counts/s. SCN-*Bmal1*-KD: mean = 47.41 counts/s, min = 19.27 counts/s, max = 54.09 counts/s. The ranges of the experimental groups are overlapping. Error bars indicate mean and range.

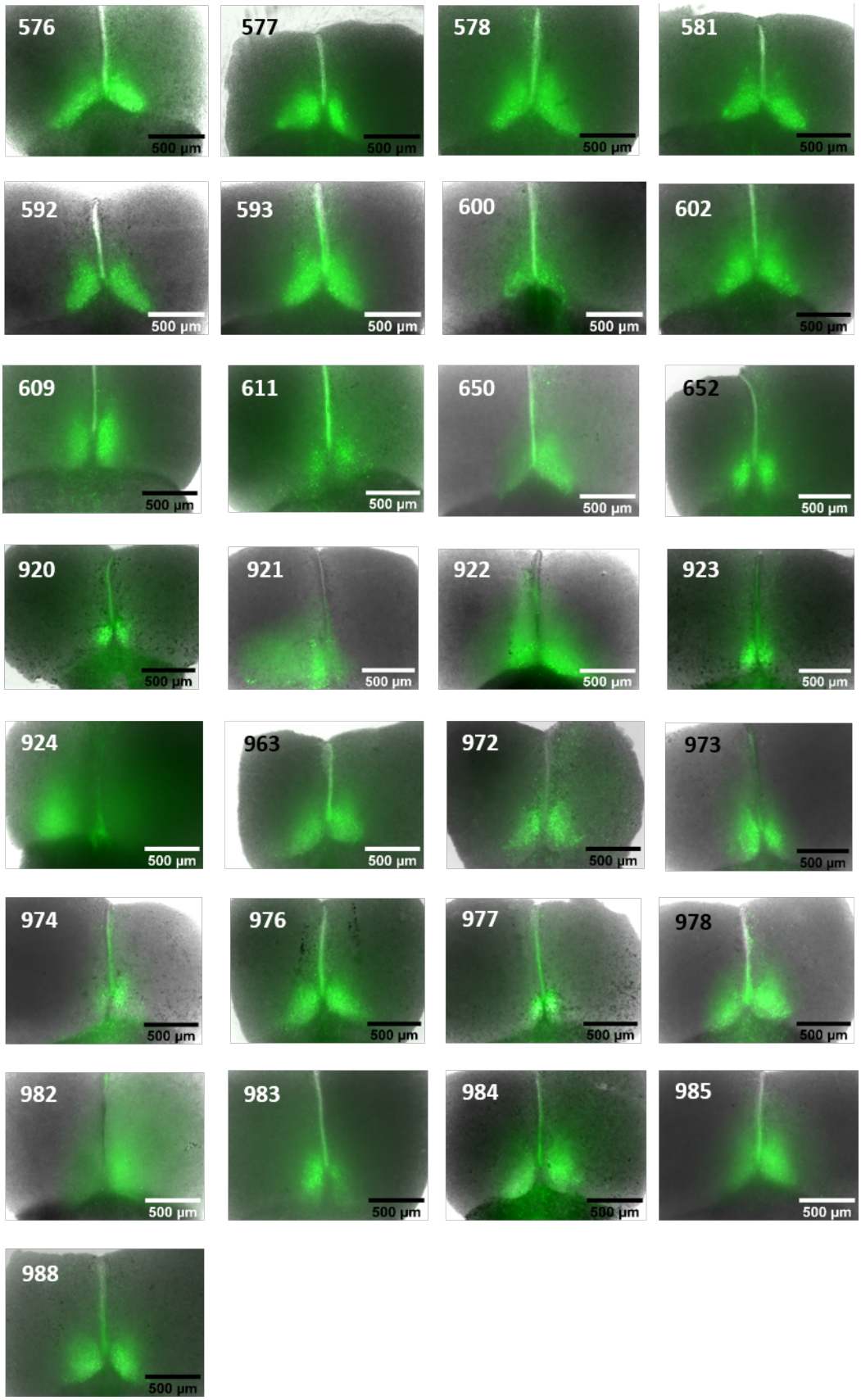

Figure S2. Microscopic SCN images of control animals. Upon sacrifice, brains of control animals were harvested and a 300 µm thick SCN slice was isolated for each experimental animal. After a week of LumiCycle measurements to determine the SCN PER2::LUC rhythms, microscopic SCN images were taken. Images are bright field and GFP-merged images. Animal ID numbers are indicated at the top left. Scale bar represents 500 µm.

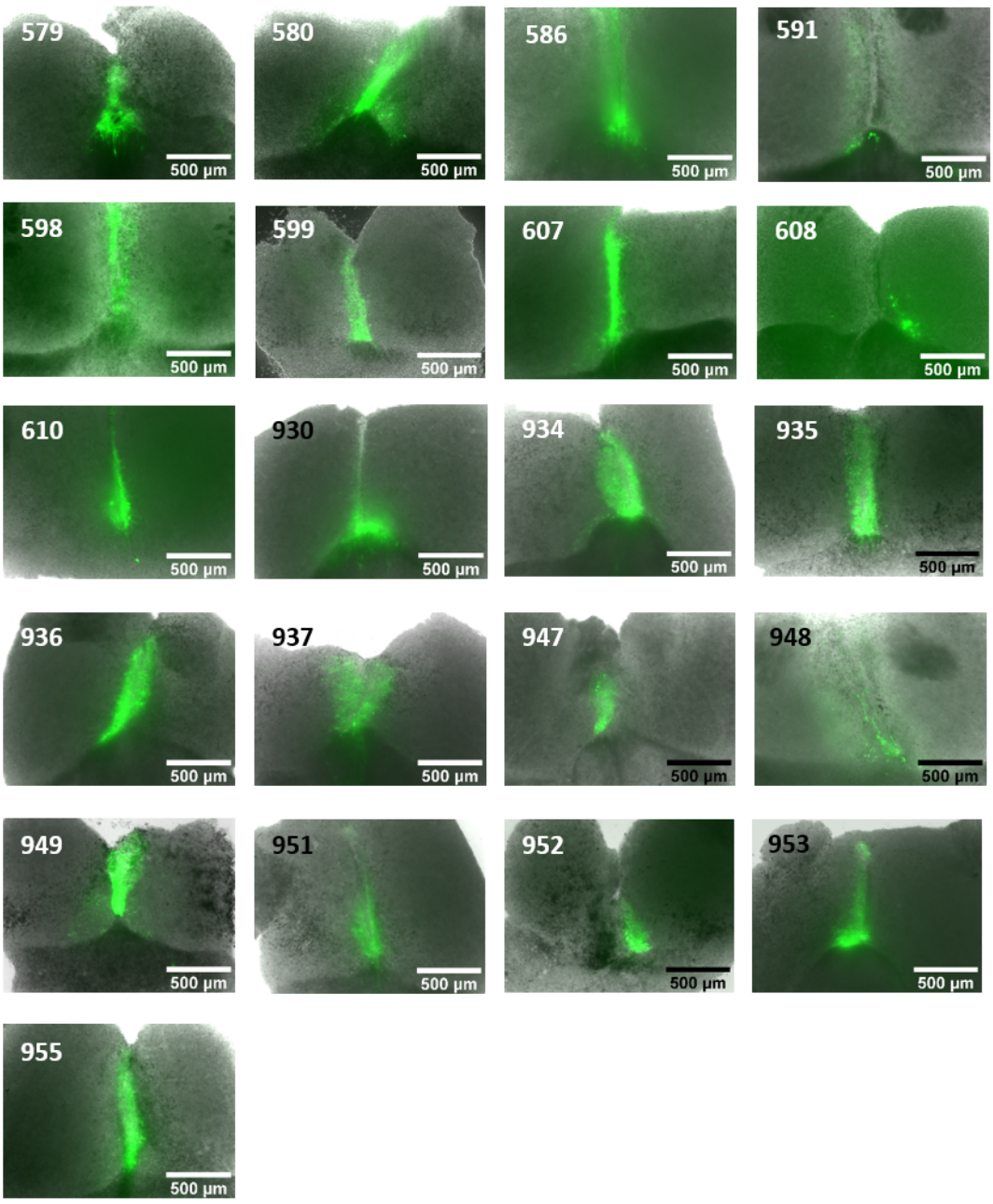

Figure S3.**Microscopic SCN images of SCN-*Bmal1*-KD animals.** Upon sacrifice, brains of SCN-*Bmal1*-KD animals were harvested and a 300 µm thick SCN slice was isolated for each experimental animal. After a week of LumiCycle measurements to determine the SCN PER2::LUC rhythms, microscopic SCN images were taken. Images are bright field and GFP-merged images. Scale bar represents 500 µm.

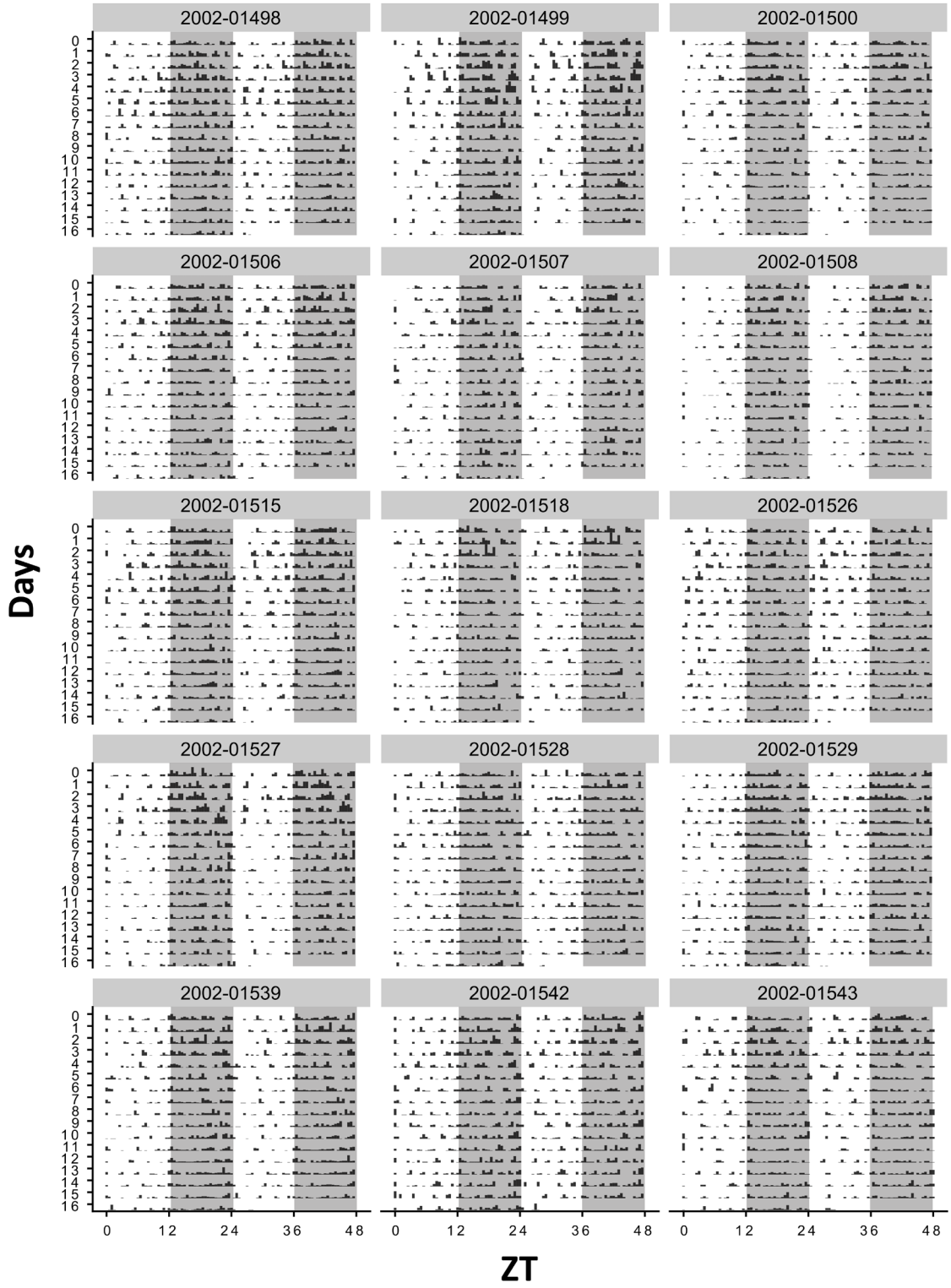

Figure S4. Double-plotted actograms for male control animals in project 2. Male control animals were placed into the IntelliCage system and subjected to a standard 12:12 LD cycle. Representative double-plotted actograms for all male control animals are displayed. Corner visits were tracked as a proxy for the animal's activity and are indicated by the black bars in the actograms. The shading of the actograms represents the LD cycle that the animal was subjected to.

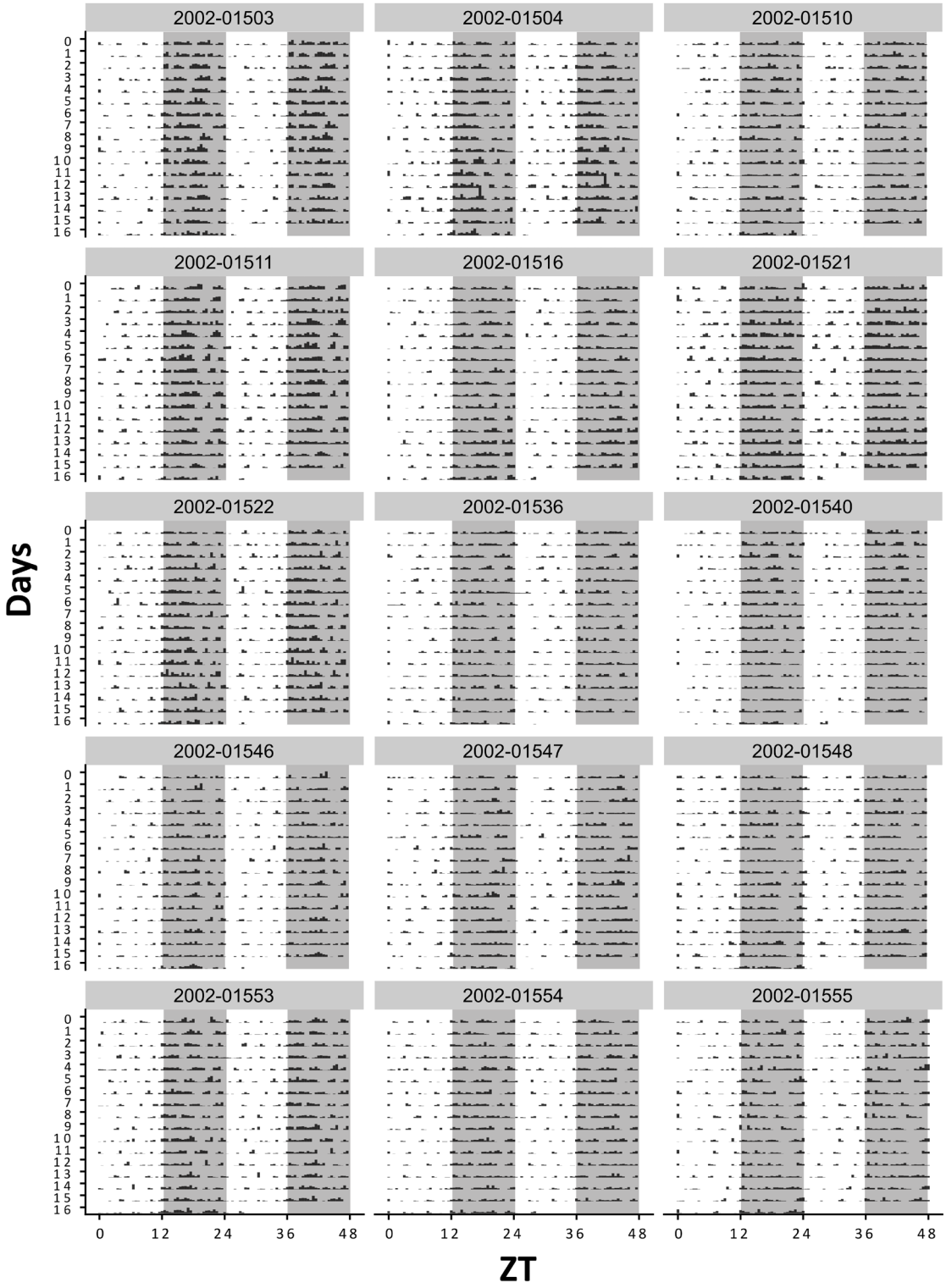

Figure S5. **Double-plotted actograms for female control animals in project 2.** Female control animals were placed into the IntelliCage system and subjected to a standard 12:12 LD cycle. Representative double-plotted actograms for all female control animals are displayed. Corner visits were tracked as a proxy for the animal's locomotor activity and are indicated by the black bars in the actograms. The shading of the actograms represents the LD cycle that the animal was subjected to.

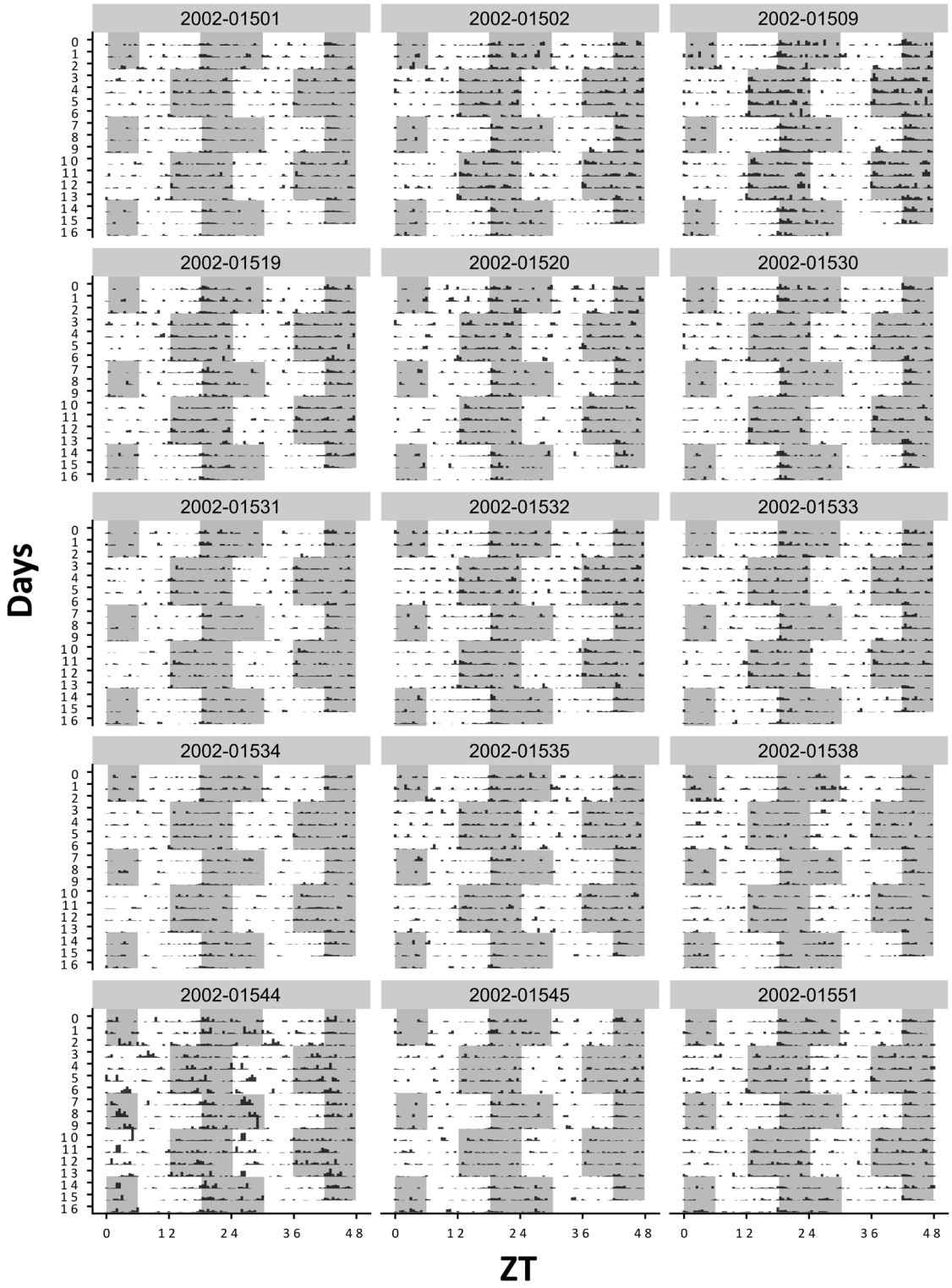

Figure S6. Double-plotted actograms for male shift work animals in project 2. Male shift work animals were placed into the IntelliCage system and subjected to alternating light cycles mimicking shift work. Representative double-plotted actograms for all male shift work animals are displayed. Corner visits were tracked as a proxy for the animal's locomotor activity and are indicated by the black bars in the actograms. The shading of the actograms represents the LD cycle that the animal was subjected to.

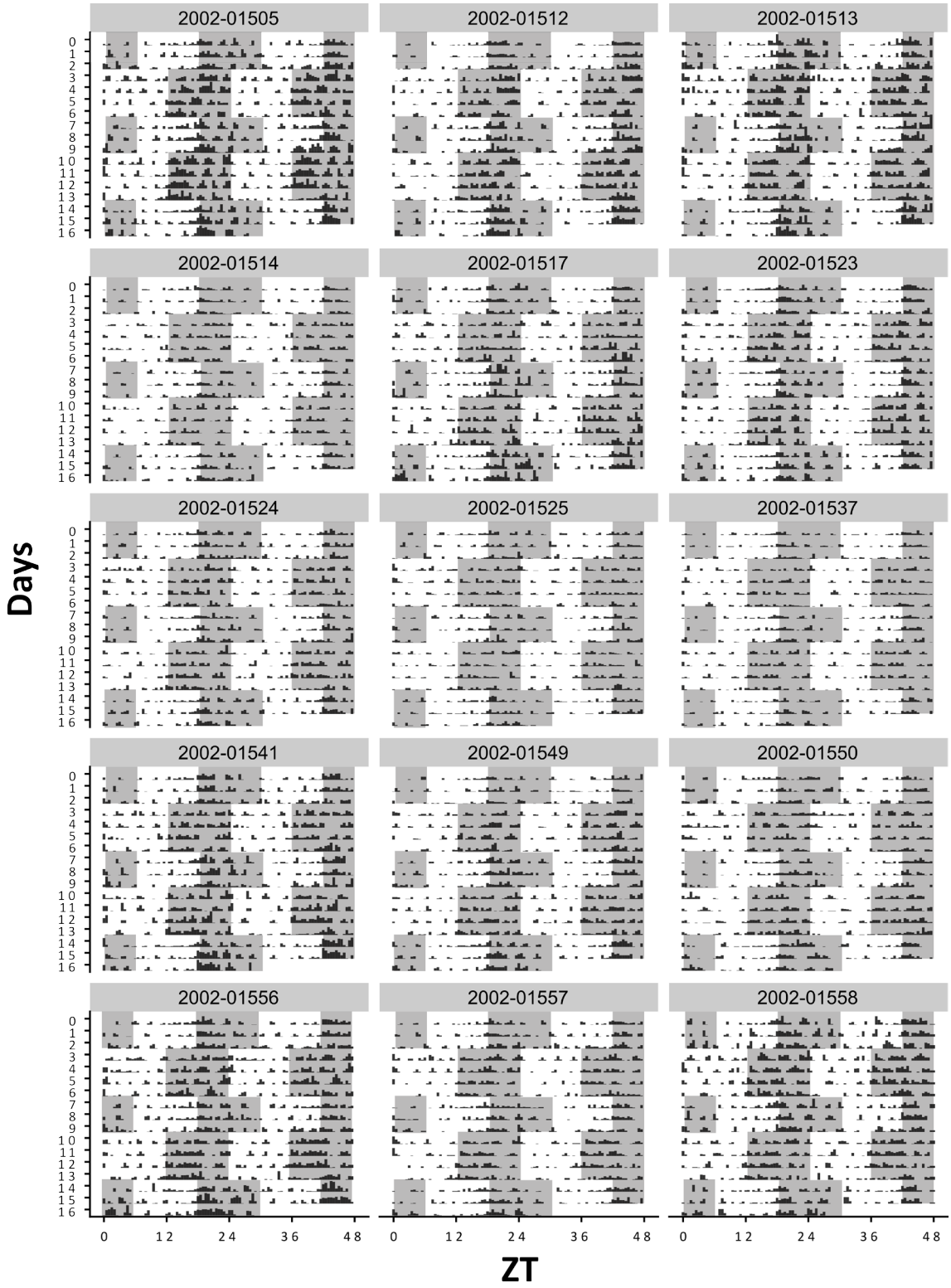

Figure S7. Double-plotted actograms for female shift work animals in project 2. Female shift work animals were placed into the IntelliCage system and subjected to alternating light cycles mimicking shift work. Representative double-plotted actograms for all female shift work animals are displayed. Corner visits were tracked as a proxy for the animal's locomotor activity and are indicated by the black bars in the actograms. The shading of the actograms represents the LD cycle that the animal was subjected to.

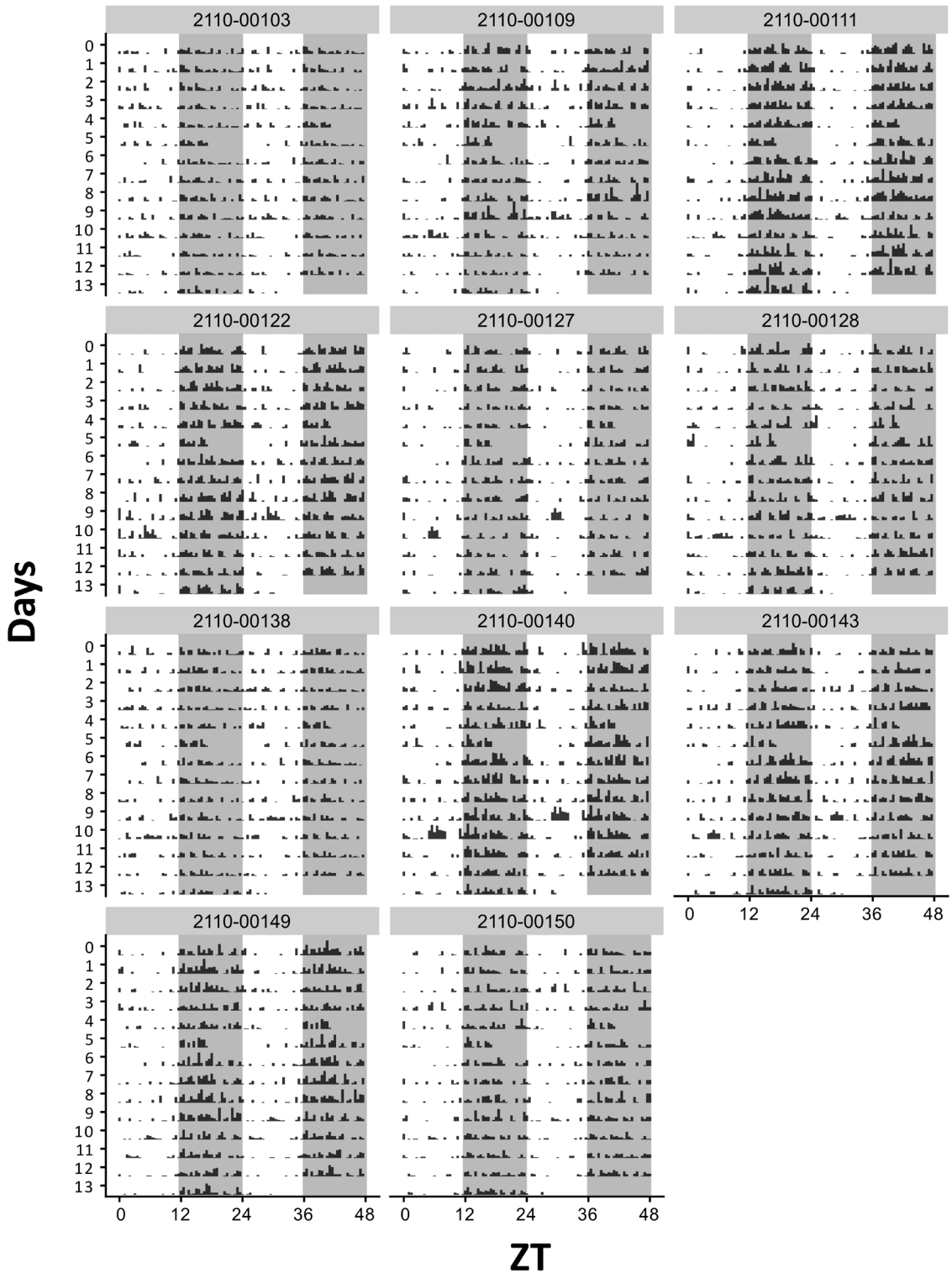

Figure S8. Double-plotted actograms for WT control animals in project 3. WT control animals were placed into the IntelliCage system and subjected to a standard 12:12 LD cycle. Representative double-plotted actograms for all WT control animals are displayed. Corner visits were tracked as a proxy for the animal's locomotor activity and are indicated by the black bars in the actograms. Due to technical reasons, some data measurements on day 5 were missing resulting in a recording gap. The shading of the actograms represents the LD cycle that the animal was subjected to.

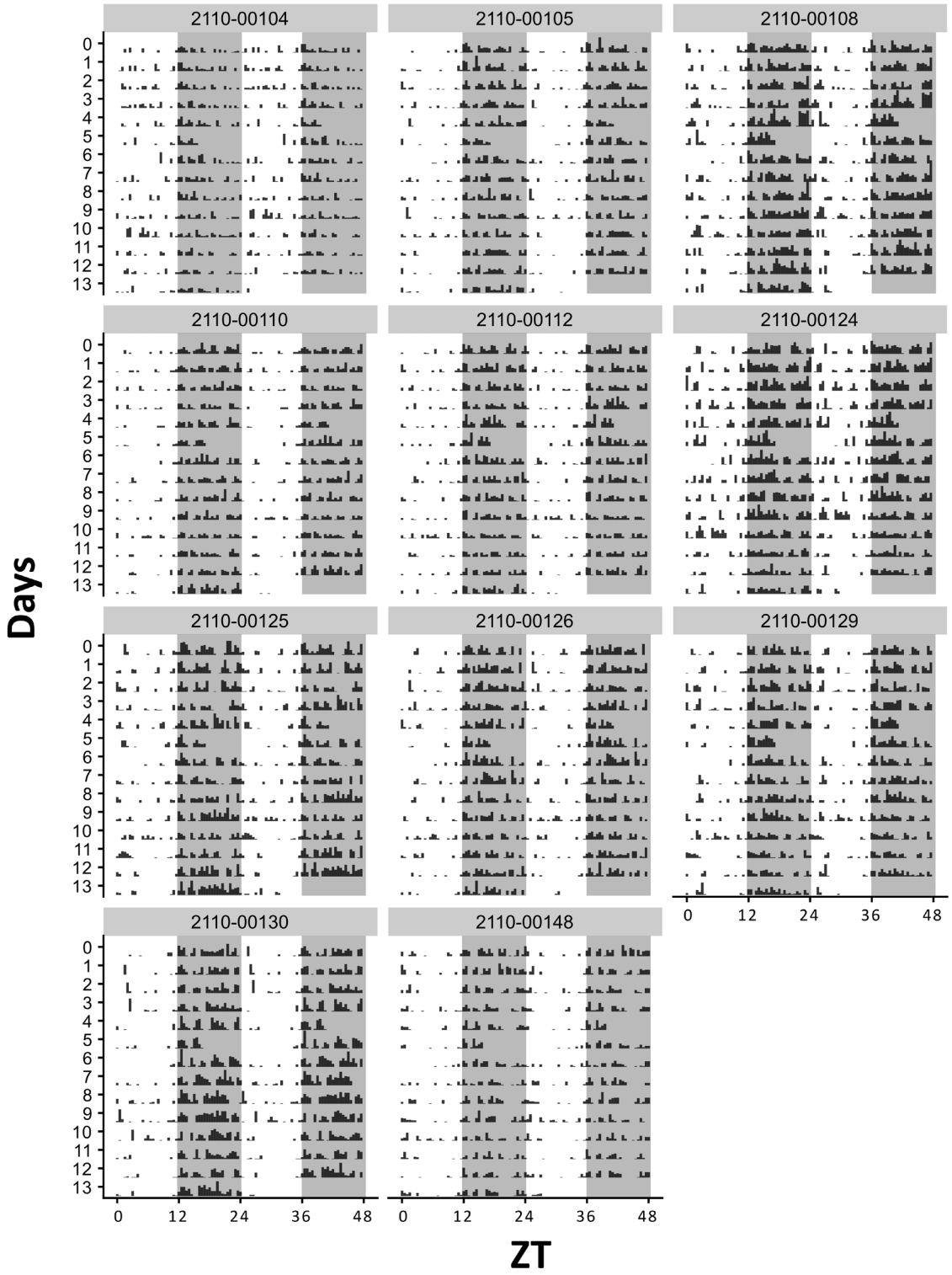

Figure S9. Double-plotted actograms for *Bmal1*$^{+/-}$ control animals in project 3. *Bmal1*$^{+/-}$ control animals were placed into the IntelliCage system and subjected to a standard 12:12 LD cycle. Representative double-plotted actograms for all *Bmal1*$^{+/-}$ control animals are displayed. Corner visits were tracked as a proxy for the animal's locomotor activity and are indicated by the black bars in the actograms. Due to technical reasons, some data measurements on day 5 were missing resulting in a recording gap. The shading of the actograms represents the LD cycle that the animal was subjected to.

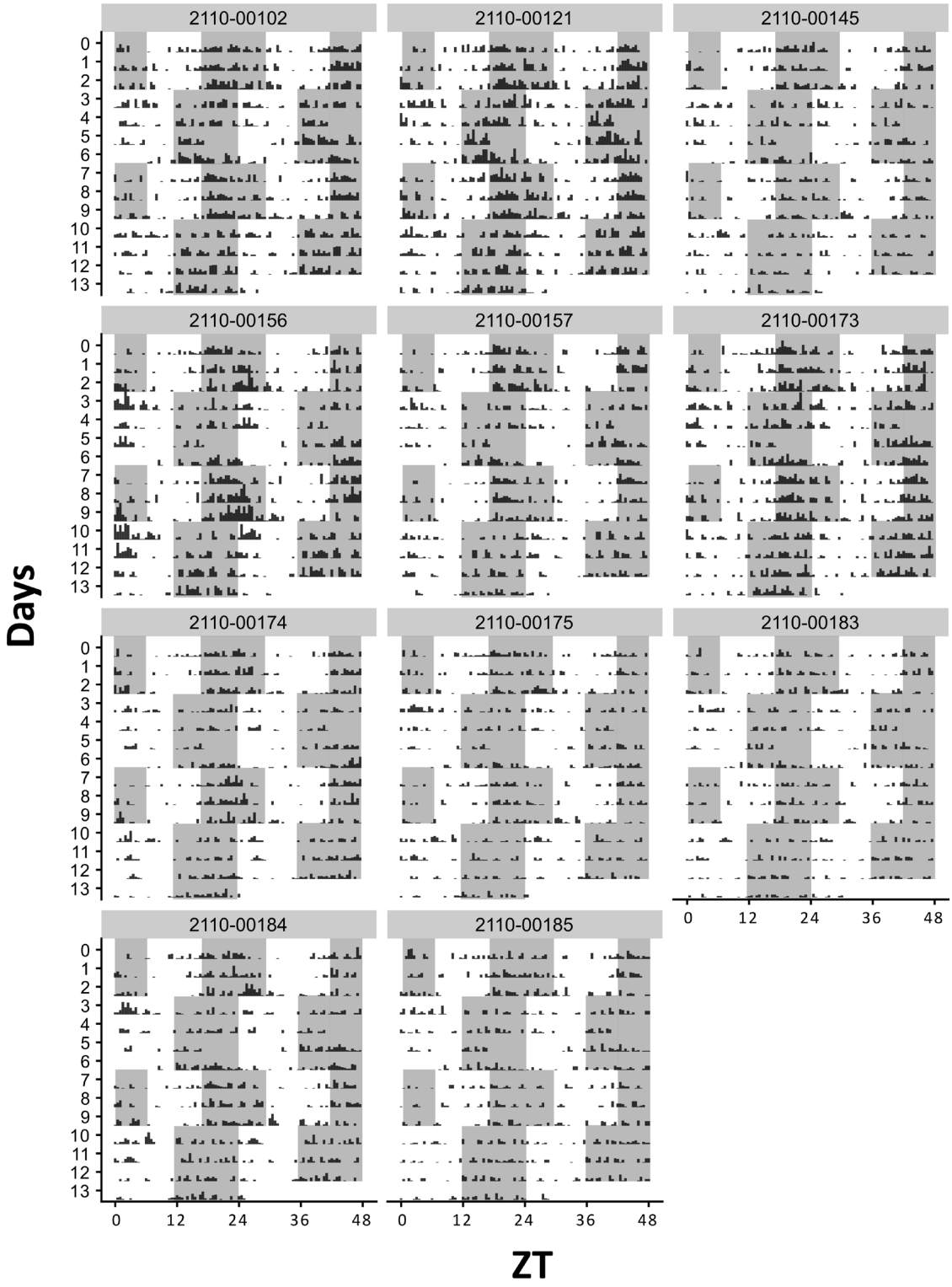

Figure S10. Double-plotted actograms for WT shift work animals in project 3. WT shift work animals were placed into the IntelliCage system and subjected to alternating light cycles mimicking shift work. Representative double-plotted actograms for all WT shift work animals are displayed. Corner visits were tracked as a proxy for the animal's locomotor activity and are indicated by the black bars in the actograms. Due to technical reasons, some data measurements on day 5 were missing resulting in a recording gap. The shading of the actograms represents the LD cycle that the animal was subjected to.

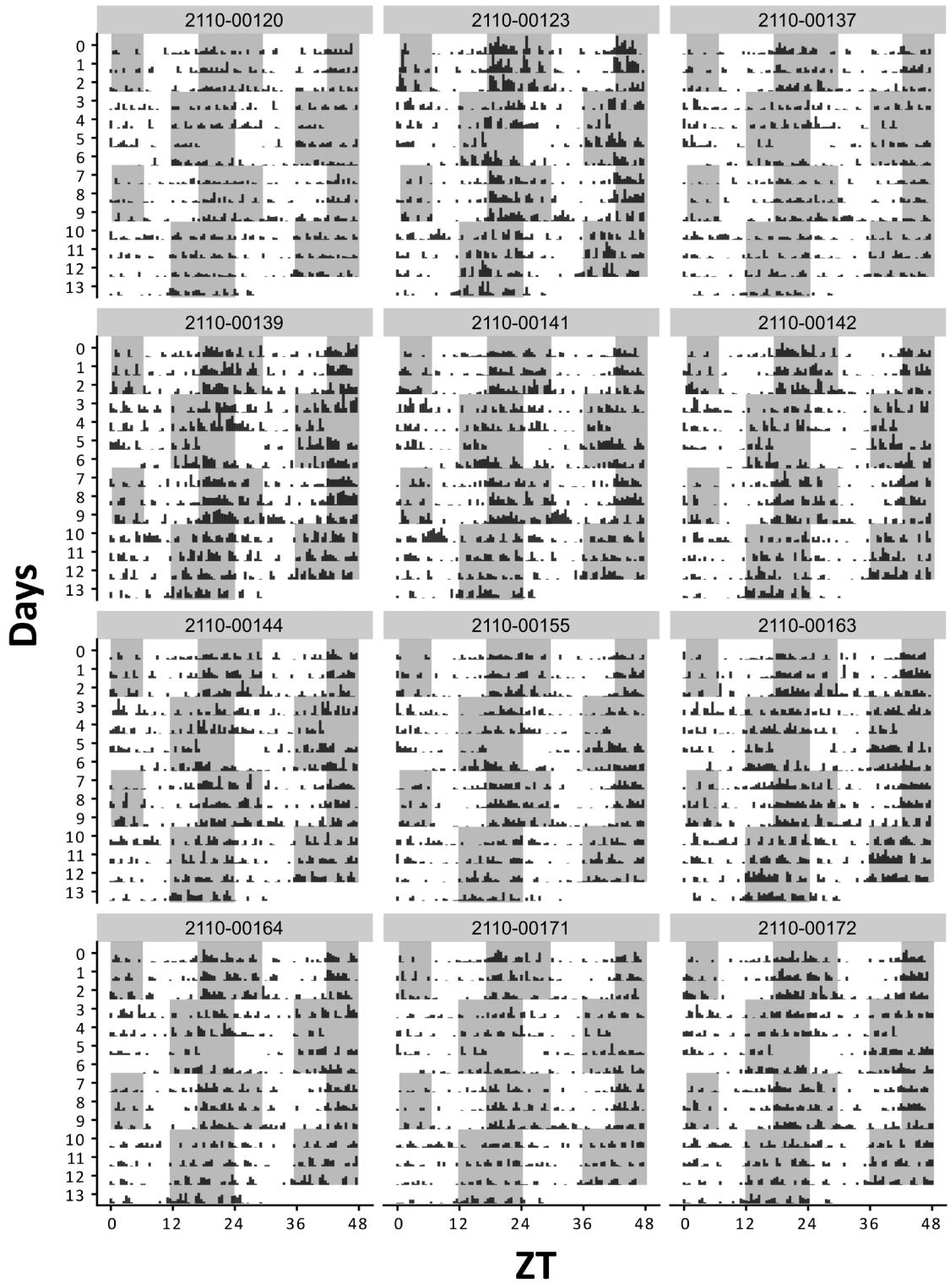

Figure S11. Double-plotted actograms for *Bmal1*$^{+/-}$ shift work animals in project 3. *Bmal1*$^{+/-}$ shift work animals were placed into the IntelliCage system and subjected to alternating light cycles mimicking shift work. Representative double-plotted actograms for all *Bmal1*$^{+/-}$ shift work animals are displayed. Corner visits were tracked as a proxy for the animal's locomotor activity and are indicated by the black bars in the actograms. Due to technical reasons, some data measurements on day 5 were missing resulting in a recording gap. The shading of the actograms represents the LD cycle that the animal was subjected to.

Appendix B: Supplementary tables

Table S1. Bioluminescence rhythm parameters and *Ppox* expression in project 1. Mean ± SD, statistical tests and their outcomes are indicated. n.s. = not significant; PAG = periaqueductal gray; SD = standard deviation; SCN = suprachiasmatic nucleus.

Tissue	Parameter	Control	SCN-*Bmal1*-KD	Statistical Test	p-value	Summary
SCN	Amplitude (counts/s) (mean ± SD)	0.1065 ± 0.0438	0.0190 ± 0.01971	Unpaired t-test	< 0.0001	****
	n - value	29	21			
	Period (h) (mean ± SD)	23.36 ± 1.150	26.05 ± 0.6882	Mann–Whitney U test	< 0.0001	****
	n-value	28	12			
	Phase (h) (mean ± SD)	18.50 ± 1.281	21.08 ± 1.547	Mann–Whitney U test	< 0.0001	****
	n - value	28	12			
PAG	Amplitude (counts/s) (mean ± SD)	0.0357 ± 0.02174	0.01968 ± 0.007736	Unpaired t-test	0.0023	**
	n - value	29	21			
	Period (h) (mean ± SD)	26.04 ± 2.054	19.2 ± 0.000	n too small for statistical analysis	-	-
	n-value	21	1			
	Phase (h) (mean ± SD)	7.384 ± 7.584	21.11 ± 0.000	n too small for statistical analysis	-	-
	n - value	21	1			
	Rhythmic slices (n - value)	21	1	Fisher's exact test	< 0.0001	****
	Non-rhythmic slices (n - value)	8	20			
Liver	Amplitude (counts/s) (mean ± SD)	0.07409 ± 0.03251	0.09984 ± 0.06392	n too small for statistical analysis	-	-
	n - value	8	3			
	Period (h) (mean ± SD)	27.63 ± 6.831	22.40 ± 1.273	n too small for statistical analysis	-	-
	n-value	6	2			
	Phase (h) (mean ± SD)	9.829 ± 5.137	8.803 ± 10.82	n too small for statistical analysis	-	-
	n - value	6	2			
Lateral Hypothalamus	*Ppox* (Fold Change) (mean ± SD)	1 ± 0.2289	0.9471 ± 0.2166	Unpaired t-test	0.5738	n.s.
	n - value	14	10			

Tissue	Group	Parameter	*Ppox* (Fold Change)	SCN amplitude (counts/s)	Statistical Test	p-value	R^2	Summary
Lateral hypothalamus	Control	*Ppox* (Fold Change) vs. SCN amplitude (counts/s) (mean ± SD)	1 ± 0.2289	0.0858 ± 0.03554	Pearson correlation coefficient	0.0268	0.3464	*
		n - value	14	14				
	SCN-*Bmal1*-KD	*Ppox* (Fold Change) vs. SCN amplitude (counts/s) (mean ± SD)	0.9471 ± 0.2166	0.02183 ± 0.00737	Pearson correlation coefficient	0.9432	0.0007	n.s.
		n - value	10	10				

Table S2. First OFT, EPM and DaLi box test in project 1. Mean ± SD, statistical tests and their outcomes are indicated. DaLi box = dark-light box; EPM = elevated plus maze; n.s. = not significant; OFT = open field test; SD = standard deviation.

Test	Parameter	Control	SCN-*Bmal1*-KD	Statistical Test	p-value	Summary
OFT	Distance traveled (m) (mean ± SD)	30.95 ± 6.153	34.65 ± 11.21	Unpaired t-test	0.2617	n.s.
	n - value	17	12			
	Center entries (mean ± SD)	73.35 ± 16.34	79.92 ± 20.71	Unpaired t-test	0.3485	n.s.
	n - value	17	12			
	Center time (s) (mean ± SD)	263.1 ± 53.50	250.8 ± 58.93	Unpaired t-test	0.5623	n.s.
	n - value	17	12			
EPM	Distance traveled (m) (mean ± SD)	10.18 ± 2.236	14.42 ± 5.114	Unpaired t-test	0.0052	**
	n - value	17	12			
	Open arm entries (mean ± SD)	14.71 ± 4.195	28.50 ± 5.126	Unpaired t-test	< 0.0001	****
	n - value	17	12			
	Open arm time (s) (mean ± SD)	42.84 ± 20.20	161.9 ± 62.81	Unpaired t-test	< 0.0001	****
	n - value	17	12			
	Open arm distance (% of total distance) (mean ± SD)	8.006 ± 5.809	19.04 ± 9.332	Unpaired t-test	0.0005	***
	n - value	17	12			
DaLi box	Entries into light (mean ± SD)	14.69 ± 5.868	18.90 ± 6.625	Unpaired t-test	0.0216	*
	n - value	29	21			
	Time in light (s) (mean ± SD)	143.0 ± 78.20	162.5 ± 60.87	Unpaired t-test	0.3469	n.s.
	n - value	29	21			
	Latency to light entry (s) (mean ± SD)	52.47 ± 103.7	31.39 ± 20.46	Mann–Whitney U test	0.0636	#
	n - value	29	21			

Table S3. EPM and DaLi box test over time in project 1. Mean ± SD, statistical tests and their outcomes are indicated. DaLi box = dark-light box; DF = degrees of freedom; EPM = elevated plus maze; n.s. = not significant; SD = standard deviation.

Test	Parameter	Experimental group	Time		Statistical test		Source of variation		
			Time point 1	Time point 2			Experimental Group	Time	Experimental Group x Time
EPM	Distance traveled (m) (mean ± SD)	Control	9.053 ± 1.492	8.496 ± 1.655	Two-way repeated measures ANOVA	DF	1	1	1
	n - value		9	9		F-value	8.806	1.781	0.4121
	Distance traveled (m) (mean ± SD)	SCN-*Bmal1*-KD	13.92 ± 5.873	12.33 ± 3.308		p-value	0.0091	0.2008	0.53
	n - value		9	9		Summary	**	n.s.	n.s.
	Open arm entries (mean ± SD)	Control	13.78 ± 4.604	13.00 ± 4.610		DF	1	1	1
	n - value		9	9		F-value	50.7	2.507	1.41
	Open arm entries (mean ± SD)	SCN-*Bmal1*-KD	27.67 ± 6.344	22.22 ± 5.848		p-value	< 0.0001	0.1329	0.2523
	n - value		9	9		Summary	****	n.s.	n.s.
	Open arm time (s) (mean ± SD)	Control	41.43 ± 23.05	53.59 ± 27.19		DF	1	1	1
	n - value		9	9		F-value	27.49	0.02978	0.9391
	Open arm time (s) (mean ± SD)	SCN-*Bmal1*-KD	157.2 ± 66.76	139.8 ± 71.72		p-value	< 0.0001	0.8652	0.3469
	n - value		9	9		Summary	****	n.s.	n.s.
	Open arm distance (% of total distance) (mean ± SD)	Control	7.547 ± 6.413	11.30 ± 6.756		DF	1	1	1
	n - value		9	9		F-value	6.489	0.346	1.181
	Open arm distance (% of total distance) (mean ± SD)	SCN-*Bmal1*-KD	17.64 ± 9.015	16.52 ± 9.213		p-value	0.0215	0.5646	0.2933
	n - value		9	9		Summary	*	n.s.	n.s.
DaLi box	Entries into light	Control	9.750 ± 4.652	12.50 ± 2.777		DF	1	1	1
	n - value		8	8		F-value	8.149	1.031	1.236
	Entries into light	SCN-*Bmal1*-KD	17.88 ± 7.259	17.75 ± 5.701		p-value	0.0127	0.3272	0.2849
	n - value		8	8		Summary	*	n.s.	n.s.
	Latency to light entry (s) (mean ± SD)	Control	113.2 ± 113.2	69.80 ± 76.57		DF	1	1	1
	n - value		8	8		F-value	3.606	0.1962	0.8644
	Latency to light entry (s) (mean ± SD)	SCN-*Bmal1*-KD	20.66 ± 14.84	36.05 ± 26.11		p-value	0.0784	0.6646	0.3683
	n - value		8	8		Summary	#	n.s.	n.s.

Table S4. OFT and DaLi box test over time in project 1. Mean ± SD, statistical tests and their outcomes are indicated. DaLi box = dark-light box; DF = degrees of freedom; n.s. = not significant; OFT = open field test; SD = standard deviation.

Test	Parameter	Experimental group	Time		Statistical test		Source of variation			Statistical Test	Comparison	Uncorrected p-value	Corrected p-value	Summary
			Time point 1	Time point 2			Experimental Group	Time	Experimental Group x Time					
OFT	Distance traveled (m) (mean ± SD)	Control	36.05 ± 26.11	21.08 ± 8.932	Two-way repeated measures ANOVA	DF	1	1	1	Fisher's LSD test + Bonferroni correction	Control day vs. control night	0.0019	0.0038	**
	n - value		9	9		F-value	2.411	23.67	0.1444					
	Distance traveled (m) (mean ± SD)	SCN-*Bmal1*-KD	34.99 ± 11.75	27.95 ± 8.823		p-value	0.1401	0.0002	0.7089		SCN-*Bmal1*-KD day vs. SCN-*Bmal1*-KD night	0.0059	0.0118	*
	n - value		9	9		Summary	n.s.	***	n.s.					
	Center entries (mean ± SD)	Control	76.00 ± 21.42	50.22 ± 20.39		DF	1	1	1		Control day vs. control night	< 0.0001	0.0010	***
	n - value		9	9		F-value	1.253	52.45	0.08543					
	Center entries (mean ± SD)	SCN-*Bmal1*-KD	84.33 ± 20.80	60.56 ± 12.43		p-value	0.2795	< 0.0001	0.7738		SCN-*Bmal1*-KD day vs. SCN-*Bmal1*-KD night	0.0002	0.0003	***
	n - value		9	9		Summary	n.s.	****	n.s.					
	Center time (s) (mean ± SD)	Control	60.56 ± 12.43	222.5 ± 86.74		DF	1	1	1		Control day vs. control night	0.0727	0.1455	n.s.
	n - value		9	9		F-value	0.2929	4.826	0.2701					
	Center time (s) (mean ± SD)	SCN-*Bmal1*-KD	259.2 ± 51.91	221.4 ± 80.70		p-value	0.5958	0.0431	0.6104		SCN-*Bmal1*-KD day vs. SCN-*Bmal1*-KD night	0.253	0.506	n.s.
	n - value		9	9		Summary	n.s.	*	n.s.					
DaLi box	Time in light (s) (mean ± SD)	Control	90.81 ± 53.48	182.0 ± 116.6		DF	1	1	1		Control day vs. control night	0.0070	0.0139	*
	n - value		8	8		F-value	0.8766	10.54	1.488					
	Time in light (s) (mean ± SD)	SCN-*Bmal1*-KD	148.4 ± 65.56	189.8 ± 73.78		p-value	0.365	0.0058	0.2427		SCN-*Bmal1*-KD day vs. SCN-*Bmal1*-KD night	0.1737	0.3473	n.s.
	n - value		8	8		Summary	n.s.	**	n.s.					

Table S5. First TST, first LH and second LH test in project 1. Mean ± SD, statistical tests and their outcomes are indicated. LH = learned helplessness; n.s. = not significant; SD = standard deviation; TST = tail suspension test.

Test	Parameter	Control	SCN-*Bmal1*-KD	Statistical Test	p-value	Summary
First TST	Time immobile (s) (mean ± SD)	183.9 ± 54.89	183.6 ± 76.28	Unpaired t-test	0.9879	n.s.
	n - value	29	21			
	Transitions between mobile and immobile episodes (mean ± SD)	23 ± 10.69	20.14 ± 9.074	Unpaired t-test	0.326	n.s.
	n - value	29	21			
	Immobility latency (s) (mean ± SD)	77.27 ± 52.89	74.33 ± 38.94	Unpaired t-test	0.8304	n.s.
	n - value	29	21			
First LH	Latency (s) (mean ± SD)	18.72 ± 8.162	19.70 ± 6.873	n too small for statistical analysis	-	-
	n - value	8	3			
	Number of failures (mean ± SD)	9.625 ± 7.558	10.33 ± 8.505	n too small for statistical analysis	-	-
	n - value	8	3			
Second LH	Latency (s) (mean ± SD)	15.35 ± 8.302	14.03 ± 6.062	Unpaired t-test	0.5975	n.s.
	n - value	20	16			
	Number of failures (mean ± SD)	7.950 ± 8.817	5.250 ± 4.107	Unpaired t-test	0.267	n.s.
	n - value	20	16			

Table S6. TST over time in project 1. Mean ± SD, statistical tests and their outcomes are indicated. DF = degrees of freedom; n.s. = not significant; SD = standard deviation; TST = tail suspension test.

Test	Parameter	Experimental group	Time		Statistical test		Source of variation		
			Time point 1	Time point 2			Experimental Group	Time	Experimental Group x Time
TST	Time immobile (s) (mean ± SD)	Control	167.3 ± 54.01	205.0 ± 73.43	Two-way repeated measures ANOVA	DF	1	1	1
	n - value		9	9		F-value	0.5129	2.785	0.00224
	Time immobile (s) (mean ± SD)	SCN-*Bmal1*-KD	150.7 ± 48.16	186.3 ± 94.97		p-value	0.4842	0.1146	0.9628
	n - value		9	9		Summary	n.s.	n.s.	n.s.
	Transitions between mobile and immobile episodes (mean ± SD)	Control	24.89 ± 10.83	21.78 ± 10.65		DF	1	1	1
	n - value		9	9		F-value	0.1361	2.977	0.1191
	Transitions between mobile and immobile episodes (mean ± SD)	SCN-*Bmal1*-KD	24.33 ± 7.632	19.67 ± 6.124		p-value	0.717	0.1037	0.7345
	n - value		9	9		Summary	n.s.	n.s.	n.s.
	Immobility latency (s) (mean ± SD)	Control	19.67 ± 6.124	98.93 ± 27.62		DF	1	1	1
	n - value		9	9		F-value	1.567	0.7266	0.2452
	Immobility latency (s) (mean ± SD)	SCN-*Bmal1*-KD	56.03 ± 30.98	91.43 ± 97.91		p-value	0.2287	0.4066	0.6272
	n - value		9	9		Summary	n.s.	n.s.	n.s.

Table S7. Cognitive and reward-related parameters assessed in the IntelliCage system in project 1. Mean ± SD, statistical tests and their outcomes are indicated. AU = arbitrary unit; AUC = area under the curve; n.s. = not significant; SD = standard deviation.

Test	Parameter	Control	SCN-*Bmal1*-KD	Statistical Test	p-value	Summary
Y-maze	Spontaneous alternations (mean ± SD)	41.25 ± 9.421	46.13 ± 7.220	Unpaired t-test	0.2319	n.s.
	n - value	12	8			
Reversal learning	Preference Score (AU) (mean ± SD)	0.4856 ± 0.1160	0.5555 ± 0.2475	Unpaired t-test	0.4038	n.s.
	n - value	12	8			
Serial reversal learning	AUC of Learning Curve (AU) (mean ± SD)	1.119 ± 0.09087	1.078 ± 0.2148	Unpaired t-test	0.5654	n.s.
	n - value	12	8			
Sucrose preference test	Preference Score (AU) (mean ± SD)	0.8207 ± 0.2197	0.9669 ± 0.04839	Mann–Whitney U test	0.0246	*
	n - value	12	8			
	Sucrose licks (mean ± SD)	6415 ± 2656	10638 ± 4614	Unpaired t-test	0.0178	*
	n - value	12	8			
	Water licks (mean ± SD)	507.3 ± 556.8	125.4 ± 190.2	Mann–Whitney U test	0.0306	*
	n - value	12	8			
	Total licks (mean ± SD)	6922 ± 2443	10764 ± 4518	Unpaired t-test	0.0236	*
	n - value	12	8			
Place learning	Preference Score (AU) (mean ± SD)	0.5324 ± 0.1946	0.7781 ± 0.08022	Mann–Whitney U test	0.0030	**
	n - value	12	8			

Table S8. Absolute weight, percent weight gain and food consumption from Week 0 – 6 in project 1. Mean ± SD is indicated. SD = standard deviation.

Experimental group	Parameter	Weeks after stereotactic injection						
		0	1	2	3	4	5	6
Control	Weight (g) (mean ± SD)	22.35 ± 1.509	22.58 ± 1.371	24.09 ± 1.745	25.32 ± 2.159	26.29 ± 2.627	27.54 ± 3.242	28.87 ± 3.845
	n - value	29	29	29	29	29	29	29
SCN-*Bmal1*-KD	Weight (g) (mean ± SD)	22.06 ± 0.8669	23.28 ± 1.098	26.01 ± 2.519	27.97 ± 3.747	29.04 ± 4.625	29.45 ± 4.694	29.29 ± 4.367
	n - value	21	21	21	21	21	21	21
Control	Weight gain (%) (mean ± SD)	0 ± 0	1.148 ± 3.749	7.916 ± 6.605	13.48 ± 9.309	17.84 ± 11.34	23.44 ± 14.17	29.46 ± 17.03
	n - value	29	29	29	29	29	29	29
SCN-*Bmal1*-KD	Weight gain (%) (mean ± SD)	0 ± 0	5.654 ± 6.049	17.99 ± 11.34	26.80 ± 16.48	31.68 ± 20.64	33.56 ± 21.24	32.90 ± 20.14
	n - value	21	21	21	21	21	21	21
Control	Food consumption/ animal/week (g) (mean ± SD)	-	25.71 ± 0	28.66 ± 0	29.47 ± 3.120	26.09 ± 2.038	30.75 ± 5.544	28.28 ± 4.630
	n - value	-	1	1	2	2	2	2
SCN-*Bmal1*-KD	Food consumption/ animal/week (g) (mean ± SD)	-	25.49 ± 0	31.16 ± 0	33.01 ± 6.341	26.44 ± 5.970	26.86 ± 2.720	23.59 ± 1.339
	n - value	-	1	1	2	2	2	2

Table S9. Absolute weight, percent weight gain and food consumption from Week 7 – 17 in project 1. Mean ± SD is indicated. SD = standard deviation.

Experimental group	Parameter	Weeks after stereotactic injection										
		7	**8**	**9**	**10**	**11**	**12**	**13**	**14**	**15**	**16**	**17**
Control	Weight (g) (mean ± SD)	29.80 ± 4.344	30.26 ± 4.938	29.97 ± 4.946	30.67± 5.533	32.03 ± 6.062	33.01 ± 6.565	33.34 ± 7.084	33.76 ± 7.453	34.14 ± 7.615	34.09 ± 7.665	33.84 ± 8.278
	n - value	29	29	25	21	21	21	21	21	21	21	21
SCN-*Bmal1*-KD	Weight (g) (mean ± SD)	29.14 ± 4.550	30.07 ± 4.757	29.62 ± 4.740	28.76 ± 4.824	30.07 ± 5.471	30.47 ± 5.716	30.29 ± 5.913	30.03 ± 5.653	30.77 ± 6.251	30.88 ± 6.227	31.12 ± 6.427
	n - value	21	21	19	18	18	18	18	18	18	18	18
Control	Weight gain (%) (mean ± SD)	33.62 ± 19.21	35.61 ± 21.69	34.76 ± 23.00	38.01 ± 25.54	44.20 ± 28.22	48.75 ± 31.19	50.12 ± 33.14	52.00 ± 34.62	53.79 ± 35.78	53.74 ± 36.96	52.55 ± 39.24
	n - value	29	29	25	21	21	21	21	21	21	21	21
SCN-*Bmal1*-KD	Weight gain (%) (mean ± SD)	32.18 ± 20.78	36.42 ± 21.69	34.81 ± 21.79	30.57 ± 21.58	36.52 ± 24.54	38.36 ± 25.90	37.57 ± 26.67	36.38 ± 25.60	39.72 ± 28.14	40.25 ± 28.16	41.27 ± 28.85
	n - value	21	21	19	18	18	18	18	18	18	18	18
Control	Food consumption/ animal/week (g) (mean ± SD)	31.30 ± 0	31.18 ± 0	27.28 ± 5.527	29.10 ± 8.557	31.65 ± 1.887	34.21 ± 0	30.36 ± 4.547	28.97 ± 1.928	28.86 ± 2.134	31.64 ± 2.872	28.30 ± 4.319
	n - value	1	1	2	2	2	1	2	2	2	2	2
SCN-*Bmal1*-KD	Food consumption/ animal/week (g) (mean ± SD)	22.17 ± 0	26.75 ± 0	25.88 ± 1.085	22.34 ± 6.598	24.10 ± 2.391	28.83 ± 0	26.24 ± 0.7607	23.99 ± 4.523	25.94 ± 0.4101	27.46 ± 4.099	26.38 ± 0.2022
	n - value	1	1	2	2	2	1	2	2	2	2	2

Table S10. Statistics for absolute weight, percent weight gain and food consumption in project 1. Statistical tests and their outcomes are indicated. DF = degrees of freedom; n.s. = not significant.

Time frame	Parameter	Statistical test		Source of variation		
				Experimental Group	Time	Experimental Group x Time
Week 0 - 17	Absolute weight (g)	Mixed-effects analysis (Repeated-Measured)	DF	1	17	17
			F-value	0.6237	62.13	7.472
			p-value	0.4335	< 0.0001	< 0.0001
			Summary	n.s.	****	****
	Weight gain (%)	Mixed-effects analysis (Repeated-Measured)	DF	1	17	17
			F-value	0.2572	60.93	7.241
			p-value	0.6144	< 0.0001	< 0.0001
			Summary	n.s.	****	****
Week 0 - 6	Weight gain (%)	Two-way repeated measures ANOVA	DF	1	6	6
			F-value	6.930	110.4	5.192
			p-value	0.0114	< 0.0001	0.004
			Summary	*	****	****
Week 7 - 17	Weight gain (%)	Mixed-effects analysis (Repeated-Measured)	DF	1	10	10
			F-value	1.502	19.74	5.251
			p-value	0.2264	< 0.0001	< 0.0001
			Summary	n.s.	****	****
Week 0 - 17	Food consumption / animal / week (g)	Mixed-effects analysis (Repeated-Measured)	DF	1	16	16
			F-value	1.115	0.9491	0.8486
			p-value	0.4016	0.5341	0.6264
			Summary	n.s.	n.s.	n.s.

Table S11. Fat pads in project 1. Mean ± SD, statistical tests and their outcomes are indicated. BAT = brown adipose tissue; gWAT = gonadal white adipose tissue; iWAT = inguinal white adipose tissue; n.s. = not significant; SD = standard deviation.

Measurement	Parameter	Control	SCN-*Bmal1*-KD	Statistical Test	p-value	Summary
Fat Pad weight at sacrifice	% gWAT (mean ± SD)	5.443 ± 3.691	6.127 ± 4.797	Mann–Whitney U test	0.8916	n.s.
	n - value	29	21			
	% iWAT (mean ± SD)	2.216 ± 1.837	2.106 ± 1.549	Unpaired t-test	0.8239	n.s.
	n - value	29	21			
	% BAT (mean ± SD)	0.4345 ± 0.1637	0.3605 ± 0.1040	Unpaired t-test	0.0754	#
	n - value	29	21			

Table S12. Day vs. night metabolic cage parameters in project 1. Mean ± SD is indicated. SD = standard deviation.

Measurement	Parameter	Experimental group	Phase	
			Day	Night
Day vs. night locomotor activity	Activity (counts) (mean ± SD)	Control	398321 ± 166779	575838 ± 124789
	n - value		19	19
	Activity (counts) (mean ± SD)	SCN-*Bmal1*-KD	380019 ± 185351	466379 ± 208107
	n - value		15	15
Day vs. night food consumption	Food intake (g) (mean ± SD)	Control	7.906 ± 2.455	13.94 ± 7.184
	n - value		19	19
	Food intake (g) (mean ± SD)	SCN-*Bmal1*-KD	10.77 ± 5.636	11.29 ± 5.446
	n - value		15	15
Day vs. night water consumption	Water intake (ml) (mean ± SD)	Control	17.02 ± 8.721	24.34 ± 13.22
	n - value		19	19
	Water intake (ml) (mean ± SD)	SCN-*Bmal1*-KD	17.54 ± 11.37	21.80 ± 15.05
	n - value		15	15
Day vs. night respiratory exchange rate	Respiratory exchange rate (mean ± SD)	Control	0.9044 ± 0.03460	0.9250 ± 0.04235
	n - value		12	12
	Respiratory exchange rate (mean ± SD)	SCN-*Bmal1*-KD	0.9018 ± 0.05680	0.9021 ± 0.06900
	n - value		8	8
Day vs. night energy expenditure	Energy expenditure (kcal/h/kg) (mean ± SD)	Control	5.741 ± 0.6609	6.304 ± 0.8538
	n - value		12	12
	Energy expenditure (kcal/h/kg) (mean ± SD)	SCN-*Bmal1*-KD	5.382 ± 0.6673	5.631 ± 0.8917
	n - value		8	8

Table S13. Statistics for day vs. night metabolic cage parameters in project 1. Statistical tests and their outcomes are indicated. DF = degrees of freedom; n.s. = not significant.

Measurement	Statistical test		Source of variation			Statistical Test	Comparison	Uncorrected p-value	Corrected p-value	Summary
			Experimental group	Phase	Experimental group x phase					
Day vs. night locomotor activity	Two-way repeated measures ANOVA	DF	1	1	1	Fisher's LSD test + Bonferroni correction	Control day vs. control night	< 0.0001	< 0.0001	****
		F-value	1.1387	32.24	3.847					
		p-value	0.2476	< 0.0001	0.0586		SCN-*Bmal1*-KD day vs. SCN-*Bmal1*-KD night	0.0183	0.0367	*
		Summary	n.s.	****	#					
Day vs. night food consumption		DF	1	1	1		Control day vs. control night	0.0003	0.0007	***
		F-value	0.004855	8.406	5.95					
		p-value	0.9449	0.0067	0.0204		SCN-*Bmal1*-KD day vs. SCN-*Bmal1*-KD night	0.7603	> 0.9999	n.s.
		Summary	n.s.	**	*					
Day vs. night water consumption		DF	1	1	1		Control day vs. control night	< 0.0001	< 0.0001	****
		F-value	0.0615	29.01	2.015					
		p-value	0.8057	< 0.0001	0.1654		SCN-*Bmal1*-KD day vs. SCN-*Bmal1*-KD night	0.0123	0.0246	*
		Summary	n.s.	****	n.s.					
Day vs. night respiratory exchange rate		DF	1	1	1		Control day vs. control night	0.0274	0.0549	#
		F-value	0.3472	2.367	2.24					
		p-value	0.563	0.1413	0.1518		SCN-*Bmal1*-KD day vs. SCN-*Bmal1*-KD night	0.9788	> 0.9999	n.s.
		Summary	n.s.	n.s.	n.s.					
Day vs. night energy expenditure		DF	1	1	1		Control day vs. control night	< 0.0001	0.0002	***
		F-value	2.277	21.36	3.206					
		p-value	0.1486	0.0002	0.0902		SCN-*Bmal1*-KD day vs. SCN-*Bmal1*-KD night	0.0843	0.1685	n.s.
		Summary	n.s.	***	#					

Table S14. Overall metabolic cage parameters in project 1. Mean ± SD, statistical tests and their outcomes are indicated. n.s. = not significant; SD = standard deviation.

Measurement	Parameter	Control	SCN-*Bmal1*-KD	Statistical Test	p-value	Summary
Total locomotor activity	Activity (counts) (mean ± SD)	974159 ± 246701	853064 ± 402868	Mann–Whitney U test	0.0138	*
	n - value	19	15			
Total food consumption	Food intake (g) (mean ± SD)	21.85 ± 7.698	22.06 ± 9.844	Unpaired t-test	0.9449	n.s.
	n - value	19	15			
Total water consumption	Water intake (ml) (mean ± SD)	41.36 ± 21.28	39.34 ± 26.18	Mann–Whitney U test	0.5836	n.s.
	n - value	19	15			
Mean respiratory exchange rate	Respiratory exchange rate (mean ± SD)	0.9147 ± 0.03579	0.9019 ± 0.06132	Unpaired t-test	0.563	n.s.
	n - value	12	8			
Mean energy expenditure	Energy expenditure (kcal/h/kg) (mean ± SD)	6.022 ± 0.7354	5.507 ± 0.7688	Unpaired t-test	0.1486	n.s.
	n - value	12	8			

Table S15. First GTT and ITT in project 1. Mean ± SD, statistical tests and their outcomes are indicated. DF = degrees of freedom; GTT = glucose tolerance test; ITT = insulin tolerance test; SD = standard deviation.

Test	Time	Parameter	Experimental group		Statistical test		Source of variation		
			Control	SCN-*Bmal1*-KD			Experimental Group	Time	Experimental Group x Time
Glucose tolerance test	0 min	Glucose (mg/dL) (mean ± SD)	166.3 ± 34.77	129.8 ± 20.28	Two-way repeated measures ANOVA	DF	1	5	5
		n - value	29	21					
	15 min	Glucose (mg/dL) (mean ± SD)	391.4 ± 70.69	265.6 ± 51.71		F-value	52.65	198.1	8.574
		n - value	29	21					
	30 min	Glucose (mg/dL) (mean ± SD)	382.0 ± 72.23	265.2 ± 65.84		p-value	< 0.0001	< 0.0001	< 0.0001
		n - value	29	21					
	60 min	Glucose (mg/dL) (mean ± SD)	300.6 ± 61.7	218.2 ± 55.7		Summary	****	****	****
		n - value	29	21					
	90 min	Glucose (mg/dL) (mean ± SD)	245.9 ± 44.75	162.1 ± 33.35					
		n - value	29	21					
	120 min	Glucose (mg/dL) (mean ± SD)	204.5 ± 46.19	144.7 ± 25.81					
		n - value	29	21					
Insulin tolerance test	0 min	Glucose (mg/dL) (mean ± SD)	182.8 ± 32.21	127.1 ± 33.99		DF	1	5	5
		n - value	29	20					
	15 min	Glucose (mg/dL) (mean ± SD)	177.6 ± 51.96	107.2 ± 25.58		F-value	31.25	46.34	3.065
		n - value	29	20					
	30 min	Glucose (mg/dL) (mean ± SD)	123.5 ± 43.45	79.55 ± 21.60		p-value	< 0.0001	< 0.0001	0.0106
		n - value	29	20					
	60 min	Glucose (mg/dL) (mean ± SD)	118.8 ± 40.14	79.95 ± 20.73		Summary	****	****	*
		n - value	29	20					
	90 min	Glucose (mg/dL) (mean ± SD)	128 ± 44.63	85.35 ± 20.84					
		n - value	29	20					
	120 min	Glucose (mg/dL) (mean ± SD)	137.0 ± 44.03	94.0 ± 27.15					
		n - value	29	20					

Table S16. AOC and fasting glucose for the first GTT and ITT in project 1. Mean ± SD, statistical tests and their outcomes are indicated. AOC = area of the curve; GTT = glucose tolerance test; ITT = insulin tolerance test; n.s. = not significant; SD = standard deviation.

Test	Parameter	Control	SCN-*Bmal1*-KD	Statistical Test	p-value	Summary
Glucose Tolerance Test 1	AOC (mg/dL x min) (mean ± SD)	15120 ± 6035	9241 ± 4676	Unpaired t-test	0.0005	***
	n - value	29	21			
	Fasting glucose (6-hour fasting) (mg/dL) (mean ± SD)	166.3 ± 34.77	129.8 ± 20.28	Unpaired t-test	< 0.0001	****
	n - value	29	21			
Insulin Tolerance Test 1	AOC (mg/dL x min) (mean ± SD)	5973 ± 3229	4568 ± 2835	Mann–Whitney U test	0.1019	n.s.
	n - value	29	20			
	Fasting glucose (4-hour fasting) (mg/dL) (mean ± SD)	182.8 ± 32.21	127.1 ± 33.99	Mann–Whitney U test	< 0.0001	****
	n - value	29	20			

Table S17. **GTT and ITT over time in project 1.** Mean ± SD, statistical tests and their outcomes are indicated. DF = degrees of freedom; GTT = glucose tolerance test; ITT = insulin tolerance test; n.s. = not significant; SD = standard deviation.

Test	Parameter	Experimental group	Time		Statistical test		Source of variation		
			Time point 1	Time point 2			Experimental Group	Time	Experimental Group x Time
Glucose tolerance test	AOC (mg/dL x min) (mean ± SD)	Control	14002 ± 5751	17877 ± 6016	Two-way repeated measures ANOVA	DF	1	1	1
	n - value		9	9		F-value	27.16	1.88	0.744
	AOC (mg/dL x min) (mean ± SD)	SCN-*Bmal1*-KD	8055 ± 3274	8938 ± 3301		p-value	< 0.0001	0.1893	0.4011
	n - value		9	9		Summary	****	n.s.	n.s.
	Fasting glucose (6-hour fasting) (mg/dL) (mean ± SD)	Control	160.8 ± 28.53	164.7 ± 37.79		DF	1	1	1
	n - value		9	9		F-value	13.74	0.1046	0.0009
	Fasting glucose (6-hour fasting) (mg/dL) (mean ± SD)	SCN-*Bmal1*-KD	127.8 ± 12.33	131.0 ± 35.19		p-value	0.0019	0.7506	0.9762
	n - value		9	9		Summary	**	n.s.	n.s.
Insulin tolerance test	AOC (mg/dL x min) (mean ± SD)	Control	5158 ± 3149	2650 ± 2519		DF	1	1	1
	n - value		8	8		F-value	2.843	2.909	1.626
	AOC (mg/dL x min) (mean ± SD)	SCN-*Bmal1*-KD	3030 ± 1417	2668 ± 1108		p-value	0.1124	0.1087	0.2216
	n - value		9	9		Summary	n.s.	n.s.	n.s.
	Fasting glucose (6-hour fasting) (mg/dL) (mean ± SD)	Control	198.9 ± 11.93	178.4 ± 35.98		DF	1	1	1
	n - value		8	8		F-value	14.9	0.7334	2.569
	Fasting glucose (6-hour fasting) (mg/dL) (mean ± SD)	SCN-*Bmal1*-KD	134.0 ± 42.14	140.2 ± 29.98		p-value	0.0015	0.4052	0.1298
	n - value		9	9		Summary	**	n.s.	n.s.

Table S18. Glucose measurements in project 1. Mean ± SD is indicated. Cumulative day glucose = ZT1 + ZT5 + ZT9. Cumulative night glucose = ZT13 + ZT17 + ZT21. SD = standard deviation; ZT = Zeitgeber time.

Measurement	Time point	Parameter	Experimental group	
			Control	SCN-*Bmal1*-KD
24-hour glucose	ZT1	Glucose (mg/dL) (mean ± SD)	170.0 ± 38.77	134.9 ± 19.89
		n - value	9	9
	ZT5	Glucose (mg/dL) (mean ± SD)	165.2 ± 31.88	146.4 ± 24.06
		n - value	9	9
	ZT9	Glucose (mg/dL) (mean ± SD)	175.4 ± 39.80	137.3 ± 18.88
		n - value	9	9
	ZT13	Glucose (mg/dL) (mean ± SD)	172.0 ± 26.28	133.8 ± 18.42
		n - value	9	9
	ZT17	Glucose (mg/dL) (mean ± SD)	194.4 ± 34.38	150.1 ± 35.07
		n - value	9	9
	ZT21	Glucose (mg/dL) (mean ± SD)	186.9 ± 32.74	142.1 ± 20.03
		n - value	9	9
Measurement	**Experimental group**	**Parameter**	**Phase**	
			Day	**Night**
Cumulative day vs. night Glucose	Control	Glucose (mg/dL) (mean ± SD)	510.7 ± 67.92	553.3 ± 67.58
		n - value	9	9
	SCN-*Bmal1*-KD	Glucose (mg/dL) (mean ± SD)	418.7 ± 47.10	426 ± 67.58
		n - value	9	9

Table S19. Statistics for glucose measurements in project 1. Statistical tests and their outcomes are indicated. DF = degrees of freedom; n.s. = not significant; ZT = Zeitgeber time.

Measurement	Statistical test		Source of variation		
			Experimental group	ZT	Experimental group x ZT
24-hour glucose	Two-way repeated measures ANOVA	DF	1	5	5
		F-value	15.52	1.918	0.7127
		p-value	0.0012	0.1005	0.5157
		Summary	**	n.s.	n.s.

Measurement	Statistical test		Source of variation			Statistical Test	Comparison	Uncorrected p-value	Corrected p-value	Summary
			Experimental group	Phase	Experimental group x phase					
Cumulative day vs. night Glucose	Two-way repeated measures ANOVA	DF	1	1	1	Fisher's LSD test + Bonferroni correction	Control day vs. control night	0.0005	0.0010	**
		F-value	15.52	12.94	6.462					
		p-value	0.0012	0.002	0.0217		SCN-*Bmal1*-KD day vs. SCN-*Bmal1*-KD night	0.4664	0.9328	n.s.
		Summary	**	**	*					

Table S20. IntelliCage data in project 2. Mean ± SD, statistical tests and their outcomes are indicated. DF = degrees of freedom; nocturnality score = (parameter during dark phase - parameter during light phase) / (parameter during dark phase + parameter during light phase); SD = standard deviation.

Test	Parameter	Sex	Paradigm		Statistical test		Source of variation			Statistical Test	Comparison	Uncorrected p-value	Corrected p-value	Summary
			Control	Shift work			Sex	Shift work	Sex x shift work					
Intelli-Cage	Overall corner visits (mean ± SD)	Male	2801 ± 353.5	1922 ± 389.2	Two-way ANOVA	DF	1	1	1	Fisher's LSD test + Bonferroni correction	Male control vs. Male shift work	0.0014	0.0027	**
	n - value		15	15		F-value	96.11	22.15	0.00415					
	Overall corner visits (mean ± SD)	Female	4594 ± 902.9	3739 ± 970.8		p-value	< 0.0001	< 0.0001	0.9488		Female control vs. Female shift work	0.0018	0.0036	**
	n - value		15	15		Summary	****	****	n.s.					
	Nocturnality (mean ± SD)	Male	0.4571 ± 0.1016	0.3812 ± 0.08336		DF	1	1	1		Male control vs. Male shift work	0.0089	0.0177	*
	n - value		15	15		F-value	15.08	44.31	8.136					
	Nocturnality (mean ± SD)	Female	0.5916 ± 0.04484	0.4017 ± 0.06280		p-value	0.0003	< 0.0001	0.0061		Female control vs. Female shift work	< 0.0001	< 0.0001	****
	n - value		14	15		Summary	***	****	**					

Table S21. OFT and transitions in the TST in project 2. Mean ± SD is indicated. OFT = open field test; SD = standard deviation; TST = tail suspension test.

Test	Parameter	Sex	Paradigm	
			Control	Shift work
OFT	Distance traveled (m) (mean ± SD)	Male	17.66 ± 4.259	19.74 ± 5.315
	n - value		18	18
	Distance traveled (m) (mean ± SD)	Female	19.25 ± 3.013	20.10 ± 4.067
	n - value		11	12
	Center entries (mean ± SD)	Male	42.78 ± 11.70	46.28 ± 9.510
	n - value		18	18
	Center entries (mean ± SD)	Female	43.42 ± 10.26	48.42 ± 10.08
	n - value		12	12
	Center time (s) (mean ± SD)	Male	132.5 ± 30.16	133.5 ± 36.18
	n - value		18	18
	Center time (s) (mean ± SD)	Female	117.0 ± 42.06	113.1 ± 39.22
	n - value		12	12
	Transitions mobile / immobile episodes (mean ± SD)	Male	33.67 ± 6.553	31.22 ± 8.434
	n - value		18	18
	Transitions mobile / immobile episodes (mean ± SD)	Female	22.83 ± 6.520	28.00 ± 5.394
	n - value		12	12
TST	Transitions mobile / immobile episodes (mean ± SD)	Male	24.67 ± 6.544	24.71 ± 9.816
	n - value		18	17
	Transitions mobile / immobile episodes (mean ± SD)	Female	15.33 ± 6.499	24.17 ± 9.989
	n - value		12	12

Table S22. Statistics for OFT and transitions in the TST in project 2. Statistical tests and their outcomes are indicated. DF = degrees of freedom; n.s. = not significant; OFT = open field test; TST = tail suspension test.

Test	Parameter	Statistical test		Source of variation			Statistical Test	Comparison	Uncorrected p-value	Corrected p-value	Summary
				Sex	Shift work	Sex x shift work					
OFT	Distance traveled	Two-way ANOVA	DF	1	1	1	Fisher's LSD test + Bonferroni correction	Male control vs. Male shift work	0.1607	0.3215	n.s.
			F-value	0.6963	1.553	0.2787					
			p-value	0.4076	0.2179	0.5996		Female control vs. Female shift work	0.6476	> 0.9999	n.s.
			Summary	n.s.	n.s.	n.s.					
	Center entries		DF	1	1	1		Male control vs. Male shift work	0.3203	0.6406	n.s.
			F-value	0.2533	2.372	0.07387					
			p-value	0.6167	0.1292	0.7868		Female control vs. Female shift work	0.2471	0.4942	n.s.
			Summary	n.s.	n.s.	n.s.					
	Center time		DF	1	1	1		Male control vs. Male shift work	0.9309	> 0.9999	n.s.
			F-value	3.522	0.02137	0.06569					
			p-value	0.0658	0.8843	0.7987		Female control vs. Female shift work	0.796	> 0.9999	n.s.
			Summary	#	n.s.	n.s.					
	Transitions mobile / immobile episodes		DF	1	1	1		Male control vs. Male shift work	0.2978	0.5956	n.s.
			F-value	14.61	0.5479	4.283					
			p-value	0.0003	0.4623	0.0431		Female control vs. Female shift work	0.0751	0.1502	n.s.
			Summary	***	n.s.	*					
TST	Transitions mobile / immobile episodes		DF	1	1	1		Male control vs. Male shift work	0.989	> 0.9999	n.s.
			F-value	4.978	4.02	3.95					
			p-value	0.0298	0.0499	0.0519		Female control vs. Female shift work	0.0122	0.0244	*
			Summary	*	*	#					

Table S23. EPM and DaLi box test in project 2. Mean ± SD is indicated. DaLi box = dark-light box; EPM = elevated plus maze; SD = standard deviation.

Test	Parameter	Sex	Paradigm	
			Control	Shift work
EPM	Open arm entries (mean ± SD)	Male	6.000 ± 3.102	9.111 ± 3.563
	n - value		17	18
	Open arm entries (mean ± SD)	Female	14.33 ± 7.499	8.000 ± 2.523
	n - value		12	12
	Open arm time (s) (mean ± SD)	Male	16.36 ± 12.93	21.81 ± 14.34
	n - value		17	18
	Open arm time (s) (mean ± SD)	Female	33.97 ± 15.67	16.80 ± 8.007
	n - value		12	12
	Open arm distance (m) (mean ± SD)	Male	0.1786 ± 0.2722	0.2768 ± 0.3123
	n - value		17	18
	Open arm distance (m) (mean ± SD)	Female	0.4286 ± 0.3256	0.2488 ± 0.1975
	n - value		11	12
DaLi box	Entries into light (mean ± SD)	Male	6.722 ± 3.286	7.167 ± 5.090
	n - value		18	18
	Entries into light (mean ± SD)	Female	9.000 ± 3.801	5.100 ± 3.035
	n - value		10	10
	Time in light (s) (mean ± SD)	Male	52.64 ± 32.59	50.33 ± 32.50
	n - value		18	18
	Time in light (s) (mean ± SD)	Female	58.69 ± 29.91	32.12 ± 19.71
	n - value		10	10
	Distance in light (m) (mean ± SD)	Male	2.937 ± 1.522	2.992 ± 2.992
	n - value		18	18
	Distance in light (m) (mean ± SD)	Female	4.243 ± 2.688	2.045 ± 1.249
	n - value		10	10

Table S24. Statistics for EPM and DaLi box test in project 2. Statistical tests and their outcomes are indicated. DaLi box = dark-light box; DF = degrees of freedom; EPM = elevated plus maze; n.s. = not significant.

Test	Parameter	Statistical test		Source of variation			Statistical Test	Comparison	Uncorrected p-value	Corrected p-value	Summary
				Sex	Shift work	Sex x shift work					
EPM	Open arm entries	Two-way ANOVA	DF	1	1	1	Fisher's LSD test + Bonferroni correction	Male control vs. Male shift work	0.0406	0.0812	#
			F-value	9.644	1.92	16.49					
			p-value	0.003	0.1715	0.0002		Female control vs. Female shift work	0.0008	0.0017	**
			Summary	**	n.s.	***					
	Open arm time		DF	1	1	1		Male control vs. Male shift work	0.2275	0.455	n.s.
			F-value	3.24	2.807	10.45					
			p-value	0.0774	0.0995	0.0021		Female control vs. Female shift work	0.0024	0.0047	**
			Summary	#	#	**					
	Open arm distance		DF	1	1	1		Male control vs. Male shift work	0.3178	0.6356	n.s.
			F-value	2.099	0.2835	3.292					
			p-value	0.1533	0.5966	0.0753		Female control vs. Female shift work	0.1345	0.269	n.s.
			Summary	n.s.	n.s.	#					
DaLi box	Entries into light		DF	1	1	1		Male control vs. Male shift work	0.741	> 0.9999	n.s.
			F-value	0.0089	2.384	3.769					
			p-value	0.9252	0.1286	0.0576		Female control vs. Female shift work	0.0343	0.0686	#
			Summary	n.s.	n.s.	#					
	Time in light		DF	1	1	1		Male control vs. Male shift work	0.8196	> 0.9999	n.s.
			F-value	0.5193	2.931	2.068					
			p-value	0.4743	0.0928	0.1564		Female control vs. Female shift work	0.0548	0.1097	n.s.
			Summary	n.s.	#	n.s.					
	Distance in light		DF	1	1	1		Male control vs. Male shift work	0.9304	> 0.9999	n.s.
			F-value	0.1197	4.282	4.727					
			p-value	0.7307	0.0435	0.0343		Female control vs. Female shift work	0.0107	0.0215	*
			Summary	n.s.	*	*					

Table S25. TST, sucrose preference test, LH test and pain sensitivity in project 2. Mean ± SD is indicated. LH = learned helplessness; SD = standard deviation; TST = tail suspension test.

Test	Parameter	Sex	Paradigm	
			Control	Shift work
TST	Time immobile (s) (mean ± SD)	Male	215.5 ± 34.34	201.8 ± 41.62
	n - value		18	16
	Time immobile (s) (mean ± SD)	Female	160.2 ± 75.24	158.9 ± 56.52
	n - value		12	12
	Immobility latency (s) (mean ± SD)	Male	66.07 ± 24.44	73.03 ± 26.71
	n - value		18	16
	Immobility latency (s) (mean ± SD)	Female	86.51 ± 34.84	71.18 ± 44.02
	n - value		12	12
Sucrose preference test	Preference Score (AU) (mean ± SD)	Male	0.3501 ± 0.08766	0.3229 ± 0.09317
	n - value		15	15
	Preference Score (AU) (mean ± SD)	Female	0.2571 ± 0.1719	0.2292 ± 0.08196
	n - value		15	15
LH	Latency (s) (mean ± SD)	Male	16.27 ± 7.840	7.539 ± 3.427
	n - value		16	16
	Latency (s) (mean ± SD)	Female	9.866 ± 2.453	13.59 ± 7.182
	n - value		10	9
	Number of failures (mean ± SD)	Male	8.188 ± 7.111	0.6667 ± 1.175
	n - value		16	15
	Number of failures (mean ± SD)	Female	0.9000 ± 1.449	6.000 ± 6.442
	n - value		10	9
Pain sensitivity	Pain threshold (mA) (mean ± SD)	Male	0.06250 ± 0.02176	0.05750 ± 0.02517
	n - value		16	16
	Pain threshold (mA) (mean ± SD)	Female	0.1040 ± 0.02271	0.09556 ± 0.02603
	n - value		10	9

Table S26. Statistics for TST, sucrose preference test, LH test and pain sensitivity in project 2. Statistical tests and their outcomes are indicated. DF = degrees of freedom; LH = learned helplessness; n.s. = not significant; TST = tail suspension test.

Test	Parameter	Statistical test		Source of variation			Statistical Test	Comparison	Uncorrected p-value	Corrected p-value	Summary
				Sex	Shift work	Sex x shift work					
TST	Time immobile	Two-way ANOVA	DF	1	1	1	Fisher's LSD test + Bonferroni correction	Male control vs. Male shift work	0.4396	0.8792	n.s.
			F-value	12.75	0.2997	0.2073					
			p-value	0.0008	0.5863	0.6507		Female control vs. Female shift work	0.9522	> 0.9999	n.s.
			Summary	***	n.s.	n.s.					
	Immobility latency		DF	1	1	1		Male control vs. Male shift work	0.5303	> 0.9999	n.s.
			F-value	1.18	0.2391	1.696					
			p-value	0.2821	0.6268	0.1983		Female control vs. Female shift work	0.2469	0.4937	n.s.
			Summary	n.s.	n.s.	n.s.					
Sucrose preference test	Preference Score		DF	1	1	1		Male control vs. Male shift work	0.5187	> 0.9999	n.s.
			F-value	9.918	0.8648	0.00013					
			p-value	0.0026	0.3564	0.9909		Female control vs. Female shift work	0.5084	> 0.9999	n.s.
			Summary	**	n.s.	n.s.					
LH	Latency		DF	1	1	1		Male control vs. Male shift work	< 0.0001	0.0002	***
			F-value	0.01127	2.242	13.86					
			p-value	0.9159	0.141	0.0005		Female control vs. Female shift work	0.1669	0.3339	n.s.
			Summary	n.s.	n.s.	***					
	Number of failures		DF	1	1	1		Male control vs. Male shift work	0.0001	0.0002	***
			F-value	0.4574	0.7019	19.08					
			p-value	0.5022	0.4065	< 0.0001		Female control vs. Female shift work	0.0299	0.0598	#
			Summary	n.s.	n.s.	****					
Pain sensitivity	Pain threshold		DF	1	1	1		Male control vs. Male shift work	0.5555	> 0.9999	n.s.
			F-value	33.19	0.948	0.06222					
			p-value	< 0.0001	0.3352	0.8041		Female control vs. Female shift work	0.4442	0.8884	n.s.
			Summary	****	n.s.	n.s.					

Table S27. Weight and fat pads in project 2. Mean ± SD is indicated. BAT = brown adipose tissue; BW = body weight; gWAT = gonadal white adipose tissue; iWAT = inguinal white adipose tissue; SD = standard deviation.

Measurement	Parameter	Sex	Paradigm	
			Control	Shift work
Weight at start	Weight (g) (mean ± SD)	Male	23.43 ± 1.679	22.55 ± 2.352
	n - value		18	18
	Weight (g) (mean ± SD)	Female	19.31 ± 0.568	19.53 ± 1.414
	n - value		12	12
Weight at sacrifice	Weight gain (%) (mean ± SD)	Male	15.53 ± 3.806	22.03 ± 11.12
	n - value		17	18
	Weight gain (%) (mean ± SD)	Female	7.626 ± 3.285	7.320 ± 4.708
	n - value		12	11
gWAT	% gWAT of BW (mean ± SD)	Male	0.9550 ± 0.2172	0.9374 ± 0.2157
	n - value		18	18
	% gWAT of BW (mean ± SD)	Female	0.8072 ± 0.2074	1.018 ± 0.4936
	n - value		12	11
iWAT	% iWAT of BW (mean ± SD)	Male	0.4445 ± 0.1269	0.4666 ± 0.1082
	n - value		18	18
	% iWAT of BW (mean ± SD)	Female	0.6332 ± 0.1694	0.7380 ± 0.2684
	n - value		12	11
BAT	% BAT of BW (mean ± SD)	Male	0.2850 ± 0.03356	0.2855 ± 0.07098
	n - value		18	18
	% BAT of BW (mean ± SD)	Female	0.2874 ± 0.06618	0.2714 ± 0.05100
	n - value		12	11

Table S28. Statistics for weight and fat pads in project 2. Statistical tests and their outcomes are indicated. BAT = brown adipose tissue; BW = body weight; DF = degrees of freedom; gWAT = gonadal white adipose tissue; iWAT = inguinal white adipose tissue; n.s. = not significant.

Measurement	Parameter	Statistical test		Source of variation			Statistical Test	Comparison	Uncorrected p-value	Corrected p-value	Summary
				Sex	Shift work	Sex x shift work					
Weight at start	Weight	Two-way ANOVA	DF	1	1	1	Fisher's LSD test + Bonferroni correction	Male control vs. Male shift work	0.1313	0.2627	n.s.
			F-value	61.24	0.5207	1.477					
			p-value	< 0.0001	0.4735	0.2294		Female control vs. Female shift work	0.7512	> 0.9999	n.s.
			Summary	****	n.s.	n.s.					
Weight at sacrifice	Weight gain		DF	1	1	1		Male control vs. Male shift work	0.0085	0.0171	*
			F-value	35.77	2.682	3.239					
			p-value	< 0.0001	0.1073	0.0775		Female control vs. Female shift work	0.9173	> 0.9999	n.s.
			Summary	****	n.s.	#					
gWAT	% gWAT of BW		DF	1	1	1		Male control vs. Male shift work	0.8539	> 0.9999	n.s.
			F-value	0.1935	1.596	2.232					
			p-value	0.6617	0.2119	0.1409		Female control vs. Female shift work	0.0833	0.1665	n.s.
			Summary	n.s.	n.s.	n.s.					
iWAT	% iWAT of BW		DF	1	1	1		Male control vs. Male shift work	0.6905	> 0.9999	n.s.
			F-value	27.04	2.056	0.8731					
			p-value	< 0.0001	0.1573	0.3542		Female control vs. Female shift work	0.1354	0.2708	n.s.
			Summary	****	n.s.	n.s.					
BAT	% BAT of BW		DF	1	1	1		Male control vs. Male shift work	0.9792	> 0.9999	n.s.
			F-value	0.1458	0.2616	0.296					
			p-value	0.7041	0.6111	0.5886		Female control vs. Female shift work	0.5023	> 0.9999	n.s.
			Summary	n.s.	n.s.	n.s.					

Table S29. Weight measurements and food consumption over time in project 2. Mean ± SD is indicated. SD = standard deviation.

Parameter	Sex	Experimental paradigm	Weeks after initiation of shift work paradigm							
			0	1	2	3	4	5	6	7
Weight (g) (mean ± SD)	Male	Control	23.43 ± 1.679	24.83 ± 1.531	25.45 ± 1.407	26.34 ± 1.350	26.53 ± 1.308	27.27 ± 1.528	27.50 ± 1.572	28.16 ± 1.095
n - value			18	18	18	18	18	18	18	12
Weight (g) (mean ± SD)	Male	Shift work	22.55 ± 2.352	24.96 ± 2.086	25.91 ± 2.052	26.76 ± 2.060	27.01 ± 2.007	27.58 ± 2.156	28.04 ± 2.064	28.38 ± 2.522
n - value			18	18	18	18	18	18	18	12
Weight (g) (mean ± SD)	Female	Control	19.31 ± 0.568	19.87 ± 0.7024	20.27 ± 0.676	20.43 ± 0.5726	20.40 ± 0.6715	20.81 ± 0.7513	21.04 ± 0.7038	21.23 ± 0.3955
n - value			12	12	12	12	12	12	12	8
Weight (g) (mean ± SD)	Female	Shift work	19.53 ± 1.414	19.73 ± 1.649	20.63 ± 1.705	20.82 ± 1.496	21.20 ± 1.656	21.36 ± 1.356	21.20 ± 1.338	21.60 ± 1.838
n - value			12	12	12	12	12	12	12	8
Weight gain (%) (mean ± SD)	Male	Control	0 ± 0	6.055 ± 1.978	8.774 ± 2.965	11.95 ± 3.399	12.70 ± 3.834	15.71 ± 3.694	16.71 ± 3.113	17.54 ± 4.287
n - value			18	18	18	17	17	17	17	11
Weight gain (%) (mean ± SD)	Male	Shift work	0 ± 0	11.13 ± 6.131	15.45 ± 7.584	19.38 ± 9.579	20.61 ± 10.34	23.12 ± 10.81	25.18 ± 10.88	28.84 ± 9.369
n - value			18	18	18	18	18	18	18	12
Weight gain (%) (mean ± SD)	Female	Control	0 ± 0	2.899 ± 2.389	4.969 ± 1.987	5.845 ± 1.862	5.665 ± 2.272	7.799 ± 3.477	9.012 ± 3.364	10.29 ± 2.314
n - value			12	12	12	12	12	12	12	8
Weight gain (%) (mean ± SD)	Female	Shift work	0 ± 0	0.9891 ± 3.253	5.564 ± 3.370	6.651 ± 4.169	8.582 ± 4.587	9.475 ± 4.032	8.641 ± 3.157	8.242 ± 4.336
n - value			12	12	12	12	12	12	12	8
Food consumption/animal (g) (mean ± SD)	Male	Control	-	-	34.94 ± 7.238	28.57 ± 1.814	27.79 ± 3.236	25.57 ± 1.227	27.38 ± 1.072	28.98 ± 2.582
n - value			-	-	3	3	3	3	3	3
Food consumption/animal (g) (mean ± SD)	Male	Shift work	-	-	30.02 ± 2.578	27.14 ± 4.165	27.57 ± 4.452	26.13 ± 6.817	28.19 ± 4.155	32.63 ± 0.0106
n - value			-	-	3	3	3	3	3	2
Food consumption/animal (g) (mean ± SD)	Female	Control	-	-	23.85 ± 0.1956	24.21 ± 0.03299	23.32 ± 0.7319	22.03 ± 0.7896	20.40 ± 0.1886	22.43 ± 4.745
n - value			-	-	2	2	2	2	2	2
Food consumption/animal (g) (mean ± SD)	Female	Shift work	-	-	27.26 ± 2.269	30.32 ± 0.000	22.94 ± 1.080	25.21 ± 1.914	24.35 ± 1.811	26.16 ± 5.268
n - value			-	-	2	1	2	2	2	2

Table S30. Statistics for weight measurements and food consumption over time in project 2. Statistical tests and their outcomes are indicated. DF = degrees of freedom; n.s. = not significant.

Parameter	Statistical test		Source of variation						
			Time	Sex	Shift work	Time x sex	Time x shift work	Sex x shift work	Time x sex x shift work
Absolute weight (g)	Mixed-effects analysis (Repeated-Measured)	DF	7	1	1	7	7	1	7
		F-value	227.5	203.3	0.4617	46.75	4.023	0.002224	2.8232
		p-value	< 0.0001	< 0.0001	0.4996	< 0.0001	0.0003	0.9626	0.0069
		Summary	****	****	n.s.	****	***	n.s.	**
Weight gain (%)	Mixed-effects analysis (Repeated-Measured)	DF	7	1	1	7	7	1	7
		F-value	194.1	45.55	7.049	28.7	5.349	5.963	3.871
		p-value	< 0.0001	< 0.0001	0.0103	< 0.0001	< 0.0001	0.0178	0.0004
		Summary	****	****	*	****	****	*	***
Food consumption/ animal/week (g)	Mixed-effects analysis (Repeated-Measured)	DF	5	1	1	5	5	1	5
		F-value	3.405	7.083	0.889	1.6	0.755	1.479	0.8663
		p-value	0.0158	0.0375	0.3822	0.1925	0.5896	0.2696	0.5159
		Summary	*	*	n.s.	n.s.	n.s.	n.s.	n.s.

Table S31. Locomotor activity, food consumption and water consumption in the metabolic cages in project 2. Mean ± SD is indicated. Nocturnality score = (parameter during dark phase - parameter during light phase) / (parameter during dark phase + parameter during light phase); SD = standard deviation.

Measurement	Parameter	Sex	Paradigm	
			Control	Shift work
Locomotor activity	Overall (light beam breaks) (mean ± SD)	Male	1044717 ± 551880	868509 ± 155716
	n - value		6	5
	Overall (light beam breaks) (mean ± SD)	Female	1057332 ± 253551	994258 ± 236641
	n - value		5	5
	Nocturnality (mean ± SD)	Male	0.2739 ± 0.1388	0.3793 ± 0.1407
	n - value		4	6
	Nocturnality (mean ± SD)	Female	0.5890 ± 0.05056	0.3784 ± 0.03864
	n - value		5	4
Food consumption	Overall (g) (mean ± SD)	Male	11.97 ± 1.406	11.04 ± 2.172
	n - value		6	5
	Overall (g) (mean ± SD)	Female	8.860 ± 0.7033	9.326 ± 1.288
	n - value		4	5
	Nocturnality (mean ± SD)	Male	0.4840 ± 0.1848	0.4322 ± 0.2465
	n - value		6	6
	Nocturnality (mean ± SD)	Female	0.5211 ± 0.2112	0.3658 ± 0.1948
	n - value		5	5
Water consumption	Overall (ml) (mean ± SD)	Male	13.81 ± 1.381	13.36 ± 2.562
	n - value		6	5
	Overall (ml) (mean ± SD)	Female	12.51 ± 1.155	16.87 ± 3.616
	n - value		5	5
	Nocturnality (mean ± SD)	Male	0.5359 ± 0.1806	0.3991 ± 0.1739
	n - value		6	6
	Nocturnality (mean ± SD)	Female	0.4617 ± 0.1200	0.3483 ± 0.1714
	n - value		5	5

Table S32. Statistics for locomotor activity, food consumption and water consumption in the metabolic cages in project 2. Statistical tests and their outcomes are indicated. DF = degrees of freedom; nocturnality score = (parameter during dark phase - parameter during light phase) / (parameter during dark phase + parameter during light phase); n.s. = not significant.

Measurement	Parameter	Statistical test		Source of variation			Statistical Test	Comparison	Uncorrected p-value	Corrected p-value	Summary
				Sex	Shift work	Sex x shift work					
Locomotor activity	Overall	Two-way ANOVA	DF	1	1	1	Fisher's LSD test + Bonferroni correction	Male control vs. Male shift work	0.4193	0.8386	n.s.
			F-value	0.2021	0.6043	0.1351					
			p-value	0.6587	0.4476	0.7178		Female control vs. Female shift work	0.7801	> 0.9999	n.s.
			Summary	n.s.	n.s.	n.s.					
	Nocturnality		DF	1	1	1		Male control vs. Male shift work	0.1473	0.2946	n.s.
			F-value	9.966	1.116	10.08					
			p-value	0.0065	0.3075	0.0063		Female control vs. Female shift work	0.0102	0.0204	*
			Summary	**	n.s.	**					
Food consumption	Overall		DF	1	1	1		Male control vs. Male shift work	0.3294	0.6589	n.s.
			F-value	12.36	0.1118	1.028					
			p-value	0.0029	0.7425	0.3258		Female control vs. Female shift work	0.6534	> 0.9999	n.s.
			Summary	**	n.s.	n.s.					
	Nocturnality		DF	1	1	1		Male control vs. Male shift work	0.6761	> 0.9999	n.s.
			F-value	0.02613	1.308	0.3264					
			p-value	0.8734	0.2677	0.5749		Female control vs. Female shift work	0.2607	0.5215	n.s.
			Summary	n.s.	n.s.	n.s.					
Water consumption	Overall		DF	1	1	1		Male control vs. Male shift work	0.754	> 0.9999	n.s.
			F-value	1.157	3.632	5.505					
			p-value	0.2971	0.0737	0.0313		Female control vs. Female shift work	0.0091	0.0182	*
			Summary	n.s.	#	*					
	Nocturnality		DF	1	1	1		Male control vs. Male shift work	0.1678	0.3357	n.s.
			F-value	0.7843	3.14	0.02747					
			p-value	0.3875	0.0933	0.8702		Female control vs. Female shift work	0.2912	0.5823	n.s.
			Summary	n.s.	#	n.s.					

Table S33. Respiratory exchange rate and energy expenditure in the metabolic cages in project 2. Mean ± SD is indicated. Nocturnality score = (parameter during dark phase - parameter during light phase) / (parameter during dark phase + parameter during light phase); SD = standard deviation.

Measurement	Parameter	Sex	Paradigm	
			Control	Shift work
Respiratory exchange rate	Mean (mean ± SD)	Male	0.7801 ± 0.03732	0.7782 ± 0.05946
	n - value		6	5
	Mean (mean ± SD)	Female	0.8352 ± 0.01268	0.8379 ± 0.01255
	n - value		5	5
	Nocturnality (mean ± SD)	Male	0.07373 ± 0.03603	0.07173 ± 0.02786
	n - value		6	6
	Nocturnality (mean ± SD)	Female	0.05396 ± 0.0082	0.04583 ± 0.02206
	n - value		5	5
Energy expenditure	Mean (kcal/h/kg) (mean ± SD)	Male	6.206 ± 0.3067	6.244 ± 0.4425
	n - value		6	5
	Mean (kcal/h/kg) (mean ± SD)	Female	5.664 ± 0.06553	6.411 ± 0.4975
	n - value		5	5
	Nocturnality (mean ± SD)	Male	0.1077 ± 0.03114	0.08544 ± 0.00866
	n - value		6	6
	Nocturnality (mean ± SD)	Female	0.1561 ± 0.00641	0.1093 ± 0.03687
	n - value		5	5

Table S34. Statistics for respiratory exchange rate and energy expenditure in the metabolic cages in project 2. Statistical tests and their outcomes are indicated. DF = degrees of freedom; nocturnality score = (parameter during dark phase - parameter during light phase) / (parameter during dark phase + parameter during light phase); n.s. = not significant.

Measurement	Parameter	Statistical test		Source of variation			Statistical Test	Comparison	Uncorrected p-value	Corrected p-value	Summary
				Sex	Shift work	Sex x shift work					
Respiratory exchange rate	Mean	Two-way ANOVA	DF	1	1	1	Fisher's LSD test + Bonferroni correction	Male control vs Male shift work	0.9351	> 0.9999	n.s.
			F-value	13.09	0.0009	0.02079					
			p-value	0.0021	0.9765	0.8871		Female control vs. Female shift work	0.9055	> 0.9999	n.s.
			Summary	**	n.s.	n.s.					
	Nocturnality		DF	1	1	1		Male control vs. Male shift work	0.8971	> 0.9999	n.s.
			F-value	4.068	0.1999	0.07306					
			p-value	0.0589	0.6601	0.79		Female control vs. Female shift work	0.633	> 0.9999	n.s.
			Summary	#	n.s.	n.s.					
Energy expenditure	Mean		DF	1	1	1		Male control vs. Male shift work	0.8653	> 0.9999	n.s.
			F-value	1.382	6.047	4.932					
			p-value	0.2559	0.0249	0.0402		Female control vs. Female shift work	0.0048	0.0096	**
			Summary	n.s.	*	*					
	Nocturnality		DF	1	1	1		Male control vs. Male shift work	0.1327	0.2653	n.s.
			F-value	11.84	10.83	1.363					
			p-value	0.0029	0.0041	0.2582		Female control vs. Female shift work	0.0074	0.0148	*
			Summary	**	**	n.s.					

Table S35. GTT in project 2. Mean ± SD, statistical tests and their outcomes are indicated. DF = degrees of freedom; GTT = glucose tolerance test; n.s. = not significant; SD = standard deviation.

Test	Time	Parameter	Sex	Paradigm		Statistical test		Source of variation						
				Control	Shift work			Time	Sex	Shift work	Time x sex	Time x shift work	Sex x shift work	Time x sex x shift work
Glucose tolerance test	0 min	Glucose (mg/dL) (mean ± SD)	Male	134.9 ± 24.24	127.4 ± 18.36	Three-way repeated measures ANOVA	DF	5	1	1	5	5	1	5
		n - value		18	17									
		Glucose (mg/dL) (mean ± SD)	Female	124.2 ± 17.48	125.5 ± 22.18									
		n - value		12	11									
	15 min	Glucose (mg/dL) (mean ± SD)	Male	346.3 ± 42.93	348.5 ± 50.43									
		n - value		18	17									
		Glucose (mg/dL) (mean ± SD)	Female	316.4 ± 69.44	334.5 ± 47.56									
		n - value		12	11									
	30 min	Glucose (mg/dL) (mean ± SD)	Male	309.7 ± 60.39	332.9 ± 54.92		F-value	346.2	14.06	0.3453	2.351	0.8441	0.04932	0.5867
		n - value		18	17									
		Glucose (mg/dL) (mean ± SD)	Female	275.8 ± 55.01	281.5 ± 47.48									
		n - value		12	11									
	60 min	Glucose (mg/dL) (mean ± SD)	Male	215.3 ± 26.65	217.8 ± 27.64		p-value	< 0.0001	0.0004	0.5592	0.0412	0.5195	0.8251	0.7102
		n - value		18	17									
		Glucose (mg/dL) (mean ± SD)	Female	184.5 ± 30.08	188.0 ± 27.66									
		n - value		12	11									
	90 min	Glucose (mg/dL) (mean ± SD)	Male	186.0 ± 26.94	194.2 ± 23.80									
		n - value		18	17									
		Glucose (mg/dL) (mean ± SD)	Female	165.6 ± 28.26	165.7 ± 32.31									
		n - value		12	11									
	120 min	Glucose (mg/dL) (mean ± SD)	Male	165.6 ± 23.86	166.1 ± 25.98		Summary	****	***	n.s.	*	n.s.	n.s.	n.s.
		n - value		18	17									
		Glucose (mg/dL) (mean ± SD)	Female	164.8 ± 20.58	149.2 ± 29.45									
		n - value		12	11									

Table S36. **AOC for the GTT and ITT in project 2.** Mean ± SD, statistical tests and their outcomes are indicated. AOC = area of the curve; DF = degrees of freedom; GTT = glucose tolerance test; ITT = insulin tolerance test; n.s. = not significant; SD = standard deviation.

Test	Parameter	Sex	Paradigm		Statistical test		Source of variation			Statistical Test	Comparison	Uncorrected p-value	Corrected p-value	Summary
			Control	Shift work			Sex	Shift work	Sex x shift work					
Glucose Tolerance Test	AOC (mg/dl x min) (mean ± SD)	Male	11522 ± 3200	13243 ± 2738	Two-way ANOVA	DF	1	1	1	Fisher's LSD test + Bonferroni correction	Male control vs. Male shift work	0.0941	0.1883	n.s.
	n - value		18	17		F-value	7.947	1.623	0.7588					
	AOC (mg/dl x min) (mean ± SD)	Female	9959 ± 2972	10282 ± 3009		p-value	0.0067	0.2081	0.3875		Female control vs. Female shift work	0.7963	> 0.9999	n.s.
	n - value		12	11		Summary	**	n.s.	n.s.					
Insulin Tolerance Test	AOC (mg/dl x min) (mean ± SD)	Male	4788 ± 2091	5248 ± 1560		DF	1	1	1		Male control vs. Male shift work	0.2424	0.4849	n.s.
	n - value		18	17		F-value	16.21	0.00045	2.171					
	AOC (mg/dl x min) (mean ± SD)	Female	3343 ± 2385	2496 ± 1466		p-value	0.0002	0.9831	0.1465		Female control vs. Female shift work	0.3478	0.6957	n.s.
	n - value		12	10		Summary	***	n.s.	n.s.					

Table S37. ITT in project 2. Mean ± SD, statistical tests and their outcomes are indicated. DF = degrees of freedom; ITT = insulin tolerance test; n.s. = not significant; SD = standard deviation.

Test	Time	Parameter	Sex	Paradigm		Statistical test		Source of variation						
				Control	Shift work			Time	Sex	Shift work	Time x sex	Time x shift work	Sex x shift work	Time x sex x shift work
Insulin tolerance test	0 min	Glucose (mg/dL) (mean ± SD)	Male	134.2 ± 19.58	134.2 ± 23.04	Three-way repeated measures ANOVA	DF	5	1	1	5	5	1	5
		n - value		18	18									
		Glucose (mg/dL) (mean ± SD)	Female	132.1 ± 21.42	109.3 ± 16.76									
		n - value		12	10									
	15 min	Glucose (mg/dL) (mean ± SD)	Male	94.89 ± 9.529	95.44 ± 15.14		F-value	99.92	2.568	12.25	11.37	0.96	3.553	1.346
		n - value		18	18									
		Glucose (mg/dL) (mean ± SD)	Female	111.4 ± 14.91	96.80 ± 7.099									
		n - value		12	10									
	30 min	Glucose (mg/dL) (mean ± SD)	Male	89.72 ± 14.02	87.06 ± 17.58									
		n - value		18	18									
		Glucose (mg/dL) (mean ± SD)	Female	93.25 ± 10.31	82.80 ± 82.80									
		n - value		12	10									
	60 min	Glucose (mg/dL) (mean ± SD)	Male	84.78 ± 17.63	72.56 ± 14.26		p-value	< 0.0001	0.1149	0.0009	< 0.0001	0.4428	0.0648	0.2452
		n - value		18	18									
		Glucose (mg/dL) (mean ± SD)	Female	86.42 ± 16.63	73.90 ± 13.14									
		n - value		12	10									
	90 min	Glucose (mg/dL) (mean ± SD)	Male	91.83 ± 15.54	80.72 ± 11.59									
		n - value		18	18									
		Glucose (mg/dL) (mean ± SD)	Female	111.5 ± 18.50	92.60 ± 15.68									
		n - value		12	10									
	120 min	Glucose (mg/dL) (mean ± SD)	Male	104.7 ± 14.28	100.1 ± 15.51		Summary	****	n.s.	***	****	n.s.	#	n.s.
		n - value		18	18									
		Glucose (mg/dL) (mean ± SD)	Female	130.3 ± 25.90	109.4 ± 18.91									
		n - value		12	10									

Table S38. SCN and PAG bioluminescence parameters in project 2. Mean ± SD is indicated. PAG = periaqueductal gray; SD = standard deviation; SCN = suprachiasmatic nucleus.

Tissue	Parameter	Sex	Paradigm	
			Control	Shift work
SCN	Phase (h) (mean ± SD)	Male	21.28 ± 0.9302	21.90 ± 1.048
	n - value		15	15
	Phase (h) (mean ± SD)	Female	23.64 ± 0.4896	24.66 ± 1.647
	n - value		7	8
	Period (h) (mean ± SD)	Male	25.15 ± 0.2264	25.25 ± 0.3502
	n - value		15	15
	Period (h) (mean ± SD)	Female	25.14 ± 0.4117	24.98 ± 0.3151
	n - value		7	8
	Amplitude (counts/s) (mean ± SD)	Male	0.2149 ± 0.04222	0.2007 ± 0.05626
	n - value		15	15
	Amplitude (counts/s) (mean ± SD)	Female	0.1738 ± 0.06926	0.1978 ± 0.05680
	n - value		7	8
PAG	Phase (h) (mean ± SD)	Male	2.279 ± 2.296	1.885 ± 1.937
	n - value		13	12
	Phase (h) (mean ± SD)	Female	6.198 ± 1.988	5.462 ± 1.196
	n - value		6	6
	Period (h) (mean ± SD)	Male	25.69 ± 0.7921	25.41 ± 0.6571
	n - value		13	12
	Period (h) (mean ± SD)	Female	25.47 ± 0.7174	26.28 ± 0.7679
	n - value		6	6
	Amplitude (counts/s) (mean ± SD)	Male	0.05007 ± 0.01726	0.05083 ± 0.01962
	n - value		13	12
	Amplitude (counts/s) (mean ± SD)	Female	0.07995 ± 0.02707	0.07278 ± 0.01966
	n - value		6	6

Table S39. Statistics for SCN and PAG bioluminescence parameters in project 2. Statistical tests and their outcomes are indicated. DF = degrees of freedom; n.s. = not significant; PAG = periaqueductal gray; SCN = suprachiasmatic nucleus.

Tissue	Parameter	Statistical test		Source of variation			Statistical Test	Comparison	Uncorrected p-value	Corrected p-value	Summary
				Sex	Shift work	Sex x shift work					
SCN	Phase	Two-way ANOVA	DF	1	1	1	Fisher's LSD test + Bonferroni correction	Male control vs. Male shift work	0.1195	0.2391	n.s.
			F-value	55.83	5.781	0.3264					
			p-value	< 0.0001	0.0208	0.5709		Female control vs. Female shift work	0.0759	0.1519	n.s.
			Summary	****	*	n.s.					
	Period		DF	1	1	1		Male control vs. Male shift work	0.3942	0.7884	n.s.
			F-value	2.056	0.1135	1.768					
			p-value	0.1592	0.7379	0.191		Female control vs. Female shift work	0.3138	0.6276	n.s.
			Summary	n.s.	n.s.	n.s.					
	SCN		DF	1	1	1		Male control vs. Male shift work	0.4781	0.9562	n.s.
			F-value	1.643	0.08178	1.235					
			p-value	0.207	0.7763	0.2729		Female control vs. Female shift work	0.3975	0.7949	n.s.
			Summary	n.s.	n.s.	n.s.					
PAG	Phase		DF	1	1	1		Male control vs. Male shift work	0.6257	> 0.9999	n.s.
			F-value	28.58	0.6491	0.05979					
			p-value	< 0.0001	0.4262	0.8083		Female control vs. Female shift work	0.5273	> 0.9999	n.s.
			Summary	****	n.s.	n.s.					
	Period		DF	1	1	1		Male control vs. Male shift work	0.3411	0.6823	n.s.
			F-value	1.584	1.066	4.55					
			p-value	0.217	0.3094	0.0404		Female control vs. Female shift work	0.0628	0.1255	n.s.
			Summary	n.s.	n.s.	*					
	SCN		DF	1	1	1		Male control vs. Male shift work	0.9255	> 0.9999	n.s.
			F-value	13.4	0.2049	0.3137					
			p-value	0.0009	0.6537	0.5792		Female control vs. Female shift work	0.542	> 0.9999	n.s.
			Summary	***	n.s.	n.s.					

Table S40. Liver bioluminescence parameters and the phase relationship between the SCN and subordinate clocks in project 2. Mean ± SD is indicated. PAG = periaqueductal gray; SD = standard deviation; SCN = suprachiasmatic nucleus.

Measurement	Parameter	Sex	Paradigm	
			Control	Shift work
Liver	Phase (h) (mean ± SD)	Male	2.407 ± 2.421	2.307 ± 3.622
	n - value		13	11
	Phase (h) (mean ± SD)	Female	3.542 ± 1.167	4.136 ± 0.9497
	n - value		6	8
	Period (h) (mean ± SD)	Male	23.64 ± 2.008	22.75 ± 1.421
	n - value		13	11
	Period (h) (mean ± SD)	Female	23.41 ± 1.733	22.65 ± 0.8832
	n - value		7	8
	Amplitude (counts/s) (mean ± SD)	Male	0.1240 ± 0.05100	0.1551 ± 0.04876
	n - value		12	11
	Amplitude (counts/s) (mean ± SD)	Female	0.1435 ± 0.05116	0.1350 ± 0.04614
	n - value		7	8
Phase relationship	ΔSCN-PAG (h) (mean ± SD)	Male	4.876 ± 2.863	3.581 ± 2.012
	n - value		13	12
	ΔSCN-PAG (h) (mean ± SD)	Female	6.455 ± 1.881	4.405 ± 1.324
	n - value		6	6
	ΔSCN-Liver (h) (mean ± SD)	Male	5.068 ± 2.025	4.244 ± 3.687
	n - value		13	11
	ΔSCN-Liver (h) (mean ± SD)	Female	4.684 ± 2.493	3.588 ± 1.556
	n - value		7	8

Table S41. Statistics for liver bioluminescence parameters and the phase relationship between the SCN and subordinate clocks in project 2. Statistical tests and their outcomes are indicated. DF = degrees of freedom; n.s. = not significant; PAG = periaqueductal gray; SCN = suprachiasmatic nucleus.

Measurement	Parameter	Statistical test		Source of variation			Statistical Test	Comparison	Uncorrected p-value	Corrected p-value	Summary
				Sex	Shift work	Sex x shift work					
Liver	Phase	Two-way ANOVA	DF	1	1	1	Fisher's LSD test + Bonferroni correction	Male control vs. Male shift work	0.9231	> 0.9999	n.s.
			F-value	3.029	0.08423	0.1662					
			p-value	0.0908	0.7734	0.686		Female control vs. Female shift work	0.6642	> 0.9999	n.s.
			Summary	#	n.s.	n.s.					
	Period		DF	1	1	1		Male control vs. Male shift work	0.192	0.3839	n.s.
			F-value	0.09431	2.371	0.01249					
			p-value	0.7606	0.1326	0.9117		Female control vs. Female shift work	0.3687	0.7375	n.s.
			Summary	n.s.	n.s.	n.s.					
	Amplitude		DF	1	1	1		Male control vs. Male shift work	0.1409	0.2817	n.s.
			F-value	0.0003711	0.474	1.451					
			p-value	0.9847	0.4958	0.2367		Female control vs. Female shift work	0.7423	> 0.9999	n.s.
			Summary	n.s.	n.s.	n.s.					
Phase relationship	ΔSCN-PAG		DF	1	1	1		Male control vs. Male shift work	0.1484	0.2968	n.s.
			F-value	2.117	4.482	0.1854					
			p-value	0.1552	0.0419	0.6696		Female control vs. Female shift work	0.1307	0.2613	n.s.
			Summary	n.s.	*	n.s.					
	ΔSCN-Liver		DF	1	1	1		Male control vs. Male shift work	0.4466	0.8931	n.s.
			F-value	0.3632	1.239	0.02482					
			p-value	0.5506	0.2732	0.8757		Female control vs. Female shift work	0.4232	0.8465	n.s.
			Summary	n.s.	n.s.	n.s.					

Table S42. IntelliCage data in project 3. Mean ± SD, statistical tests and their outcomes are indicated. DF = degrees of freedom; n.a. = not applicable; nocturnality score = (parameter during dark phase - parameter during light phase) / (parameter during dark phase + parameter during light phase); n.s. = not significant; SD = standard deviation; WT = wild type.

Test	Parameter	Genotype	Paradigm		Statistical test		Source of variation			Statistical Test	Comparison	Uncorrected p-value	Corrected p-value	Summary
			Control	Shift work			Genotype	Shift work	Genotype x shift work					
Intelli-Cage	Overall corner visits (mean ± SD)	WT	1078 ± 286.4	858.2 ± 320.6	Two-way ANOVA	DF	1	1	1	Fisher's LSD test + Bon-ferroni correction	n.a.	n.a.	n.a.	n.a.
	n - value		11	11		F-value	18.95	0.5079	2.074					
	Overall corner visits (mean ± SD)	*Bmal1*$^{+/-}$	1375 ± 396.5	1449 ± 353.1		p-value	< 0.0001	0.4801	0.1575		n.a.	n.a.	n.a.	n.a.
	n - value		11	12		Summary	****	n.s.	n.s.					
	Nocturnality (mean ± SD)	WT	0.5030 ± 0.1086	0.4316 ± 0.09671		DF	1	1	1		WT control vs. WT shift work	0.0895	0.2686	n.s.
	n - value		10	11		F-value	3.323	21.11	4.439		WT control vs. *Bmal1*$^{+/-}$ control	0.0105	0.0316	*
	Nocturnality (mean ± SD)	*Bmal1*$^{+/-}$	0.6157 ± 0.1051	0.4235 ± 0.06311		p-value	0.076	< 0.0001	0.0416					
	n - value		10	12		Summary	#	****	*		*Bmal1*$^{+/-}$ control vs. *Bmal1*$^{+/-}$ shift work	< 0.0001	< 0.0001	****

Table S43. OFT in project 3. Mean ± SD, statistical tests and their outcomes are indicated. DF = degrees of freedom; n.s. = not significant; OFT = open field test; SD = standard deviation; WT = wild type.

Test	Parameter	Genotype	Paradigm		Statistical test		Source of variation		
			Control	Shift work			Genotype	Shift work	Genotype x shift work
OFT	Distance traveled (m) (mean ± SD)	WT	7.129 ± 2.109	12.61 ± 3.163	Two-way ANOVA	DF	1	1	1
	n - value		11	11		F-value	18.6	28.24	0.01019
	Distance traveled (m) (mean ± SD)	*Bmal1*$^{+/-}$	11.60 ± 4.684	16.87 ± 3.134		p-value	< 0.0001	< 0.0001	0.9201
	n - value		11	12		Summary	****	****	n.s.
	Center entries (mean ± SD)	WT	23.00 ± 6.213	31.36 ± 8.164		DF	1	1	1
	n - value		11	11		F-value	14.11	16.94	1.832
	Center entries (mean ± SD)	*Bmal1*$^{+/-}$	30.27 ± 13.14	46.83 ± 11.46		p-value	0.0005	0.0002	0.1833
	n - value		11	12		Summary	***	***	n.s.
	Center time (s) (mean ± SD)	WT	196.9 ± 74.31	195.6 ± 43.78		DF	1	1	1
	n - value		11	11		F-value	7.258	0.4456	0.5551
	Center time (s) (mean ± SD)	*Bmal1*$^{+/-}$	141.2 ± 58.39	164.1 ± 33.29		p-value	0.0102	0.5082	0.4605
	n - value		11	12		Summary	*	n.s.	n.s.

Table S44. EPM in project 3. Mean ± SD, statistical tests and their outcomes are indicated. DF = degrees of freedom; EPM = elevated plus maze; n.a. = not applicable; n.s. = not significant; SD = standard deviation; WT = wild type.

Test	Parameter	Genotype	Paradigm		Statistical test		Source of variation			Statistical Test	Comparison	Uncorrected p-value	Corrected p-value	Summary
			Control	Shift work			Genotype	Shift work	Genotype x shift work					
EPM	Distance traveled (m) (mean ± SD)	WT	2.273 ± 1.068	3.793 ± 0.9924	Two-way ANOVA	DF	1	1	1	Fisher's LSD test + Bonferroni correction	n.a.	n.a.	n.a.	n.a.
	n - value		11	11		F-value	7.328	9.375	0.3244					
	Distance traveled (m) (mean ± SD)	*Bmal1*$^{+/-}$	3.645 ± 1.947	4.688 ± 1.400		p-value	0.0099	0.0039	0.5721		n.a.	n.a.	n.a.	n.a.
	n - value		11	12		Summary	**	**	n.s.					
	Open arm entries (mean ± SD)	WT	2.500 ± 1.080	5.000 ± 1.897		DF	1	1	1		WT control vs. WT shift work	0.002	0.0061	**
	n - value		10	11		F-value	0.1697	3.396	8.566					
	Open arm entries (mean ± SD)	*Bmal1*$^{+/-}$	3.818 ± 2.316	3.250 ± 1.357		p-value	0.6826	0.0728	0.0056		WT control vs. *Bmal1*$^{+/-}$ control	0.0897	0.2692	n.s.
	n - value		11	12		Summary	n.s.	#	**		*Bmal1*$^{+/-}$ control vs. *Bmal1*$^{+/-}$ shift work	0.4373	> 0.9999	n.s.
	Open arm time (s) (mean ± SD)	WT	3.555 ± 1.761	7.320 ± 3.602		DF	1	1	1		n.a.	n.a.	n.a.	n.a.
	n - value		11	10		F-value	0.4406	3.137	0.3634					
	Open arm time (s) (mean ± SD)	*Bmal1*$^{+/-}$	5.564 ± 4.375	7.417 ± 8.329		p-value	0.5106	0.0842	0.55		n.a.	n.a.	n.a.	n.a.
	n - value		11	12		Summary	n.s.	#	n.d.					

Table S45. DaLi box test in project 3. Mean ± SD, statistical tests and their outcomes are indicated. DF = degrees of freedom; DaLi box = dark-light box; n.s. = not significant; SD = standard deviation; WT = wild type.

Test	Parameter	Genotype	Paradigm		Statistical test		Source of variation		
			Control	Shift work			Genotype	Shift work	Genotype x shift work
DaLi box	Entries into light (mean ± SD)	WT	2.909 ± 1.921	3.818 ± 1.601	Two-way ANOVA	DF	1	1	1
	n - value		11	11		F-value	1.472	11.93	2.517
	Entries into light (mean ± SD)	*Bmal1*$^{+/-}$	2.727 ± 1.737	5.182 ± 1.079		p-value	0.2321	0.0013	0.1205
	n - value		11	11		Summary	n.s.	**	n.s.
	Time in light (s) (mean ± SD)	WT	28.07 ± 23.52	22.01 ± 8.654		DF	1	1	1
	n - value		10	10		F-value	0.01728	0.00042	1.19
	Time in light (s) (mean ± SD)	*Bmal1*$^{+/-}$	21.15 ± 20.83	27.44 ± 16.92		p-value	0.8961	0.9838	0.2821
	n - value		10	12		Summary	n.s.	n.s.	n.s.
	Distance in light (m) (mean ± SD)	WT	1.205 ± 1.006	1.480 ± 0.8463		DF	1	1	1
	n - value		11	11		F-value	0.0021	1.665	0.09218
	Distance in light (m) (mean ± SD)	*Bmal1*$^{+/-}$	1.133 ± 0.9534	1.577 ± 0.9249		p-value	0.9638	0.2042	0.763
	n - value		11	11		Summary	n.s.	n.s.	n.s.
	Latency to light entry (s) (mean ± SD)	WT	32.72 ± 46.31	76.94 ± 80.29		DF	1	1	1
	n - value		10	11		F-value	0.1405	4.562	0.00023
	Latency to light entry (s) (mean ± SD)	*Bmal1*$^{+/-}$	40.22 ± 26.14	85.07 ± 91.10		p-value	0.7098	0.039	0.988
	n - value		10	12		Summary	n.s.	*	n.s.

Table S46. TST, sucrose preference test and LH test in project 3. Mean ± SD, statistical tests and their outcomes are indicated. DF = degrees of freedom; LH = learned helplessness; n.s. = not significant; SD = standard deviation; TST = tail suspension test; WT = wild type.

Test	Parameter	Genotype	Paradigm		Statistical test		Source of variation		
			Control	Shift work			Genotype	Shift work	Genotype x shift work
TST	Time immobile (s) (mean ± SD)	WT	115.7 ± 53.30	117.8 ± 47.03	Two-way ANOVA	DF	1	1	1
	n - value		11	11		F-value	0.08148	2.161	2.564
	Time immobile (s) (mean ± SD)	*Bmal1*$^{+/-}$	145.3 ± 50.98	97.18 ± 57.51		p-value	0.7767	0.1492	0.117
	n - value		11	12		Summary	n.s.	n.s.	n.s.
	Immobility latency (s) (mean ± SD)	WT	87.95 ± 35.64	73.00 ± 27.68		DF	1	1	1
	n - value		11	11		F-value	0.9269	0.2671	2.829
	Immobility latency (s) (mean ± SD)	*Bmal1*$^{+/-}$	78.72 ± 27.03	106.9 ± 64.07		p-value	0.3414	0.6081	0.1004
	n - value		10	12		Summary	n.s.	n.s.	n.s.
Sucrose preference test	Preference Score (AU) (mean ± SD)	WT	0.2878 ± 0.1507	0.3327 ± 0.2967		DF	1	1	1
	n - value		11	11		F-value	0.4511	2.065	0.4401
	Preference Score (AU) (mean ± SD)	*Bmal1*$^{+/-}$	0.2103 ± 0.1279	0.3322 ± 0.1602		p-value	0.5056	0.1583	0.5108
	n - value		11	12		Summary	n.s.	n.s.	n.s.
LH	Latency (s) (mean ± SD)	WT	9.096 ± 5.463	6.909 ± 3.362		DF	1	1	1
	n - value		8	8		F-value	2.672	0.3311	0.3734
	Latency (s) (mean ± SD)	*Bmal1*$^{+/-}$	10.98 ± 5.513	11.05 ± 6.522		p-value	0.1122	0.5692	0.5456
	n - value		9	10		Summary	n.s.	n.s.	n.s.
	Number of failures (mean ± SD)	WT	2.500 ± 3.625	1.125 ± 1.808		DF	1	1	1
	n - value		8	8		F-value	2.601	0.1085	0.3594
	Number of failures (mean ± SD)	*Bmal1*$^{+/-}$	4.000 ± 4.664	4.400 ± 5.777		p-value	0.1169	0.7441	0.5532
	n - value		9	10		Summary	n.s.	n.s.	n.s.

Table S47. Weight at start and fat pads in project 3. Mean ± SD, statistical tests and their outcomes are indicated. BAT = brown adipose tissue; BW = body weight; DF = degrees of freedom; gWAT = gonadal white adipose tissue; iWAT = inguinal white adipose tissue; n.s. = not significant; SD = standard deviation; WT = wild type.

Measurement	Parameter	Genotype	Paradigm		Statistical test		Source of variation		
			Control	Shift work			Genotype	Shift work	Genotype x shift work
Weight at start	Weight gain (%) (mean ± SD)	WT	19.90 ± 1.636	19.65 ± 0.9040	Two-way ANOVA	DF	1	1	1
	n - value		11	11		F-value	2.325	0.1382	0.05012
	Weight gain (%) (mean ± SD)	*Bmal1*$^{+/-}$	20.46 ± 1.725	20.40 ± 1.370		p-value	0.1349	0.712	0.824
	n - value		11	12		Summary	n.s.	n.s.	n.s.
gWAT	% gWAT of BW (mean ± SD)	WT	0.8387 ± 0.2798	0.9237 ± 0.3450		DF	1	1	1
	n - value		10	11		F-value	0.2097	0.6649	0.05514
	% gWAT of BW (mean ± SD)	*Bmal1*$^{+/-}$	0.8948 ± 0.2421	0.9418 ± 0.1613		p-value	0.6495	0.4198	0.8156
	n - value		11	11		Summary	n.s.	n.s.	n.s.
iWAT	% iWAT of BW (mean ± SD)	WT	0.5655 ± 0.08214	0.6231 ± 0.1821		DF	1	1	1
	n - value		9	11		F-value	0.001669	1.105	0.1112
	% iWAT of BW (mean ± SD)	*Bmal1*$^{+/-}$	0.5777 ± 0.1291	0.6075 ± 0.1225		p-value	0.9676	0.2997	0.7406
	n - value		11	12		Summary	n.s.	n.s.	n.s.
BAT	% BAT of BW (mean ± SD)	WT	0.4407 ± 0.04926	0.4397 ± 0.05106		DF	1	1	1
	n - value		10	11		F-value	0.05115	0.5023	0.6089
	% BAT of BW (mean ± SD)	*Bmal1*$^{+/-}$	0.4330 ± 0.02933	0.4537 ± 0.05018		p-value	0.8222	0.4826	0.4398
	n - value		11	12		Summary	n.s.	n.s.	n.s.

Table S48. Weight measurements and food consumption over time in project 3. Mean ± SD is indicated. SD = standard deviation; WT = wild type.

Genotype	Paradigm	Parameter	Weeks after initiation of shift work paradigm							
			0	1	2	3	4	5	6	7
WT	Control	Weight (g) (mean ± SD)	19.90 ± 1.636	20.36 ± 1.542	20.78 ± 1.611	21.21 ± 1.425	21.60 ± 1.727	21.84 ± 1.691	22.35 ± 2.068	22.55 ± 2.370
		n - value	11	11	11	11	11	11	10	8
WT	Shift work	Weight (g) (mean ± SD)	19.65 ± 0.9040	20.52 ± 1.022	20.96 ± 1.018	21.55 ± 0.6647	21.65 ± 1.154	21.99 ± 0.9577	22.25 ± 1.294	23.53 ± 0.8425
		n - value	11	11	11	10	11	11	11	8
Bmal1$^{+/-}$	Control	Weight (g) (mean ± SD)	20.46 ± 1.725	20.78 ± 1.557	21.28 ± 1.844	21.83 ± 1.785	22.12 ± 1.606	22.63 ± 1.690	22.97 ± 1.628	23.61 ± 1.779
		n - value	11	11	11	11	11	11	11	8
Bmal1$^{+/-}$	Shift work	Weight (g) (mean ± SD)	20.40 ± 1.370	21.08 ± 1.459	21.79 ± 1.431	22.34 ± 1.226	22.86 ± 1.523	22.82 ± 1.414	23.23 ± 1.597	23.95 ± 1.434
		n - value	12	12	12	12	12	12	12	8
WT	Control	Weight gain (%) (mean ± SD)	0 ± 0	2.365 ± 2.427	4.471 ± 2.136	5.578 ± 2.424	8.649 ± 4.882	9.834 ± 4.135	12.08 ± 4.982	13.54 ± 4.437
		n - value	11	11	11	10	11	11	10	8
WT	Shift work	Weight gain (%) (mean ± SD)	0 ± 0	4.425 ± 1.437	6.683 ± 1.972	8.447 ± 2.205	10.19 ± 2.701	11.94 ± 2.479	13.22 ± 2.546	17.60 ± 3.163
		n - value	11	11	11	11	11	11	11	8
Bmal1$^{+/-}$	Control	Weight gain (%) (mean ± SD)	0 ± 0	1.618 ± 2.406	4.018 ± 3.213	6.747 ± 3.766	8.247 ± 3.500	10.75 ± 4.313	12.50 ± 5.388	13.03 ± 2.162
		n - value	11	11	11	11	11	11	11	8
Bmal1$^{+/-}$	Shift work	Weight gain (%) (mean ± SD)	0 ± 0	3.335 ± 2.175	6.877 ± 3.364	9.607 ± 2.654	12.09 ± 3.380	11.93 ± 3.400	14.44 ± 1.563	14.18 ± 3.981
		n - value	12	12	12	12	12	12	11	8
WT	Control	Food consumption/animal (g) (mean ± SD)	-	23.28182 ± 0	23.09818 ± 0	N.A.	23.53273 ± 0	23.5 ± 0	23.194 ± 0	26.94 ± 0
		n - value	-	1	1	1	1	1	1	1
WT	Shift work	Food consumption/animal (g) (mean ± SD)	-	23.64 ± 0	24.36273 ± 0	21.85546 ± 0	22.51636 ± 0	24.56 ± 0	23.70273 ± 0	24.75412 ± 0
		n - value	-	1	1	1	1	1	1	1
Bmal1$^{+/-}$	Control	Food consumption/animal (g) (mean ± SD)	-	26.05364 ± 0	24.74273 ± 0	23.10455 ± 0	24.32182 ± 0	24.62818 ± 0	27.14727 ± 0	27.88588 ± 0
		n - value	-	1	1	1	1	1	1	1
Bmal1$^{+/-}$	Shift work	Food consumption/animal (g) (mean ± SD)	-	25.22167 ± 0	27.6725 ± 0	24.33 ± 0	24.93917 ± 0	23.66333 ± 0	24.42 ± 0	23.97111 ± 0
		n - value	-	1	1	1	1	1	1	1

Table S49. Statistics for weight measurements and food consumption over time in project 3. Statistical tests and their outcomes are indicated. DF = degrees of freedom; n.s. = not significant; WT = wild type.

Parameter	Statistical test		Source of variation						
			Time	Genotype	Shift work	Time x genotype	Time x shift work	Genotype x shift work	Time x genotype x shift work
Absolute weight (g)	Mixed-effects analysis (Repeated-measures)	DF	7	1	1	7	7	1	7
		F-value	234.4	2.534	0.2599	1.58	2.058	0.05899	1.23
		p-value	< 0.0001	0.1191	0.6129	0.1414	0.0483	0.8093	0.2861
		Summary	****	n.s.	n.s.	n.s.	*	n.s.	n.s.
Weight gain (%)	Mixed-effects analysis (Repeated-measures)	DF	7	1	1	7	7	1	7
		F-value	227.4	0.000002	7.727	1.851	2.023	0.00097	1.151
		p-value	< 0.0001	0.9987	0.0082	0.0779	0.0524	0.9754	0.3314
		Summary	****	n.s.	**	n.s.	n.s.	n.s.	n.s.

Table S50. Locomotor activity, food consumption and water consumption in the metabolic cages in project 3. Mean ± SD, statistical tests and their outcomes are indicated. DF = degrees of freedom; nocturnality score = (parameter during dark phase - parameter during light phase) / (parameter during dark phase + parameter during light phase); n.s. = not significant; SD = standard deviation; WT = wild type.

Measurement	Parameter	Genotype	Paradigm		Statistical test		Source of variation		
			Control	Shift work			Genotype	Shift work	Genotype x shift work
Locomotor activity	Overall (light beam breaks) (mean ± SD)	WT	809229 ± 340290	999820 ± 117281	Two-way ANOVA	DF	1	1	1
	n - value		4	4		F-value	2.177	1.222	0.01524
	Overall (light beam breaks) (mean ± SD)	*Bmal1*$^{+/-}$	1071654 ± 250951	1310162 ± 640527		p-value	0.1658	0.2907	0.9038
	n - value		4	4		Summary	n.s.	n.s.	n.s.
	Nocturnality (mean ± SD)	WT	0.4020 ± 0.06410	0.3996 ± 0.1004		DF	1	1	1
	n - value		4	4		F-value	0.02804	0.1079	0.1363
	Nocturnality (mean ± SD)	*Bmal1*$^{+/-}$	0.3902 ± 0.1985	0.4308 ± 0.02116		p-value	0.8698	0.7482	0.7184
	n - value		4	4		Summary	n.s.	n.s.	n.s.
Food consumption	Overall (g) (mean ± SD)	WT	7.340 ± 1.226	6.583 ± 0.5548		DF	1	1	1
	n - value		4	4		F-value	0.01387	1.362	0.2071
	Overall (g) (mean ± SD)	*Bmal1*$^{+/-}$	7.183 ± 0.8690	6.850 ± 0.9611		p-value	0.9082	0.2659	0.6572
	n - value		4	4		Summary	n.s.	n.s.	n.s.
	Nocturnality (mean ± SD)	WT	0.6492 ± 0.1842	0.5502 ± 0.1772		DF	1	1	1
	n - value		4	4		F-value	0.01384	1.212	0.07293
	Nocturnality (mean ± SD)	*Bmal1*$^{+/-}$	0.6212 ± 0.07040	0.5612 ± 0.1150		p-value	0.9083	0.2925	0.7917
	n - value		4	4		Summary	n.s.	n.s.	n.s.
Water consumption	Overall (ml) (mean ± SD)	WT	6.627 ± 0.3553	6.643 ± 0.6788		DF	1	1	1
	n - value		3	3		F-value	11.71	0.2617	0.3293
	Overall (ml) (mean ± SD)	*Bmal1*$^{+/-}$	7.698 ± 0.3212	7.407 ± 0.5404		p-value	0.0076	0.6212	0.5801
	n - value		4	3		Summary	**	n.s.	n.s.
	Nocturnality (mean ± SD)	WT	0.6322 ± 0.1221	0.4628 ± 0.1817		DF	1	1	1
	n - value		3	3		F-value	0.7411	5.623	0.0056
	Nocturnality (mean ± SD)	*Bmal1*$^{+/-}$	0.6866 ± 0.1140	0.5276 ± 0.04039		p-value	0.4117	0.0418	0.942
	n - value		4	3		Summary	n.s.	*	n.s.

Table S51. RER and EE in the metabolic cages in project 3. Mean ± SD, statistical tests and their outcomes are indicated. DF = degrees of freedom; EE = energy expenditure; nocturnality score = (parameter during dark phase - parameter during light phase) / (parameter during dark phase + parameter during light phase); n.s. = not significant; RER = respiratory exchange rate; SD = standard deviation; WT = wild type.

Measurement	Parameter	Genotype	Paradigm		Statistical test		Source of variation		
			Control	Shift work			Genotype	Shift work	Genotype x shift work
Respiratory exchange rate	Mean (mean ± SD)	WT	0.7172 ± 0.06655	0.7031 ± 0.06401	Two-way ANOVA	DF	1	1	1
	n - value		4	4		F-value	0.008628	0.6319	0.0696
	Mean (mean ± SD)	*Bmal1*$^{+/-}$	0.7217 ± 0.02138	0.6936 ± 0.04809		p-value	0.9275	0.4421	0.7964
	n - value		4	4		Summary	n.s.	n.s.	n.s.
	Nocturnality (mean ± SD)	WT	0.09233 ± 0.03089	0.07879 ± 0.02730		DF	1	1	1
	n - value		4	4		F-value	1.29	1.44	0.01519
	Nocturnality (mean ± SD)	*Bmal1*$^{+/-}$	0.1082 ± 0.02516	0.09152 ± 0.01407		p-value	0.2783	0.2532	0.904
	n - value		4	4		Summary	n.s.	n.s.	n.s.
Energy expenditure	Mean (kcal/h/kg) (mean ± SD)	WT	7.835 ± 0.6098	7.954 ± 0.7100		DF	1	1	1
	n - value		4	4		F-value	1.17	0.4757	0.1067
	Mean (kcal/h/kg) (mean ± SD)	*Bmal1*$^{+/-}$	8.084 ± 0.3337	8.418 ± 0.8663		p-value	0.3007	0.5036	0.7496
	n - value		4	4		Summary	n.s.	n.s.	n.s.
	Nocturnality (mean ± SD)	WT	0.1175 ± 0.02055	0.08579 ± 0.02179		DF	1	1	1
	n - value		4	4		F-value	3.515	4.889	0.1144
	Nocturnality (mean ± SD)	*Bmal1*$^{+/-}$	0.1366 ± 0.02628	0.1133 ± 0.02983		p-value	0.0854	0.0472	0.7411
	n - value		4	4		Summary	#	*	n.s.

Table S52. GTT in project 3. Mean ± SD, statistical tests and their outcomes are indicated. DF = degrees of freedom; GTT = glucose tolerance test; n.s. = not significant; SD = standard deviation; WT = wild type.

Test	Time	Parameter	Genotype	Paradigm		Statistical test		Source of variation						
				Control	Shift work			Time	Genotype	Shift work	Time x genotype	Time x shift work	Genotype x shift work	Time x genotype x shift work
Glucose tolerance test	0 min	Glucose (mg/dL) (mean ± SD)	WT	135.6 ± 14.19	118.8 ± 17.09	Three-way repeated measures ANOVA	DF	5	1	1	5	5	1	5
		n - value		11	11									
		Glucose (mg/dL) (mean ± SD)	*Bmal1*$^{+/-}$	149.5 ± 35.83	114.6 ± 12.77									
		n - value		11	12									
	15 min	Glucose (mg/dL) (mean ± SD)	WT	270.0 ± 38.29	255.4 ± 29.11		F-value	205.8	0.4244	8.199	0.4452	2.339	1.472	0.526
		n - value		11	11									
		Glucose (mg/dL) (mean ± SD)	*Bmal1*$^{+/-}$	260.8 ± 65.71	254.9 ± 38.73									
		n - value		11	12									
	30 min	Glucose (mg/dL) (mean ± SD)	WT	196.9 ± 30.25	208.9 ± 18.38									
		n - value		11	11									
		Glucose (mg/dL) (mean ± SD)	*Bmal1*$^{+/-}$	204.0 ± 33.44	202.4 ± 33.00									
		n - value		11	12									
	60 min	Glucose (mg/dL) (mean ± SD)	WT	171.3 ± 17.08	164.4 ± 13.62		p-value	< 0.0001	0.5184	0.0066	0.8165	0.043	0.232	0.7564
		n - value		11	11									
		Glucose (mg/dL) (mean ± SD)	*Bmal1*$^{+/-}$	183.4 ± 28.25	161.5 ± 21.16									
		n - value		11	12									
	90 min	Glucose (mg/dL) (mean ± SD)	WT	144.3 ± 13.29	128.6 ± 13.16									
		n - value		11	11									
		Glucose (mg/dL) (mean ± SD)	*Bmal1*$^{+/-}$	159.5 ± 28.52	131.0 ± 12.23									
		n - value		11	12									
	120 min	Glucose (mg/dL) (mean ± SD)	WT	134.1 ± 14.63	128.5 ± 15.91		Summary	****	n.s.	**	n.s.	*	n.s.	n.s.
		n - value		11	11									
		Glucose (mg/dL) (mean ± SD)	*Bmal1*$^{+/-}$	148.8 ± 20.76	123.9 ± 13.94									
		n - value		11	12									

Table S53. ITT in project 3. Mean ± SD, statistical tests and their outcomes are indicated. DF = degrees of freedom; ITT = insulin tolerance test; n.s. = not significant; SD = standard deviation; WT = wild type.

Test	Time	Parameter	Genotype	Paradigm		Statistical test		Source of variation						
				Control	Shift work			Time	Genotype	Shift work	Time x genotype	Time x shift work	Genotype x shift work	Time x genotype x shift work
Insulin tolerance test	0 min	Glucose (mg/dL) (mean ± SD)	WT	121.9 ± 23.34	108.5 ± 20.00	Three-way repeated measures ANOVA	DF	5	1	1	5	5	1	5
		n - value		10	11									
		Glucose (mg/dL) (mean ± SD)	*Bmal1*$^{+/-}$	120.8 ± 16.23	106.6 ± 12.98									
		n - value		11	11									
	15 min	Glucose (mg/dL) (mean ± SD)	WT	87.10 ± 14.96	84.82 ± 13.14		F-value	57.19	0.005438	10.07	0.4288	0.8655	0.758	1.826
		n - value		10	11									
		Glucose (mg/dL) (mean ± SD)	*Bmal1*$^{+/-}$	89.18 ± 11.81	83.36 ± 8.744									
		n - value		11	11									
	30 min	Glucose (mg/dL) (mean ± SD)	WT	87.20 ± 11.01	75.27 ± 11.19									
		n - value		10	11									
		Glucose (mg/dL) (mean ± SD)	*Bmal1*$^{+/-}$	87.82 ± 12.84	79.55 ± 21.89									
		n - value		11	11									
	60 min	Glucose (mg/dL) (mean ± SD)	WT	77.80 ± 8.443	69.45 ± 13.66		p-value	< 0.0001	0.8168	0.0029	0.8282	0.5053	0.3893	0.1094
		n - value		10	11									
		Glucose (mg/dL) (mean ± SD)	*Bmal1*$^{+/-}$	83.09 ± 9.060	72.82 ± 16.05									
		n - value		11	11									
	90 min	Glucose (mg/dL) (mean ± SD)	WT	97.20 ± 12.81	80.00 ± 12.32									
		n - value		10	11									
		Glucose (mg/dL) (mean ± SD)	*Bmal1*$^{+/-}$	89.27 ± 11.23	88.45 ± 16.81									
		n - value		11	11									
	120 min	Glucose (mg/dL) (mean ± SD)	WT	105.0 ± 13.87	84.27 ± 13.64		Summary	****	n.s.	**	n.s.	n.s.	n.s.	n.s.
		n - value		10	11									
		Glucose (mg/dL) (mean ± SD)	*Bmal1*$^{+/-}$	94.36 ± 11.75	91.64 ± 18.54									
		n - value		11	11									

Table S54. AOC for the GTT and ITT in project 3. Mean ± SD, statistical tests and their outcomes are indicated. AOC = area of the curve; DF = degrees of freedom; GTT = glucose tolerance test; ITT = insulin tolerance test; n.s. = not significant; SD = standard deviation; WT = wild type.

Test	Parameter	Genotype	Paradigm		Statistical test		Source of variation		
			Control	Shift work			Genotype	Shift work	Genotype x shift work
Glucose Tolerance Test	AOC (mg/dl x min) (mean ± SD)	WT	4931 ± 2084	6039 ± 2128	Two-way ANOVA	DF	1	1	1
	n - value		11	11		F-value	0.8602	0.8614	0.4828
	AOC (mg/dl x min) (mean ± SD)	*Bmal1*$^{+/-}$	6038 ± 2738	6198 ± 2086		p-value	0.3592	0.3589	0.4912
	n - value		10	12		Summary	n.s.	n.s.	n.s.
Insulin Tolerance Test	AOC (mg/dl x min) (mean ± SD)	WT	2948 ± 1638	3797 ± 2312		DF	1	1	1
	n - value		9	12		F-value	0.007243	0.03412	2.733
	AOC (mg/dl x min) (mean ± SD)	*Bmal1*$^{+/-}$	3855 ± 1764	2792 ± 1538		p-value	0.9326	0.8544	0.1066
	n - value		10	11		Summary	n.s.	n.s.	n.s.

Acknowledgements

The time of my dissertation was certainly an exciting, but also very challenging one. I would like to sincerely thank the people who made this journey possible.

I would like to express my gratitude to my supervisor, **Dr. Dominic Landgraf**, for his support, advice, and guidance throughout my dissertation project. Thank you for giving me with the opportunity to delve into the exciting field of circadian biology.

I am thankful to **Prof. Dr. Moritz Rossner**, head of the Molecular Neurobiology Department, for providing the necessary scientific environment and infrastructure for this dissertation project.

I would also like to thank my TAC members, **Prof. Dr. Maria del Sagrario Robles Martinez**, and **Dr. Jan Deussing**, for their scientific input during my TAC meetings. Thank you for being approachable despite your numerous responsibilities.

Moreover, I am thankful to many members of the Molecular Neurobiology Department:

To **Dr. Charlotte Kling** and **Min Chen**, who gave me scientific and emotional support whenever needed. Charly, you deserve a special thank you for the *Ppox* quantifications as well as the help with the statistical analyses of the metabolic cage and IntelliCage data. Thank you both for laughing, crying, and eating a ridiculous number of snacks with me. You truly were the best colleagues I could have imagined – thank you for always standing by my side.

To **Lisa Echtler**, **Annika Geiger**, **Naomi Springer**, **Katharina Laurent, and Pia Pickelmann** for their technical assistance during behavioral and metabolic experiments. Working with you was always a pleasure.

To **Jessica Bly** and **Wilma Vogel** for their support in animal care. You two kept the mouse unit running.

To **Dr. Niels Jensen** for leading the mouse unit. This is a very challenging and laborious task, which deserves recognition.

To **Dr. Marius Stephan** for setting up the IntelliCage system in our department and for introducing me to FlowR for statistical analyses. Thank you for always providing a solution to the countless issues one encounters during a PhD. Your incredible patience and serenity during stressful times helped me more than once.

To **Dr. Sergi Papiol** for his statistical advice, guidance and supporting words.

To **Dr. Alexander Herholt** for his advice on virus production.

To **Dr. Sven Wichert** for his IT-related help.

And to the whole **Molecular Neurobiology Department** and particularly the **Circadian Biology Group** for providing an enjoyable atmosphere to work in.

Furthermore, I am thankful:

To **Dr. Rosa Hüttl** for her training in stereotactic injections and providing the necessary equipment. Your help was very appreciated.

To **Isabel Oßwald**, for excellently coordinating the IMPRS-TP program and always having an open door.

To the **IMPRS-TP** for being a scientifically stimulating graduate school and providing financial support.

And to the **Deutsche Forschungsgemeinschaft** (Emmy-Noether-Programm) for funding my work.

Lastly, I would like to thank my family and friends for their continuous encouragement, support, and love. I am incredibly lucky to have wonderful people in my life and I apologize for not listing every single one of you. However, I would still like to highlight a few people who particularly shaped my life during the PhD. **Lotte**, thank you for being the most kind-hearted, inspiring, and empowering flatmate I could have asked for. Danke auch dir, **Julian**, dass du mir während dieser herausfordernden Zeit immer bedingungslos und liebevoll zur Seite gestanden hast. **Mama** und **Mimi**, ihr seid meine größten Supporter und ohne euch würde ich heute nicht hier stehen. Wo auch immer ich bin, ich trage euch stets in meinem Herzen (und auf meinem Fuß) – M^3.

Affidavit

Affidavit

Frisch, Muriel Katja

Surname, first name

Nußbaumstraße 7

Street

80336, Munich, Germany

Zip code, town, country

I hereby declare, that the submitted thesis entitled:

Contribution of Genetic and Environmental Circadian Disruptions to the Development of Comorbid Behavioral and Metabolic Deficits in Mice

is my own work. I have only used the sources indicated and have not made unauthorised use of services of a third party. Where the work of others has been quoted or reproduced, the source is always given.

I further declare that the dissertation presented here has not been submitted in the same or similar form to any other institution for the purpose of obtaining an academic degree.

Munich, 19.05.2023
place, date

Muriel Katja Frisch
Signature doctoral candidate

Confirmation of congruency

LMU LUDWIG-MAXIMILIANS-UNIVERSITÄT MÜNCHEN

Promotionsbüro
Medizinische Fakultät

MMRS

Confirmation of congruency between printed and electronic version of the doctoral thesis

Frisch, Muriel Katja

Surname, first name

Nußbaumstraße 7

Street

80336, Munich, Germany

Zip code, town, country

I hereby declare, that the submitted thesis entitled:

Contribution of Genetic and Environmental Circadian Disruptions to the Development of Comorbid Behavioral and Metabolic Deficits in Mice

is congruent with the printed version both in content and format.

Munich, 19.05.2023
place, date

Muriel Katja Frisch
Signature doctoral candidate

List of publications

Hühne-Landgraf A, **Frisch MK**, Laurent K, Wehr MC, Rossner MJ, Landgraf D**. Rescue of Comorbid Behavioral and Metabolic Phenotypes of Arrhythmic Mice by Restoring Circadian Cryptochrome1/2 Expression in the Suprachiasmatic Nucleus**. [Manuscript submitted for publication]. 2023. Department of Molecular Neurobiology, Clinic of Psychiatry and Psychotherapy, University Hospital, Ludwig Maximilian University.